

Some pages of this thesis may have been removed for copyright restrictions.

If you have discovered material in AURA which is unlawful e.g. breaches copyright, (either yours or that of a third party) or any other law, including but not limited to those relating to patent, trademark, confidentiality, data protection, obscenity, defamation, libel, then please read our [Takedown Policy](#) and [contact the service](#) immediately

APPLICATIONS OF REISSNER'S PRINCIPLE
TO
STRUCTURAL DYNAMICS

by

Ahmad. Ali. Youssefi, BSc, MSc

A thesis submitted for the degree of
Doctor of Philosophy

Mechanical Engineering Department
The University of Aston in Birmingham

July 1983

Applications of Reissner's Principle to Structural Dynamics

PhD

by

1983

Ahmad. A. Youssefi

The analysis and prediction of the dynamic behaviour of structural components plays an important role in modern engineering design. In this work, the so-called "mixed" finite element models based on Reissner's variational principle are applied to the solution of free and forced vibration problems, for beam and plate structures. The mixed beam models are obtained by using elements of various shape functions ranging from simple linear to complex cubic and quadratic functions. The elements were in general capable of predicting the natural frequencies and dynamic responses with good accuracy.

An isoparametric quadrilateral element with 8-nodes was developed for application to thin plate problems. The element has 32 degrees of freedom (one deflection, two bending and one twisting moment per node) which is suitable for discretization of plates with arbitrary geometry. A linear isoparametric element and two non-conforming displacement elements (4-node and 8-node quadrilateral) were extended to the solution of dynamic problems. An auto-mesh generation program was used to facilitate the preparation of input data required by the 8-node quadrilateral elements of mixed and displacement type.

Numerical examples were solved using both the mixed beam and plate elements for predicting a structure's natural frequencies and dynamic response to a variety of forcing functions. The solutions were compared with the available analytical and displacement model solutions.

The mixed elements developed have been found to have significant advantages over the conventional displacement elements in the solution of plate type problems. A dramatic saving in computational time is possible without any loss in solution accuracy. With beam type problems, there appears to be no significant advantages in using mixed models.

Key words:

REISSNER'S PRINCIPLE
MIXED FINITE ELEMENT
BEAM AND THIN PLATE
DYNAMIC ANALYSIS

ACKNOWLEDGEMENTS

I wish to express my sincere gratitude to my project supervisor Mr T.H. Richards for his valuable help, guidance and encouragement during the entire period of the project.

It is also my pleasure to acknowledge the assistance of various members of the Department of Mechanical Engineering at the University of Aston in Birmingham. My particular gratitude goes to Dr C.W. Chuen, R. Firoozian and Gerald Seet.

The patience and understanding of Mrs. S. Glendon during the typing of the thesis is also worth special mention.

The Department of Mechanical Engineering of the University of Aston in Birmingham is acknowledged for the financial assistance during the course of this work.

CONTENTS

	<u>Page</u>
SUMMARY	i
ACKNOWLEDGEMENTS	ii
LIST OF CONTENTS	iii
LIST OF FIGURES	viii
LIST OF TABLES	xiii
NOTATIONS	xiv
<u>CHAPTER ONE:</u> INTRODUCTION	1
<u>CHAPTER TWO:</u> VARIATIONAL METHODS IN STRUCTURAL MECHANICS	
2.1 Introduction	6
2.2 Basic relations	7
2.2.1 Equations of dynamic equilibrium	8
2.2.2 Strain-displacement relations	8
2.2.3 Compatibility conditions	8
2.2.4 Stress-strain relations	9
2.2.5 Boundary conditions	10
2.3 Classical variational principles	13
2.3.1 Lagrange's principle for elasticity problems	14
2.3.2 Minimum potential energy principle	16
2.3.3 Hamilton's principle	
2.4 Multi-field variational principles - Lagrange's relaxation principle	20
2.4.1 The generalization of minimum potential energy principle	20
2.4.2 E. Reissner's principle	24
2.4.3 Reissner's principle - extension to dynamical problems	26
2.5 Approximate methods	28
2.5.1 Rayleigh-Ritz method	28
2.5.2 The finite element method	30
2.5.3 The mixed finite element method	32
<u>CHAPTER THREE:</u> DYNAMIC ANALYSIS OF ELASTIC BEAMS AND PLATES	
3.1 Introduction	33
3.2 Response of a beam to an applied force	34

3.2.1	Equations of motion	34
3.2.2	Solution of the equations of motion	36
3.3	Reissner principle applied to flexural motion of beams	40
3.4	Basic equations - Thin plate theory	42
3.4.1	Plate displacement components	42
3.4.2	Stress-strain relations	43
3.4.3	Relations between internal moments, stresses and displacements	44
3.4.4	Derivation of the governing differential equations	45
3.4.5	Boundary conditions	47
3.5	Hamilton's principle - Thin plate theory	51
3.6	Reissner's principle - applied to plate bending	54
3.6.1	Introduction	54
3.6.2	Reissner's functional for plate bending	54
3.7	Methods for the solution of dynamic plate problems	60
3.7.1	Free vibration of thin rectangular plates	60
3.7.2	Forced vibration analysis of thin plates	65
<u>CHAPTER FOUR:</u>	APPLICATION OF REISSNER'S PRINCIPLE IN FINITE ELEMENT FORMULATION	
4.1	Introduction	68
4.2	Finite element models	70
4.3	Discretized Reissner functional - Interelement continuity requirements	73
4.3.1	Discretized Reissner's principle - Beam bending problems	76
4.3.2	Discretized Reissner's principle - Plate bending problems	77
4.4	Finite element formulation	79
4.4.1	General approach	79
4.4.2	Derivation of the mixed element equations	80

4.5	Evaluation of the damping matrix	88
4.5.1	Importance of damping	88
4.5.2	The element damping matrix	89
4.6	Solution of dynamic equilibrium equations	91
4.6.1	Direct integration method - Wilson θ method	93
4.6.2	Mode superposition method - Duhammel integral	96
4.6.3	Comparison between mode superposition and direct integration methods	98
<u>CHAPTER FIVE:</u>	<u>SURVEY OF LITERATURE ON PLATE PROBLEMS</u>	100
<u>CHAPTER SIX:</u>	<u>TREATMENT OF BEAM AND PLATE VIBRATION PROBLEMS BY MIXED FINITE ELEMENT METHOD</u>	
6.1	Introduction	106
6.2	Derivation of the mixed beam element properties	107
6.2.1	Mixed finite element properties	107
6.3	Computer implementation of the mixed beam elements	113
6.4	Mixed finite element formulation - thin plates	114
6.5	Derivation of mixed element properties - thin plates	120
6.5.1	Element shape functions	120
6.5.2	Transformation	121
6.5.3	Slope matrices	123
6.5.4	Shear force intensity matrix	124
6.5.5	Normal twisting moment along each element side	125
6.5.6	Mixed element matrices and load vector	126
6.5.7	Approximate integration of element matrices - Gauss-quadrature rule	130
6.6	Assembly of the overall matrices and load vector	134
6.7	Boundary conditions	136
6.8	Matrix condensation of the mixed governing equations	139

3.2.1	Equations of motion	34
3.2.2	Solution of the equations of motion	36
3.3	Reissner principle applied to flexural motion of beams	40
3.4	Basic equations - Thin plate theory	42
3.4.1	Plate displacement components	42
3.4.2	Stress-strain relations	43
3.4.3	Relations between internal moments, stresses and displacements	44
3.4.4	Derivation of the governing differential equations	45
3.4.5	Boundary conditions	47
3.5	Hamilton's principle - Thin plate theory	51
3.6	Reissner's principle - applied to plate bending	54
3.6.1	Introduction	54
3.6.2	Reissner's functional for plate bending	54
3.7	Methods for the solution of dynamic plate problems	60
3.7.1	Free vibration of thin rectangular plates	60
3.7.2	Forced vibration analysis of thin plates	65

CHAPTER FOUR: APPLICATION OF REISSNER'S PRINCIPLE IN FINITE ELEMENT FORMULATION

4.1	Introduction	68
4.2	Finite element models	70
4.3	Discretized Reissner functional - Interelement continuity requirements	73
4.3.1	Discretized Reissner's principle - Beam bending problems	76
4.3.2	Discretized Reissner's principle - Plate bending problems	77
4.4	Finite element formulation	79
4.4.1	General approach	79
4.4.2	Derivation of the mixed element equations	80

CHAPTER SEVEN:COMPUTER ALGORITHMS AND
PROGRAMS STRUCTURE

7.1	Introduction	142
7.2	Classification of the sections of the program	143
7.3	Subprogram Feinput	145
7.4	Subprogram Cmatrx	148
7.5	Subprogram Excitn	148
7.6	Subprogram Rspipt	149
7.7	Subprogram Qaux	150
7.8	Algorithms for the generation of element matrices and load vector	154
7.8.1	Subprogram Mnsws	154
7.8.2	Subprogram Heform	155
7.8.3	Subprogram Geform	156
7.8.4	Subprogram Transf	156
7.8.5	Subprogram Meform	157
7.8.6	Subprogram Loadap	158
7.9	Algorithms for the assembly of the overall matrices	171
7.10	Elimination of the nodal moment degrees of freedom	175
7.11	Subprogram Dampmat	176
7.12	Subprogram Initil	176
7.13	Subprogram Wilsnsol	177
7.14	Subprogram Duhammel	178

CHAPTER EIGHT:APPLICATIONS OF MIXED BEAM AND
PLATE FINITE ELEMENTS IN FREE AND
FORCED VIBRATION PROBLEMS

8.1	Introduction	182
8.2	Numerical examples on free vibration of beams	184
8.3	Numerical examples on forced vibration of beams	192
8.3.1	Response of a cantilever to a transient force	192
8.3.2	Response of a cantilever to a ramp force input	193
8.3.3	Response of a clamped-clamped beam to a step force input	194

8.3.4	Response of a clamped-simply supported beam to half sine pulse input	194
8.3.5	Response of a clamped-simply supported beam to a ramp force input (damping included)	195
8.3.6	Response of a cantilever to a step moment input at the tip	195
8.4	Numerical examples on free vibration of plates	202
8.4.1	Simply-supported plate	222
8.4.2	Clamped-simply supported square plate	223
8.4.3	Cantilevered square plate	224
8.5	Numerical examples on forced vibration of plates	234
8.5.1	Simply-supported square plate under uniform loading, varying sinusoidally with time	234
8.5.2	Simply-supported square plate under point load, step force input	235
8.5.3	Clamped square plate under point load, step force input	236
8.5.4	The effect of time step size, Δt on the numerical stability and accuracy of the solution	237
8.5.5	The effect of number of modes on the accuracy of the solution from mode superposition method	239
<u>CHAPTER NINE:</u>	DISCUSSION AND CONCLUSIONS	268
9.1	Further improvements	272
REFERENCES		273
APPENDIX A	Direct method for evaluation of damping matrix	278
APPENDIX B	Input data for mesh generation program	281
APPENDIX C	Computer program listings	287

LIST OF FIGURES

<u>Figure</u>	<u>Title</u>	<u>Page</u>
2.1	Elastic body subject to external forces	12
2.2	Stress and displacement components	12
2.3	Boundary forces	12
3.1	Beam subjected to dynamic loading. (a) beam properties and coordinates. (b) forces acting on a differential element	35
3.2	Thin plate subjected to distributed loading	48
3.3	Stress components on a plate element	48
3.4	Moments and shear notation	49
3.5	Forces and moments on an element of a plate	50
3.6	Simply supported rectangular plate, Navier's method	67
3.7	Rectangular plate with two opposite edges simply-supported - Levy's method	67
4.1	A rectangular plane stress/strain finite element	87
4.2	Characteristics of typical dynamic loading	92
6.1	Beam finite element	110
6.2	Finite element idealisation of a plate	119
6.3	Isoparametric quadratic plate element	133
6.4	Typical boundary node	138
7.1	Nodal connection array for a quarter of SSSS plate	146
7.2	Flow diagram for SUB Qaux	152
7.3	Flow diagram for SUB Mnsws	160
7.4	Flow diagram for SUB Heform	162
7.5	Flow diagram for SUB Geform	163
7.6	Flow diagram for SUB Transf	164
7.7	Flow diagram for the construction of element matrices	165
7.8	Flow diagram for SUB Meform	167
7.9	Flow diagram for SUB Loadap	168

7.10	Flow diagram for SUB Ghasemb	172
7.11	Flow diagram for SUB Masemb	174
7.12	Flow diagram for SUB Dampmat	174
7.13	Flow diagram for SUB Wilsnsol	180
8.1	Types of plate bending elements (a,b) mixed elements (c,d) non-conforming elements	183
8.2	Zero energy modes in elements MB7 (a), MB8 (b) and MB5 (c)	186
8.3	Cantilever beam used in free vibration tests	187
8.4	Prediction of 1st natural frequency of CF beam: Elements D & MB1	188
8.5	Prediction of 1st natural frequency of CF beam: Elements D & MB2	188
8.6	Prediction of 1st natural frequency of CF beam: Elements D & MB3	189
8.7	Prediction of 1st natural frequency of CF beam: Elements D & MB4	189
8.8	Prediction of 1st natural frequency of CF beam: Elements D & MB5	190
8.9	Prediction of 1st natural frequency of CF beam: Elements D & MB6	190
8.10	Tip displacement response of cantilever to half sine pulse input F.E models with 2 d.o.f	198
8.11	Bending moment response of cantilever to half sine input at $x = 0.0$ F.E models with 2 d.o.f	199
8.12	Tip displacement response of cantilever to half sine pulse input F.E models with 4 d.o.f.	200
8.13	Bending moment response of a cantilever to half sine pulse input at $x = 0.0$ F.E models with 4 d.o.f	201
8.14	Tip displacement response of a cantilever to ramp input F.E. models with 2 d.o.f	202
8.15	Bending moment response of cantilever to ramp force input $x = 0.0$ F.E. models with 2 d.o.f	203
8.16	Tip displacement response of cantilever to ramp force input F.E models with 4 d.o.f	204
8.17	Bending moment response of cantilever to ramp force input F.E. models with 4 d.o.f	205
8.18	Bending moment response of cantilever to ramp input at $x = 0.0$ F.E. models with 6 d.o.f.	206

8.19	Mid-point deflection response of a CC beam to step force input	207
8.20	Bending moment response of a CC beam at $x = 0.0$ to step force input F.E. models with 2 and 3 d.o.f.	208
8.21	Bending moment response of a CC beam at $x = 0.0$ to step force input F.E. models with 6, 7 d.o.f	209
8.22	Mid-point displacement response of CS beam to half sine pulse input F.E. models with 3 d.o.f	210
8.23	Bending moment response of CS beam to half sine pulse input F.E. models with 3 d.o.f.	211
8.24	Mid-point displacement response of CS beam to half sine pulse input F.E. models with 7 d.o.f.	212
8.25	Bending moment response of CS beam to half sine pulse input F.E. models with 7 d.o.f	213
8.26	Mid-point displacement response of a damped CS beam to ramp force input	214
8.27	Mid-point moment response of a damped CS beam to ramp force input	215
8.28	Tip deflection response of a cantilever to step moment input F.E. models with 2 d.o.f	216
8.29	Bending moment response at $x = 0$ of a cantilever to step moment input F.E. models, with 2 d.o.f	217
8.30	Tip deflection response of cantilever to step moment input F.E. models with 4 d.o.f.	218
8.31	Bending moment response at $x = 0.0$ of cantilever to step moment input F.E. models, with 4 d.o.f	219
8.32	Tip deflection response of cantilever to step moment input F.E. models with 8 d.o.f.	220
8.33	Bending moment response at $x = 0.0$ of cantilever to step moment input F.E. models, with 8 d.o.f	221
8.34	Finite element discretisations for a simply supported square plate used in free vibration tests	226
8.35	Prediction of lowest natural frequency of SSSS plate (QR4 and QR8 elements)	227
8.36	Prediction of second natural frequency of SSSS plate (QR4 and QR8 elements)	227
8.37	Prediction of lowest natural frequency of SSSS plate (QR4, QR8, QD4 and QD8 elements)	228
8.38	Prediction of fifth natural frequency of SSSS plate (QR4, QR8, QD4 and QD8 elements)	228

8.39	Prediction of lowest natural frequency of CSCS plate (QR4 and QR8 elements)	229
8.40	Prediction of second natural frequency of CSCS plate (QR4 and QR8 elements)	229
8.41	Prediction of third natural frequency of CSCS plate (QR4 and QR8 elements)	230
8.42	Prediction of fourth natural frequency of CSCS plate (QR4 and QR8 elements)	230
8.43	Prediction of second natural frequency of CSCS plate (QR4, QR8, QD4 and QD8 elements)	231
8.44	Prediction of third natural frequency of CSCS Plate	231
8.45	Finite element meshes used for the analysis of a thin simply-supported plate under steady state sinusoidal loading	241
8.46	Deflection W , vs time; t at the centre of simply supported plate under uniform loading varying sinusoidally with time (QR4 and QD4 elements)	242
8.47	Deflection W , vs time; t at the centre of simply supported plate under uniform loading, varying sinusoidally with time (QR8 and QD8 elements)	243
8.48	Bending moment M_x , vs time; t at the centre of SSSS plate under uniform loading varying sinusoidally with time (QR4 and QD4 elements)	244
8.49	Bending moment M_x , vs time; t at the centre of SSSS plate under uniform loading varying sinusoidally with time (QR8 and QD8 elements)	245
8.50	Bending moment M_x , vs time; t at the centre of SSSS plate (QR8, QD8 and exact solutions)	246
8.51	Finite element meshes used for the analysis of a square plate under transient point load	247
8.52	Deflection W , vs time; t at the centre of SSSS plate under transient point load (QR4 element)	248
8.53	Deflection W , vs time; t at the centre of SSSS plate under transient point load (QR8 element)	249
8.54	Deflection W , vs time; t at the centre of SSSS plate under transient point load (QD4 and QD8 elements)	250
8.55	Bending moment, M_x , vs time; t at the centre of SSSS plate; transient point load (QR4 element)	251

8.56	Bending moment M_x , vs time; t at the centre of SSSS plate, transient point load (QR8 element)	252
8.57	Bending moment M_x , vs time; t at the centre of SSSS plate, transient point load (QD4 and QD8 elements)	253
8.58	Deflection W , vs time, t at the centre of clamped plate under transient point load (QD4 and QD8 elements)	254
8.59	Bending moment M_x , vs time, t at the centre of clamped plate under transient point load (QD4 and QD8 elements)	255
8.60	Deflection w , vs time, t at the centre of clamped plate under transient point load (QR4 and QD8 elements)	256
8.61	Bending moment M_x , vs time, t at the centre of clamped plate, transient point load (QR4 and QD8 elements)	257
8.62	Deflection W , vs time, t at the centre of clamped plate under transient point load (QR8 and QD8 elements)	258
8.63	Bending moment M_x , vs time, t at the centre of clamped plate under transient point load (QR8 and QD8 elements)	259
8.64	Simply supported square plate subjected to (a) step function input, and (b) impulsive input	260
8.65	Displacement response predicted with increasing time step size Δt ; Wilson θ method, $\theta = 1.4$ (Case a)	261
8.66	Displacement response predicted with increasing time step size Δt ; Wilson θ method, $\theta = 1.4$ (Case b)	262
8.67	Bending moment response predicted with increasing time step size Δt , Wilson θ method (case a)	263
8.68	Bending moment response predicted with increasing time step Δt , Wilson θ method (case b)	264
8.69	Displacement response by mode superposition method (a - 1 mode, b - 3 modes)	265
8.70	Bending moment response by mode superposition method (a - 1 mode, b - 3 modes)	266
8.71	Forced response of a SSSS plate by mode superposition method using 12 modes	267

LIST OF TABLES

<u>Table</u>	<u>Title</u>	<u>Page</u>
6.1	Mixed beam elements (C1 and C0 continuous elements)	111
6.2	Gauss quadrature points	132
6.3	Thin plate boundary conditions	137
8.1	% error in the first three natural frequencies of cantilever beam - C1 elements	191
8.2	% error in the first three natural frequencies of cantilever beam - C0 elements	191
8.3	Beam forced vibration problems	197
8.4	Eigenvalues of a square simply supported plate	232
8.5	Eigenvalues of a clamped-simply supported square plate	232
8.6	Vibration eigenvalues of square cantilever plate	233
8.7	Computer execution time at response analysis process by Wilson θ method ($\Delta t = .001$ sec)	238

NOTATIONS

The following is a list of the principal symbols used in this thesis. Rectangular matrices are indicated by [], and column vectors by { }. Overbars denote specified quantities. Dot over a symbol denotes derivative with respect to time.

a, b	dimensions of a plate in x and y directions, respectively
A	cross sectional area of a beam, plate middle plane area
B_n	jump term
$[B]$	operational matrix
c	damping coefficient
$[C]$	compliance matrix; damping matrix
D	flexural rigidity of a plate
$[D]$	elasticity matrix
d.o.f.	degree of freedom
E	elastic modulus
F_x, F_y, F_z	components of body forces per unit volume
$\{F\}_{nc}, \{F\}_c$	vectors of non-conservative and conservative body forces respectively
$[g], [h]$	mixed element matrices
G	shear modulus
h	plate thickness
$[G], [H]$	Overall mixed matrices
I	second moment of inertia
$[I]$	Identity matrix
$[J]$	Jacobian matrix
i, j, k	dummy subscripts
$[K]$	overall stiffness matrix
l	beam element length
L	length of a beam

$[l], [L_k]$	direction cosine transformation matrices
$[L]$	strain-displacement matrix
l, m, n	direction cosines
$[m]$	element mass matrix
$[M]$	overall mass matrix
M	Bending moment in a beam
M_x, M_y, M_{xy}	Bending and twisting moments in a plate
$\{M\}_e$	vector of nodal bending (and twisting) moments for element (e)
n, s	normal and tangential directions
N_1, N_2, \dots, N_8	Interpolation functions
p	distributed load on a beam or plate
P	concentrated load
$\{p\}_e$	distributed load intensities
$\{q\}$	principal coordinates vector
Q_x, Q_y, Q_n	shearing forces in a plate
$\{Q\}_e$	specific impressed forces
$\{r\}_e$	element consistent load vector
$\{R\}$	overall load vector
S, S_u, S_σ	General surface and surfaces where displacements and stresses are prescribed respectively
t	Time
T	kinetic energy
$\{T\}, T_x, T_y, T_z$	surface traction vector and components
T_0	kinetic energy density
$\{u\}, u, v, w$	displacement vector and components
$\{u\}_e$	element nodal displacement vector
$\{U\}, \{u\}_0$	overall displacement vectors
$\{\hat{U}\}$	mode shape vector
U, U^*	potential energy and complementary potential energy
V	volume
V_n	effective shearing force

W	transverse deflection
$\{w\}_e$	element nodal deflection vector
$\{w^*\}$	overall deflection vector
x, y, z	cartesian coordinates
T.D.O.F.	Total number of degrees of freedom in mixed models (displacements and moments).
α, β	angles, parameters
β_x, β_y	rotations
δ	variational operator
$\{\epsilon\}$	strain vector (includes both normal and shear strains)
ζ	modal damping ratio
$\lambda_1, \lambda_2, \dots, \lambda_9$	Lagrange multipliers
ν	poisson ratio
ξ, η	natural coordinates
π_p	potential energy functional
π_R, π^R	Reissner functional for static and dynamic analysis, respectively
ρ	mass per unit volume
ω	natural frequency
ω_D	damped natural frequency
$\{\sigma\}$	stress vector (includes both normal and shear stresses)

CHAPTER 1

INTRODUCTION

1. INTRODUCTION

The increased complexity of engineering structures, and demands for increased precision in design predictions has brought about a need for obtaining accurate and efficient models to represent the behaviour of the structure under various conditions of loading. Over the past two decades, the finite element technique has played an important role as a means of obtaining adequate solutions to problems which are otherwise intractable. In this work, the so-called "mixed formulation" is employed to develop finite element models for beam and plate type structures. Free and forced vibration problems are tackled and the efficiency of these models are ascertained with reference to the conventional displacement type formulation.

The finite element technique pioneered by Turner, Clough, Martin and Topp (1) in 1956, rapidly became a very popular means for the computer solution of complex problems, particularly in the field of structural engineering. In this method, an actual continuum is imagined divided into a series of elements which are connected at a finite number of points known as nodal points. This reduces the problem from one having an infinite number of degrees of freedom to one with a finite number. The approach then involves the approximation of a variational expression (functional) in terms of nodal variables of unknown magnitudes within each element. The extremization of the functional with respect to these unknowns yields the element characteristic matrices. The procedure is repeated for each element in turn and the overall structural properties are computed by adding contributions from individual elements. Finally, standard solution algorithms for discrete parameter systems are utilized to determine the unknowns. Various schemes have been offered which use either the displacements or the stresses or a combination of both as

the basic variables. Most practical elements are formulated by use of assumed displacement fields and the potential energy principle. In this method the displacements are chosen as the prime unknowns, with the stresses being determined from the calculated displacement field. The approximation involved is that the equilibrium equations are not satisfied exactly, but only in an integral sense. The continuity of displacements is required because of the method's dependence on the potential energy theorem. Alternatively it is possible to proceed with the stresses as the primary unknowns, an approach which is called "the equilibrium method". In this method, the minimum complementary energy principle is used. The assumed stress field is chosen so as to satisfy the equilibrium conditions within and across the element boundaries, and the compatibility conditions are satisfied in a 'mean'. A more general variational principle is that of Reissner (2), in which the primary field variables, are both displacements and stresses. The application of this principle results in finite element discretisations with nodal displacement and stress variables: these are classed as "mixed models". Since both compatibility and equilibrium are violated, on a strictly point by point basis, no preference is given to either displacement or stress fields. The mixed finite element models have received wide spread applications in problems dealing with bending components such as plates and shells. Mixed formulation permits the relaxation of the interelement compatibility conditions which are generally difficult to satisfy in problems dealing with flexural components. This allows the use of low order shape functions for displacements and moments which results in a decrease of computational effort.

The mixed element was first introduced by Herrmann (3), used in the solution of static plate bending problems and demonstrated the specific features of the mixed formulation in the finite element

method. Numerous other mixed plate elements have been presented, (4), (5), (6). Of particular interest are the works by Mota Soares (7), and Tsay and Reddy (8) who applied the isoparametric concept to mixed element formulation for the solution of free vibration problems. Excellent results were reported for this type of formulation.

In this thesis mixed models have been applied to beam and plate type structures to take advantage of the superiority of the mixed element over the displacement type element in this class of problems. The following problems are investigated:

- (i) Free vibration analysis (Mode shapes and frequencies).
- (ii) Forced vibration analysis (Time history response of displacements and moments).

A generalized version of Reissner principle has been derived which incorporates damping forces as non-conservative external forces.

The beam elements were examined by employing various interpolations for deflection and moment fields. It has been shown in this work that the element can favourably predict the natural modes and frequencies of the free vibration problem. The elements have also been tested in the forced vibration problems to determine the time history response of displacements and moments. The results compare favourably with known exact and displacement type element solutions. Only the two beam elements with (parabolic-linear) and (linear-parabolic) interpolations for displacement and moment, failed to produce meaningful results: in these elements the mixed matrix rank is of lower order than required. Redundant zero energy modes are produced which cannot be removed by application of kinematic boundary conditions. The success of the linear isoparametric element in Reference (7) prompted

the development of a new quadratic mixed element, to be used in the solution of thin plate problems. The element has eight nodes with four degrees of freedom at each node. (One deflection and three moments). The geometric, displacement and moment fields are assumed to vary parabolically within each element. Two computer programs were written which dealt with the free and forced vibration problems separately. The programs are capable of analyzing plates of variable thickness, and various loading and support conditions. Furthermore the plate may have orthotropic properties coinciding with the coordinate axes. The element can be applied to plates of arbitrary plan form with the proper transformation of the moments on the boundary. The transient solutions are obtained by either direct integration or modal analysis techniques.

In order to obtain a basis for the comparison of results, the following elements have also been applied and extended to the dynamic case.

- (i) 4-node and 8-node non-conforming displacement type elements, Ref. (9).
- (ii) Linear quadrilateral mixed element, (Ref. (7)).

Using the developed quadratic element, some free vibration problems are solved for plates with various edge conditions. The results from these are then compared with the exact solution (10) and those obtained using the elements named in (i) and (ii). Despite their simplicity, mixed elements yield reasonable (good) accuracy for the modal frequencies. It is also observed that, for a particular number of degrees of freedom the quadratic mixed element yields higher accuracy in the prediction of modal frequencies.

The transient displacements and moments are obtained for a simply supported square plate under dynamic loading. The results are presented graphically with the exact and other types of elements. The advantages gained in using the mixed models over the displacement type elements may be summed up as follows:

- (i) Mixed models calculate the transient displacements and moments with comparable degree of accuracy.
- (ii) The eigen problem is condensed to yield a set of equations in terms of nodal displacements only. The condensation of moment degrees of freedom is an exact operation whereas in displacement formulation some accuracy is lost in the reduction of the eigen problem.
- (iii) In engineering application, stress is often the quantity which is of prime interest. With a mixed model, this quantity is obtained directly through a simple matrix transformation procedure. With a displacement model, however, this quantity is obtained using a differentiation process from an approximate displacement field. This procedure is somewhat lengthy, time consuming and inherently yields reduced accuracy compared with the displacements, whereas the matrix multiplication required by mixed models offer a faster and more efficient way for the calculation of stresses. In forced vibration applications, where the stress field is to be calculated at incrementals of time, this effect is most noticeable.

CHAPTER 2

VARIATIONAL METHODS
IN
STRUCTURAL MECHANICS

2.1 INTRODUCTION

The variational or energy methods have long been used to study the behaviour of elastic structures as an alternative to the direct "vectorial" approach. Much of the interest and of the fascination of variational principles lies in the fact that a set of equations is replaced by the stationarity of a single functional in characterizing the dynamics of a system. The variational principles of an elasticity problem do, however, provide the governing equations of the problem as the stationary conditions of a functional and, in that sense, are equivalent to the governing equations. However, the variational approach has several advantages:

- (i) The functional subject to variation has usually a definite physical meaning and is invariant under coordinate transformation. Thus, the problem can be easily formulated in any coordinate system.
- (ii) When a problem of elasticity cannot be solved exactly, variational method provides a convenient means for obtaining approximate solutions. The accuracy of the solution is improved by increasing the number of degrees of freedom.
- (iii) A variational problem with subsidiary conditions may be transformed into an equivalent problem that can be solved more easily than the original. Transformation is achieved by the Lagrange multiplier technique. Thus a family of variational principles which are equivalent to each other are derived.

In this chapter, the basic equations which govern the distribution of stress and deformation in elastic bodies are briefly presented. Lagrange's principle will be introduced as the root of all modern variational principles, from which the principle of minimum potential energy and Hamilton's principle are derived. Other variational

principles such as minimum complementary potential energy may also be derived in a similar manner (11).

Generalized principles including that of Reissner's are summarised with reference to three dimensional dynamical problems. Some approximate methods of analysis, applicable to problems involving deformations and vibrations of elastic bodies are discussed. The following notations are used:

- (a) The matrix notation.
- (b) The generally employed scalar notation.
- (c) Cartesian coordinates (x,y,z) are used throughout.

2.2 BASIC RELATIONS

The formulation of the governing differential equations of elasticity is well established (12), (13). Thus, suppose a body deforms under the action of external and inertial forces, which are in equilibrium in accordance with d'Alembert's principle, and each point undergoes a small displacement represented by the components u, v, w parallel to the directions of the coordinate axes, Figure (2.1). The state of stress at a point of the body is defined by nine components of stress, Figure (2.2).

$$\begin{bmatrix} \sigma_x & \tau_{yx} & \tau_{zx} \\ & \sigma_y & \tau_{zy} \\ & & \sigma_z \end{bmatrix} \quad (2.1)$$

The governing equations may be summarized as follows:

2.2.1 Equations of dynamic equilibrium

The equations of equilibrium of an elementary particle $dx dy dz$ subject to body forces $\{F\}$, and undergoing accelerations $\frac{\partial^2}{\partial t^2} \begin{Bmatrix} u \\ v \\ w \end{Bmatrix}$ are:

$$\begin{aligned} \frac{\partial \sigma_x}{\partial x} + \frac{\partial \tau_{xy}}{\partial y} + \frac{\partial \tau_{xz}}{\partial z} + F_x &= \rho \frac{\partial^2 u}{\partial t^2}, \quad \tau_{xy} = \tau_{yx} \\ \frac{\partial \tau_{xy}}{\partial x} + \frac{\partial \sigma_y}{\partial y} + \frac{\partial \tau_{yz}}{\partial z} + F_y &= \rho \frac{\partial^2 v}{\partial t^2}, \quad \tau_{xz} = \tau_{zx} \\ \frac{\partial \tau_{xz}}{\partial x} + \frac{\partial \tau_{yz}}{\partial y} + \frac{\partial \sigma_z}{\partial z} + F_z &= \rho \frac{\partial^2 w}{\partial t^2}, \quad \tau_{yz} = \tau_{zy} \end{aligned} \quad (2.2)$$

2.2.2 Strain-displacement relations

The small displacement-strain relations are derived from purely geometrical considerations and are given by:

$$\begin{bmatrix} \epsilon_x \\ \epsilon_y \\ \epsilon_z \\ \gamma_{xy} \\ \gamma_{xz} \\ \gamma_{zy} \end{bmatrix} = \begin{bmatrix} \frac{\partial}{\partial x} & 0 & 0 \\ 0 & \frac{\partial}{\partial y} & 0 \\ 0 & 0 & \frac{\partial}{\partial z} \\ \frac{\partial}{\partial y} & \frac{\partial}{\partial x} & 0 \\ \frac{\partial}{\partial z} & 0 & \frac{\partial}{\partial x} \\ 0 & \frac{\partial}{\partial z} & \frac{\partial}{\partial y} \end{bmatrix} \begin{bmatrix} u \\ v \\ w \end{bmatrix} = [L] \{u\} \quad (2.3)$$

where $[L]$ is a matrix of differential operators.

2.2.3 Compatibility conditions

The necessary and sufficient conditions that the six strain components can be derived from three single-valued functions (equation

2.3) are called the compatibility conditions:

$$\begin{aligned}
 \frac{\partial^2 \epsilon_x}{\partial y^2} + \frac{\partial^2 \epsilon_y}{\partial x^2} &= \frac{\partial^2 \gamma_{xy}}{\partial x \partial y} ; & 2 \frac{\partial^2 \epsilon_x}{\partial y \partial z} &= \frac{\partial}{\partial x} \left(-\frac{\partial \gamma_{yz}}{\partial x} + \frac{\partial \gamma_{zx}}{\partial y} + \frac{\partial \gamma_{xy}}{\partial z} \right) \\
 \frac{\partial^2 \epsilon_y}{\partial z^2} + \frac{\partial^2 \epsilon_z}{\partial y^2} &= \frac{\partial^2 \gamma_{yz}}{\partial y \partial z} ; & 2 \frac{\partial^2 \epsilon_y}{\partial z \partial x} &= \frac{\partial}{\partial y} \left(\frac{\partial \gamma_{yz}}{\partial x} - \frac{\partial \gamma_{zx}}{\partial y} + \frac{\partial \gamma_{xy}}{\partial z} \right) \\
 \frac{\partial^2 \epsilon_z}{\partial x^2} + \frac{\partial^2 \epsilon_x}{\partial z^2} &= \frac{\partial^2 \gamma_{xz}}{\partial x \partial z} ; & 2 \frac{\partial^2 \epsilon_z}{\partial x \partial y} &= \frac{\partial}{\partial z} \left(\frac{\partial \gamma_{yz}}{\partial x} + \frac{\partial \gamma_{zx}}{\partial y} - \frac{\partial \gamma_{xy}}{\partial z} \right)
 \end{aligned} \tag{2.4}$$

2.2.4 Stress-strain relations

The stress-strain relations are given by the generalized Hooke's law and can be represented in matrix form as:

$$\begin{aligned}
 \text{and } \{\sigma\} &= [D] \{\epsilon\} \\
 \{\epsilon\} &= [D]^{-1} \{\sigma\} = [C] \{\sigma\}
 \end{aligned} \tag{2.5}$$

where $[C]$ is a matrix of material compliances, and

$$\{\sigma\}^t = [\sigma_x \quad \sigma_y \quad \sigma_z \quad \tau_{xy} \quad \tau_{yz} \quad \tau_{xz}] \tag{2.6}$$

$\{\epsilon\}$ is given by (2.3). In the most general case, the matrix $[C]$ can contain up to twenty-one independent constants. Such a material is said to be anisotropic. A material which has three planes of elastic symmetry may be defined by nine independent constants. Such a material is said to be orthotropic and if the three planes of elastic symmetry coincide with x-y, x-z, y-z planes then:

$$[C] = \begin{bmatrix} \frac{1}{E_x} & \frac{-\nu_{yx}}{E_y} & \frac{-\nu_{zx}}{E_z} & 0 & 0 & 0 \\ & \frac{1}{E_y} & \frac{-\nu_{zy}}{E_z} & 0 & 0 & 0 \\ & & \frac{1}{E_z} & 0 & 0 & 0 \\ & & & \frac{1}{G_{xy}} & 0 & 0 \\ & & & & \frac{1}{G_{yz}} & 0 \\ & & & & & \frac{1}{G_{xz}} \end{bmatrix} \quad (2.7)$$

For an isotropic material (which has complete elastic symmetry) only two independent constants are required, then

$$[C] = \frac{1}{E} \begin{bmatrix} 1 & -\nu & -\nu & 0 & 0 & 0 \\ -\nu & 1 & -\nu & 0 & 0 & 0 \\ -\nu & -\nu & 1 & 0 & 0 & 0 \\ 0 & 0 & 0 & 2(1+\nu) & 0 & 0 \\ 0 & 0 & 0 & 0 & 2(1+\nu) & 0 \\ 0 & 0 & 0 & 0 & 0 & 2(1+\nu) \end{bmatrix} \quad (2.8)$$

where E is the Young's modulus for the material and ν is its Poisson's ratio.

2.2.5 Boundary conditions

The boundary of a solid, S , may be subjected either to prescribed displacements or stresses. Equilibrium requirements must be met in the interior (Eqn.2.2) and part of the surface boundary S_σ where tractions are prescribed, that is

$$\begin{aligned} T_x &= \bar{T}_x \\ T_y &= \bar{T}_y \\ T_z &= \bar{T}_z \end{aligned} \quad \text{on } S_\sigma \quad (2.9)$$

where $\{\bar{T}\}$ denote prescribed values of tractions. The components of surface traction T , Fig. (2.3), are given by:

$$\begin{aligned} T_x &= \sigma_x \cdot l + \tau_{xy} \cdot m + \tau_{xz} \cdot n \\ T_y &= \tau_{yx} \cdot l + \sigma_y \cdot m + \tau_{yz} \cdot n \\ T_z &= \tau_{zx} \cdot l + \tau_{yz} \cdot m + \sigma_z \cdot n \end{aligned} \quad (2.10)$$

l, m, n being the direction cosines of the unit vector normal to the boundary. On the other hand, displacements are prescribed on part S_u of the boundary and the geometrical conditions given by:

$$u = \bar{u}, \quad v = \bar{v}, \quad w = \bar{w} \quad \text{on } S_u \quad (2.11)$$

The whole surface S is therefore the sum of S_σ and S_u that is:

$$S = S_\sigma + S_u$$

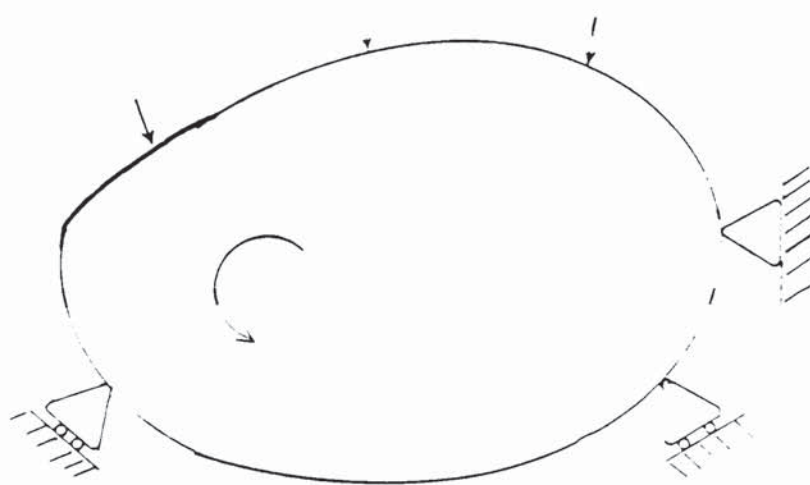


Fig 2.1 Elastic body subject to external forces.

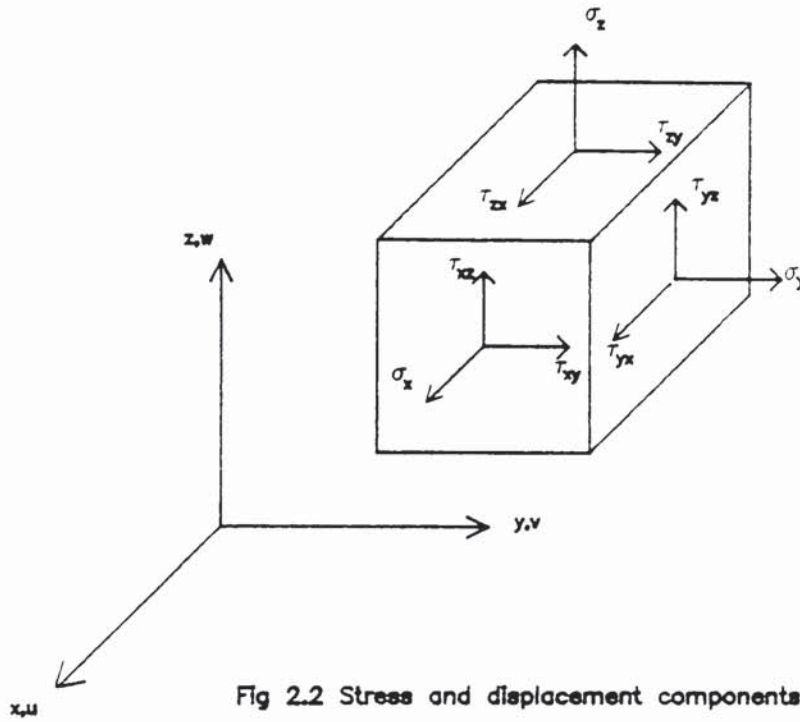


Fig 2.2 Stress and displacement components.

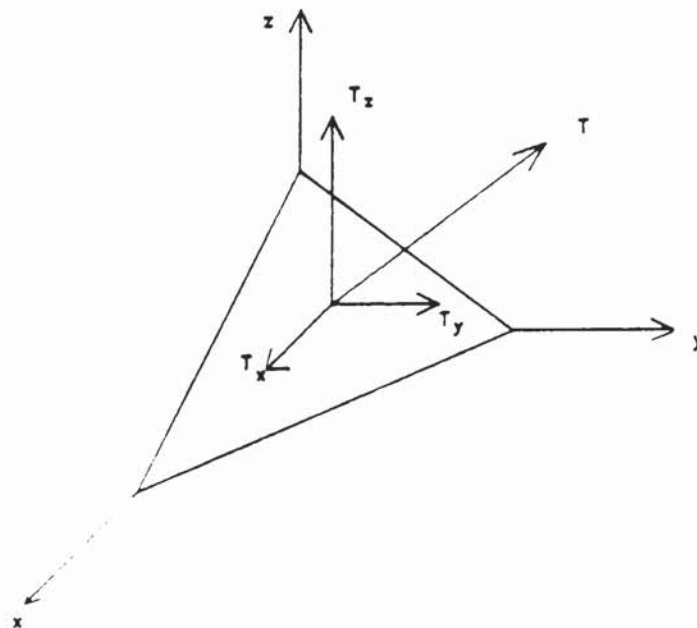


Fig 2.3 Boundary conditions.

2.3 CLASSICAL VARIATIONAL PRINCIPLES

The above summary has implied the use of Newton's laws of motion and geometry. The problem may be alternatively formulated from an integral point of view by means of d'Alembert's principle. Using the concept of variations for the interpretation of problems in mechanics. Lagrange (1736-1813) reformulated d'Alembert's principle thus yielding "Lagrange's principle". In its most general form, this principle may be stated as:

$$\int (\{d Q\}_e^t - \{\ddot{u}\}^t dm) \{\delta u\} = 0, \quad (2.12)$$

where $\{Q\}_e$ are the impressed forces, m is the mass of the mechanical system and $\{u\}$ are its displacements. Lagrange's principle may be considered as the starting point for developing the more general variational principles which are freed from some or all restrictions. Thus, combining (2.12) with the Lagrange relaxation principle, one will be able to tackle any problem in mechanics in terms of a variational principle. Based on (2.12), some useful variational principles have been developed (11) which deal with problems in structural mechanics.

This section describes in brief the classical variational principles applicable to non-conservative systems. A knowledge of this is necessary to enable the understanding of the work described in the later sections.

2.3.1 Lagrange's principle for elasticity problems

For problems in structural engineering, Lagrange's principle, Equation (2.12) must be reformulated in terms of internal and external forces for an elastic, continuous body. Let V be the volume of the body. Then, set

$$\{dQ\}_e = \{Q\}_e dV, \quad dm = \rho dV$$

where $\{Q\}_e$ are the specific impressed forces and ρ is the mass density of the body. The impressed forces may be written as:

$$\{Q\}_e = \{Q\}_{ext} + \{Q\}_{int} \quad (2.13)$$

where $\{Q\}_{ext}$ and $\{Q\}_{int}$ are the external and internal forces respectively. Therefore, (2.12), changes into:

$$\int_V \{Q\}_{ext}^t \{\delta u\} dV + \int_V \{Q\}_{int}^t \{\delta u\} dV - \int_V \rho \{\ddot{u}\}^t \{\delta u\} dV = 0 \quad (2.14)$$

In (2.14) variations $\{\delta u\}$, the so-called virtual distortions, must be small and since the reactions have not been taken into account, they must be restricted to such ones that satisfy the prescribed kinematical constraints imposed on the body at the points of application of the reactions.

The external forces $\{Q\}_{ext}$ consist of $\{F\}$, (body forces per unit volume), and $\{T\}$, (distributed surface tractions per unit surface).

Hence,

$$\begin{aligned} \int_V \{Q\}_{ext}^t \{\delta u\} dV &= \int_V (F_x \delta u + F_y \delta v + F_z \delta w) dV \\ &+ \int_S (T_x \delta u + T_y \delta v + T_z \delta w) dS - \delta U_{ext} \end{aligned} \quad (2.15)$$

where U_{ext} is the potential of the external forces as far as these are conservative. Now, the surface S of the body consists of a part S_σ on which surface loads $\{T\} = \{\bar{T}\}$ are prescribed, and of a part S_u on which displacements $\{u\} = \{\bar{u}\}$ are prescribed. Then

$$\int_S \{T\}^t \{\delta u\} dS = \int_{S_\sigma} \{\bar{T}\}^t \{\delta u\} dS, \quad (2.16)$$

Since $\{\delta u\} = 0$ on S_u . Therefore with (2.16) in (2.15), we have:

$$\int_V \{Q\}_{\text{ext}}^t \{\delta u\} dV = \int_V \{F\}_{\text{nc}}^t \{\delta u\} dV + \int_{S_\sigma} \{\bar{T}\}_{\text{nc}}^t \{\delta u\} dS - \delta U_{\text{ext}} \quad (2.17)$$

The integral involving the internal forces is given by:

$$\int_V \{Q\}_{\text{int}}^t \{\delta u\} dV = - \int_V (\sigma_x \delta \epsilon_x + \sigma_y \delta \epsilon_y + \dots) dV = - \int_V \{\sigma\}^t \{\delta \epsilon\} dV \quad (2.18)$$

where $\{\sigma\}$ and $\{\epsilon\}$ denote the vectors of stress and strain components respectively. Hooke's law, equation (2.5) is given by:

$$\{\sigma\} = [D] \{\epsilon\} \quad (2.5)$$

Thus

$$\{\sigma\}^t \{\delta \epsilon\} = \{\epsilon\}^t [D] \{\delta \epsilon\} = \delta \left[\frac{1}{2} \{\epsilon\}^t [D] \{\epsilon\} \right] = \delta U_0 \quad (2.19)$$

The quantity

$$U_0 = \frac{1}{2} \{\epsilon\}^t [D] \{\epsilon\} \quad (2.20)$$

is the potential (strain) energy density of the internal forces.

For isotropic elastic material, Equation (2.20) may be expanded as:

$$U_0 = \frac{E}{2(1+\nu)} (\epsilon_x^2 + \epsilon_y^2 + \epsilon_z^2 + \frac{1}{2} (\gamma_{xy}^2 + \gamma_{xz}^2 + \gamma_{yz}^2)) + \frac{E\nu}{2(1+\nu)(1-2\nu)} (\epsilon_x + \epsilon_y + \epsilon_z)^2 \quad (2.21)$$

which may also be expressed in terms of displacement components (u, v, w) by using the strain-displacement relations (2.3), thus

$$U_0(u, v, w) = \frac{E}{2(1+\nu)} \left(\left(\frac{\partial u}{\partial x} \right)^2 + \left(\frac{\partial v}{\partial y} \right)^2 + \left(\frac{\partial w}{\partial z} \right)^2 \right) + \frac{E\nu}{2(1+\nu)(1-2\nu)} \left(\frac{\partial u}{\partial x} + \frac{\partial v}{\partial y} + \frac{\partial w}{\partial z} \right)^2 \\ + \frac{E}{4(1+\nu)} \left(\left(\frac{\partial v}{\partial z} + \frac{\partial w}{\partial y} \right)^2 + \left(\frac{\partial w}{\partial x} + \frac{\partial u}{\partial z} \right)^2 + \left(\frac{\partial u}{\partial y} + \frac{\partial v}{\partial x} \right)^2 \right) \quad (2.22)$$

Now using (2.19) in (2.18) yields:

$$\int_V \{Q\}_{int}^t \{\delta u\} dV = - \int_V \delta U_0 dV = -\delta \int_V U_0 dV = -\delta U_{int} \quad (2.23)$$

where U_{int} is called the potential energy of the internal forces.

Substituting (2.17) and (2.23), back into (2.14) yields:

$$\int_V \{F\}_{nc}^t \{\delta u\} dV + \int_{S_\sigma} \{\bar{T}\}_{nc}^t \{\delta u\} dS - \delta U_{ext} - \delta U_{int} - \int_V \rho \{\ddot{u}\}^t \{\delta u\} dV = 0 \quad (2.24)$$

This expression represents Lagrange's principle for the elastic continuous body and is useful in applications to elasticity problems in which external forces may not be derivable from potential functions.

2.3.2 Minimum potential energy principle

In this section minimum potential energy principle will be derived from Lagrange's principle (Eqn. 2.24). The following restrictive assumptions are made:

- (i) The problem is a static one. Then,

$$\{\ddot{u}\} = 0 \quad (2.25)$$

- (ii) The problem is a conservative one. In other words the external forces possess a potential. Then,

$$\int_V \{F\}_{nc}^t \{\delta u\} dV + \int_{S_\sigma} \{\bar{T}\}_{nc}^t \{\delta u\} dS = 0 \quad (2.26)$$

Under the above assumptions, Lagrange's principle (2.24) changes into:

$$- \delta (U_{ext} + U_{int}) = 0 \quad (2.27)$$

Let

$$\pi_p = U_{int} + U_{ext} = \int_V U_0 dV - \int_V \{F\}_c^t \{u\} dV - \int_{S_\sigma} \{\bar{T}\}_c^t \{u\} dS \quad (2.28)$$

be the total potential energy of the elastic body where now both $\{F\}_c$ and $\{\bar{T}\}_c$ are conservative forces, then

$$\delta \pi_p = 0, \quad \pi_p = \text{minimum} \quad (2.29)$$

It can be proved that U_0 is a positive definite quantity (12). With (2.29), one has obtained the minimum potential energy principle which may be stated as follows:

For a kinematically admissible displacement field related to a stress field satisfying the equilibrium conditions, the total potential energy assumes a minimum value as compared to values resulting from any other admissible displacement field.

2.3.3 Hamilton's principle

Hamilton's principle may be derived from the general Lagrange's principle. For an elastic body the principle is given by Equation (2.24):

$$\int_V \{F\}_{nc}^t \{\delta u\} dV + \int_{S_\sigma} \{T\}_{nc}^t \{\delta u\} dS - \delta U_{ext} - \delta U_{int} - \int_V \rho \{\ddot{u}\}^t \{\delta u\} dV = 0 \quad (2.24)$$

As before it is required that $\{\delta u\}$ be consistent with the prescribed constraint conditions. Now however, the virtual distortion is

further restricted by demanding that the variations $\{\delta u\}$ be zero at all points in the body at two arbitrary instant of time t_1 and t_2 , that is:

$$\{\delta u\}_{\text{at } t_1} = \{\delta u\}_{\text{at } t_2} = 0 \quad (2.30)$$

Integrating (2.24) with respect to t results in

$$\int_{t_1}^{t_2} \left[\int_V \{F\}_{nc}^t \{\delta u\} dV + \int_{S_\sigma} \{\bar{T}\}_{nc}^t \{\delta u\} dS - \delta U_{\text{ext}} - \delta U_{\text{int}} \right] dt - \int_{t_1}^{t_2} \left[\int_V \rho \{\ddot{u}\}^t \{\delta u\} dV \right] dt = 0 \quad (2.31)$$

Now since

$$\int_{t_1}^{t_2} \rho \{\ddot{u}\}^t \{\delta u\} dt = \left[\rho \{\dot{u}\}^t \{\delta u\} \right]_{t_1}^{t_2} - \int_{t_1}^{t_2} \rho \{\dot{u}\}^t \{\delta \dot{u}\} dt \quad (2.32)$$

and since (2.30) shall hold true, (2.32) changes into:

$$\int_{t_1}^{t_2} \rho \{\ddot{u}\}^t \{\delta u\} dt = - \int_{t_1}^{t_2} \rho \{\dot{u}\}^t \{\delta \dot{u}\} dt \quad (2.33)$$

with the kinetic energy density defined as:

$$T_0 = \frac{1}{2} \rho \{\dot{u}\}^t \{\dot{u}\} \quad (2.34)$$

$$\text{then } \delta T_0 = \rho \{\dot{u}\}^t \{\delta \dot{u}\} \quad (2.35)$$

and consequently (2.31) becomes equal to

$$\int_{t_1}^{t_2} \left[\int_V \{F\}_{nc}^t \{\delta u\} dV + \int_{S_\sigma} \{\bar{T}\}_{nc}^t \{\delta u\} dS - \delta U_{int} - \delta U_{ext} \right] dt + \int_{t_1}^{t_2} \delta T dt = 0 \quad (2.36)$$

where T is the kinetic energy of the system.

Equation (2.36) is a general statement of Hamilton's principle for elasticity problems with non-conservative external forces. It may be re-written as follows:

$$\delta \int_{t_1}^{t_2} (T - U_{int} - U_{ext}) dt = - \int_{t_1}^{t_2} \left[\int_V \{F\}_{nc}^t \{\delta u\} dV + \int_{S_\sigma} \{\bar{T}\}_{nc}^t \{\delta u\} dS \right] dt \neq 0 \quad (2.36a)$$

which means $(T - U_{int} - U_{ext})$ is not even stationary. For many mechanical systems, the dissipative forces can be idealised by simple viscous damping forces $\{F_d\} = -c\{\dot{u}\}$, then equation (2.36) reads as follows:

$$\delta \int_{t_1}^{t_2} (T - U_{int} - U_{ext}) dt - \int_{t_1}^{t_2} \int_V c\{\dot{u}\}^t \{\delta u\} dV dt = 0 \quad (2.36b)$$

For conservative systems equation (2.26) holds and (2.36) changes into:

$$\delta \int_{t_1}^{t_2} (T - U_{ext} - U_{int}) dt = 0 \quad (2.37)$$

or simply:
$$\delta \int_{t_1}^{t_2} (T - \pi_p) dt = 0 \quad (2.38)$$

where $\pi_p = U_{ext} + U_{int}$ is the total potential energy of the system.

Equation (2.38) represents Hamilton's classical principle and may be applied to an elastic body subjected to external conservative forces.

2.4 MULTI-FIELD VARIATIONAL PRINCIPLES - LAGRANGE'S RELAXATION PRINCIPLE

As mentioned earlier in section 2.1, variational principles may be used conveniently as a means of constructing approximate solutions to boundary value problems in linear elasticity. The crucial point in applying it is the selection of appropriate coordinate functions which should satisfy certain restrictive conditions. The principle of minimum potential energy for instance requires that the displacement field be a continuous function of position and also satisfy the geometric boundary conditions of the problem under investigation. In practice it is often desirable to relax these requirements and thus widen the function space from which coordinate functions are chosen for comparison. This may be achieved by modifying the classical variational principles so that all continuity and boundary conditions become natural ones. From the point of view of mechanics it means applying Lagrange's relaxation principle. In the next section, it will be shown how to modify the minimum potential energy and thus obtain the generalized potential energy principle. Lagrange's relaxation principle introduces new fields in the modified variational statement and thus increases the number of independent variables subject to variations.

2.4.1 The Generalization of Minimum Potential Energy Principle

In the development of the minimum potential energy principle, the assumption is made that the strains are related to displacements according to (2.3), i.e.

$$\{\epsilon\} - [L] \{u\} = \{0\} \quad \text{in the region} \quad (2.3)$$

and that

$$\{u\} - \{\bar{u}\} = 0 \quad \text{on the boundary } S_u \quad (2.11)$$

Restrictions on the conditions of compatibility (2.3) and the geometric boundary conditions (2.11) may be removed by means of the Lagrange multiplier technique (see references (14),(15)). Thus the functional in (2.28) is modified to yield:

$$\begin{aligned} \pi_g &= \int U_0 dV - \int_V \{F\}_C^t \{u\} dV - \int_{S_\sigma} \{\bar{T}\}_C^t \{u\} dS \\ &- \int_V \left[\left(\epsilon_x - \frac{\partial u}{\partial x} \right) \lambda_1 + \dots + \left(\gamma_{xz} - \frac{\partial w}{\partial x} - \frac{\partial u}{\partial z} \right) \lambda_6 \right] dV \quad (2.39) \\ &- \int_{S_u} \left[(u - \bar{u}) \lambda_7 + (v - \bar{v}) \lambda_8 + (w - \bar{w}) \lambda_9 \right] dS \end{aligned}$$

where λ_1 to λ_9 are the corresponding multipliers. The modified principle is therefore stated as follows:

$$\delta \pi_g = 0 \quad (2.40)$$

with no auxiliary constraint conditions.

Now it may be shown that the above principle provides, indeed, the differential equation of the problem under consideration and in addition all the boundary conditions, as natural conditions of the variational principle (2.40).

The independent quantities subject to variations in the functional (2.39) are: six strain components, three displacements and nine Lagrange multipliers $\lambda_1, \dots, \lambda_6$ and $(\lambda_7, \lambda_8, \lambda_9)$. Performing the variation with respect to these quantities, it is observed that:

$$\begin{aligned}
\delta \pi_g = & \int_V \left[\left(\frac{\partial U_0}{\partial \epsilon_x} \delta \epsilon_x + \dots + \frac{\partial U_0}{\partial \gamma_{xz}} \delta \gamma_{xz} \right) - \{ \bar{F} \}^t \{ \delta u \} \right] dV - \int_{S_\sigma} \{ \bar{T} \}^t \{ \delta u \} dS \\
& - \int_V \left[\left(\epsilon_x - \frac{\partial u}{\partial x} \right) \delta \lambda_1 + \dots + \left(\gamma_{xz} - \frac{\partial w}{\partial x} - \frac{\partial u}{\partial z} \right) \delta \lambda_6 \right] dV \quad (2.41) \\
& - \int_{S_u} \left[(u - \bar{u}) \delta \lambda_7 + (v - \bar{v}) \delta \lambda_8 + (w - \bar{w}) \delta \lambda_9 \right] dS \\
& - \int_V \left[\left(\delta \epsilon_x - \frac{\partial (\delta u)}{\partial x} \right) \lambda_1 + \dots + \left(\delta \gamma_{xz} - \frac{\partial (\delta w)}{\partial x} - \frac{\partial (\delta u)}{\partial z} \right) \lambda_6 \right] dV \\
& - \int_{S_u} \left[\delta u \lambda_7 + \delta v \lambda_8 + \delta w \lambda_9 \right] dS = 0
\end{aligned}$$

Integrating by parts, where appropriate using Green's formula, and rearranging the terms yields:

$$\begin{aligned}
\delta \pi_g = & \int_V \left[\left(\frac{\partial U_0}{\partial \epsilon_x} - \lambda_1 \right) \delta \epsilon_x + \dots + \left(\frac{\partial U_0}{\partial \gamma_{xz}} - \lambda_6 \right) \delta \gamma_{xz} \right] dV \\
& - \int_V \left[\left(\frac{\partial \lambda_1}{\partial x} + \frac{\partial \lambda_4}{\partial y} + \frac{\partial \lambda_6}{\partial z} + F_x \right) \delta u + (\dots) \delta v + (\dots) \delta w \right] dV \quad (2.42) \\
& + \int_{S_\sigma} \left[(T_x - \bar{T}_x) \delta u + (T_y - \bar{T}_y) \delta v + (T_z - \bar{T}_z) \delta w \right] dS + \\
& + \int_{S_u} \left[(T_x - \lambda_7) \delta u + (\dots) \delta v + (\dots) \delta w \right] dS \\
& - \int_V \left[\left(\epsilon_x - \frac{\partial u}{\partial x} \right) \delta \lambda_1 + \dots + \left(\gamma_{xz} - \frac{\partial w}{\partial x} - \frac{\partial u}{\partial z} \right) \delta \lambda_6 \right] dV \\
& - \int_{S_u} \left[(u - \bar{u}) \delta \lambda_7 + (\dots) \delta \lambda_8 + (w - \bar{w}) \delta \lambda_9 \right] dS = 0
\end{aligned}$$

The conditions for π_g to be stationary are, then

$$\frac{\partial U_0}{\partial \epsilon_x} = \lambda_1 \dots; \quad \frac{\partial U_0}{\partial \gamma_{xz}} = \lambda_6 \quad \text{in } V \quad (2.43)$$

$$T_x = \lambda_7; \quad T_y = \lambda_8; \quad T_z = \lambda_9 \quad \text{on } S_u \quad (2.44)$$

$$\frac{\partial \lambda_1}{\partial x} + \frac{\partial \lambda_4}{\partial y} + \frac{\partial \lambda_6}{\partial z} + F_x = 0; \quad \text{etc.} \quad \text{in } V \quad (2.45)$$

$$T_x = \bar{T}_x; \quad T_y = \bar{T}_y; \quad T_z = \bar{T}_z \quad \text{on } S_\sigma \quad (2.46)$$

$$\epsilon_x = \frac{\partial u}{\partial x}; \quad \dots; \quad \gamma_{xz} = \frac{\partial w}{\partial x} + \frac{\partial u}{\partial z} \quad \text{in } V \quad (2.47)$$

$$u = \bar{u}; \quad v = \bar{v}; \quad w = \bar{w} \quad \text{on } S_u \quad (2.48)$$

These are the so-called Euler-Lagrange equations of the Principle (2.40). The last two equations give the constraints satisfaction and from the others it is seen that the Lagrange multipliers may be identified as follows:

$$\lambda_1 = \sigma_x, \quad \lambda_2 = \sigma_y, \dots, \quad \lambda_6 = \tau_{xz} \quad (2.49)$$

and

$$\lambda_7 = T_x, \quad \lambda_8 = T_y, \quad \lambda_9 = T_z \quad (2.50)$$

with this identification the variational principle is known as the Hu-Washizu principle and can be stated as a stationary requirement for the function (2.51).

$$\begin{aligned} \pi_{HW} = & \int_V U_0 dV - \int_V \{F\}_c^t \{u\} dV - \int_{S_\sigma} \{\bar{T}\}_c^t \{u\} dS - \int_V \{\sigma\}^t (\{\epsilon\} - [L]\{u\}) dV \\ & - \int_{S_u} \{T\}^t (\{u\} - \{\bar{u}\}) dS \end{aligned} \quad (2.51)$$

The independent quantities subject to variation in the functional (2.51) consist of the stresses $\{\sigma\}$, strains $\{\epsilon\}$ and displacements

{u} with no subsidiary conditions. On taking variations with respect to these quantities, it is found that the stationary conditions are given by Equation (2.43) through (2.48), with λ 's replaced by stresses { σ } and {T} as in Equations (2.49), (2.50) (see reference (14)).

2.4.2 E. Reissner's principle

For a linear elastic solid, the so-called complementary strain energy density (U_0^*) is defined as

$$U_0^* = \frac{1}{2} \{\sigma\}^t [C] \{\sigma\} \quad (2.52)$$

thus it can be easily shown that

$$U_0 = \{\sigma\}^t \{\epsilon\} - U_0^* \quad (2.53)$$

holds true.

Substituting from (2.53) into (2.51), the strain components can be eliminated from the functional (2.51) to yield another principle known as Reissner's Principle (2).

Then,

$$\begin{aligned} \pi_R = & - \int_V U_0^* dV + \int_V \{\sigma\}^t [L] \{u\} dV - \int_V \{F\}_C^t \{u\} dV - \int_{S_\sigma} \{T\}_C^t \{u\} dS \\ & - \int_{S_u} \{T\}^t (\{u\} - \{\bar{u}\}) dS \end{aligned} \quad (2.54)$$

where now only { σ } and {u} are independent variables, with no subsidiary conditions. Carrying out the variations we get:

$$\begin{aligned}
\delta \pi_R &= \int_V \left[\{\delta \sigma\}^t [L] \{u\} + \{\sigma\}^t [L] \{\delta u\} - \frac{\partial U_0^*}{\partial \{\sigma\}} \{\delta \sigma\} \right] dV \\
&- \int_V \{F\}^t \{\delta w\} dV - \int_{S_\sigma} \{\bar{T}\}^t \{\delta u\} dS - \int_{S_u} \{\delta T\}^t (\{u\} - \{\bar{u}\}) dS \\
&- \int_{S_u} \{T\}^t \{\delta u\} dS \tag{2.55}
\end{aligned}$$

The second term on the right of the above equation may be recast as follows (making use of the integral theorem of Gauss).

$$\begin{aligned}
\int_V \{\sigma\}^t [L] \{\delta u\} dV &= \int_{S = S_\sigma + S_u} \left[(\sigma_x \cdot l + \tau_{xy} \cdot m + \tau_{xz} \cdot n) \delta u + (\dots) \delta v \right. \\
&+ \left. (\tau_{xz} \cdot l + \tau_{yz} \cdot m + \sigma_z \cdot n) \delta w \right] dS \tag{2.56} \\
&- \int_V \left[\left(\frac{\partial \sigma_x}{\partial x} + \frac{\partial \tau_{xy}}{\partial y} + \frac{\partial \tau_{xz}}{\partial z} \right) \delta u + (\dots) \delta v + \left(\frac{\partial \tau_{xz}}{\partial x} + \frac{\partial \tau_{yz}}{\partial y} + \frac{\partial \sigma_z}{\partial z} \right) \delta w \right] dV
\end{aligned}$$

substituting equation (2.56) into (2.55) yields:

$$\begin{aligned}
\delta \pi_R &= - \int_V \left[\left(\frac{\partial \sigma_x}{\partial x} + \frac{\partial \tau_{xy}}{\partial y} + \frac{\partial \tau_{xz}}{\partial z} + F_x \right) \delta u + (\dots) \delta v + (\dots) \delta w \right] dV \\
&- \int_V \left[\left(\frac{\partial U_0^*}{\partial \sigma_x} - \frac{\partial u}{\partial x} \right) \delta \sigma_x + \dots + \left(\frac{\partial U_0^*}{\partial \tau_{xz}} - \frac{\partial u}{\partial z} - \frac{\partial w}{\partial x} \right) \delta \tau_{xz} \right] dV \tag{2.57} \\
&- \int_{S_\sigma} \{\delta u\}^t (\{T\} - \{\bar{T}\}) dS - \int_{S_u} \{\delta T\}^t (\{u\} - \{\bar{u}\}) dS
\end{aligned}$$

with $\{\delta u\}$ and $\{\delta \sigma\}$ as arbitrary independent quantities, the following relations are obtained as Euler equations and natural boundary conditions of the functional (2.54).

- (a) - The equations of equilibrium in V
- (b) - The strain-displacement relations in V
- (c) - The requirements that $T_x = \bar{T}_x$, etc. on S_σ
- (d) - The requirements that $u = \bar{u}$, etc. on S_u

2.4.3 Reissner's principle - extension to dynamical problems

Reissner's principle, equation (2.54), is applicable to static problems in which all forces, internal and external ones are derivable from a potential. In this section the principle is modified to the case of dynamic problems with non-conservative damping forces. To the author's knowledge this has not been attempted before.

Hamilton's principle, equation (2.36) may be modified in a manner similar to section (2.4.1) for static problems. Thus the dynamical version of Reissner's principle is obtained. Assuming that all the external forces are conservative and derivable from potential functions, the new Principle may be written as follows:

$$\delta \int_{t_1}^{t_2} \pi_R^D dt = \delta \int_{t_1}^{t_2} \left[\int_V (-T_0 - U_0^* + \{\sigma\}^t [L] \{u\}) dV - \int_V \{F\}_C^t \{u\} dV - \int_{S_\sigma} \{\bar{T}\}_C^t \{u\} dS - \int_{S_u} \{T\}^t (\{u\} - \{\bar{u}\}) dS \right] dt = 0 \quad (2.58)$$

where

$$\pi_R^D = \pi_R - T$$

may be referred to as Reissner's dynamical functional. Carrying out the variations indicated in (2.58), we find that, as in the static case, the stationary conditions are the differential equations of dynamic equilibrium, strain-displacement relations and all mechanical and geometrical boundary conditions. Reissner's principle is thus seen

to give equal emphasis to the conditions of equilibrium and compatibility since both appear as Euler-Lagrange equations of the functional π_R .

When damping forces are also included, Hamilton's principle equation (2.36b) may be generalized by means of Lagrange multipliers, thus generalized Reissner's principle is obtained which may be stated as follows:

$$\delta \int_{t_1}^{t_2} \left[\int_V (-T_0 - U_0^* + \{\sigma\}^t [L] \{u\}) dV - \int_V \{F\}_c^t \{u\} dV - \int_{S_\sigma} \{\bar{T}\}_c^t \{u\} dS - \int_{S_u} \{T\}^t (\{u\} - \{\bar{u}\}) dS \right] dt + \int_{t_1}^{t_2} \int_V c \{\dot{u}\}^t \{\delta u\} dV dt = 0 \quad (2.59)$$

2.5 APPROXIMATE METHODS

Problems of any complexity are governed by a set of simultaneous differential equations stemming from Newton's laws of motion. These equations can be regarded as the Euler-Lagrange equations of a functional with one or several dependent variables. The principal approach in approximate methods is to work with the functional for the purpose of finding approximate solution to the corresponding differential equations. In this connection, the variational methods of Ritz (16), Galerkin (16) and Kantorovich (17) have been extensively used, with the displacement finite element method becoming increasingly applied in recent years. In the next section, Rayleigh-Ritz method is outlined. The finite element method which may be interpreted as a piece-wise Rayleigh-Ritz method will be described in detail in the following chapters.

2.5.1 Rayleigh-Ritz method

The most notable approximate procedure is the Rayleigh-Ritz method (16), which was originally developed for use with the potential energy functional. In this method the structure's displacement field is approximated by functions which contain a finite number of independent coefficients. The assumed functions are chosen to satisfy the kinematic boundary conditions, but they need not satisfy the mechanical boundary conditions (ones involving forces and moments). The following displacement field components are thus employed for expressing the total potential energy.

$$\begin{aligned} u &= u_0(x,y,z) + \sum_{i=1}^n a_i \psi_i(x,y,z) \\ v &= v_0(x,y,z) + \sum_{i=1}^n b_i \psi_i(x,y,z) \end{aligned} \quad (2.60)$$

continued:

$$w = \gamma_0(x,y,z) + \sum_{i=1}^n c_i \gamma_i(x,y,z) \quad (2.60)$$

where φ_0 , ψ_0 and γ_0 satisfy the kinematic boundary conditions on S_u while the remaining functions are zero there. The scheme for the Ritz method is to choose the values of the unknown coefficients so as to minimize the total potential energy. Thus substituting equation (2.60) into the potential energy functional equation (2.28), and performance of the integration results in $\pi_p = \pi_p(a_i, b_i, c_i)$ $i=1,2,\dots,n$ then for a stationary π_p , $\delta\pi_p = 0$ which is equivalent to

$$\frac{\partial \pi_p}{\partial a_i} = 0$$

$$\frac{\partial \pi_p}{\partial b_i} = 0 \quad i = 1, 2, \dots, n \quad (2.61)$$

$$\frac{\partial \pi_p}{\partial c_i} = 0$$

This process yields $3n$ simultaneous algebraic equations in the undetermined coefficients a_i , b_i , c_i . For dynamical problems the Rayleigh-Ritz procedure can be used in conjunction with Hamilton's principle (16). Thus the equations of motion are obtained which may be expressed in matrix notation as

$$[K] \{a\} + [M] \{\ddot{a}\} = \{R\} \quad (2.62)$$

where $\{a\}$ and $\{R\}$ are the generalized coordinates and generalized forces respectively. The response is obtained by solving equation (2.62), using an appropriate direct integration or mode superposition method (see section 4.6).

For free vibration $\{R\} = 0$ in (2.62) and, with harmonic motion:

$$([K] - \omega^2[M]) \{a\} = \{0\} \quad (2.63)$$

which may be solved by standard eigen value solution routines (18).

The Rayleigh-Ritz method may also be applied with the Reissner's functional. Now forces and displacements are independently represented by shape functions satisfying the "forced" boundary conditions (16), and the constants are found as before by rendering the functional stationary.

2.5.2 The finite element method

The finite element method pioneered by Turner et al (1) and Clough (19), is the most significant development in structural analysis in recent years. With the development of powerful digital computers the f.e.m. has gained considerable popularity and become a very important tool in the analysis of structural problems and in the broad field of continuum mechanics (20), (21). The basic concept of the method, when applied to problems of structural analysis, is that a continuum (structure) can be modelled analytically by its subdivision into regions (the finite elements) in each of which the behaviour is described by a separate set of assumed functions representing the stresses or displacements in that region. Then it is possible by the use of the appropriate energy functional and a procedure similar to the Rayleigh-Ritz technique to derive an element matrix equation which may have generalized displacements, stresses or both, at the nodal points, as unknowns to be evaluated.

The Rayleigh-Ritz technique is applied to each element in turn

and the overall problem is examined by assembling all the individual element properties in a suitable manner.

Although the two procedures of Ritz and finite element are theoretically identical, in practice, the finite element method has most important advantages over a conventional Ritz analysis. A particular difficulty associated with a conventional Ritz analysis is the selection of appropriate Ritz functions. In order to solve accurately for large displacement or stress gradients, many functions may be needed. However, these functions also unnecessarily cover the regions in which the displacements and stresses vary slowly and where not many functions are required. Another difficulty arises when the total region of interest is made up of subregions with different kinds of strain. In such a case, the Ritz functions used for one region are not appropriate for the other regions and special displacement continuity conditions must be enforced. No such difficulties arise in the finite element procedure and it may be applied to represent highly irregular and complex structures and loading conditions.

The so-called displacement finite element method, based on the principle of minimum potential energy, is the most well known of all and has been applied to static, dynamic, buckling and a whole range of other problems (20), (21), (22), (23). The compatibility conditions imposed on the assumed displacement field can be satisfied without major difficulties in C_0 continuity problems; for example, in plane stress and plane strain problems or the analysis of three-dimensional solids. However, in the analysis of bending problems, such as plate and shell analysis (C_1 problems), continuity of displacement first derivatives along inter-element boundaries is difficult to maintain. Furthermore, considering complex analyses in

which completely different finite elements must be used to idealize different regions of the structure, compatibility may be almost impossible to maintain. Difficulties with inter-element compatibility requirements render attractive alternative formulations based on a mixed variational principle.

2.5.3 The mixed finite element method

The most general variational principle is that of Reissner, in which the primary field variables are both displacements and stresses. The application of this principle results in finite element discretizations with nodal displacements and stress variables, referred to as mixed models. By using the Reissner functional in one of the several possible alternatives (22), (24), inter-element continuity conditions may be conveniently relaxed allowing the use of stress/displacement shape functions of lower order which ease the computational effort. Another advantage of finite element mixed models is that stresses and displacements are obtained with similar degrees of accuracy, thus avoiding the decrease in accuracy characteristic of the displacement method due to the process of differentiating approximate displacements to obtain the strains (and hence the stresses) once the displacement are evaluated. The mixed method was first investigated by Herrmann (3) in the static plate bending analysis.

CHAPTER 3

DYNAMIC ANALYSIS
OF
ELASTIC BEAMS AND PLATES

3.1 INTRODUCTION

The prediction of dynamic behaviour of structural elements in the form of beams and plates due to transient forces is a problem of practical importance, with applications in the design of vehicles, aircraft, missiles, etc.

In the absence of continuously applied external forces, the structure undergoes a motion due to inertia and elastic forces only. Natural frequencies and modal shapes can be determined from a free vibration analysis of the structure. Knowledge of the natural frequencies helps the designer avoid the peak resonances which occur in the vicinity of the natural frequencies. More detailed knowledge of the mode shapes may be used to estimate bending stresses excited in a vibratory mode. The free vibration results only give information for each mode independent of the rest. The more important class of problems is when the structure experiences external dynamic loads. Displacements and stresses developed under such circumstances are of great importance to the structural analyst.

A recent survey by Leissa (25, 26) uncovers more than 200 references which deal with problems involving the free, undamped vibration of plates. Forced vibration problems, however, have not received as much attention, largely due to the increased complexity of such problems. For convenience for subsequent references the basic equations governing the motions of elastic beams and plates are reviewed. Hamilton's principle (2.36) and the Reissner functional (2.54) will be specialized for plate problems. Finally, the available classical methods of solving dynamic plate problems will be outlined.

3.2 RESPONSE OF A BEAM TO AN APPLIED FORCE

3.2.1. Equation of motion

In this section, the equations of motion for a straight, non-uniform beam, Fig. (3.1) are formulated. It is assumed that vibration occurs in one of the principal planes of the beam and the effects of rotatory inertia and of transverse shear deformation are negligible.

The significant physical properties of the beam include the flexural stiffness $EI(x)$, and the mass per unit length $\rho A(x)$. In addition, the resistance to transverse velocity, $c(x)$ is included to represent the damping mechanisms in the beam. A distributed force $p(x)$ is applied on the beam, which is a function of time $f(t)$ and acts in the z direction. The equations of motion can readily be derived by considering the equilibrium of forces acting on the differential segment of the beam. Fig. (3.1b). Thus summing all the forces acting vertically leads to the first dynamic-equilibrium relationship:

$$\frac{\partial Q}{\partial x} = -p(x) f(t) + \rho A \frac{\partial^2 w}{\partial t^2} + c(x) \frac{\partial w}{\partial t} \quad (3.1)$$

where $w(x,t)$ is the deflection at any section x at time t and $Q(x,t)$ is the shearing force.

The second equilibrium relationship is obtained by summing moments about the centre line of the element (neglecting products of small quantities), gives:

$$\frac{\partial M(x,t)}{\partial x} = Q(x,t) \quad (3.2)$$

Differentiating Eqn. (3.2) with respect to x and substituting into

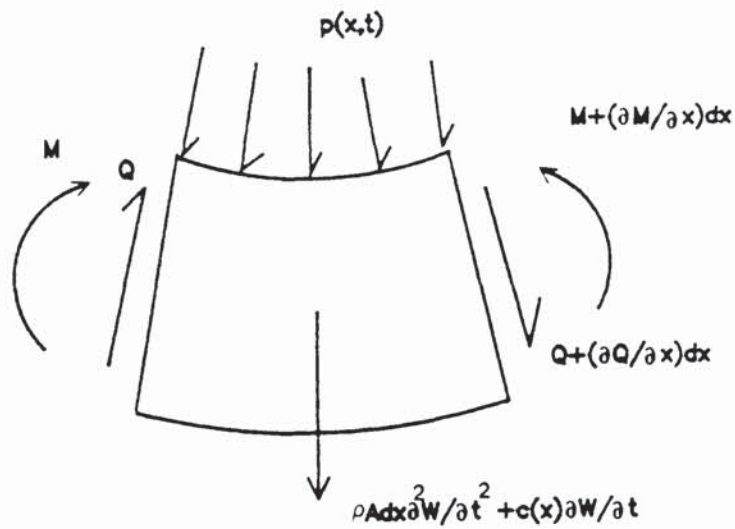
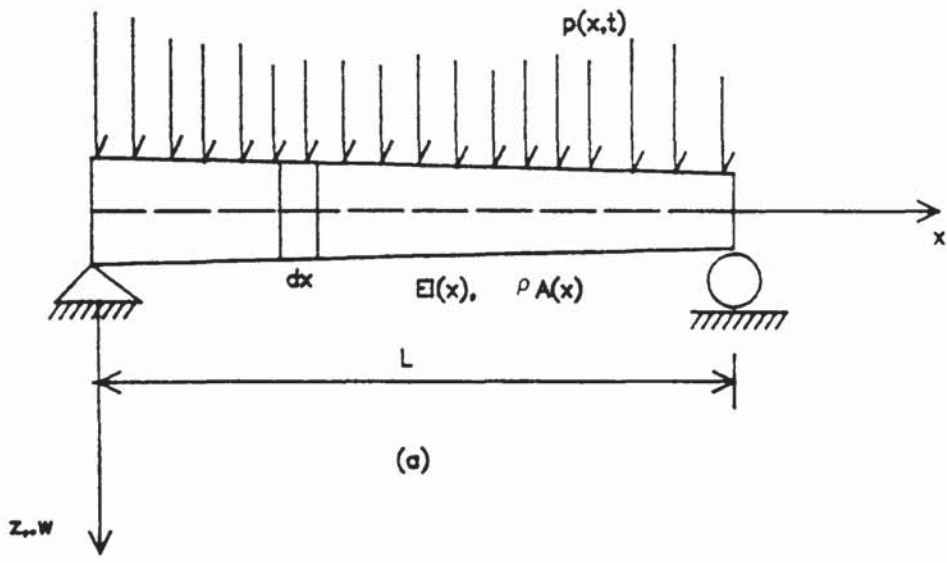


Fig 3.1 Beam subjected to dynamic loading.(a) beam properties and coordinates.(b) forces acting on a differential element.

Equation (3.1) yields after rearrangements:

$$\frac{\partial^2 M(x,t)}{\partial x^2} - \rho A \frac{\partial^2 w(x,t)}{\partial t^2} - c(x) \frac{\partial w}{\partial t} = - p(x) f(t) \quad (3.3)$$

Finally, introducing the basic moment-curvature relationship of elementary beam theory ($M = -EI \frac{\partial^2 w}{\partial x^2}$) leads to the partial differential equation of motion in terms of w and its derivatives only.

$$\frac{\partial^2}{\partial x^2} (EI \frac{\partial^2 w}{\partial x^2}) + \rho A(x) \frac{\partial^2 w}{\partial t^2} + c(x) \frac{\partial w}{\partial t} = + p(x) f(t) \quad (3.4)$$

Equation (3.4) is valid for both uniform and non-uniform beams.

3.2.2 Solution of the equations of motion

Free vibration - the general equation for transverse undamped free vibration of a beam may be obtained from equation (3.4) with $p(x,t) = c(x) \frac{\partial w}{\partial t} = 0$, thus:

$$\frac{\partial^2}{\partial x^2} (EI \frac{\partial^2 w}{\partial x^2}) = - \rho A \frac{\partial^2 w}{\partial t^2} \quad (3.5)$$

For the free vibration, $w(x,t)$ must be a harmonic function of time, i.e.

$$w(x,t) = \hat{w}(x) \sin(\omega t + \alpha) \quad (3.6)$$

substituting (3.6) in (3.5) and assuming that $EI(x)$ is constant we have:

$$\frac{d^4 \hat{w}}{dx^4} - \frac{\rho A \omega^2}{EI} \hat{w} = 0 \quad (3.7)$$

The general form of the solution for equation (3.7) becomes:

$$\hat{w} = c_1 \sin \lambda x + c_2 \cos \lambda x + c_3 \sinh \lambda x + c_4 \cosh \lambda x$$

where $\lambda = \left(\frac{\rho A \omega^2}{EI} \right)^{\frac{1}{2}}$ (3.8)

Two conditions expressing the displacement, slope, moment, or shear force will be defined at each end of the beam. These may be used to determine the four constants c_1 to c_4 (to within an arbitrary constant) and will also provide an expression (called the frequency equation) from which the frequency parameter λ can be evaluated. The total response is thus obtained by superimposing the individual mode shapes. That is:

$$w(x,t) = \sum_{i=1}^{\infty} \hat{w}_i \sin(\omega_i t + \alpha) \quad (3.9)$$

The natural frequencies and the mode shapes for the first few modes of beams with different end conditions have been tabulated in Ref. (27).

The orthogonality conditions for uniform and non-uniform beams with simple and general end conditions are derived in Ref. (28). The following orthogonality relationships exist for a beam with the standard (simply supported, clamped, free) end conditions:

$$\int_0^L \rho A \hat{w}_i(x) \hat{w}_j(x) dx = 0 \quad (a)$$

$$\int_0^L \hat{w}_i(x) \frac{d^2}{dx^2} \left[EI(x) \frac{d^2 \hat{w}_j(x)}{dx^2} \right] dx = 0 \quad (b) \quad (3.10)$$

$$\int_0^L \hat{w}_i''(x) \hat{w}_j''(x) EI(x) dx = 0 \quad (c)$$

Also it can be shown that:

$$\int_0^L \hat{w}_i \frac{d^2}{dx^2} \left[EI \frac{d^2 \hat{w}_i}{dx^2} \right] dx = \omega_i^2 \int_0^L \rho A \hat{w}_i^2 dx \quad (3.11)$$

Response: A solution of equation (3.4) will be sought in the form of an infinite series of the normal modes multiplied by the time-dependent generalized coordinates. That is:

$$w(x,t) = \sum_{i=1}^{\infty} \hat{w}_i(x) q_i(t) \quad (3.12)$$

substituting for w from (3.12) in (3.4), multiplying by w_j and integrating with respect to x over the length of the beam,

$$\begin{aligned} & \int_0^L \rho A \hat{w}_j \sum_i (\hat{w}_i \ddot{q}_i) dx + \int_0^L \hat{w}_j \frac{d^2}{dx^2} \left[EI \sum_i \frac{d^2 \hat{w}_i}{dx^2} q_i \right] dx \\ & + \int_0^L c(x) \hat{w}_j \sum_i (\hat{w}_i \dot{q}_i) dx = \int_0^L p(x) \hat{w}_j f(t) dx \end{aligned} \quad (3.13)$$

Applying orthogonality relations, equations (3.10) and (3.11) together with the assumption of proportional damping leads to:

$$\ddot{q}_i(t) + 2 \xi_i \omega_i \dot{q}_i(t) + \omega_i^2 q_i(t) = p_i(x) f(t) \quad (3.14)$$

where

$$p_i(x) = \frac{\int_0^L p(x) \hat{w}_i(x) dx}{\int_0^L \rho A [\hat{w}_i(x)]^2 dx} \quad (3.15)$$

If the variation of the applied force with time is given, the principal coordinates q_i , may be determined from equation (3.14),

using Duhammel integral or other direct numerical integration methods. The complete dynamic response is found by substituting in equation (3.12).

3.3 REISSNER PRINCIPLE APPLIED TO FLEXURAL MOTION OF BEAMS

To discuss the Reissner principle for the one dimensional technical theory of beams, consider a beam of length L , subject to a uniform transverse load $p(x,t)$ per unit length, Fig. (3.1a). For this beam, the stress field $\{\sigma\}$ is the moment M , the displacement field $\{u\}$ is the transverse displacement w , and the strain field is the curvature w'' ($\epsilon_x = -zw''$). Hence, the Reissner principle, Equation (2.59), can be written as:

$$\delta \int_{t_1}^{t_2} \left[- \int_0^L \left(\rho A \left(\frac{dw}{dt} \right)^2 + \frac{M^2}{2EI} + M \frac{d^2w}{dx^2} \right) dx - \int_0^L w^t p(x,t) dx + \frac{dw}{dx} \bar{M} \Big|_0^L \right] dt + \int_{t_1}^{t_2} \left[\int_0^L c(x) \dot{w} \delta w dx \right] dt = 0 \quad (3.16)$$

where \bar{M} represents the prescribed end moments. Taking variations with respect to w and M , and equating to zero yields the stationary conditions for (3.16) as:

- (i) The equilibrium equations (3.3)
- (ii) The moment-curvature relation ($M = -EI \frac{d^2w}{dx^2}$)
- (iii) The appropriate Boundary Conditions on $x = 0$ and $x = L$.

In finite element applications, the variables M and w can be approximated independently, but the latter would have to show continuous slope according to standard 'Integrating' rules (20). It is possible to relax this condition by integrating by parts of the term $M \frac{d^2w}{dx^2}$ in Eqn. (3.16). Thus Reissner's principle may be re-written as:

$$\delta \int_{t_1}^{t_2} \left[\int_0^L (-\rho A \dot{w}^2 - \frac{M^2}{2EI} + M'w') dx - \int_0^L w^t p(x,t) dx + \frac{cW}{dx} (M - \bar{M}) \Big|_0^L \right] dt$$

$$+ \int_{t_1}^{t_2} \int_0^L c(x) \dot{w} \delta \dot{w} dx dt = 0 \quad (3.17)$$

In the present work, equations (3.16) and (3.17), have been used to develop several beam finite element models with different interpolation functions (see section 6.1). The behaviour of these elements in free and forced vibration problems is studied and numerical examples are presented in Chapter 8.

3.4 BASIC EQUATIONS - THIN PLATE THEORY

A plate of uniform thickness (h) is considered (Figure 3.2), such that its middle surface coincides with the x - y plane and the free surfaces of the plate are the planes $z = \pm \frac{1}{2} h$. If h is small compared to other in plane dimensions, the following assumptions may be made with regard to small deflections of the plate.

- (i) The direct stress in the transverse direction σ_z is considered negligible.
- (ii) Membrane stresses in the middle plane of the plate are neglected.
- (iii) Plane sections that are initially normal to the middle plane remain plane and normal to it. This is equivalent to neglecting the transverse shear effects ($\gamma_{xz} = \gamma_{yz} = 0$).
- (iv) Transverse displacement w of any point of the plate is identical to that of the point (below or above it) in the middle surface.

3.4.1 Plate displacement components

From the third and fourth assumptions, the plate displacement field is given as

$$\begin{aligned}w(x,y,z,t) &= w(x,y,0,t) = W(x,y,t) \\u &= -z \frac{\partial W}{\partial x} \\v &= -z \frac{\partial W}{\partial y}\end{aligned}\tag{3.18}$$

Therefore the strain in a plane at a distance z from the middle surface is given by the expression

$$\begin{bmatrix} \epsilon_x \\ \epsilon_y \\ \gamma_{xy} \end{bmatrix} = \begin{bmatrix} \frac{\partial u}{\partial x} \\ \frac{\partial v}{\partial y} \\ \frac{\partial u}{\partial y} + \frac{\partial v}{\partial x} \end{bmatrix} = -z \begin{bmatrix} \frac{\partial^2 W}{\partial x^2} \\ \frac{\partial^2 W}{\partial y^2} \\ \frac{2\partial^2 W}{\partial x \partial y} \end{bmatrix} \quad (a) \quad (3.19)$$

$$\text{and } \sigma_z = \tau_{xz} = \tau_{yz} = 0 \quad (b)$$

3.4.2 Stress-strain relations

With $\sigma_z = 0$, the stress-strain relations for an orthotropic plate with principal directions of orthotropy coinciding with the x and y axes can be written in matrix notations as:

$$\begin{bmatrix} \sigma_x \\ \sigma_y \\ \tau_{xy} \end{bmatrix} = \begin{bmatrix} 1/E_x & -\nu_{yx}/E_y & 0 \\ -\nu_{xy}/E_x & 1/E_y & 0 \\ 0 & 0 & 1/G_{xy} \end{bmatrix} \begin{bmatrix} \epsilon_x \\ \epsilon_y \\ \gamma_{xy} \end{bmatrix} \quad (3.20)$$

Assuming that the material is isotropic the equations become:

$$\begin{bmatrix} \sigma_x \\ \sigma_y \\ \tau_{xy} \end{bmatrix} = \frac{E}{1-\nu^2} \begin{bmatrix} 1 & \nu & 0 \\ \nu & 1 & 0 \\ 0 & 0 & \frac{1-\nu}{2} \end{bmatrix} \begin{bmatrix} \epsilon_x \\ \epsilon_y \\ \gamma_{xy} \end{bmatrix} \quad (3.21)$$

Stresses τ_{xz} and τ_{yz} can only be evaluated from the equilibrium conditions (2.2).

3.4.3 Relations between internal moments, stresses and displacements

Integration of the direct stresses across the thickness of the plate yields stress resultants in the form of direct (M_x, M_y) and twisting (M_{xy}) moments per unit length (Fig. 3.3).

$$\begin{bmatrix} M_x \\ M_y \\ M_{xy} \end{bmatrix} = \int_{-h/2}^{h/2} \begin{bmatrix} \sigma_x \\ \sigma_y \\ \tau_{xy} \end{bmatrix} z dz \quad (3.22)$$

and the shear force intensities (Q_x, Q_y) are given by:

$$\begin{bmatrix} Q_x \\ Q_y \end{bmatrix} = \int_{-h/2}^{h/2} \begin{bmatrix} \tau_{xz} \\ \tau_{yz} \end{bmatrix} dz \quad (3.23)$$

Using equations (3.19) - (3.22), the following expression may be derived for stress resultants (M_x, M_y, M_{xy}) in terms of curvatures.

$$\begin{bmatrix} M_x \\ M_y \\ M_{xy} \end{bmatrix} = D \begin{bmatrix} 1 & \nu & 0 \\ \nu & 1 & 0 \\ 0 & 0 & \frac{1-\nu}{2} \end{bmatrix} \begin{bmatrix} -\frac{\partial^2 W}{\partial x^2} \\ -\frac{\partial^2 W}{\partial y^2} \\ -2\frac{\partial^2 W}{\partial x \partial y} \end{bmatrix} \quad (3.24)$$

where D is the plate bending rigidity; $D = \frac{Eh^3}{12(1-\nu^2)}$

Comparing equations (3.19) and (3.24), the following relation is obtained

$$\begin{bmatrix} \sigma_x \\ \sigma_y \\ \tau_{xy} \end{bmatrix} = \frac{12z}{h^3} \begin{bmatrix} M_x \\ M_y \\ M_{xy} \end{bmatrix} \quad (3.25)$$

If a transformation of coordinates (n,s,z) is required, simple equilibrium considerations yields (see Fig. 3.4)

$$\begin{bmatrix} M_s \\ M_n \\ M_{ns} \end{bmatrix} = \begin{bmatrix} \sin^2\alpha & \cos^2\alpha & -\sin 2\alpha \\ \cos^2\alpha & \sin^2\alpha & \sin 2\alpha \\ -\frac{1}{2}\sin 2\alpha & \frac{1}{2}\sin 2\alpha & \cos 2\alpha \end{bmatrix} \begin{bmatrix} M_x \\ M_y \\ M_{xy} \end{bmatrix} \quad (3.26)$$

and

$$Q_n = \begin{bmatrix} \cos\alpha & \sin\alpha \end{bmatrix} \begin{Bmatrix} Q_x \\ Q_y \end{Bmatrix} \quad (3.27)$$

where α is the angle between outward normal n and the x-axis.

3.4.4 Derivation of the governing differential equations

The governing differential equation of plate flexural motion can be derived by examining, on a differential element, the equilibrium of forces with respect to the vertical direction z and of moments about the x and y axes, respectively. In addition to the applied transverse force per unit area, $p(x,y) f(t)$ there is an inertia force $(\rho h \frac{\partial^2 W}{\partial t^2})$ and a damping force $(c \frac{\partial W}{\partial t})$ per unit area acting in the z direction. (Fig. 3.5).

$$\frac{\partial M_x}{\partial x} + \frac{\partial M_{xy}}{\partial y} - Q_x = 0$$

$$\frac{\partial M_{xy}}{\partial x} + \frac{\partial M_y}{\partial y} - Q_y = 0 \quad (3.28)$$

$$\frac{\partial Q_x}{\partial x} + \frac{\partial Q_y}{\partial y} + p(x,y,t) = \rho h \frac{\partial^2 W}{\partial t^2} + c(x,y) \frac{\partial W}{\partial t}$$

Eliminating Q_x and Q_y from above equations yields

$$\frac{\partial^2 M_x}{\partial x^2} + 2 \frac{\partial^2 M_{xy}}{\partial x \partial y} + \frac{\partial^2 M_y}{\partial y^2} + p(x,y) f(t) = \rho h \frac{\partial^2 W}{\partial t^2} + c \frac{\partial W}{\partial t} \quad (3.29)$$

Substituting from equation (3.24) into (3.29) gives the equilibrium equation for an element of the plate in terms of W and its derivatives.

$$D \left[\frac{\partial^4 W}{\partial x^4} + 2 \frac{\partial^4 W}{\partial x^2 \partial y^2} + \frac{\partial^4 W}{\partial y^4} \right] + \rho h \frac{\partial^2 W}{\partial t^2} + c \frac{\partial W}{\partial t} = p(x,y) f(t) \quad (3.30)$$

which may also be written as:

$$D \left[\frac{\partial}{\partial x} \left(\frac{\partial}{\partial x} \nabla^2 W \right) + \frac{\partial}{\partial y} \left(\frac{\partial}{\partial y} \nabla^2 W \right) \right] - p(x,y,t) = -\rho h \ddot{W} - c \dot{W}$$

Comparing this with the last relation in (3.28) results in

$$Q_x = -D \frac{\partial}{\partial x} (\nabla^2 W)$$

$$Q_y = -D \frac{\partial}{\partial y} (\nabla^2 W) \quad (3.31)$$

For a dynamic problem $W(x,y,t)$ must satisfy equation (3.30) together with the boundary conditions.

3.4.5 Boundary Conditions

To solve the plate equation (3.30) one needs to satisfy the boundary conditions for the given plate problem. Since equation (3.30) is a 4th order differential equation no more than two, either geometrical or mechanical boundary conditions can be imposed at a boundary. The mechanical boundary conditions may consist of the normal moment M_n , the twisting moment M_{ns} and the normal shear force intensity Q_n . Since 3 conditions are too many for the thin plate theory, the twisting moment M_{ns} and the normal shear force intensity Q_n must be reduced into one quantity, the so-called normal effective shear force intensity given by (29) as

$$V_n = Q_n + \frac{\partial M_{ns}}{\partial s} \quad (3.32)$$

the boundary conditions can thus be imposed as:

either $M_n = \bar{M}_n$ or $\frac{\partial W}{\partial n}$ is prescribed

either $V_n = \bar{V}_n$ or W is prescribed

For a simply-supported boundary

$$M_n = -D \left[\frac{\partial^2 W}{\partial n^2} + \nu \frac{\partial^2 W}{\partial s^2} \right] = 0$$

$$W = 0$$

For a built in boundary

$$\frac{\partial W}{\partial n} = 0$$

$$W = 0$$

and for a free boundary

$$M_n = 0, \quad V_n = Q_n + \frac{\partial M_{ns}}{\partial s} = 0$$

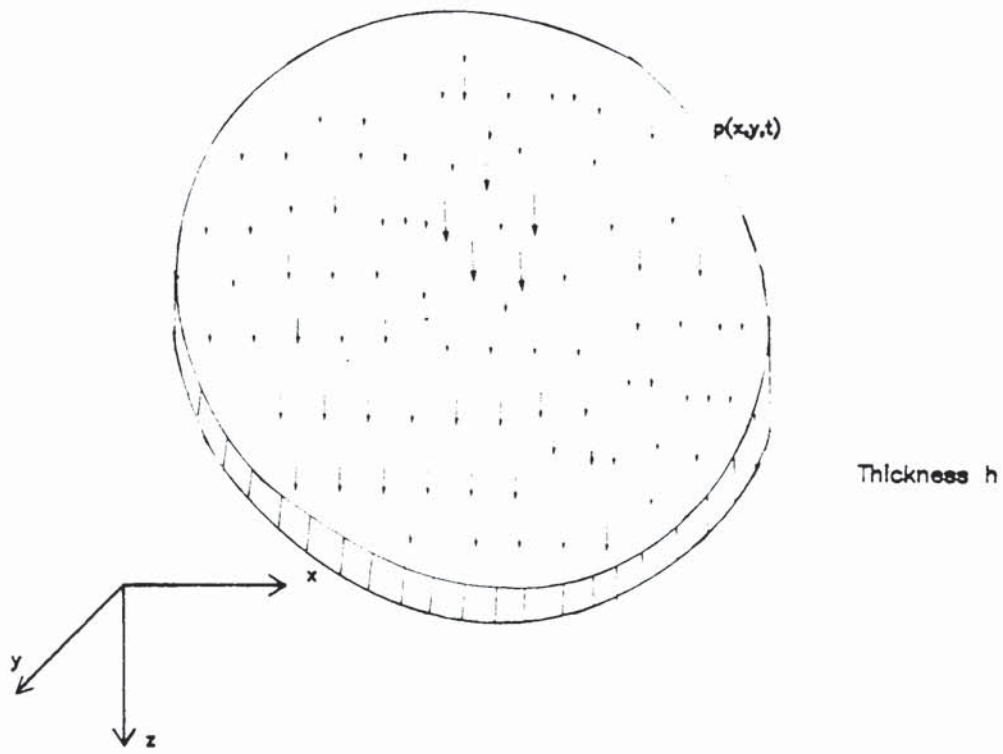


Fig 3.2 Thin plate subjected to distributed loading.

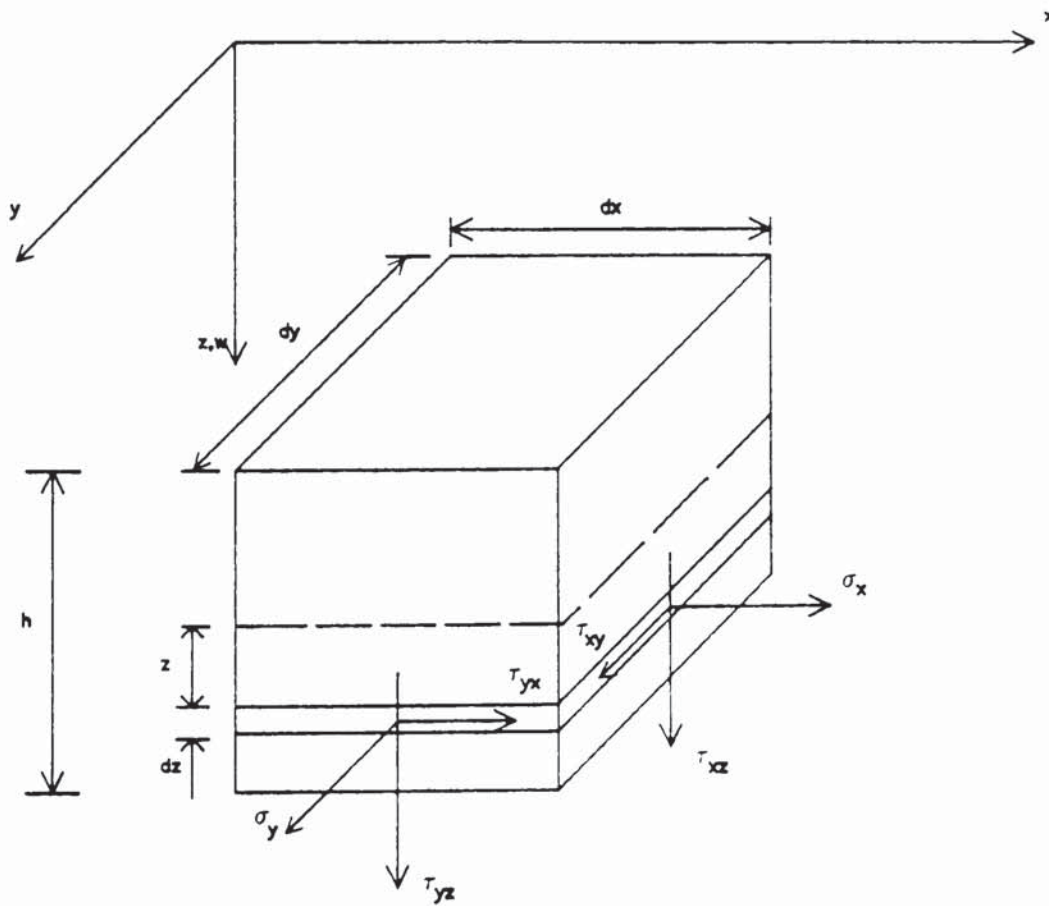


Fig 3.3 Stress components on a plate element.

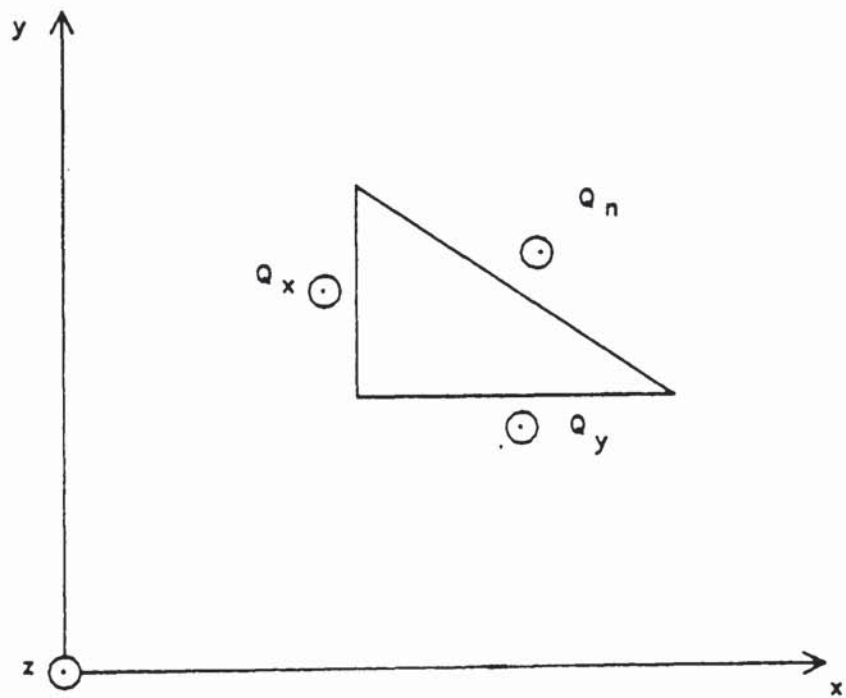
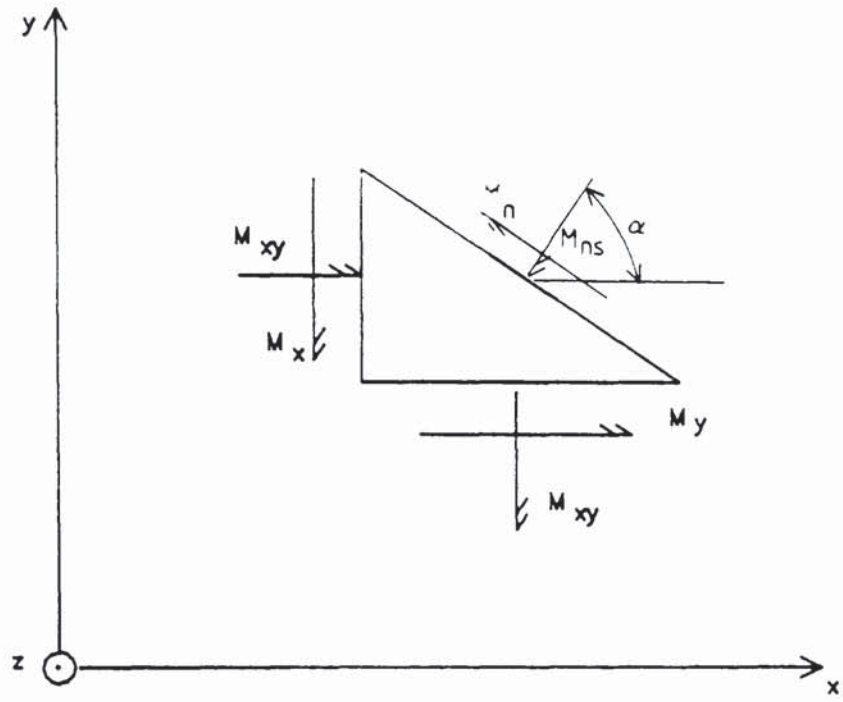


Fig 3.4 Moments and shear notations.

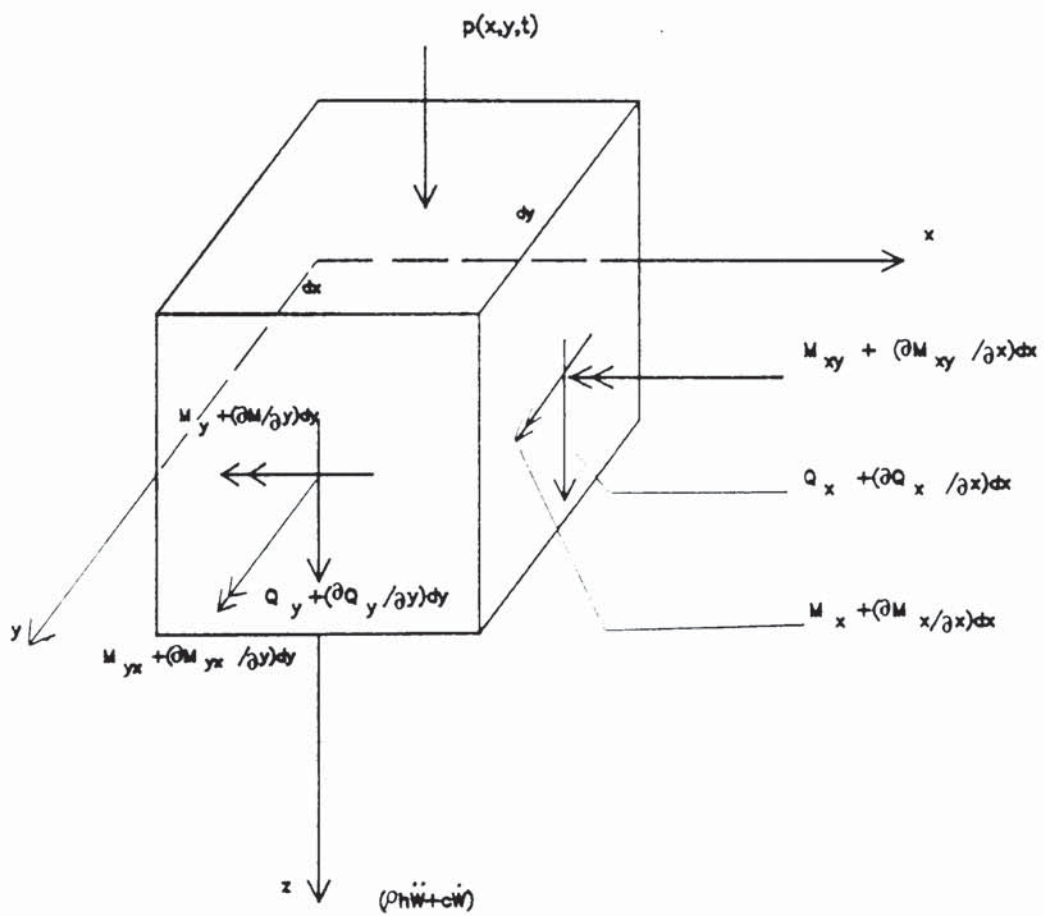


Fig 3.5 Forces and moments on an element of a plate

3.5 HAMILTON'S PRINCIPLE - THIN PLATE THEORY

Hamilton's principle, equation (2.36) may be specialized for the plate bending theory. Let the plate be subject to a distributed lateral load $p(x,y,t)$ per unit area of the middle surface in the direction of the z -axis (Fig. 3.2). On the part of the side boundary S_σ , external forces are prescribed, defined per unit area of the side boundary $(\bar{T}_x, \bar{T}_y, \bar{T}_z)$. On the remaining part of the boundary S_u , geometrical boundary conditions are prescribed. Then, Hamilton's principle for the present problem can be written as follows:

$$\int_{t_1}^{t_2} \left[\int_{S_\sigma} \{\bar{T}\}_{nc}^t \{\delta u\} dS + \int_A p(x,y,t) \delta W dA \right] dt + \int_{t_1}^{t_2} (\delta T - \delta U) dt = 0 \quad (3.33)$$

The kinetic energy (T) is given by

$$T = \frac{1}{2} \int_A \int_{-h/2}^{h/2} (\rho \dot{W}^2) dz dx dy = \frac{1}{2} \int_A \rho h \left(\frac{\partial W}{\partial t} \right)^2 dx dy \quad (3.34)$$

where the effects of rotary inertia are neglected

and the strain energy U_{int} becomes

$$U = \frac{E}{2(1-\nu^2)} \int_A \int_{-h/2}^{h/2} \left(\epsilon_x^2 + 2\nu \epsilon_x \epsilon_y + \epsilon_y^2 + \frac{(1-\nu)}{2} \gamma_{xy}^2 \right) dz dx dy \quad (3.35)$$

substituting from equation (3.19) and integrating with respect to z over the plate thickness yields:

$$U = \frac{1}{2} \int_A D \left\{ \left(\frac{\partial^2 W}{\partial x^2} + \frac{\partial^2 W}{\partial y^2} \right)^2 - 2(1-\nu) \left[\frac{\partial^2 W}{\partial x^2} \cdot \frac{\partial^2 W}{\partial y^2} - \left(\frac{\partial^2 W}{\partial x \partial y} \right)^2 \right] \right\} dx dy \quad (3.36)$$

Using equations (2.10) and (3.18), the integral involving the boundary tractions may be written as:

$$\int_{S_\sigma} (\bar{T}_x \delta u + \bar{T}_y \delta v + \bar{T}_z \delta w) dS = - \int_{s_\sigma} \int_{-h/2}^{h/2} \left[(\bar{\sigma}_x 1 + \bar{\tau}_{xy} m) \delta (W,x) + (\bar{\tau}_{xy} 1 + \bar{\sigma}_y m) \delta (W,y) \right] z dz ds + \int_{s_\sigma} \int_{-h/2}^{h/2} (\bar{\tau}_{zx} 1 + \bar{\tau}_{yz} m) \delta W dz ds \quad (3.37)$$

Integrating over the thickness yields

$$\int_{S_\sigma} \{\bar{T}\}^t \{\delta u\} dS = - \int_{s_\sigma} \left[(\bar{M}_x 1 + \bar{M}_{xy} m) \delta (W,x) + (\bar{M}_{xy} 1 + \bar{M}_y m) \delta (W,y) - (Q_x 1 + Q_y m) \delta W \right] ds \quad (3.38)$$

The quantities $\delta \left(\frac{\partial W}{\partial x} \right)$ and $\delta \left(\frac{\partial W}{\partial y} \right)$ can be expressed in terms of

$$\delta \left(\frac{\partial W}{\partial n} \right) \text{ and } \delta \left(\frac{\partial W}{\partial s} \right). \quad \text{Thus}$$

$$\delta \left(\frac{\partial W}{\partial x} \right) = \delta \left(\frac{\partial W}{\partial n} \right) 1 - \delta \left(\frac{\partial W}{\partial s} \right) m \quad (3.39)$$

$$\delta \left(\frac{\partial W}{\partial y} \right) = \delta \left(\frac{\partial W}{\partial n} \right) m + \delta \left(\frac{\partial W}{\partial s} \right) 1$$

Substituting from (3.39) into (3.38) yields:

$$\int_{S_\sigma} \{\bar{T}\}^t \{\delta u\} dS = - \int_{s_\sigma} \left[\bar{M}_n \delta (W,n) - \bar{M}_{ns} (\delta W,s) - \bar{Q}_n \delta W \right] ds \quad (3.40)$$

Substituting from (3.34), (3.36) and (3.40) into Equation (3.33), Hamilton's principle is finally reduced to:

$$\begin{aligned}
& \delta \int_{t_1}^{t_2} \frac{1}{2} \int_A \left\{ \rho h \dot{W}^2 - D \left(\left(\frac{\partial^2 W}{\partial x^2} + \frac{\partial^2 W}{\partial y^2} \right)^2 - 2(1-\nu) \left[\frac{\partial^2 W}{\partial x^2} \cdot \frac{\partial^2 W}{\partial y^2} - \left(\frac{\partial^2 W}{\partial x \partial y} \right)^2 \right] \right\} dx \, dy \, dt \\
& + \int_{t_1}^{t_2} \int_A P(x,y,t) \delta W \, dx \, dy \, dt + \int_{t_1}^{t_2} \int_{S_\sigma} \left[-\bar{M}_n^\delta (W,n) + \bar{M}_{ns}^\delta (W,s) \right. \\
& \left. + Q_n \delta W \right] ds \, dt = 0 \tag{3.41}
\end{aligned}$$

With the geometrical boundary conditions satisfied a priori, the above principle yields the equation of motion (3.30) and mechanical boundary conditions on S_σ .

3.6 REISSNER'S PRINCIPLE APPLIED TO PLATE BENDING

3.6.1 Introduction

Reissner's principle for static problems, equation (2.54) has been used to develop a system of two-dimensional equations for transverse bending of plates (2). This system of equations is of such a nature that three boundary conditions can and must be prescribed along the edge of the plate. In this section, the dynamic Reissner principle, Eqn. (2.58) will be specialised for an elastic plate where the effects of transverse shear stresses τ_{xz} , τ_{yz} as well as rotary inertia are included. This derivation is similar to the one used in (2). The Principle will then be simplified to correspond to the classical plate theory. The first derivation is referred to as "moderately thick plate" theory.

3.6.2 Reissner's functional for plate bending

As before, a plate of thickness h is considered. The faces of the plate are the planes $z = \pm h/2$ which are taken to be free from tangential traction but under normal pressure $p(x,y,t)$. Thus

$$\tau_{xz} = \tau_{yz} = 0 \quad \text{at } z = \pm h/2, \quad (\sigma_z)_{z = -h/2} = p(x,y,t) \quad (3.42)$$

For an isotropic material which obeys Hooke's law, the variational principle (2.58) may be written as follows:

$$\delta \int_{t_1}^{t_2} \left\{ \int_A \int_{-h/2}^{h/2} (-T_0 - U_0^* + \{\sigma\}^t [L]\{u\}) dz dx dy - \int_A p(x,y,t) W dx dy - \int_{s_\sigma} \int_{-h/2}^{h/2} \{\bar{T}\}_c \{u\} dz ds - \int_{s_u} \int_{-h/2}^{h/2} \{\bar{T}\}^t (\{u\} - \{\bar{u}\}) dz ds \right\} dt = 0 \quad (3.43)$$

As in the classical theory of thin plates, it is assumed that the bending stresses are distributed linearly over the plate thickness, i.e.

$$\begin{bmatrix} \sigma_x \\ \sigma_y \\ \tau_{xy} \end{bmatrix} = \frac{12z}{h^3} \begin{bmatrix} M_x \\ M_y \\ M_{xy} \end{bmatrix} \quad (3.25)$$

Expressions for the transverse shear stresses may be obtained by means of the differential equations of equilibrium which satisfy the conditions that the faces of the plate are free from shear stress, then

$$\begin{bmatrix} \tau_{xz} \\ \tau_{yz} \end{bmatrix} = \frac{3}{2h} \left(1 - \frac{4z^2}{h^2}\right) \begin{bmatrix} Q_x \\ Q_y \end{bmatrix} \quad (3.44)$$

$$\text{and } \sigma_z = 0$$

For the displacement field, it is assumed that

$$u = z \beta_x \quad (3.45)$$

$$v = z \beta_y$$

$$w = w(x,y,z,t) = w(x,y,t) = W$$

where β_x and β_y are "average rotations" of the normal to the middle

plane of the plate such that

$$\int_{-h/2}^{h/2} \sigma_x u \, dz = M_x \beta_x, \quad \int_{-h/2}^{h/2} \sigma_y v \, dz = M_y \beta_y \quad (3.46)$$

and W is a mean transverse deflection with respect to the plate thickness such that

$$\int_{-h/2}^{h/2} \tau_{xz} W(x,y,z) \, dz = Q_x W \quad (3.47)$$

For the boundary terms in (3.43) we have

$$\int_{-h/2}^{h/2} \bar{T}_x z \, dz = \bar{M}_x l + \bar{M}_{xy} \cdot m, \quad \int_{-h/2}^{h/2} \bar{T}_y z \, dz = M_{xy} \cdot l + M_y m$$

and

$$\int_{-h/2}^{h/2} \bar{T}_z \, dz = Q_x l + Q_y m \quad (3.48)$$

Introducing the above assumptions into the functional (3.43), and integrating with respect to z we obtain:

$$\begin{aligned}
& \delta \int_{t_1}^{t_2} \left[\int_A \frac{1}{2} \left\{ \frac{\rho h^3}{12} \left[\left(\frac{\partial \beta_x}{\partial t} \right)^2 + \left(\frac{\partial \beta_y}{\partial t} \right)^2 \right] - \rho h \dot{w}^2 - \frac{12}{E h^3} (M_x^2 + M_y^2 - 2\nu M_x M_y) \right. \right. \\
& + 2(1+\nu) M_{xy}^2 - \frac{12}{5hE} (1+\nu) (Q_x^2 + Q_y^2) + 2 \left[M_x \frac{\partial \beta_x}{\partial x} + M_y \frac{\partial \beta_y}{\partial y} + M_{xy} \left(\frac{\partial \beta_x}{\partial y} + \frac{\partial \beta_y}{\partial x} \right) \right. \\
& + Q_y \left(\beta_y + \frac{\partial w}{\partial y} \right) + Q_x \left(\beta_x + \frac{\partial w}{\partial x} \right) \left. \right\} dx dy - \int_A P(x,y) W dx dy \\
& - \int_{\sigma} (\bar{M}_n \beta_n + \bar{M}_{ns} \beta_s + \bar{Q}_n W) ds - \int_u \left[M_n (\beta_n - \bar{\beta}_n) + M_{ns} (\beta_s - \bar{\beta}_s) \right. \\
& \left. + Q_n (W - \bar{W}) \right] ds \left. \right] dt = 0 \tag{3.49}
\end{aligned}$$

The stationary conditions for the above functional are:

(i) The equations of equilibrium:

$$\begin{aligned}
\frac{\partial M_x}{\partial x} + \frac{\partial M_{xy}}{\partial y} - Q_x &= \frac{\rho h^3}{12} \ddot{\beta}_x \\
\frac{\partial M_y}{\partial y} + \frac{\partial M_{xy}}{\partial x} - Q_y &= \frac{\rho h^3}{12} \ddot{\beta}_y \\
\frac{\partial Q_x}{\partial x} + \frac{\partial Q_y}{\partial y} + p(x,y,t) &= \rho h \ddot{w}
\end{aligned} \tag{3.50}$$

(ii) Stress-displacement relations:

$$\begin{aligned}
M_x &= D \left(\frac{\partial \beta_x}{\partial x} + \nu \frac{\partial \beta_y}{\partial y} \right) \\
M_y &= D \left(\nu \frac{\partial \beta_x}{\partial x} + \frac{\partial \beta_y}{\partial y} \right) \\
M_{xy} &= \frac{Gh^3}{12} \left(\frac{\partial \beta_x}{\partial y} + \frac{\partial \beta_y}{\partial x} \right) \\
Q_x &= \frac{5Gh}{6} \left(\beta_x + \frac{\partial w}{\partial x} \right) \\
Q_y &= \frac{5Gh}{6} \left(\beta_y + \frac{\partial w}{\partial y} \right)
\end{aligned} \tag{3.51}$$

(iii) Boundary conditions

Geometrical boundary conditions are

$$\beta_n = \bar{\beta}_n, \quad \beta_s = \bar{\beta}_s, \quad w = \bar{w}, \quad \text{on } s_u \quad (3.52)$$

and mechanical boundary conditions

$$M_n = \bar{M}_n, \quad M_{ns} = \bar{M}_{ns}, \quad Q_n = \bar{Q}_n \quad \text{on } s_\sigma \quad (3.53)$$

These are the Euler equations corresponding to $\delta \pi_R^D = 0$ which govern the behaviour of plates, including the effect of transverse shear deformation and rotatory inertia.

For thin plates, the complementary strain energy due to the stresses σ_z , τ_{xz} and τ_{yz} are assumed negligible, i.e.

$$\frac{12}{5hE} (Q_x^2 + Q_y^2) = 0 \quad (3.54)$$

and the rotations are:

$$\begin{aligned} \beta_x &= -\frac{\partial w}{\partial x} & \beta_y &= -\frac{\partial w}{\partial y} \\ \beta_n &= -\frac{\partial w}{\partial n} & \beta_s &= -\frac{\partial w}{\partial s} \end{aligned} \quad (3.55)$$

in accordance with the classical assumptions as presented in section (3.4). Using equations (3.54) and (3.55) in the expression for Reissner's principle equation (3.49), we obtain:

$$\begin{aligned}
& \delta \int_{t_1}^{t_2} \int_A \left[\frac{\rho h}{2} \left(\frac{\partial W}{\partial t} \right)^2 + \frac{6}{Eh^3} (M_x^2 + M_y^2 - 2\nu M_x M_y + 2(1+\nu) M_{xy}^2) + M_x \frac{\partial^2 W}{\partial x^2} \right. \\
& + M_y \frac{\partial^2 W}{\partial y^2} + M_{xy} \frac{\partial^2 W}{\partial x \partial y} \left. \right] dx dy - \int_A p(x,y,t) W dx dy \\
& + \int_{S_\sigma} (\bar{M}_n \frac{\partial W}{\partial n} + \bar{M}_{ns} \frac{\partial W}{\partial s} - \bar{Q}_n W) ds - \int_{S_u} (M_n (\frac{\partial W}{\partial n} - \bar{\frac{\partial W}{\partial n}}) + M_{ns} (\frac{\partial W}{\partial s} - \bar{\frac{\partial W}{\partial s}}) \\
& + Q_n (W - \bar{W})) ds \left. \right\} dt + \int_{t_1}^{t_2} \int_A cW \delta W dx dy dt = 0 \quad (3.56)
\end{aligned}$$

In which the term due to damping is included according to section (2.4.3).

The quantities subject to variations in (3.56) are M_x , M_y , M_{xy} , W .

The Euler-Lagrange equations can be shown to be the equations of equilibrium (3.29), and the curvature-moment relations (3.24). As boundary conditions we will obtain:

(i) geometrical boundary conditions

$$\begin{aligned}
W &= \bar{W} \\
&\quad \text{on } S_u \\
\frac{\partial W}{\partial n} &= \frac{\partial \bar{W}}{\partial n}
\end{aligned} \quad (3.57)$$

(ii) mechanical boundary conditions

$$\begin{aligned}
V_n &= \bar{V}_n \\
M_n &= \bar{M}_n \\
&\quad \text{on } S_\sigma
\end{aligned} \quad (3.58)$$

where V_n is the effective shear force intensity. Reissner's principle, (3.56) may be transformed into simpler forms for use with the finite element method (see section 4.3.2).

3.7 METHODS FOR THE SOLUTION OF DYNAMIC PLATE PROBLEMS

3.7.1 Free vibration of thin rectangular plates

The subsequent study of the forced motion of elastic plates will require certain basic relations which are obtained from the study of free vibrations with homogeneous boundary conditions. The familiar equation of motion for free vibration of thin plates is obtained by setting of $p = 0$ in equation (3.30), then

$$D (\nabla^4 W (x,y,t)) + \rho \frac{\partial^2 W}{\partial t^2} = 0 \quad (3.59)$$

where $\nabla^4 = \nabla^2 \nabla^2$ is the biharmonic differential operator and the effect of damping is neglected.

Assuming a harmonic motion, we may write

$$W (x,y,t) = \hat{W} (x,y) \sin (\omega t) \quad (3.60)$$

Here $\hat{W} (x,y)$ is the shape function describing the modes of vibration of the middle plane of the plate and ω is the natural frequency of the vibrations. Substitution of equation (3.60) into equation (3.59) gives:

$$\nabla^4 \hat{W} = \lambda^* \hat{W} \quad (3.61)$$

where
$$\lambda^* = \frac{\rho h}{D} \cdot \omega^2 \quad (3.62)$$

Equation (3.61) is an eigenvalue equation whose exact solution will consist of infinite series of frequencies and associated normal modes (eigenvalues and eigenvectors). We shall now briefly illustrate exact and approximate methods to a few situations of the type that we

will subsequently treat by finite elements.

a) Exact solution method

Exact solutions to the eigenvalue equation (3.61) exist for very few cases where the shape and boundary conditions of the plate are suitable. In the case of a rectangular plate with simply supported edges (Fig. 3.6), Navier's method (29) is the classical method of analysis. The shape functions $\hat{W}(x,y)$ can be given by double trigonometric series in the form of equation (3.63).

$$\hat{W}(x,y) = \sin \frac{m\pi x}{a} \sin \frac{n\pi y}{b} \quad (3.63)$$

This function completely satisfies the conditions at the edges which require that

$$\begin{aligned} \hat{W} = \frac{\partial^2 \hat{W}}{\partial x^2} &= 0 && \text{at } x = 0 \quad \text{and } x = a \\ \hat{W} = \frac{\partial^2 \hat{W}}{\partial y^2} &= 0 && \text{at } y = 0 \quad \text{and } y = b \end{aligned} \quad (3.64)$$

Substituting equation (3.63) into equation (3.61) yields:

$$D \left[\left(\frac{\pi m}{a} \right)^4 + \frac{2\pi^4 m^2 n^2}{a^2 b^2} + \left(\frac{\pi n}{b} \right)^4 \right] = \rho h \omega^2 \quad (3.65)$$

Associating ω , with the corresponding integers m and n , equation (3.65) can be represented as:

$$\frac{\rho h}{D} \omega_{mn}^2 = \pi^4 \left[\left(\frac{m}{a} \right)^2 + \left(\frac{n}{b} \right)^2 \right]^2 \quad (3.66)$$

solving for ω_{mn} gives

$$\omega_{mn} = \pi^2 \left[\left(\frac{m}{a} \right)^2 + \left(\frac{n}{b} \right)^2 \right] \sqrt{\frac{D}{\rho h}} \quad (3.67)$$

for $m, n = 1, 2, 3, \dots$

ω_{mn} are the natural frequencies (eigenvalues) and the corresponding natural modes (eigenfunctions) are:

$$\hat{W}_{mn}(x,y) = \sin \frac{m\pi x}{a} \sin \frac{n\pi y}{b} \quad (3.63)$$

The free vibration of the plate is a superposition of all the modes with proper amplitudes.

$$W(x,y,t) = \sum_{m=1}^{\infty} \sum_{n=1}^{\infty} \left(\sin \frac{m\pi x}{a} \sin \frac{n\pi y}{b} \right) (A_{mn} \sin \omega_{mn} t + B_{mn} \cos \omega_{mn} t) \quad (3.68)$$

where the double infinity of constants A_{mn} and B_{mn} are determined to satisfy the initial conditions:

$$\begin{aligned} W(x,y,0) &= \phi(x,y) \\ \frac{\partial W(x,y,0)}{\partial t} &= \psi(x,y) \end{aligned} \quad (3.69)$$

with ϕ and ψ as known functions. Now making use of the orthogonality property of the eigenfunctions that is

$$\int_A (\hat{W}_{rs}) (\hat{W}_{pq}) dx dy = \frac{ab}{4} (\delta_{rs} \cdot \delta_{pq}) \quad (3.70)$$

it may be shown that the unknowns A_{mn} and B_{mn} are determined from the following relations

$$A_{mn} = \frac{4}{ab\omega_{mn}} \int_A \psi(x,y) \sin \frac{m\pi x}{a} \sin \frac{n\pi y}{b} dx dy \quad (3.71)$$

and

$$B_{mn} = \frac{4}{ab} \int_A \phi(x,y) \sin \frac{m\pi x}{a} \sin \frac{n\pi y}{b} dx dy$$

Thus the free vibration problem for a rectangular simply supported plate is solved. Levy's type of solution can be applied to rectangular plates which are simply supported along a pair of opposite edges (say at $x = 0$ and at $x = a$) while the other edges ($y = 0$ and $y = b$) are supported in an arbitrary manner (Fig. 3.7). The shape function $\hat{W}(x,y)$ can take the form of equation (3.72) which satisfies the boundary conditions on $x = 0$ and $x = a$

$$\hat{W}(x,y) = Y_{mn}(y) \sin \left(\frac{m\pi x}{a} \right) \quad (3.72)$$

$Y_{mn}(y)$ is yet to be determined and must satisfy appropriate boundary conditions at $y = 0$ and $y = b$. Substituting equation (3.72) into equation (3.61), a fourth order ordinary differential equation in $Y(y)$ is obtained

$$Y_{mn}^{IV} - 2 \frac{m^2 \pi^2}{a^2} Y_{mn}'' + \left(\frac{m^4 \pi^4}{a^4} - \frac{\rho h \omega_{mn}^2}{D} \right) Y_{mn} = 0 \quad (3.73)$$

The general solution of equation (3.73) is given in reference (30) as:

$$Y_{mn}(y) = c_1 e^{-\alpha y} + c_2 e^{\alpha y} + c_3 \cos \beta y + c_4 \sin \beta y \quad (3.74)$$

where

$$\alpha = \sqrt{\omega_{mn}^2 \frac{\rho h}{D} + \frac{m^2 \pi^2}{a^2}} \quad (a)$$

$$\beta = \sqrt{\omega_{mn}^2 \frac{\rho h}{D} - \frac{m^2 \pi^2}{a^2}} \quad (b)$$

The constants c_1 , c_2 , c_3 and c_4 can be eliminated by application of boundary conditions at $y = 0$ and $y = b$ to give the frequency equations from which ω is determined. Details will not be given here. The equation has been solved for different plate ratios a/b and the results for all possible combinations of clamped, free and simply-supported conditions on $y = 0$ and $y = b$ are given by Leissa (31).

(b) Approximate solution - Rayleigh-Ritz method

When the plate does not have two parallel edges simply supported, no single expression of the form

$$\hat{W}(x,y) = X(x) Y(y)$$

satisfies the plate equation and all the boundary conditions. It is therefore necessary to resort to various approximate methods for this purpose, the method of Rayleigh and Ritz and the finite element method have gained increased popularity in the solution of plate problems with complex geometry, loading and boundary conditions. The general method of Rayleigh and Ritz was described in section 2.5.1. In the application to plates, the series approximation for \hat{W} is taken in the form

$$\hat{W}(x,y) = \sum_{i=1}^I \sum_{j=1}^J X_i(x) Y_j(y) \quad (3.76)$$

The functions $X_i(x)$ and $Y_j(y)$ must be chosen to satisfy any geometric boundary conditions. Leissa (10) has used appropriate beam modal functions for $X(x)$ and $Y(y)$ to determine natural frequencies for several modes for all combinations of clamped, simply supported and free edges. Application of the finite element method to plate problems will be described in the following chapter.

3.7.2 Forced vibration analysis of thin plates

The equation of motion for the forced, damped vibration of a plate is given by equation (3.30).

$$D\nabla^4 W + \rho h \frac{\partial^2 W}{\partial t^2} + c \frac{\partial W}{\partial t} = p(x,y) f(t) \quad (3.30)$$

where $p(x,y)$ is the applied force per unit surface area.

The solution of the above equation can be obtained by normal mode superposition method using the normal modes $\hat{W}(x,y)$, of the undamped system (32). Thus the exact and approximate methods of determining natural frequencies and modes can be extended to the determination of response. For a rectangular plate which is simply supported on two parallel edges ($x = 0$ and $x = a$) the normal modes are given by equation (3.72),

$$\hat{W}(x,y) = Y_{mn}(y) \sin \frac{m\pi x}{a} \quad (3.72)$$

It can be shown (28) that for any combination of homogeneous boundary conditions on $y = 0$ and $y = b$,

$$\int_0^b Y_{mn}(y) Y_{im}(y) dy = 0 \quad i \neq n \quad (3.77)$$

Also the modal functions $Y_{mn}(y)$ must satisfy the differential equation (3.73). We seek a solution for equation (3.30) in the form

$$W(x,y,t) = \sum_m \sum_n Y_{mn}(y) \sin \frac{m\pi x}{a} q_{mn}(t) \quad (3.78)$$

where $q_{mn}(t)$, a principal coordinate, is a function of time. Substituting for W from equation (3.78) in equation (3.30) and using equation (3.73) yields:

$$\sum_m \sum_n \rho h Y_{mn} \sin \frac{m\pi x}{a} \ddot{q}_{mn} + \frac{c}{\rho h} \dot{q}_{mn} + \omega_{mn}^2 q_{mn} = p(x,y) f(t) \quad (3.79)$$

multiplying equation (3.79) by $Y_{ns}(y) \sin \frac{s\pi x}{a}$, integrating over the area of the plate and using equation (3.77) and the orthogonal property of functions $\sin \frac{m\pi x}{a}$, a set of uncoupled equations is obtained: (damping is assumed proportional)

$$\ddot{q}_{mn} + 2 \xi_{mn} \omega_{mn} \dot{q}_{mn} + \omega_{mn}^2 q_{mn} = P_{mn} f(t) \quad (3.80)$$

$m,n = 1,2,\dots$

$$P_{mn} = \int_0^a \int_0^b p(x,y) Y_{mn}(y) \sin \frac{m\pi x}{a} dx dy \quad (3.81)$$

The solution of equation (3.80) may be obtained using the Duhammel integral (section 4.6) and then the complete dynamic response is found by substituting in equation (3.78).

For the response analysis of a plate with general boundary conditions, either The Rayleigh-Ritz (section 2.5.1) or finite element methods (section 2.5.2) may be used.

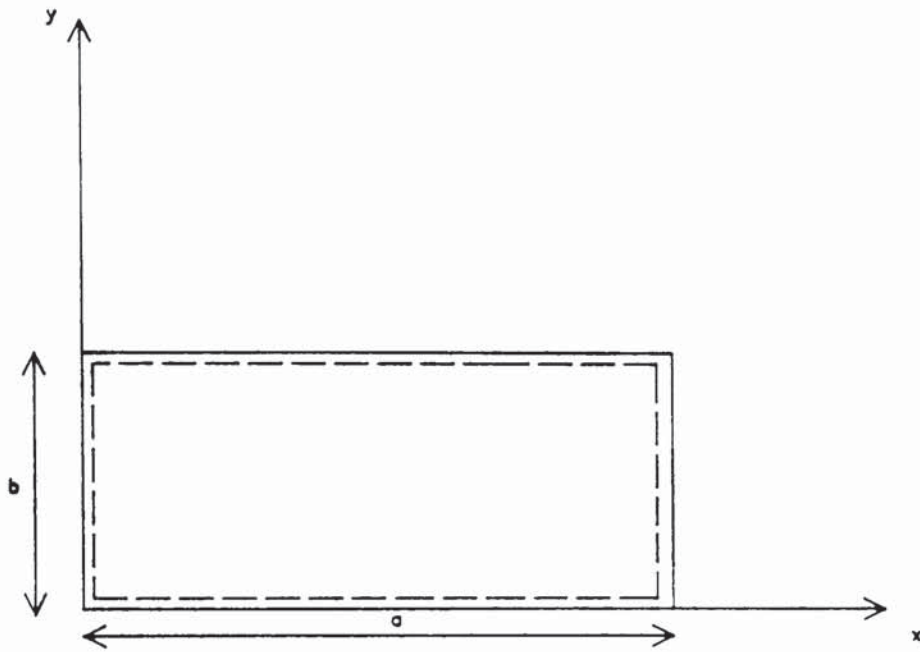


Fig 3.6 Simply supported rectangular plate ,Navier's method

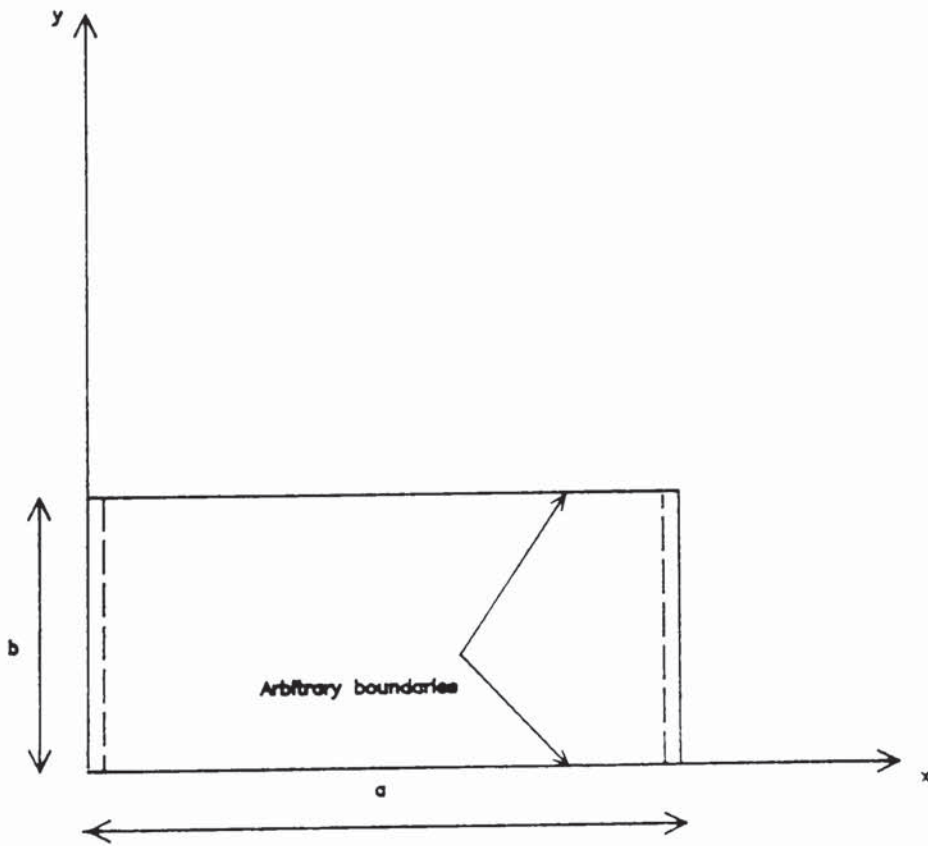


Fig 3.7 Rectangular plate with two opposite edges simply supported , Levy's method



CHAPTER 4

APPLICATIONS OF REISSNER'S PRINCIPLE
IN
FINITE ELEMENT FORMULATION

4.1 INTRODUCTION

Prior to the work of Reissner "on a variational theorem in elasticity" published in 1950 (2), approximate solutions to elasticity problems were obtained by means of the principle of stationary potential energy and the principle of stationary complementary energy. The principle of minimum potential energy is well adapted to elasticity problems that are formulated in terms of displacements. In this theorem, the stress-displacement relations (2.3) are used as equations of constraint which define the components of stress in terms of appropriate displacement derivatives. The corresponding variational equations (Euler-Lagrange equations) are the equilibrium equations in the interior and on the boundary S_σ of the solid. The complementary energy principle is, on the other hand, suited to problems that are formulated in terms of stresses. In this theorem, the differential equations of equilibrium serve to restrict the class of admissible stress variations and the variational equations are equivalent to the system of stress-displacement relations. As a result of the above constraint conditions introduced in the variational principles, the approximate solutions are such that part of the complete system of differential equations is satisfied exactly while the remaining equations are satisfied only approximately. Reissner's principle may be derived from either the potential energy or the complementary energy principle by introducing the appropriate constraint conditions into the variational statement through the Lagrange multiplier technique. The resulting variational theorem simultaneously provides the differential equations of equilibrium, the stress-displacement relations and the boundary conditions. Thus approximate solutions can be obtained in such a manner that there is no preferential treatment of either one of the two kinds of differential equations which occur in practice. In this section,

the current finite element models are briefly reviewed. A new version of Reissner principle is derived which is suitable for finite element analyses of plate and shell type structures. Finally, the essential steps in formulating the mixed element equations are described.

4.2 FINITE ELEMENT MODELS

Variational principles in structural mechanics have acquired a significant practical importance as the basis for numerical methods of analysis. When used in conjunction with finite element techniques, variational principles exhibit comparative advantages pertaining to algebraic simplicity of forming and solving the equations, number of unknowns per nodal point, accuracy of the various types of unknowns, convergence properties, etc. According to a study carried out by Pian and Tong (24) the current finite element models may be divided into four basic types: 1967,

- (i) Compatible models (compatibility satisfied, equilibrium violated).
- (ii) Equilibrium models (equilibrium satisfied, compatibility violated).
- (iii) Hybrid models.
- (iv) Mixed models (equilibrium violated, compatibility violated).

The first class contains the compatible displacement model which is derived from minimum potential energy principle. Based on an assumed displacement field continuous over the entire solid, the principle yields a system of equations with the nodal displacements as unknowns. Although the potential energy principle is the predominant approach to the formulation of finite element equations, it is not always the most convenient approach. In many practical situations, it becomes extremely difficult to choose an element displacement field that will satisfy all the conditions of inter-element displacement continuity. Plate and shell elements, for example, require the continuity of both displacement and its derivatives across the element boundaries. No simple displacement

functions are capable of satisfying these requirements. A modified potential energy functional may be derived for application to finite element analysis. In the new formulation, the displacement functions are chosen independently for each individual element while inter-element compatibility conditions are accommodated by including Lagrange multiplier terms in the functional. In application to finite element analysis, equilibrating tractions are assumed along the interelement boundaries in addition to the assumed continuous displacement fields in each element. This method is thus called a hybrid-displacement method (33). Both compatible and hybrid displacement models produce better results for displacements than stresses.

The second class contains the equilibrium model (34) which is derived from the principle of minimum complementary energy and is based on an assumed equilibrium stress field within and across the element boundaries. It is customary to use stress functions as primary field variables and the nodal values of such variables are the unknowns of the final system of equations. A dual hybrid method can be formulated, for which compatible displacement functions are assumed along the interelement boundaries in addition to the assumed equilibrating stress field in each element (35). According to the above classification hybrid models fall into the third category. The results from the equilibrium and hybrid-stress models are, as one would expect, more in favour of stresses. The fourth method, derived from the Reissner's principle, presented in section (4.4.2) is called the mixed method (3), (36) with nodal values of both displacements and stresses as unknowns. In mixed models, the field variables should only maintain a degree of continuity such that the functional of the variational problem is defined, i.e. it must be finite. Mixed formulation, in general yields a

solution with balanced accuracy in displacements and stresses. It will be seen in the following section that there exists a wide degree of freedom in the application of Reissner's principle to the finite element method.

4.3 DISCRETIZED REISSNER FUNCTIONAL-INTERELEMENT CONTINUITY REQUIREMENTS

In the solution of boundary value problems by approximate methods, the continuity requirements placed on the approximating functions depend on the order of the governing differential equations and its variational formulation. Reissner's principle leads directly to mixed formats of the element force-displacement equations. Because the Euler equations of this functional are the more basic equations of elasticity, with lower order derivatives, the continuity requirements on the assumed fields are of lower order than for the conventional variational principles. In the finite element formulation, the functional for the complete system is comprised of the sum of functionals of (n) individual regions (elements) π^j , such that

$$\pi = \sum_{j=1}^n \pi^j \quad j = 1, 2, \dots, n \quad (4.1)$$

Thus approximating functions must be such that their derivatives up to the highest order occurring in the corresponding Euler equations are continuous within each discrete element. The admissibility on the inter element boundary conditions may be broadened to the degree that the assumed functions shall only possess continuous derivatives in such a manner that the functional of the variational problem is defined (24). The interelement boundary conditions may be further relaxed by considering the displacement continuity or traction reciprocity conditions* as conditions of constraint that can be included in the variational statement by means of Lagrange multiplier terms as additional variables along the element boundary. General

* That is $\{T\}_b = -\{T\}_a$ on S_0 where $\{T\}$ are the boundary tractions and a, b denote the elements at the two sides of the boundary.

discussions of this topic have been made by Prager (37), Pian (24) and by Nemat-Nasser (38).

In accordance with equation (4.1), Reissner's Principle (2.54) can be written in a discretized form as

$$\pi R = \sum \left\{ \int_{V_n} \left[-U_0^* (\sigma) + \{\sigma\}^t [L] \{u\} - \{\bar{F}\}^t \{u\} \right] dV - \int_{S_{\sigma n}} \{\bar{T}\}^t \{u\} dS - \int_{S_{u n}} \{T\}^t (\{u\} - \{\bar{u}\}) dS - B_n \right\} \quad (4.2)$$

where $\{T\} = [1]\{\sigma\}$ represents boundary tractions. V_n indicates the volume of the nth element. For the boundary of the nth element, $S_{\sigma n}$ is the portion over which the surface tractions $\{\bar{T}\}$ are prescribed while over $S_{u n}$ the displacements $\{u\}$ are prescribed. The term B_n , arises from possible jump functions of the derivatives of $\{u\}$ across the interelement boundaries. For example if the displacements $\{u\}$ are continuous, $B_n = 0$ and if $\{u\}$ are not continuous along S_n of the nth element while the surface tractions are in equilibrium with the tractions of the adjacent element, then

$$B_n = \int_{S_n} \{T\}^t \{u\} dS \quad (4.3)$$

The independent variables subject to variations are still $\{\sigma\}$ and $\{u\}$ with subsidiary conditions that $\{T\}$ are in equilibrium along the interelement boundary, i.e.

$$\{T\}_a = - \{T\}_b \quad \text{on } S_n \quad (4.4)$$

where (a) and (b) are the elements at the two sides of the boundary. When tractions are not in equilibrium at the two sides of the boundary, equation (4.4) must be introduced as a condition of constraint.

The corresponding Lagrange multipliers are the boundary displacements $\{\bar{u}\}$ which are independent of the displacements $\{u\}$. Thus if along S_n , $\{u\}$ are discontinuous and $\{T\}$ are non-reciprocal, then

$$B_n = \int_{S_n} \{T\}^t \{u\} dS - \int_{S_n} \{T\}^t \{\bar{u}\} dS \quad (4.5)$$

The independent variables subject to variations are $\{\sigma\}$ and $\{u\}$ in each element, and $\{\bar{u}\}$ along the interelement boundaries. There are still many more versions of the π_R based on the additional variables introduced along the interelement boundaries. These functionals have been studied by Pian and Tong (39).

The functional in Reissner's principle may be transformed to a different form by integrating by parts the second term in the volume integral of equation (4.2). Then

$$\begin{aligned} \pi'_R = & \sum \left\{ \int_{V_n} \left[-U_0^* (\sigma) - ([L] \{\sigma\})^t \{u\} - \{\bar{F}\}^t \{u\} \right] dV \right. \\ & \left. - B'_n - \int_{S_{\sigma_n}} \{\bar{T}\}^t \{u\} dS - \int_{S_{u_n}} \{T\}^t (\{u\} - \{\bar{u}\}) dS \right\} \end{aligned} \quad (4.6)$$

where now

$$B'_n = B_n - \int_{S_n + S_{\sigma_n} + S_{u_n}} \{T\}^t \{u\} dS \quad (4.7)$$

$[L]'$ is the differential operator obtained in the process of integration by parts. It is seen that the new version of Reissner's principle imposes some new continuity on the stresses, but relaxes those on the displacements. This version of the Reissner functional has practical importance in application to plate and shell type structures.

4.3.1 Discretized Reissner's Principle - Beam Bending Problems

For application to beam bending problems, Reissner's Principle in the form of equations (3.16) or (3.17) may be directly employed to formulate the element relationships. The approximate shape functions for the displacement w , and the bending moment M_x , must satisfy the necessary interelement continuity conditions. This follows from the requirement that the functional be defined (20). Therefore, when using the variational principle (3.16), it is necessary to ensure the continuity of w and its slope between elements (C1 continuity). On the other hand, the variational principle (3.17) requires the shape functions to satisfy the displacement (w) continuity only (C0 continuity). Thus the latter formulation permits the use of simpler shape functions. The beam element formulation is described in section (6.2).

4.3.2 Discretized Reissner's Principle - Plate Bending Problems

For thin plates, the expression of π_R , that is equivalent to equation (4.2), is

$$\begin{aligned} \pi_R = & \sum_n \left\{ \int_{A_n} - \left[\frac{6}{Eh^3} (M_x^2 + M_y^2 - 2\nu M_x M_y + 2(1+\nu) M_{xy}^2) \right. \right. \\ & + M_x \frac{\partial^2 W}{\partial x^2} + M_y \frac{\partial^2 W}{\partial y^2} + M_{xy} \frac{\partial^2 W}{\partial x \partial y} \left. \right] dx dy - \int_{A_n} P(x,y) W dx dy - B_n \\ & - \int_{s_{\sigma_n}} (\bar{Q}_n W - \bar{M}_{ns} \bar{W}'_s - \bar{M}_n W'_{,n}) ds - \int_{s_{u_n}} \left[Q_n (W - \bar{W}) - M_{ns} (W'_{,s} - \bar{W}'_{,s}) \right. \\ & \left. - M_n (W'_{,n} - \bar{W}'_{,n}) \right] ds \left. \right\} \quad (4.8) \end{aligned}$$

where B_n depends on the different continuity conditions along the interelement boundaries. The following expression is used if all displacement continuity requirements are to be relaxed along the boundaries:

$$B_n = \int_{s_n} \left[Q_n (W - \bar{W}) - M_{ns} (W'_{,s} - \bar{W}'_{,s}) - M_n (W'_{,n} - \bar{W}'_{,n}) \right] ds \quad (4.9)$$

But when W is continuous and M_n are in equilibrium across the interelement boundary then

$$B_n = - \int_{s_n} M_n W'_{,n} ds \quad (4.10)$$

which accounts for the discontinuity of $W_{,n}$.

A convenient version for finite element implementation of plate bending problems is one which corresponds to equation (4.6) and (4.10), then

$$\begin{aligned}
 \pi'_R = & \sum \left\{ \int_{A_n} -\frac{6}{Eh^3} \left[M_x^2 + M_y^2 - 2\nu M_x M_y + 2(1+\nu) M_{xy}^2 \right] dx dy \right. \\
 & + \int_{A_n} \left[\left(\frac{\partial M_y}{\partial y} + \frac{\partial M_{xy}}{\partial x} \right) \frac{\partial W}{\partial y} + \left(\frac{\partial M_x}{\partial x} + \frac{\partial M_{xy}}{\partial y} \right) \frac{\partial W}{\partial x} \right] dx dy \\
 & - \int_{A_n} P(x,y) W dx dy - \int_{s_n} M_{ns} W'_{,s} ds - \int_{s_{\sigma n}} \left[\bar{Q}_n W - (\bar{M}_{ns} - M_{ns}) W'_{,s} \right. \\
 & \left. - (\bar{M}_n - M_n) W_{,n} \right] ds - \int_{s_{u_n}} \left[Q_n (W - \bar{W}) + M_{ns} \bar{W}'_{,s} + M_n \bar{W}_{,n} \right] ds \left. \right\} \quad (4.11)
 \end{aligned}$$

Which only requires the continuity of W and bending moment components across the element boundaries. Herrmann (3) was the first to use the above principle in the development of a finite element mixed model for static plate bending analysis. The dynamic version of this principle may be simply obtained by including the inertia and time varying forces in the functional. This will be the starting point for the development of mixed dynamic plate elements in this thesis.

4.4 FINITE ELEMENT FORMULATION

4.4.1 General Approach

The finite element method is formulated by approximating the variables in the variational functional in terms of a finite number of unknown parameters. The application of the variational principle then leads to the final matrix equation to be solved. The procedure consists of the following steps:

- 1) Definition of the finite element mesh. Depending on the problem at hand, the complete region (continuum) is subdivided into one, two or three dimensional sub-regions (finite-elements). The elements are separated by imaginary lines or surfaces interconnected at certain nodal points. For the two dimensional continuum, the elements may be of triangular, rectangular or general quadrilateral shapes. An improvement over the straight-sided triangular and rectangular elements are those with curved sides which are more easily adaptable to any given geometry.
2. Modelling of unknown variables. The field variables in the variational functional are represented by interpolating functions and generalized displacements and/or stresses at a finite number of nodal points of each element. In most cases, the interpolating functions must be such that the continuity requirements inside and across the element boundaries are satisfied.
3. Formulating the element equations. On the basis of the assumed functions of (2) above, the energy functional is expressed in terms of element generalized coordinates (displacements

and/or stresses). The application of the variational principle then leads to a set of matrix equations for individual elements. The final matrix equations representing the structure as a whole is then synthesized from element matrices.

4. Solution of the resulting system of equations. The overall matrix equation of the structure is solved for the unknown displacements and/or stresses, after imposing the appropriate geometric and/or mechanical boundary conditions. The solution of equations is a standard procedure in matrix algebra. This as well as the generation of element characteristics and synthesis of system characteristics are performed on a digital computer.

4.4.2 Derivation of the mixed element equations

If we choose to satisfy the displacement boundary conditions with our field variables models the Reissner generalized principle (equation 2.59) in matrix notation becomes:

$$\delta \int_{t_1}^{t_2} \left[\int_V (-\frac{1}{2} \rho \{\dot{u}\}^t \{\dot{u}\} - \frac{1}{2} \{\sigma\}^t [D]^{-1} \{\sigma\} + \{\sigma\}^t [L] \{u\}) dV - \int_V \{F\}_C^t \{u\} dV - \int_{S_\sigma} \{\bar{T}\}_C^t \{u\} dS \right] dt + \int_{t_1}^{t_2} \int_V c \{\dot{u}\}^t \{\delta u\} dV dt = 0 \quad (4.12)$$

Let the displacement and stress fields within an element be represented independently by:

$$\begin{aligned} \{u\} &= [\phi] \{\gamma\} & (a) \\ \{\sigma\} &= [\psi] \{\alpha\} & (b) \end{aligned} \tag{4.13}$$

where $\{u\}$ and $\{\sigma\}$ are vectors that contain all possible displacement and stress components, within the element, in the direction of the coordinate axes. $[\phi]$ and $[\psi]$ are matrices of position which in general are of different order, and $\{\gamma\}$ and $\{\alpha\}$ are the generalized parameters. The nodal values of the displacements and stresses will be

$$\{u\}_e = [A] \{\gamma\}, \quad \{\sigma\}_e = [P] \{\alpha\} \tag{4.14}$$

For a two dimensional element such as the one in figure (4.1), the nodal displacements and stresses are:

$$\begin{aligned} \{u\}_e^t &= [u_1, v_1, \dots, u_4, v_4] \\ \{\sigma\}_e^t &= [\sigma_{x_1}, \sigma_{y_1}, \tau_{xy_1}, \dots, \sigma_{x_4}, \sigma_{y_4}, \tau_{xy_4}] \end{aligned}$$

From equations (4.13) and (4.14), the element displacement and stresses will be:

$$\begin{aligned} \{u\} &= [\phi] [A]^{-1} \{u\}_e = [N_u] \{u\}_e & (a) \\ \{\sigma\} &= [\psi] [P]^{-1} \{\sigma\}_e = [N_\sigma] \{\sigma\}_e & (b) \end{aligned} \tag{4.15}$$

If the interpolating functions $[N_u]$ and $[N_\sigma]$ satisfy the interelement continuity requirements, then equation (4.12) may be utilized to derive the element matrices. Thus substituting the mixed variable model equations (4.15) into equation (4.12), we get for an element:

$$\begin{aligned}
& \delta \int_{t_1}^{t_2} \left\{ \int_{V_n} (-\frac{1}{2} \rho \{\dot{u}\}_e^t [N_u]^t [N_u] \{\dot{u}\}_e - \frac{1}{2} \{\sigma\}_e^t [N_\sigma]^t [D]^{-1} [N_\sigma] \{\sigma\}_e \right. \\
& + \{\sigma\}_e^t [N_\sigma]^t [L] [N_u] \{u\}_e) dV_n - \int_{V_n} \{F\}^t [N_u] \{u\}_e \\
& \left. + \int_{S_\sigma} \{\bar{T}\}^t [N_u] \{u\}_e dS_n \right\} dt + \int_{t_1}^{t_2} \int_{V_n} c \{\dot{u}\}_e^t [N_u]^t [N_u] \{\delta u\}_e \\
& \qquad \qquad \qquad dV_n dt = 0 \quad (4.16)
\end{aligned}$$

Now taking variations with respect to the generalized parameters $\{u\}_e$ and $\{\sigma\}_e$ yields:

$$\begin{aligned}
& \int_{t_1}^{t_2} \left[\{\delta u\}_e^t [m] \{\ddot{u}\}_e - \{\delta \sigma\}_e^t [k_{\sigma\sigma}] \{\sigma\}_e + \{\delta \sigma\}_e^t [k_{\sigma u}] \{u\}_e \right. \\
& \left. + \{\delta u\}_e^t [k_{\sigma u}]^t \{\sigma\}_e - \{\delta u\}_e^t \{r\}_e \right] dt + \int_{t_1}^{t_2} \{\delta u\}_e^t [c] \{\dot{u}\}_e dt = 0 \quad (4.17)
\end{aligned}$$

collecting terms in $\{\delta u\}_e$ and $\{\delta \sigma\}_e$ and equating to zero yields:

$$\int_{t_1}^{t_2} \{\delta u\}_e^t ([m] \{\ddot{u}\}_e + [k_{\sigma u}]^t \{\sigma\}_e + [c] \{\dot{u}\}_e - \{r\}_e) dt = 0 \quad (a)$$

and

$$\int_{t_1}^{t_2} [\{\delta \sigma\}_e^t (-[k_{\sigma\sigma}] \{\sigma\}_e + [k_{\sigma u}] \{u\}_e)] dt = 0 \quad (b) \quad (4.18)$$

therefore:

$$[m]\{\ddot{u}\}_e + [k_{\sigma u}]^t \{\sigma\}_e + [c]\{\dot{u}\}_e = \{r\}_e \quad (a)$$

and

(4.19)

$$[k_{\sigma u}]\{u\}_e - [k_{\sigma\sigma}] \{\sigma\}_e = \{0\}$$

where

$$[k_{\sigma\sigma}] = \int_{V_n} [N_\sigma]^t [D]^{-1} [N_\sigma] dV \quad (a)$$

$$[k_{\sigma u}] = \int_{V_n} [N_\sigma]^t [L] [N_u] dV \quad (b)$$

$$[m] = \int_{V_n} \rho [N_u]^t [N_u] dV \quad (c) \quad (4.20)$$

$$[c] = \int_{V_n} c [N_u]^t [N_u] dV \quad (d)$$

$$\{r\}_e = \int_{V_n} [N_u]^t \{F\}_c dV + \int_{S_{\sigma n}} [N_u]^t \{\bar{T}\}_c dS \quad (e)$$

The mixed element matrices and load vector in equation (4.20) can be assembled for the overall structure, in accordance with the rules of assembly. Thus after introducing the boundary conditions the mixed equations for the assembled structure are:

$$[M]\{\ddot{u}\}_o + [K_{\sigma u}]^t \{\sigma\}_o + [C]\{\dot{u}\}_o = \{R\} \quad (a)$$

(4.21)

$$[K_{\sigma u}]\{u\}_o - [K_{\sigma\sigma}]\{\sigma\}_o = \{o\} \quad (b)$$

where $\{u\}_0$ and $\{\sigma\}_0$ are the unknown stress and displacement vectors. For the dynamic case we solve (4.21 b) for $\{\sigma\}_0$ and substitute into (4.21a), thus,

$$\{\sigma\}_0 = [K_{\sigma\sigma}]^{-1} [K_{\sigma u}] \{u\}_0 \quad (4.22)$$

and

$$[M]\{\ddot{u}\}_0 + [K_{\sigma u}]^t [K_{\sigma\sigma}]^{-1} [K_{\sigma u}] \{u\}_0 + [C]\{\dot{u}\}_0 = \{R\} \quad (4.23)$$

or simply

$$[M]\{\ddot{u}\}_0 + [K]\{u\}_0 + [C]\{\dot{u}\}_0 = \{R\}$$

where

$$[K] = [K_{\sigma u}]^t [K_{\sigma\sigma}]^{-1} [K_{\sigma u}] \quad (4.24)$$

is a full symmetric matrix. The solution of equation (4.23) yields the time history of displacements. The stresses may be obtained by substituting for the displacements into equation (4.22).

In the case of undamped free vibrations, $[C]$ and $\{R\}$ are zero, therefore, equations (4.21) becomes:

$$-\omega^2 [M] \{\hat{u}\}_0 + [K_{\sigma u}]^t \{\hat{\sigma}\}_0 = \{0\} \quad (a) \quad (4.25)$$

$$[K_{\sigma u}] \{\hat{u}\}_0 - [K_{\sigma\sigma}] \{\hat{\sigma}\}_0 = \{0\} \quad (b)$$

where it is assumed that $\{u\}_0$ and $\{\sigma\}_0$ vary harmonically with time, i.e.

$$\{u\}_0 = \{\hat{u}\}_0 \sin \omega t \quad (a) \quad (4.26)$$

$$\{\sigma\}_0 = \{\hat{\sigma}\}_0 \sin \omega t \quad (b)$$

The eigenvalue equation may be obtained by solving (4.25 b) for $\{\hat{\sigma}\}$ and substituting into (4.25 a), thus:

$$[K] \{\hat{u}\}_0 - \omega^2 [M] \{\hat{u}\}_0 = \{0\} \quad (4.27)$$

where

$$[K] = [K_{\sigma u}]^t [K_{\sigma\sigma}]^{-1} [K_{\sigma u}] \quad (4.28)$$

conversely, it is possible to write the eigenvalue equation in terms of stress vector $\{\sigma\}_0$. Solving (4.25 a) for $\{\hat{u}\}_0$ and substituting in (4.25 b) yields:

$$[K^*] \{\hat{\sigma}\}_0 - \omega^2 [K_{\sigma\sigma}] \{\hat{\sigma}\}_0 = \{0\} \quad (4.29)$$

where

$$[K^*] = [K_{\sigma u}] [M]^{-1} [K_{\sigma u}]^t \quad (4.30)$$

This represents the eigenvalue equation in terms of stress $\{\hat{\sigma}\}_0$. Either equations (4.27) or (4.29) may be solved to yield the system eigenvalues (ω) and eigenvectors ($\{\hat{u}\}_0$ or $\{\hat{\sigma}\}_0$).

It should be noted that the number of parameters in $\{\hat{u}\}_0$ is in general different from that in $\{\hat{\sigma}\}_0$, (i.e. the number of displacement degrees of freedom is different from the number of stress degrees of freedom). This affects the rank of the matrices involved in equations (4.28) and (4.30). If the number of parameters in $\{\hat{\sigma}\}_0$ exceeds that of $\{\hat{u}\}_0$, matrix $[K^*]$ (Eqn. 4.30) will be deficient in rank and the eigenvalue equation (4.29) yields extra very low or zero

eigenvalues which have no physical significance. The converse is also possible (i.e. when the number of parameters in $\{\hat{u}\}_0$ exceeds that of $\{\hat{\sigma}\}_0$, matrix $[K]$ in (4.28) becomes deficient in rank). It is therefore advisable to attempt the solution of the eigenvalue equation with smaller matrices. This ensures that only the true system eigenvalues are obtained, thus overcoming the need to compute unwanted zero eigenvalues.

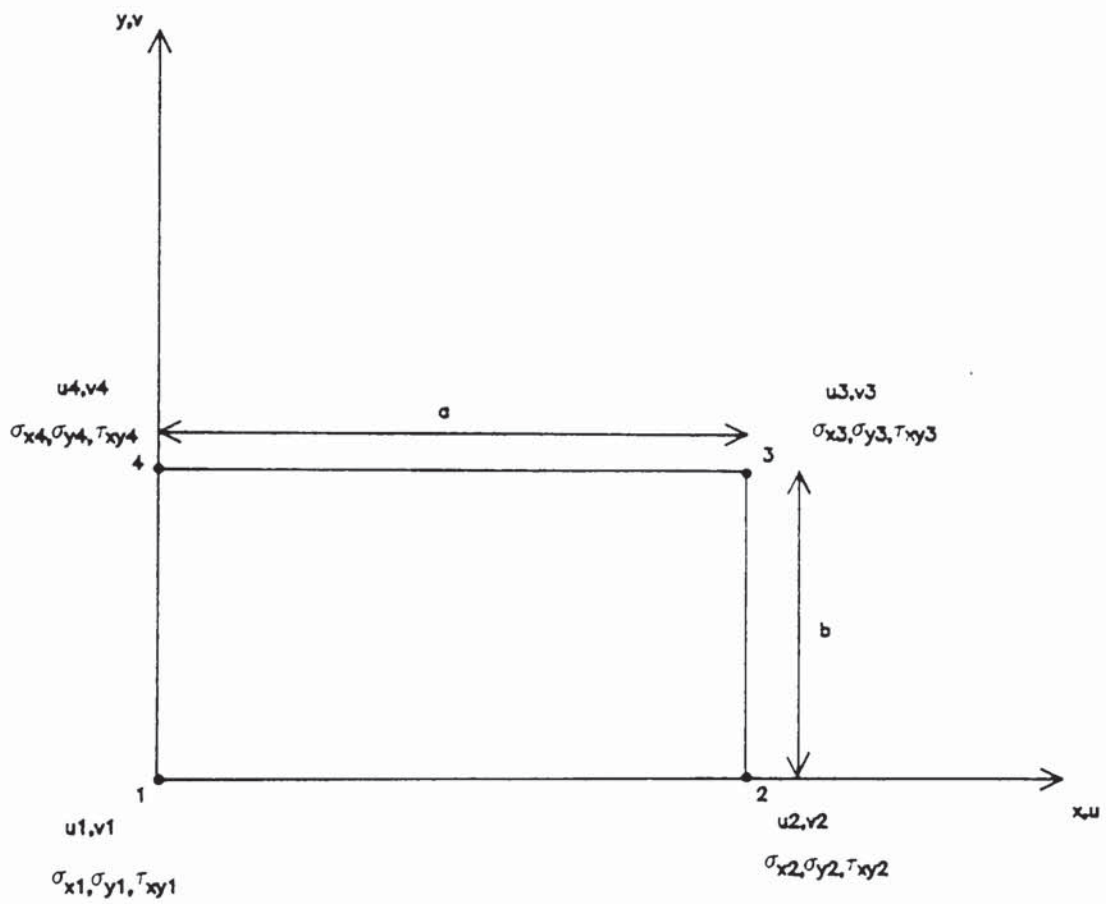


Fig 4.1 A rectangular plane stress/strain finite element

4.5 EVALUATION OF THE DAMPING MATRIX

4.5.1 Importance of Damping

Before discussing methods of solving the equations of motion, it is worth considering the importance of the damping matrix. Damping is the removal of energy from a vibratory system. The energy lost is either transmitted away from the system by some mechanism of radiation or dissipated within the system. Damping is responsible for the eventual decay of free vibrations and is of primary importance in controlling response amplitudes under conditions of steady state resonance excitation. Most structures are lightly damped (1% of the critical damping) and if they are subject to periodic force containing at least one frequency component coinciding with a structural resonance then the damping will be important. However, if the excitation is slightly off-resonance, then the response will be controlled almost entirely by the distribution of mass and stiffness properties.

The energy loss mechanisms in practical structures may be basically divided into external and internal ones. The acoustic radiation, fluid flow resistance and coulomb friction are some examples of models of external energy dissipation sources. Internal friction (damping) in materials is caused by different physical micromechanisms (40). In metals, for instance, these mechanisms include thermoelasticity, grain boundary viscosity, eddy current effects and to some extent electronic effects. For most non-metallic materials, little is known about such physical mechanisms. However, for one important class of these, namely, polymers and elastomers considerable information has been obtained as the rheological behaviour of such materials may be adequately represented

by simple mathematical models (41).

4.5.2 The element damping matrix

The finite element method can be used to generate a damping matrix for a structure where definite damping mechanisms can be recognized. If damping is viscous then equation (4.20 d) yields the so-called consistent damping matrix.

$$[c] = \int_{V_n} c_n [N_u]^t [N_u] dV_n \quad (4.20 d)$$

Viscous damping coefficients (c) equivalent to a number of different damping mechanisms can be determined by measuring the energy dissipated per cycle (E) in a dashpot undergoing sinusoidal motion $u_0 \sin \omega t$. The expression for E is (41)

$$E = \pi c \omega u_0^2 \quad (4.31)$$

The overall damping matrix C is constructed from contributions of all the elements. That is

$$[C] = \sum_n \int_{V_n} c_n [N_u]^t [N_u] dV_n \quad (4.32)$$

In practice, it is very difficult, if not impossible, to determine for general finite element assemblage the element damping parameters, in particular because the damping properties are frequency dependent. For this reason, matrix $[C]$ is in general not assembled from element damping matrices. Instead, direct methods are available (42, 43)

which incorporate the mass and stiffness matrices of the complete assemblage together with experimental results on the amount of damping in order to derive an orthogonal damping matrix for the overall structure. A knowledge of modal damping ratios is thus a prerequisite. Some experimental techniques for identification of modal parameters in lightly damped structures with uncoupled modes are described in Reference (41). Wilson and Penzien (43) have presented a direct method for the numerical evaluation of an orthogonal damping matrix. This method is applicable to lightly damped structures where the effect of modal coupling can be ignored. The final matrix is expressed as the sum of a series of matrices, each of which produces damping in a particular mode. The procedure is described in Appendix A.

4.6 SOLUTION OF DYNAMIC EQUILIBRIUM EQUATIONS

Having established the system characteristics matrices and load vector, we can proceed with the solution of dynamic equations,

$$\left[M \right] \{\ddot{U}\} + \left[K \right] \{U\} + \left[C \right] \{\dot{U}\} = \{R(t)\} \quad (4.33)$$

$\{U\}$ is the overall displacement vector and $\{R(t)\}$ is the overall load vector. The various forms of force inputs are shown in figure (4.2). The analysis of the response of any specified structural system to a prescribed dynamic loading is defined as a deterministic analysis. The non-deterministic analysis, on the other hand, corresponds to the analysis of response to a random dynamic loading. Only the deterministic analysis is considered here.

There are basically two methods of solving these equations: direct step-by-step integration or the mode superposition method (44). In the first method, the response is obtained at a series of sequential time intervals whereas the mode superposition method requires the application of a coordinate transformation prior to the numerical integration. This causes the equations to become uncoupled in the new coordinates.

The choice of which method depends on both the type of force input and the required form of response. It has been found (45) that direct step-by-step integration is most useful when only the initial transient response is required for a small number of loading cases. The normal mode superposition is preferred when there are many loading cases or when the steady state response is required.

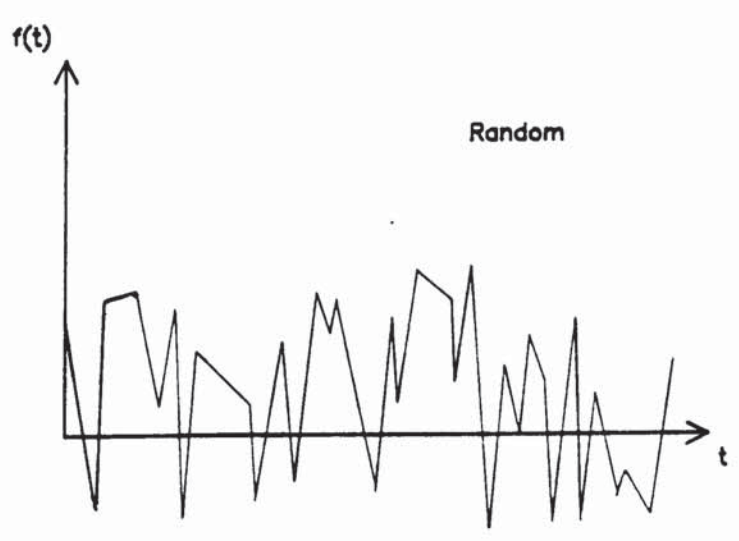
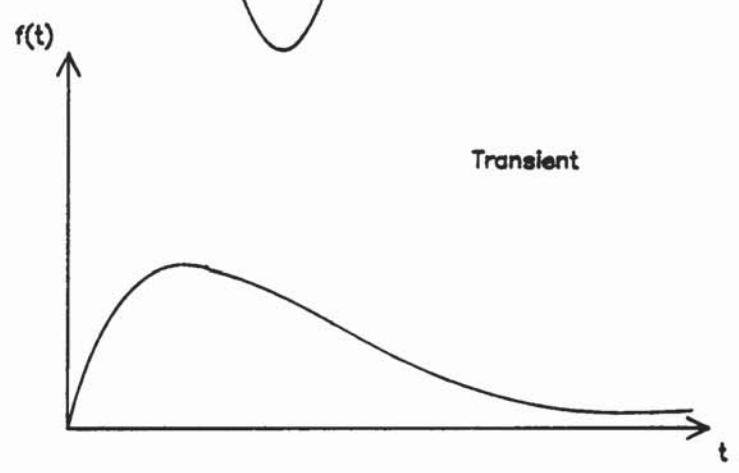
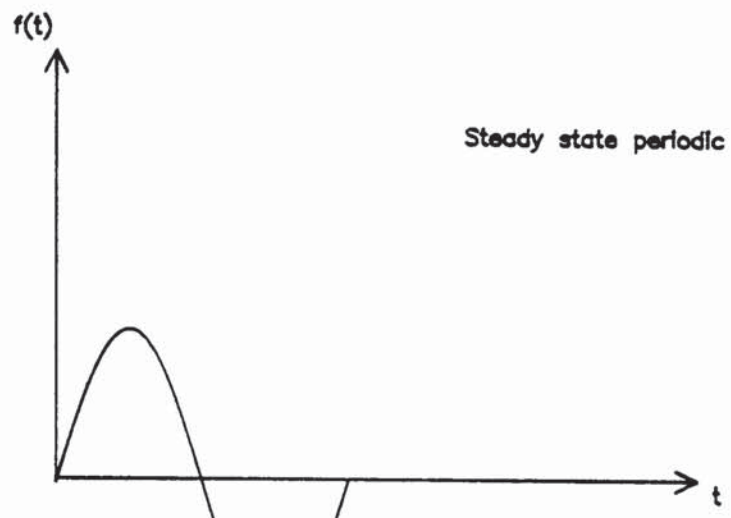


Fig 4.2 Characteristics of typical dynamic loading.

4.6.1 Direct integration method - Wilson α method

In this method, the equations in (4.33) are integrated using a numerical step-by-step procedure. A polynomial is assumed to represent the variation of displacements, velocities and acceleration within each time interval Δt . In the solution process, it is assumed that the displacement, velocity and acceleration vectors at time 0, denoted by $\{U\}_0$, $\{\dot{U}\}_0$ and $\{\ddot{U}\}_0$, respectively are known. The time span under consideration, T , is subdivided into n equal time intervals Δt (i.e. $\Delta t = \frac{T}{n}$) and the integration scheme is employed to establish an approximate solution at times 0, Δt , $2\Delta t$, ..., t , $t + \Delta t$, ..., T . Algorithms are derived by assuming that the solutions at time 0, Δt , $2\Delta t$, ..., t are known and that the solution at time $t + \Delta t$ is required next. The calculations performed to obtain the solution at time $t + \Delta t$ are typical for calculating the solution at time Δt later than considered so far, and thus establish the general algorithm which can be used to calculate the solution at all discrete time points. Some commonly used effective step-by-step solution methods are presented in reference (44). An important consideration is the choice of time interval, Δt , which is somewhat arbitrary, but should be less than the time period of the highest natural frequency to enable the complete transient response to be determined. Thus

$$\Delta t \leq \Delta t_{cr} = \frac{T_N}{\pi}$$

where T_N is the smallest period of the finite element assemblage and N is the order of the finite element system.

The Wilson θ method

The step-by-step technique of Wilson θ (44) is one of the most popular techniques for the integration in time of the equation of motion of linear structural systems.

One of the main features of the Wilson θ method is that it can be made unconditionally stable, i.e. however large the time step length Δt used in the time integration, the predicted response remains bounded. The cost of a direct integration analysis is directly proportional to the number of time steps required for solution. In the present work, the computing time and computer storage are of primary concern. Thus an unconditional stable scheme provides an attractive method of solution. The effect of time step size, Δt on numerical stability and solution accuracy is demonstrated in Chapter 8.

In Wilson θ method, a linear variation of acceleration from time t to time $t + \theta \Delta t$ is assumed, where $\theta \geq 1.0$. For unconditional stability, it is required that $\theta \geq 1.37$ and usually $\theta = 1.40$ is employed. The acceleration at any time in the interval ($t, t + \theta \Delta t$) is

$$\{\ddot{U}\}_{t+\tau} = \{\ddot{U}\}_t + \frac{\tau}{\theta \Delta t} (\{\ddot{U}\}_{t+\theta \Delta t} - \{\ddot{U}\}_t) \quad (4.35)$$

where $0 \leq \tau \leq \theta \Delta t$

Integrating (4.35) yields:

$$\{\dot{U}\}_{t+\tau} = \{\dot{U}\}_t + \{\ddot{U}\}_t \tau + \frac{\tau^2}{2\theta \Delta t} (\{\ddot{U}\}_{t+\theta \Delta t} - \{\ddot{U}\}_t) \quad (4.36)$$

and

$$\{U\}_{t+\tau} = \{U\}_t + \{\dot{U}\}_t \tau + \frac{1}{2} \{\ddot{U}\}_t \tau^2 + \frac{1}{6\theta\Delta t} \tau^3 (\{\ddot{U}\}_{t+\theta\Delta t} - \{\ddot{U}\}_t) \quad (4.37)$$

Using (4.36) and (4.37), we have, at time $t + \theta\Delta t$

$$\{\dot{U}\}_{t+\theta\Delta t} = \{\dot{U}\}_t + \frac{\theta\Delta t}{2} (\{\ddot{U}\}_{t+\theta\Delta t} + \{\ddot{U}\}_t) \quad (4.38)$$

$$\{U\}_{t+\theta\Delta t} = \{U\}_t + \theta\Delta t \{\dot{U}\}_t + \frac{\theta^2\Delta t^2}{6} (\{\ddot{U}\}_{t+\theta\Delta t} + 2\{\ddot{U}\}_t) \quad (4.39)$$

from which we can solve for $\{\ddot{U}\}_{t+\theta\Delta t}$ and $\{\dot{U}\}_{t+\theta\Delta t}$ in terms of $\{U\}_{t+\theta\Delta t}$

$$\{\ddot{U}\}_{t+\theta\Delta t} = \frac{6}{\theta^2\Delta t^2} (\{U\}_{t+\theta\Delta t} - \{U\}_t) - \frac{6}{\theta\Delta t} \{\dot{U}\}_t - 2\{\ddot{U}\}_t \quad (4.40)$$

and

$$\{\dot{U}\}_{t+\theta\Delta t} = \frac{3}{\theta\Delta t} (\{U\}_{t+\theta\Delta t} - \{U\}_t) - 2\{\dot{U}\}_t - \frac{\theta\Delta t}{2} \{\ddot{U}\}_t \quad (4.41)$$

Now the equilibrium equations (4.33) are considered at time $t + \theta\Delta t$, i.e.

$$[M]\{\ddot{U}\}_{t+\theta\Delta t} + [C]\{\dot{U}\}_{t+\theta\Delta t} + [K]\{U\}_{t+\theta\Delta t} = \{R\}_{t+\theta\Delta t} \quad (4.42)$$

where

$$\{R\}_{t+\theta\Delta t} = \{R\}_t + \theta (\{R\}_{t+\Delta t} - \{R\}_t) \quad (4.43)$$

substituting (4.40) and (4.41) into (4.42), an equation is obtained from which $\{U\}_{t+\theta\Delta t}$ can be solved. Then substituting $\{U\}_{t+\theta\Delta t}$ into (4.40) we obtain $\{\ddot{U}\}_{t+\theta\Delta t}$, which is used in (4.35), (4.36) and (4.37), all evaluated at $\tau = \Delta t$ to calculate $\{\ddot{U}\}_{t+\theta\Delta t}$, $\{\dot{U}\}_{t+\Delta t}$, and $\{U\}_{t+\Delta t}$.

The complete algorithm used in the integration is given in reference (44).

4.6.2 Mode-superposition method - Duhammel integral

In this method, the response of the general system to prescribed time-dependent forces is obtained as a sum of contributions from individual modes. The system coordinates are transformed to a new set of coordinates in order to obtain new system stiffness, mass and damping matrices which have a smaller bandwidth than the original system matrices. In systems with proportional damping an effective transformation matrix is the modal matrix which contains the eigenvectors of the free vibration equation, i.e.

$$\{U\} = [\hat{U}] \{q\} \quad (4.44)$$

If (4.44) is used to transform the variables (displacement, etc.) in equation (4.33) from the original set $\{U\}$ to a new set $\{q\}$, it can be shown that the equations in terms of the transformed variables are uncoupled. (Equation 4.45)

$$\ddot{q}_r + 2 \zeta_r \omega_r \dot{q}_r + \omega_r^2 q_r = \frac{R_r(r)}{m_r} \quad (4.45)$$

$$R_r(r) = \{\hat{U}\}_r^t \{R\} \quad r = 1, 2, \dots, N$$

Each equation can then be solved as a single degree of freedom problem. The solution to equations (4.45) is obtained by evaluating the Duhammel integral which is given by

$$q_r(t) = \frac{1}{m_r \omega_{D_r}} \int_0^t R_r(\tau) e^{-\zeta_r \omega_r (t-\tau)} \sin \omega_{D_r} (t-\tau) d\tau$$

$$+ e^{-\zeta_r \omega_r t} \left[\frac{\dot{q}_r(0) + q_r(0) \zeta_r \omega_r}{\omega_{D_r}} \sin \omega_{D_r} t + q_r(0) \cos \omega_{D_r} t \right] \quad (4.46)$$

where $\omega_{D_r} = \omega_r \sqrt{1 - \zeta_r^2}$ (4.47)

and $q_r(0)$, $\dot{q}_r(0)$ represent the initial modal displacement and velocity. These can be obtained from the specified initial displacements $\{U\}_0$ and velocity $\{\dot{U}\}_0$ expressed in the original geometric coordinates as follows for each modal component

$$q_r(0) = \frac{\{\hat{U}\}_r^t [M] \{U\}_0}{m_r} \quad (a)$$

$$\dot{q}_r(0) = \frac{\{\hat{U}\}_r^t [M] \{\dot{U}\}_0}{m_r} \quad (b)$$
(4.48)

When the response for each mode $q_r(t)$ has been determined from equation (4.46), the displacements expressed in original coordinates are given by the normal coordinate transformation, equation (4.44).

In summary, the response analysis by mode superposition requires

- (i) The solution of the eigenvalue and eigenvectors of the problem in (4.27).
- (ii) The solution of the decoupled equilibrium equations in (4.45).
- (iii) The superposition of the response in each eigenvector as given by (4.44).

4.6.3 Comparison between mode superposition and direct integration methods

In the last two sections, the methods of direct integration and mode superposition were presented which can be used in the solution of dynamic equilibrium equations of (4.33). The solutions obtained using either procedures are identical, within the numerical errors of the time integration scheme. It can therefore be said, that the choice between mode superposition analysis and direct integration is only one of numerical effectiveness. The effectiveness of a mode superposition procedure depends on the number of modes that must be included in the analysis. It has been shown by experience that for many types of practical loading (e.g. earthquake), only a fraction of the total number of decoupled equations need be considered, in order to obtain a good approximation to the actual response of the system. This means that only the first p equilibrium equations in (4.45) need be used, and that only the lowest p eigenvalues and the corresponding eigenvectors need be solved. The summation in (4.44) is carried out in the first p modes ($p \ll N$).

In general the finite element analysis approximates the lowest exact frequency accurately, little or no accuracy can, however, be expected in approximating the higher frequencies and mode shapes. Thus, there is usually little justification for including the response corresponding to higher modes in the analysis. If the lower modes of a finite element system are predicted accurately, little response is calculated in the higher modes and the inclusion of the system high-frequency response will not seriously affect the accuracy of the solution.

From the above discussion it can be concluded that the mode

superposition procedure may be more advantageous to direct integration. Significant saving in computational time can be achieved by calculating only the response for the lower modes. As the response corresponding to higher modes is in most instances inaccurate, there is no advantage in computing the higher modes of the system. A direct integration method can also be used to integrate only the first p equations in (4.45) and neglect the high frequency response of the system. This may be achieved by using an unconditionally stable scheme (Wilson θ for example) and selecting an integration time step Δt , which is much larger than the integration step used with a conditionally stable scheme.

In the present work, computer subroutines for the direct integration and mode superposition methods are provided. The subroutines can be called in the main program routine to solve the equilibrium equations.

CHAPTER 5

SURVEY OF LITERATURE ON
PLATE ELEMENTS

5. SURVEY OF LITERATURE ON PLATE ELEMENTS

Much effort has been devoted to the development of finite elements for the bending of plates. Most of this effort has been oriented towards the classical poisson-Kirchhoff theory of bending, which neglects the effect of the transverse shear deformation. The Kirchhoff assumption reduces the number of independent variables in the variational statement but introduces higher order derivatives in the formulation of plate elements. The continuity requirements imposed by this theory on "displacement" finite element models has prevented the development of simple and natural elements. Because of this an exceptionally wide variety of alternative formulation has been proposed. A survey by Gallagher (46) shows the extensive amount of literature on the subject. Some of the finite element models which have been developed in the past for the analysis of thin plates are quite briefly summarized, pointing out their advantages and shortcomings.

In the application of the finite element method to thin plate flexure, reliable and accurate formulations are available for assumed displacement (compatible) models obtained by means of potential energy principle. However, the construction of a fully compatible element is rather complicated and involves nodal derivative degrees of freedom of order greater than one. Thus the interelement compatibility inevitably leads to extensive algebraic operations in the formation of the basic element stiffness coefficients and consequently to large storage requirements and computational time. A number of investigators have developed displacement compatible (conforming) models for plate analysis. Bogner, Fox and Schmit (47) developed rectangular elements with 16 degrees of freedom, i.e. with W , $W_{,x}$, $W_{,y}$, and $W_{,xy}$ at each corner as generalized coordinates.

In this case, the displacement W and the normal slope $W_{,n}$ all vary as cubic functions along each edge, hence the interelement compatibility is satisfied.

Butlin and Leckie (48), and Mason (49) also proposed some other conforming rectangular elements. Later Cowper et al. (50) presented a general triangular element suitable for plates with arbitrary boundary shapes. The element has 18 degrees of freedom with the transverse deflection and its first and second derivatives appearing as generalized coordinates at each vertex. The element is reported to be more accurate than the conforming triangular ones previously developed by Bazeley et al. (51) and by Clough and Toucher (52). But a higher order polynomial is used to represent the displacement variation within the element.

There is a very serious drawback in using the conforming elements for practical engineering purposes such as plates with varying thickness, plates with stiffeners and plates meeting at angles. The difficulty arises since $W_{,xy}$ and other higher derivatives (strains) appear as nodal degrees of freedom. At a node where there is a change in section or a stiffener then it is wrong to require strain continuity.

The difficulties associated with compatible displacement functions have led to several attempts at ignoring the complete slope continuity while still preserving the other necessary criteria for solution convergence. Therefore non-conforming plate bending elements may be formulated which require simpler displacement fields. Since the "lower bound" solution characteristics of a rigorous minimum potential energy principle is lost, the convergence of such elements is not obvious and should be proved either by the

application of the patch test (20) or by comparison with the finite difference algorithms. Successful application of several non-conforming elements have been reported by Bazelay et al. (51). Henshell et al. (9), in particular, developed a family of curvilinear plate bending elements with non-conformable shape functions, for plate vibration and stability tests. Their basic element is a quadrilateral with four nodes but the extensions to this element provide for mid-side nodes making eight and twelve nodes in all and enabling the element to have curved sides. The elements may be used in very general folded plate structures. They concluded that the 8-node element performance was superior to the other two.

By abandoning the Kirchhoff assumption, the interelement compatibility requirement is no longer a serious problem. In the principle of minimum potential energy for plate bending, the rotation angles are used as independent variables in addition to normal deflection (53). But it is known that the so-called thick plate theory does not give reliable solutions for thin plate problems. The difficulty lies on the existence of severe constraints because of the condition of zero transverse shear strain. To capture the behaviour of thin plate theory, Wempner et al. (54) introduced the concept of "discrete Kirchhoff hypothesis" in which the constraint of zero shear strains is imposed at a discrete number of points. The method is effective, but the implementation tends to be somewhat complicated. Some improvements over this have been proposed by Fried (55). On the other hand, reduced integration by Zienkiewicz et al. (56) and by Pawsey and Clough (57) utilizes a lower order of integration and has proved to be very successful in relaxation of constraints on the transverse shear strains.

These elements are based on the assumed-displacement method, but have been shown to be equivalent to elements derived from a mixed formulation (58). An accurate quadrilateral element for thick and thin plates has been developed by Zienkiewicz et al. (56). This element possesses eight node-four corner and four mid-side with the basic three degrees of freedom per node. The transverse displacement and rotation shape functions are selected from 'serendipity' family (20). Two by two Gaussian quadrature is an essential requirement for good performance of the element.

Difficulties in the establishment of admissible displacement fields may be avoided by resorting to complementary or mixed variational principles. Equilibrium elements are based on assumed stress fields and the complementary energy principle. Forces, not displacements, are the primary unknowns of the assembled structure. Displacements are obtained by means of the stress-strain relations and integration of the strain-displacement relations.

The solution for displacements depends on the chosen integration path and in general is not a unique solution. Morely (59) has developed triangular equilibrium elements using the unknown stress resultants (values of stress function) as generalized coordinates. Fraeijs de Veubeke and Sander (50) formulated an equilibrium model which has generalized displacements as unknowns in the final matrix equations.

The specific feature of the mixed model in finite element method was first demonstrated by Herrmann (61), (3). He used the Reissner principle to develop two triangular plate elements. The first element is based on linear variation in W and in the three stress couples, while the second is based on linear variation in W and

constant moment distributions. The former has the corner values of W , M_x , M_y , and M_{xy} as unknowns, hence it has twelve degrees of freedom, the latter has the corner values of W and edge values of W, n as unknown, hence it has only six degrees of freedom.

Herrmann's second plate bending element was particularly remarkable for its algebraic simplicity and gave fairly reasonable results in the distribution of moments. The transverse displacement was, however, predicted with less accuracy, leaving room for some improvements. Based on a similar formulation, Visser (4) developed a triangular plate element with six nodes based on a parabolically varying lateral displacement distribution combined with a linearly varying moment distribution, within each element. The element has twelve degrees of freedom and is suitable for thin plate problems only.

Tahiani (62) presented two mixed elements, by considering linear distribution for the transverse displacement and moments, and parabolic variations for the transverse displacement and moments respectively. The concept of area-natural coordinates was used for the first time in a mixed formulation and the shape functions were formed in terms of these natural coordinates.

Mixed formulations for flat plates of rectangular shape were made by Kikuchi and Ando (6). The transverse displacement is assumed to vary linearly. M_x and M_y are assumed constant within the element and they are expressed in terms of normal moments along the sides of the rectangle. The element has eight degrees of freedom and is compatible with Herrmann triangular element (3).

Bron and Dhatt (63) made a detailed study of the influence of various types of mesh subdivision on the convergence properties of the mixed elements in references (61), (62). They showed that certain types of subdivision for the mixed triangular elements lead to wrong solutions. In an attempt to overcome these shortcomings, Bron and Dhatt (63) proposed general quadrilateral shape elements. The elements were reported to give excellent precision for moments and displacements.

Only a few investigations have been published on mixed models in plate dynamics. Cook (5) developed a triangular thin plate element which was tested in the solution of dynamic and buckling problems. The results, although converging to the correct answers were disappointing due to the slow rate of convergence. Mota Soares (7) developed an isoparametric linear element for moderately thick plates and the results compared favourably with other mixed and displacement models. Reddy and Tsay (8) formulated linear and quadratic isoparametric elements for vibration of thin plates. Each element has three degrees of freedom (the transverse displacement and two normal moments) at each node. Despite the simplicity, the elements yield good accuracy for frequencies.

This literature survey highlights the ability of mixed formulation in generating simple and efficient plate finite elements. The works by Kikuchi and Ando (6) and by Reddy and Tsay (8) show that in general, quadrilateral type elements are more accurate and reliable than triangles. In particular the simple formulation of isoparametric elements prompted us to develop an eight node quadrilateral element for the solution of free and forced plate vibration problems.

CHAPTER 6

TREATMENT OF BEAM & PLATE VIBRATION PROBLEMS
BY
MIXED FINITE ELEMENT METHOD

6.1 INTRODUCTION

The mixed beam elements properties are briefly described and the types of elements which have been developed for the solution of free and forced vibration of beams are illustrated. Then free and forced vibration problems of thin plates are treated by means of mixed finite element technique. Reissner principle (4.11) is used which does not require the continuity of slope across element boundaries. Based on this theorem, an isoparametric quadrilateral element with 8-nodes is developed which is applicable to thin plate theory only. The geometric, deflection and moment fields are expressed as quadratic functions of position. Mixed element matrices are evaluated by means of numerical integration in which the Gauss quadrature rule is employed. Models based on this element were used to calculate the natural frequencies and modes of vibration, and the transient displacements and moments in plate type structures.

Two computer programs are developed as described in Chapter 7, which incorporate the 8-node quadrilateral element presented in this section. Examples of results will be given in Chapter 8 to show the order to accuracy which can be achieved compared with other types of elements.

6.2 DERIVATION OF THE MIXED BEAM ELEMENT PROPERTIES

Reissner's principle, equation (3.16) for application to dynamic beam problems was developed in section (3.3). We also presented the modified version of this principle, equation (3.17). This version imposes C0 continuity requirements on the fields of bending moment and deflection. These principles can be directly incorporated in finite element formulation of beam bending problems. Several such elements have been developed in this work which are shown in Table (6.1), with the corresponding shape functions. The mixed element matrices for one of these elements will be derived in here. Other elements may be formulated in a similar manner.

6.2.1 Mixed finite element properties

Let us divide the beam into finite elements, for the eth element: (from equation 3.17)

$$\begin{aligned}
 (\delta \pi \frac{D}{R})_e &= \delta \int_{t_1}^{t_2} \left[\int_0^1 \left(-\rho A \dot{w}^2 - \frac{M^2}{2EI} + M'w' \right) dx - \int_0^1 w^t p(x,t) dx \right] dt \\
 &+ \int_{t_1}^{t_2} \left[\int_0^1 c(x) \dot{w} \delta w dx \right] dt = 0 \quad (6.1)
 \end{aligned}$$

A natural coordinate, ξ , is assumed within the element (Fig. 6.1) such that

$$x = \left[\frac{1}{2} (1-\xi) \quad \frac{1}{2} (1+\xi) \right] \begin{Bmatrix} x_1 \\ x_2 \end{Bmatrix} \quad (6.2)$$

where x_1, x_2 are the nodal coordinates at node 1 and 2, and $\xi = -1$, $\xi = +1$ respectively at node 1 and node 2.

Solving equation (6.2) for ξ and differentiating with respect to x yields:

$$\frac{d}{dx} = \frac{d\xi}{dx} \quad \frac{d}{d\xi} = \frac{2}{l} \frac{d}{d\xi} \quad (6.3)$$

hence $dx = \frac{l}{2} d\xi$ (6.4)

As an example, assume a parabolic variations for M_x and w within the element, then,

$$w_x = \left[\frac{1}{2}\xi(\xi-1) \quad \frac{1}{2}\xi(\xi+1) \quad (1-\xi^2) \right] \begin{Bmatrix} w_1 \\ w_2 \\ w_3 \end{Bmatrix} \quad (6.5)$$

$$M_x = \left[\frac{1}{2}\xi(\xi-1) \quad \frac{1}{2}\xi(\xi+1) \quad (1-\xi^2) \right] \begin{Bmatrix} M_1 \\ M_2 \\ M_3 \end{Bmatrix} \quad (6.6)$$

or $(M_x, w) = [N] (\{w\}^e, \{M\}^e)$ where $\{w\}^e$ and $\{M\}^e$ are nodal values of deflection and bending moments respectively. Hence using equation (6.3)

$$\frac{dM_x}{dx} = \frac{2}{l} \cdot \frac{dM_x}{d\xi} = \frac{1}{l} \left[(2\xi-1) \quad (2\xi+1) \quad -2\xi \right] \begin{Bmatrix} M_1 \\ M_2 \\ M_3 \end{Bmatrix} \quad (6.7)$$

i.e. $\frac{dM}{dx} = [B] \{M\}_e$

and

$$\frac{dw}{dx} = \frac{2}{l} \frac{dw}{d\xi} = [B] \{w\}_e \quad (6.8)$$

Substituting relations (6.5) to (6.8) into the Reissner equation (6.1) yields

$$\delta \int_{t_1}^{t_2} \left[-\frac{1}{2} \{\dot{w}\}_e^t [m] \{\dot{w}\}_e - \frac{1}{2} \{M\}_e^t [g] \{M\}_e + \{M\}_e^t [h] \{w\}_e - \{w\}_e^t \{r\} \right] dt + \int_{t_1}^{t_2} \{\dot{w}\}_e^t [c] \{\delta w\}_e dt = 0 \quad (6.9)$$

The corresponding matrices are then evaluated from:

$$[g] = \int_{-1}^1 [N]^t \frac{1}{EI} [N] \frac{1}{2} d\xi \quad (a)$$

$$[h] = \int_{-1}^1 [B]^t [B] \frac{1}{2} d\xi \quad (b)$$

$$[m] = \int_{-1}^1 \rho A [N]^t [N] \frac{1}{2} d\xi \quad (c) \quad (6.10)$$

$$[c] = \int_{-1}^1 c [N]^t [N] \frac{1}{2} d\xi \quad (d)$$

$$\{r\} = \int_{-1}^1 [N]^t p(x,t) \frac{1}{2} d\xi \quad (e)$$

Variations of Reissner's principle then yields the mixed governing equations (4.19).

The behaviour of the beam elements in connection with free

and forced vibration problems is investigated in Chapter 8.

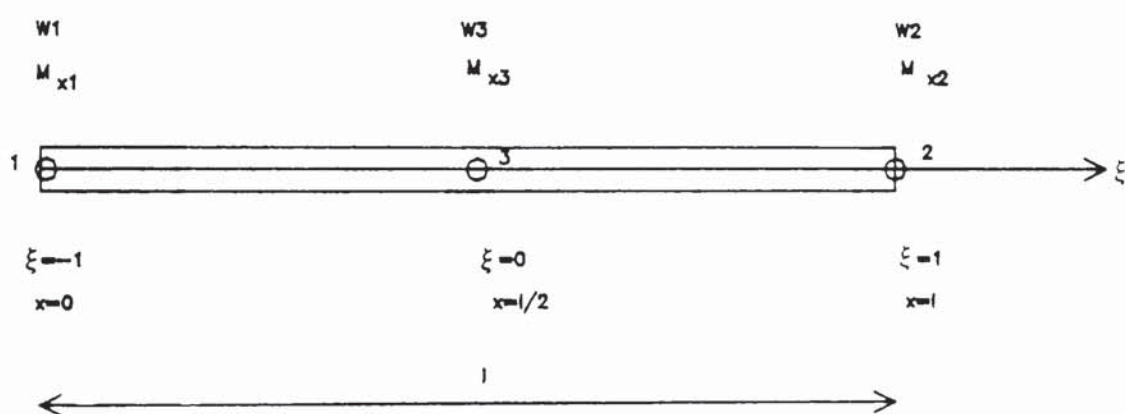


Fig 6.1 Beam finite element(MB5)

Table 6.1 Mixed beam elements, (C1 and C0 continuous elements)

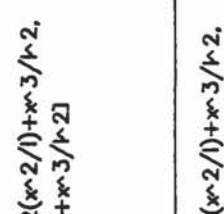
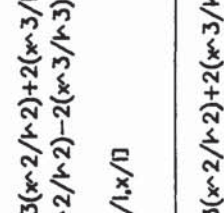
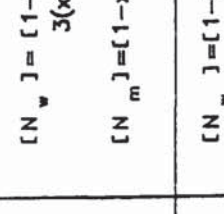
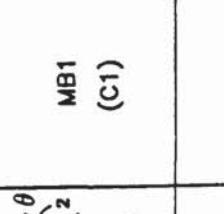
Type of element	Symbol	Displacement/Stress interpolations $0 \leq \xi \leq 1, -1 \leq \xi \leq +1$	Displacement freedoms	Stress freedoms
	MB1 (C1)	$[N_w] = [1-3(x^2/l^2)+2(x^3/l^3), x-2(x^2/l)+x^3/l^2, 3(x^2/l^2)-2(x^3/l^3), -x^2/l+x^3/l^2]$ $[N_m] = [1-x/l, x/l]$	w_x $\dot{\theta}_x$	M_x
	MB2 (C1)	$[N_w] = [1-3(x^2/l^2)+2(x^3/l^3), x-2(x^2/l)+x^3/l^2, 3(x^2/l^2)-2(x^3/l^3), -x^2/l+x^3/l^2]$ $[N_m] = [(2x-1)(x-1)/l^2, 2(x^2/l^2)-x/l, (4x-4x^2)/l^2]$	w_x $\dot{\theta}_x$	M_x
	MB3 (C1)	$[N_w] = [N_m] = [1-3(x^2/l^2)+2(x^3/l^3), x-2(x^2/l)+x^3/l^2, 3(x^2/l^2)-2(x^3/l^3), -x^2/l+x^3/l^2]$	w_x $\dot{\theta}_x$	M_x F_x
	MB4 (C0)	$[N_w] = [N_m] = [1/2(1-\xi), 1/2(1+\xi)]$	w_x	M_x

Table 6.1 Continued..

Type of element	Symbol	Displacement/Stress Interpolations	Displacement freedoms	Stress freedoms
	MB5 (CO)	$[N_w] = [N_m] =$ $[1/2(\xi^2 - \xi), 1/2(\xi^2 + \xi), (1 - \xi^2)]$	w_x	M_x
	MB6 (CO)	$[N_w] = [N_m] = [N1, N2, N3, N4]$ $N1 = 1/2(1 - \xi) + 9/16(-\xi^3 + \xi^2 + \xi - 1)$ $N2 = 1/2(1 + \xi) + 9/16(\xi^3 + \xi^2 - \xi - 1)$ $N3 = 9/16(3\xi^3 - \xi^2 - 3\xi + 1)$ $N4 = 1/16(-27\xi^3 - 9\xi^2 + 27\xi + 9)$	w_x	M_x
	MB7 (CO)	$[N_w] = [1/2(\xi^2 - \xi), 1/2(\xi^2 + \xi), (1 - \xi^2)]$ $[N_m] = [1/2(1 - \xi), 1/2(1 + \xi)]$	w_x	M_x
	MB8 (CO)	$[N_w] = [1/2(1 - \xi), 1/2(1 + \xi)]$ $[N_m] = [1/2(\xi^2 - \xi), 1/2(\xi^2 + \xi), (1 - \xi^2)]$	w_x	M_x

6.3 COMPUTER IMPLEMENTATION OF THE MIXED BEAM ELEMENTS

The series of programs written for the study of beam elements can be divided into two groups, on the basis of their functions, these being free vibration programs and response analysis programs. The former produces the eigenvalues and eigenvectors of the undamped free vibration problem. The second group of programs performs the response analysis and outputs the time history plots of the displacements and bending moments.

An important consideration in using the one-dimensional beam elements is the similarity between the calculation of different elements. For this reason and because of the familiarity and ease of formulation of one-dimensional elements, the related programs are not described in detail. However, in Appendix C, the computer listing for the forced vibration of element MB5 (defined in Table 6.1) is provided. It is believed that by showing the actual computer implementation of this element, the implementing of other beam elements is self explanatory. The input and output (I/O) variables and the flow of the program are documented within this listing. The package of mixed beam elements includes the programs VREIS1 to VREIS8 for elements MB1 to MB8 which perform the free vibration tests and the programs MBRSP1 to MBRSP5 which perform the forced vibration tests for elements MB1 to MB5.

6.4 MIXED FINITE ELEMENT FORMULATION - THIN PLATES

Reissner's principle applied to thin plate vibration theory may be derived from equation (2.59). Assuming that the prescribed normal moments, twisting moment and transverse deflection are satisfied, that is:

$$M_n = \bar{M}_n, \quad M_{ns} = \bar{M}_{ns} \quad \text{on } (s_\sigma)_e \quad (6.11)$$

and
$$W = \bar{W} \quad \text{on } (s_u)_e$$

We will obtain the following expression for Reissner's principle:

$$\begin{aligned} (\delta\pi_R^D)_e = \delta & \int_{t_1}^{t_2} \left[-\frac{1}{2} \int_{A_e} \rho h \dot{W}^2 dA - \frac{1}{2} \int_{A_e} \{M\}^t [D]^{-1} \{M\} dA \right. \\ & + \int_{A_e} \{Q\}^t \{W'\} dA - \int_A p(x,y,t) W dA - \left. \int_{s_e} M_{ns} \frac{\partial W}{\partial s} ds \right] dt \\ & + \int_{t_1}^{t_2} \left(\int_A c\dot{W}^t \delta W dA \right) dt = 0 \end{aligned} \quad (6.12)$$

in which

$$\{M\} = \begin{bmatrix} M_x & M_y & M_{xy} \end{bmatrix}^t$$

$$\{Q\} = \begin{bmatrix} Q_x & Q_y \end{bmatrix}^t = \left[\left(\frac{\partial M_x}{\partial x} + \frac{\partial M_{xy}}{\partial y} \right) \quad \left(\frac{\partial M_y}{\partial y} + \frac{\partial M_{xy}}{\partial x} \right) \right]^t$$

$$\{W'\} = \begin{bmatrix} \frac{\partial W}{\partial x} & \frac{\partial W}{\partial y} \end{bmatrix}^t$$

and the homogeneous natural boundary conditions are:

$$\frac{\partial W}{\partial n} = 0 \quad \text{on } (s_u)_e$$

$$\bar{V}_n = 0 \quad \text{on } (s_\sigma)_e$$
(6.13)

The surface integrals are evaluated over the entire area of the element and the line integral is evaluated (in an anti-clockwise direction) around each element boundary s_e .

Now consider a general thin plate divided into an arbitrary grid of finite elements (fig. 6.2). The transverse displacement W and the moments $\{M\} = \begin{bmatrix} M_x & M_y & M_{xy} \end{bmatrix}^t$ may be independently assumed within each element by:

$$W = \begin{bmatrix} N_W \end{bmatrix} \{W\}_e \quad \text{(a)}$$

$$\{M\} = \begin{bmatrix} N_M \end{bmatrix} \{M\}_e \quad \text{(b)}$$
(6.14)

$[N_W]$ and $[N_M]$ are the element displacement and bending moment shape functions respectively. For the present formulation, the trial functions should be at least linear in x and y . The element nodal parameters are given by:

$$\{W\}_e = [W_1, W_2, \dots, W_n]^t \quad (a) \quad (6.15)$$

$$\{M\}_e = [M_{x_1} \ M_{y_1} \ M_{xy_1}, \ M_{x_2} \ M_{y_2} \ M_{xy_2}, \dots, M_{x_m} \ M_{y_m} \ M_{xy_m}]^t \quad (b)$$

where n and m depend on the order of shape functions (trial functions). Note that independent approximations for the displacement and moments are used. From equation (6.14), the slopes within the element are given by:

$$\{W'\} = [N'_W] \{W\}_e \quad (6.16)$$

and on the boundary s_n ,

$$\frac{\partial W}{\partial s} = [L_W] \{W'\} = [L_W][N'_W] \{W\}_e = [Y] \{W\}_e \quad (6.17)$$

Shear force intensities are derived by differentiating (6.14b), in the interior.

$$\{Q\} = [N'_W] \{M\}_e \quad (6.18)$$

and on the boundary

$$M_{ns} = [L][N_M] \{M\}_e = [L_{ns}] \{M\}_e \quad (6.19)$$

$[L]$ and $[L_W]$ are the direction cosine matrices.

Upon substitution of the above derived equations into equation (6.12), we obtain

$$\begin{aligned}
(\delta \pi_R^D) = \delta \int_{t_1}^{t_2} & \left(-\frac{1}{2} \{\dot{W}\}_e^t [m] \{\dot{W}\}_e - \frac{1}{2} \{M\}_e^t [g] \{M\}_e \right. \\
& \left. + \{M\}_e^t [h] \{W\}_e + \{W\}_e^t \{r\} \right) dt + \int_{t_1}^{t_2} \{\dot{W}\}_e^t [c] \{\delta W\}_e dt = 0
\end{aligned} \tag{6.20}$$

where:

$$[g] = \int_{A_e} [N_M]^t [D]^{-1} [N_M] dA \quad (a)$$

$$[h] = \int_{A_e} [N'_M]^t [N'_W] dA + \int_{s_n} [L_{ns}]^t [Y] ds \quad (b) \tag{6.21}$$

$$[m] = \int_{A_e} \rho h [N_W]^t [N_W] dA \quad (c)$$

$$[c] = \int_{A_e} c [N_W]^t [N_W] dA \quad (d)$$

$$\{r\} = \int_{A_e} [N_W]^t p(x,y,t) dA_e \quad (e)$$

$[m]$ and $[c]$ represent the consistent mass and damping matrices and $\{r\}$ is the vector of equivalent nodal forces for element (e).

In order to obtain a consistent set of nodal forces corresponding to

a general distributed load, the following assumptions may be made.

$$p(x,y) = [N_p] \{p\}_e \quad (6.22)$$

in which $[N_p]$ contains the assumed functions and $\{p\}_e$ are the nodal load intensities. Thus equation (6.21e) may be re-written as:

$$\{r\} = \left(\int_{A_e} [N_W]^t [N_p] dA \right) \{p\}_e \quad (6.23)$$

Variation of $(\pi_R^D)_e$ with respect to $\{M\}_e$ and $\{W\}_e$, in succession, yields

$$-\left[g \right] \{M\}_e + \left[h \right] \{W\}_e = 0 \quad (6.24)$$

$$\left[h \right]^t \{M\}_e + \left[c \right] \{\dot{W}\}_e + \left[m \right] \{\ddot{W}\}_e = \{r\}_e$$

The above set of equations represent the mixed element matrices for an arbitrary plate finite element. We now confine our attention to the isoparametric quadrilateral element.

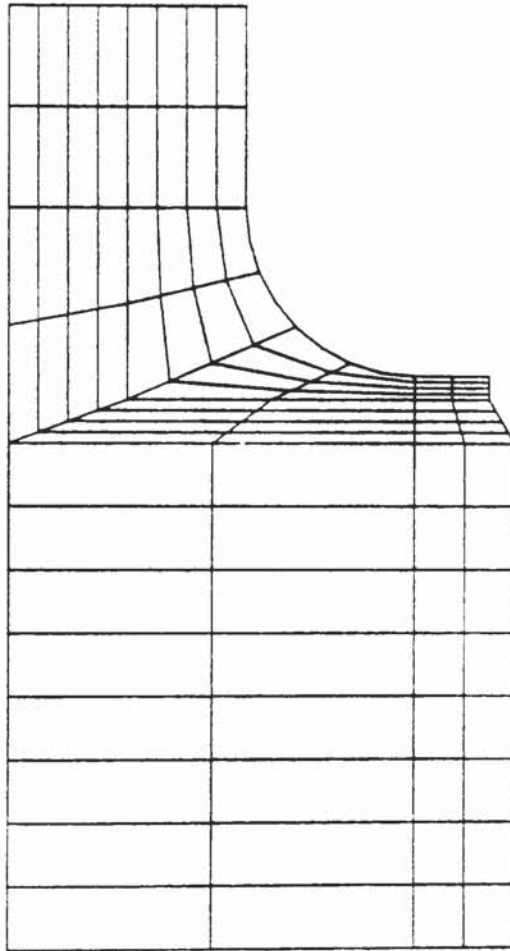


Fig 6.2 Finite element idealisation of a plate.

6.5 DERIVATION OF MIXED ELEMENT PROPERTIES - THIN PLATES

6.5.1 Element shape functions

The element under consideration is an isoparametric quadrilateral element of quadratic type (see Fig. 6.3). The element has 8 nodes with 32 degrees of freedom (one transverse deflection and two bending and one twisting moments per node). Isoparametric elements have identical geometric transformation and displacement assumptions which may be represented as:

$$(x,y) = [N_1, N_2, \dots, N_8] \left(\begin{matrix} x_1 \\ x_2 \\ \vdots \\ x_8 \end{matrix} \right), \left(\begin{matrix} y_1 \\ y_2 \\ \vdots \\ y_8 \end{matrix} \right) \quad (6.25)$$

$$W = [N_1, N_2, \dots, N_8] \begin{matrix} W_1 \\ W_2 \\ \vdots \\ W_8 \end{matrix} \quad (6.26)$$

$$\text{i.e. } W = [N_W] \{W\}_e$$

and the bending moments are given by:

$$\begin{matrix} M_x \\ M_y \\ M_{xy} \end{matrix} = \begin{bmatrix} N_1 & 0 & 0 & \dots & N_8 & 0 & 0 \\ 0 & N_1 & 0 & \dots & 0 & N_8 & 0 \\ 0 & 0 & N_1 & \dots & 0 & 0 & N_8 \end{bmatrix} \begin{bmatrix} M_{x1} \\ M_{y1} \\ M_{xy1} \\ \vdots \\ M_{x8} \\ M_{y8} \\ M_{xy8} \end{bmatrix} \quad (6.27)$$

$$\text{i.e. } \{M\} = [N_M] \{M\}_e$$

A curvilinear coordinate system (ξ, η) is defined within the element in such a way that the corners of the element have coordinates of +1 or -1. The location of local node points for each element are initially defined in terms of the cartesian coordinates (x, y) . The shape functions are:

$$\begin{aligned} N_i &= \frac{1}{4} (1 + \xi\xi_i) (1 + \eta\eta_i) (\xi\xi_i + \eta\eta_i - 1) \quad (i = 1, 2, 3, 4) \\ N_i &= \frac{1}{2} (1 - \xi^2) (1 + \eta\eta_i) \quad (i = 5, 7) \\ N_i &= \frac{1}{2} (1 - \eta^2) (1 + \xi\xi_i) \quad (i = 6, 8) \end{aligned} \quad (6.28)$$

which are the same for all three types of parameters, (geometric, displacement and moments).

6.5.2 Transformation

The evaluation of the element coefficients involves the derivatives of the shape functions (which are defined in terms of ξ and η) with respect to x and y and integration over the area of the element. Integration is performed in the transformed coordinate system and therefore various terms, such as the transformation jacobian are included in the integration to give the correct results for the original coordinate system (20).

From the chain rule of differentiation it can be shown that

$$\begin{Bmatrix} \frac{\partial N_i}{\partial \xi} \\ \frac{\partial N_i}{\partial \eta} \end{Bmatrix} = \begin{bmatrix} \frac{\partial x}{\partial \xi} & \frac{\partial y}{\partial \xi} \\ \frac{\partial x}{\partial \eta} & \frac{\partial y}{\partial \eta} \end{bmatrix} \begin{Bmatrix} \frac{\partial N_i}{\partial x} \\ \frac{\partial N_i}{\partial y} \end{Bmatrix} = [j] \begin{Bmatrix} \frac{\partial N_i}{\partial x} \\ \frac{\partial N_i}{\partial y} \end{Bmatrix} \quad (6.29)$$

where $[J]$ is the Jacobian operator relating the curvilinear coordinate derivatives to the local x,y coordinate derivatives.

The Jacobian operator can easily be found using (6.25). Inverting (6.29) gives:

$$\begin{pmatrix} \frac{\partial N_i}{\partial x} \\ \frac{\partial N_i}{\partial y} \end{pmatrix} = [J]^{-1} \begin{pmatrix} \frac{\partial N_i}{\partial \xi} \\ \frac{\partial N_i}{\partial \eta} \end{pmatrix} = \begin{bmatrix} J_{11}^* & J_{12}^* \\ J_{21}^* & J_{22}^* \end{bmatrix} \begin{pmatrix} \frac{\partial N_i}{\partial \xi} \\ \frac{\partial N_i}{\partial \eta} \end{pmatrix} \quad (6.30)$$

The inverse of $[J]$ exists provided that there is a one-to-one correspondence between the natural, (ξ,η) and local (x,y) coordinates. An operating matrix B which includes all the shape function derivatives may then be represented as:

$$[B] = \begin{bmatrix} \frac{\partial N_1}{\partial x} & \frac{\partial N_2}{\partial x} & \dots & \frac{\partial N_7}{\partial x} & \frac{\partial N_8}{\partial x} \\ \frac{\partial N_1}{\partial y} & \frac{\partial N_2}{\partial y} & \dots & \frac{\partial N_7}{\partial y} & \frac{\partial N_8}{\partial y} \end{bmatrix} = \begin{bmatrix} B_{11} & B_{12} & \dots & B_{17} & B_{18} \\ B_{21} & B_{22} & \dots & B_{27} & B_{28} \end{bmatrix} \quad (6.31)$$

in which

$$\begin{aligned} B_{11} &= J_{11}^* (1-\xi) (2\eta + \xi) / 4 + J_{12}^* (1-\eta) (2\xi + \eta) / 4 & (a) \\ B_{12} &= J_{11}^* (1-\xi) (2\eta - \xi) / 4 + J_{12}^* (1+\eta) (2\xi - \eta) / 4 & (b) \\ B_{13} &= J_{11}^* (1+\xi) (2\eta + \xi) / 4 + J_{12}^* (1+\eta) (2\xi + \eta) / 4 & (c) \\ B_{14} &= J_{11}^* (1+\xi) (2\eta - \xi) / 4 + J_{12}^* (1-\eta) (2\xi - \eta) / 4 & (d) \end{aligned} \quad (6.32)$$

etc.

Equations (6.28) and (6.32) can be used to evaluate the element matrices in (6.21). The resulting integrals are too complicated to evaluate

explicitly and therefore numerical integration must be employed.

6.5.3 Slope matrices

Differentiating equation (6.26) with respect to x and y at any point within the element gives:

$$\begin{pmatrix} \frac{\partial W}{\partial x} \\ \frac{\partial W}{\partial y} \end{pmatrix} = \begin{bmatrix} \frac{\partial N_1}{\partial x} & \frac{\partial N_2}{\partial x} & \dots & \frac{\partial N_8}{\partial x} \\ \frac{\partial N_1}{\partial y} & \frac{\partial N_2}{\partial y} & \dots & \frac{\partial N_8}{\partial y} \end{bmatrix} \begin{pmatrix} W_1 \\ W_2 \\ \vdots \\ W_8 \end{pmatrix} \quad \text{i.e.} \quad \{W'\} = [N'_W] \{W\}. \quad (6.33)$$

This relation can be evaluated by using the operating matrix B given by equations (6.31) and (6.32). Then

$$\begin{pmatrix} \frac{\partial W}{\partial x} \\ \frac{\partial W}{\partial y} \end{pmatrix} = \begin{bmatrix} B_{11} & B_{12} & \dots & B_{17} & B_{18} \\ B_{21} & B_{22} & \dots & B_{27} & B_{28} \end{bmatrix} \begin{pmatrix} W_1 \\ W_2 \\ \vdots \\ W_8 \end{pmatrix}_e \quad (6.34)$$

on the element boundary s_n , equation (6.17) can be written for each side as:

$$\frac{\partial W}{\partial s} = [L_W]_i \begin{pmatrix} \frac{\partial W}{\partial x} \\ \frac{\partial W}{\partial y} \end{pmatrix}_i \quad (6.35)$$

for $i = 1, 2, 3, 4$. Where (i) is the element side and the corresponding direction cosines matrix is given by:

$$[L_W]_i = (-\sin \beta : \cos \beta)_i \quad (6.36)$$

For each element side, β is the angle between the normal to the boundary s_n and the x-axis (Fig. 6.3). In general β is variable along curved element boundaries and therefore should be calculated numerically. A computer subroutine is written (section 7.7) which calculates β at different integration points on the element boundary.

Substituting from (6.34) into (6.35) yields:

$$\frac{\partial W}{\partial s} = (-\sin\beta \quad \cos\beta)_i \begin{bmatrix} B_{11} & B_{12} & \dots & B_{17} & B_{18} \\ B_{21} & B_{22} & \dots & B_{27} & B_{28} \end{bmatrix} \begin{Bmatrix} W_1 \\ W_2 \\ \vdots \\ W_7 \\ W_8 \end{Bmatrix} \quad (6.37)$$

$$\text{i.e. } \frac{\partial W}{\partial s} = [Y]_i \{W\}_e \quad \text{for } i = 1, 2, 3, 4$$

where

$$[Y]_i = [Y_1 \quad Y_2 \quad \dots \quad Y_7 \quad Y_8]_i \quad (a)$$

in which

$$Y_1 = (-B_{11}\sin\beta + B_{21}\cos\beta)_i, \text{ etc. } (b)$$

(6.38)

6.5.4 Shear force intensity matrix

The shear force intensities Q_x and Q_y may be expressed in terms of nodal bending moments. Differentiating the matrix relation (6.27) within the element yields:

$$\begin{Bmatrix} Q_x \\ Q_y \end{Bmatrix} = \begin{bmatrix} \frac{\partial N_1}{\partial x} & 0 & \frac{\partial N_1}{\partial y} & \dots & \frac{\partial N_8}{\partial x} & 0 & \frac{\partial N_8}{\partial y} \\ 0 & \frac{\partial N_1}{\partial y} & \frac{\partial N_1}{\partial x} & \dots & 0 & \frac{\partial N_8}{\partial y} & \frac{\partial N_8}{\partial x} \end{bmatrix} \begin{Bmatrix} M_{x1} \\ M_{y1} \\ M_{xy1} \\ \vdots \\ M_{x8} \\ M_{y8} \\ M_{xy8} \end{Bmatrix} \quad (6.39)$$

substituting the components of the operating matrix B , (6.31) in the above matrix relation yields:

$$\begin{Bmatrix} Q_x \\ Q_y \end{Bmatrix} = \left[N'_M \right]_{\xi, \eta} \{M\}_e \quad (6.40)$$

where

$$\left[N'_M \right]_{\xi, \eta} = \begin{bmatrix} B_{11} & 0 & B_{21} & \dots & B_{18} & 0 & B_{28} \\ \dots & \dots & \dots & \dots & \dots & \dots & \dots \\ 0 & B_{21} & B_{11} & \dots & 0 & B_{28} & B_{18} \end{bmatrix} \quad (\xi, \eta)$$

6.5.5 Normal twisting moment along each element side

The normal twisting moment M_{ns} in terms of the natural coordinates ξ and η and the nodal moments is given by equation (6.19). The direction cosine matrix $[L]$ is taken from relation (3.26), and is given by:

$$[L] = \begin{bmatrix} -\cos\beta & \sin\beta & : & \cos\beta & \sin\beta & : & \cos^2\beta & -\sin^2\beta \end{bmatrix}_i \quad (6.41)$$

for $i = 1, 2, 3, 4$

The components of $[L]$ are evaluated numerically at each integration point along the element boundaries. The twisting moment M_{ns} can then be represented as:

$$[m] = \int_{-1}^1 \int_{-1}^1 \rho h [N_W]^t [N_W] \det J d\xi dn \quad (c)$$

(6.44)

$$\{r\} = \int_{-1}^1 \int_{-1}^1 [N_W]^t p(x,y,t) \det J d\xi dn \quad (d)$$

The line integral in equation (6.44b) is to be evaluated along each element side. Therefore, ds is replaced by:

$$ds = \frac{\partial s}{\partial \xi} d\xi \quad (a) \quad (\eta = \text{const})$$

or (6.45)

$$ds = \frac{\partial s}{\partial \eta} d\eta \quad (b) \quad (\xi = \text{const})$$

$\frac{ds}{d\xi}$ and $\frac{ds}{d\eta}$ may be determined from the following relations:

$$\frac{ds}{d\xi} = \sqrt{\left(\frac{dx}{d\xi}\right)^2 + \left(\frac{dy}{d\xi}\right)^2}, \quad \frac{ds}{d\eta} = \sqrt{\left(\frac{dx}{d\eta}\right)^2 + \left(\frac{dy}{d\eta}\right)^2} \quad (6.46)$$

where the components $\frac{dx}{d\xi}$, etc. are evaluated using equation (6.25).

If the element edge is a straight line of length L then

$$ds = \frac{L}{2} d\xi \quad (6.47)$$

If the load $p(x,y,t)$ is not constant over the area of the plate, then it is assumed that within an element, the distribution is given by:

$$p(x,y,t) = [N_p] \{p\}_e \quad (6.22)$$

The interpolation function $[N_p] = [N_w]$ and $\{p\}_e^t = [p_1, p_2, \dots, p_7, p_8]$ is a vector with nodal pressures. Substituting from (6.22) in (6.44d) yields:

$$\{r\} = \int_{-1}^1 \int_{-1}^1 [N_w]^t [N_p] \{p\}_e \det J \, d\xi \, d\eta \quad (6.48)$$

Now the components of the element mixed matrices and load vector can be given as:

$$[g] = \begin{bmatrix} g_{11} & g_{12} & \dots & g_{17} & g_{18} \\ \vdots & \vdots & \ddots & \vdots & \vdots \\ g_{81} & g_{82} & \dots & g_{87} & g_{88} \end{bmatrix} \quad (6.49)$$

A typical submatrix (g_{ij}) linking nodes i and j is given by the expression

$$[g_{ij}] = \int_{-1}^1 \int_{-1}^1 \begin{bmatrix} N_i & C_{11} & N_j & N_i & C_{12} & N_j & N_i & C_{13} & N_j \\ N_i & C_{21} & N_j & N_i & C_{22} & N_j & N_i & C_{23} & N_j \\ N_i & C_{31} & N_j & N_i & C_{32} & N_j & N_i & C_{33} & N_j \end{bmatrix} \det J \, d\xi \, d\eta \quad (6.50)$$

For $i, j = 1, 2, 3, 4, 5, 6, 7, 8$

and,

$$[h] = \begin{bmatrix} h_{11} & h_{12} & \dots & h_{17} & h_{18} \\ \dots & \dots & \dots & \dots & \dots \\ \dots & \dots & \dots & \dots & \dots \\ h_{81} & h_{82} & \dots & h_{87} & h_{88} \end{bmatrix} \quad (6.51)$$

where

$$h_{ij} = \int_{-1}^1 \int_{-1}^1 \begin{bmatrix} B_{1i} & B_{1j} \\ B_{2i} & B_{2j} \\ B_{2i} & B_{1j} + B_{1i} & B_{2j} \end{bmatrix} \det J \, d\xi d\eta - \int_{-1}^1 \begin{bmatrix} L_{11} & N_i & Y_j \\ L_{12} & N_i & Y_j \\ L_{13} & N_i & Y_j \end{bmatrix} ds$$

$$\text{for } i, j = 1, 2, \dots, 8 \quad (6.52)$$

in which the line integral should be evaluated over the four sides of the element. The mass matrix is given by:

$$[m] = \int_{-1}^1 \int_{-1}^1 \rho h \begin{bmatrix} N_1^2 & N_1 N_2 & \dots & N_1 N_8 \\ N_2^2 & \dots & \dots & \dots \\ \dots & \dots & \dots & \dots \\ \text{Symm.} & \dots & \dots & N_8^2 \end{bmatrix} \det J \, d\xi d\eta \quad (6.53)$$

where ρ is the mass of the plate per unit volume and h is the thickness.

The load vector for $p = \text{constant}$ is:

$$\{r\} = \begin{Bmatrix} r_1 \\ r_2 \\ \vdots \\ r_8 \end{Bmatrix} = \int_{-1}^1 \int_{-1}^1 \begin{Bmatrix} N_1 \\ N_2 \\ \vdots \\ N_8 \end{Bmatrix} p \det J \, d\xi \, d\eta \quad (6.54)$$

However, if p is not constant then it is assumed that p varies parabolically within an element with $\begin{bmatrix} N_p \end{bmatrix} = \begin{bmatrix} N_w \end{bmatrix}$ we have

$$r_i = \int_{-1}^1 \int_{-1}^1 \left(\sum N_i N_j p_j \right) \det J \, d\xi \, d\eta \quad (6.55)$$

for $i, j = 1, 2, \dots, 8$

We will now outline the Gaussian numerical integration procedure which will be used in the evaluation of various matrices involved.

6.5.7. Approximate integration of element matrices. Gauss - quadrature rule

Exact integration of the matrices in equations (6.44) to (6.55) is not generally possible because the composite function which forms the integrand cannot be expressed as a polynomial. This is due to the jacobian matrix determinant $\det J$, which is used in the transformation between the global coordinate system and the natural coordinate system and is usually a variable function. It is therefore necessary to resort to numerical integration procedures to evaluate the matrix coefficients. In particular, Gaussian integration techniques have been adopted because of their convenience and accuracy.

Consider, for example the numerical integration of

$$I = \int_{-1}^{+1} f(\xi) d\xi \quad -1 \leq \xi \leq +1 \quad (6.56)$$

Using Gaussian integration, the function $f(\xi)$ is evaluated at several sampling points with coordinates $\xi_i = a_i$ within the region of integration. Each value $f(\xi_i)$ is multiplied by the appropriate "weight" W_i and added. Thus, the integration becomes a summation of products, i.e.

$$I \approx \sum_{i=1, n} f(\xi_i) W_i \quad (6.57)$$

where n is the number of points taken. The Gauss method locates the sampling points so that for a given number of them, greatest accuracy is obtained. Table (6.2) gives the appropriate Gauss quadrature coefficients for the first three orders (44). It should be noted that an n -point Gauss rule integrates a function of order $(2n-1)$ or less, exactly.

In two dimensions the function f in the integrand is a function of two variables, i.e.

$$I = \int_{-1}^{+1} \int_{-1}^{+1} f(\xi, \eta) d\xi d\eta \quad \begin{array}{l} -1 < \xi < +1 \\ -1 < \eta < +1 \end{array} \quad (6.58)$$

a product Gauss rule may be used. Therefore, the summation becomes:

$$I \approx \sum_i \sum_j W_i W_j f(\xi_i, \eta_j) \quad (6.59)$$

The 3 x 3 point Gauss quadrature is used for the evaluation of the area integrals in equation (6.59). The location of these points is shown in figure (6.3).

TABLE 6.2 Gauss quadrature points

No. of points	Locations (ξ_i, η_i)	Associated Weights, W_i
1	0.0000000	2
2	± 0.5773502691	1
3	$\pm .774596669$	$5/9$
	0.0000000	$8/9$

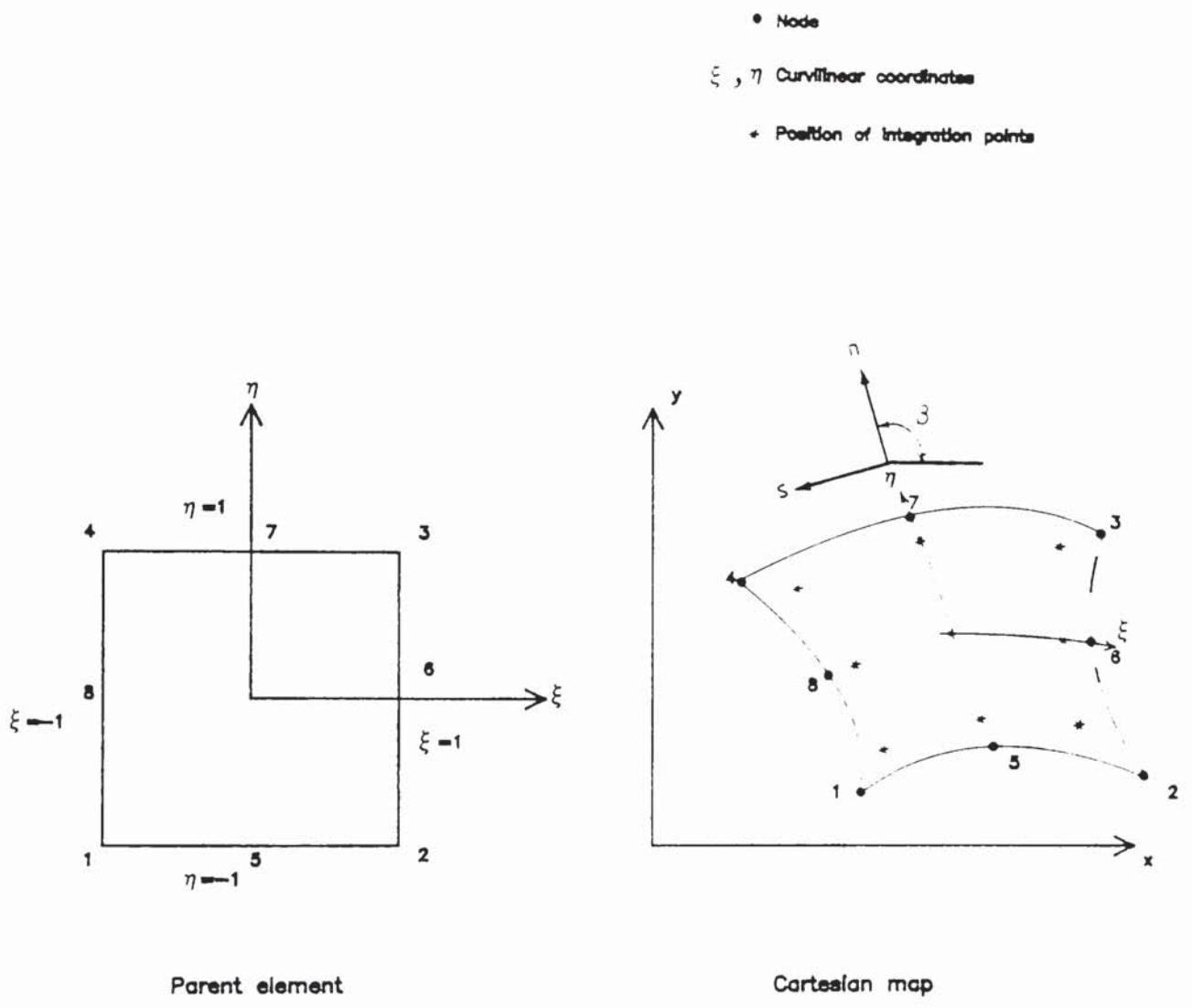


Fig 8.3 Isoparametric quadratic plate element.

6.6 ASSEMBLY OF THE OVERALL MATRICES AND LOAD VECTORS

In the preceding section the Reissner principle was applied to a single element and the individual element characteristics were established. The element matrices in equation (6.24) can be assembled in the usual manner, (64) to obtain the global matrices. Let the global deflections and moments be represented by:

$$\{W^*\} = [W_1^*, W_2^*, \dots, W_n^*]^t$$

$$\{M^*\} = [[M^*]_1, [M^*]_2, \dots, [M^*]_n]^t$$

with $[M^*]_i = \begin{bmatrix} M_x & M_y & M_{xy} \end{bmatrix}$ node i

and n representing the number of nodes. Equation (6.24) for the overall structure may now be written as:

$$- [G] \{M^*\} + [H] \{W^*\} = \{0\} \quad (6.60)$$

$$[H]^t \{M^*\} + [C] \{\dot{W}^*\} + [M] \{\ddot{W}^*\} = \{R\}$$

where the overall partitioned matrices can be represented as follows:

$$[G] = \sum_{e=1}^N [G_e] \quad (a)$$

$$[H] = \sum_{e=1}^N [H_e] \quad (b) \quad (6.61)$$

$$[C], [M] = \sum_{e=1}^N [c]_e, [m]_e \quad (c)$$

$$\{R\} = \sum_{e=1}^N \{r\}_e \quad (d) \quad N = \text{number of elements}$$

$[G_e]$, $[H_e]$, etc. have the same dimensions of $[G]$, $[H]$, ... but the only non-zero locations are those due to the coefficients of $[g]$, $[h]$, etc. for the eth element, globally located.

6.7 BOUNDARY CONDITIONS

Before proceeding to solve the problem, we must impose the kinematic (or essential) boundary conditions of equation (6.11) on the global system of equations. The constrained nodal deflections and/or moments are eliminated to yield non-singular matrices (by deleting the corresponding rows and columns). At boundary nodes where the constrained moments do not coincide with the x-y global axes, there will have to be a change of coordinates to normal and tangential components. The relation between the unknown moments for a typical boundary node (i) (Fig. 6.4) is given by:

$$\begin{Bmatrix} M_s \\ M_n \\ M_{ns} \end{Bmatrix} = \begin{bmatrix} \sin^2\beta & \cos^2\beta & -2 \sin\beta \cos\beta \\ \cos^2\beta & \sin^2\beta & 2 \sin\beta \cos\beta \\ -\cos\beta \sin\beta & \cos\beta \sin\beta & \cos^2\beta - \sin^2\beta \end{bmatrix} \begin{Bmatrix} M_x \\ M_y \\ M_{xy} \end{Bmatrix} \quad (3.26)$$

$$\text{i.e. } \{M'\}_i = [l_i] \{M^*\}_i$$

where the primed notation indicates the nodal components in the new normal axes. $[l_i]$ is the simple point transformation matrix and β is the angle between the normal of the true boundary at the i th node and the x-axis. Following a procedure similar to the one described by Mota Soares (7), the mixed-matrix governing equation is transformed to the new set of coordinates, at element level, before the assembly process. Thus for an individual element we have:

$$[g]' = [L_K]^t [g] [L_K] \quad (a)$$

and

$$[h]' = [L_K]^t [h] \quad (b)$$

where the matrix $[L_K]$ is (24 x 24) and has the following typical form:

$$[L_K] = \begin{bmatrix} I & \dots & \dots & \dots & 0 \\ \vdots & \cdot & & & \vdots \\ \vdots & & I & & 0 \\ \vdots & & & \cdot & \vdots \\ \vdots & & & & l_i \\ \vdots & & & & \vdots \\ \vdots & & & & \vdots \\ \vdots & & & & \vdots \\ 0 & & 0 & & 0 \\ 0 & \dots & 0 & \dots & I \end{bmatrix} \quad (6.63)$$

in which I is the identity matrix of the same order as l_i . The prescribed values are summarized in the following table.

TABLE 6.3

Boundary conditions	Nodal variables - Thin Plates			
	W	M_s	M_n	M_{ns}
Simply-supported	0		0	
Clamped	0			
Free			0	
Symmetrique				0

For the rest of this chapter we will assume that all the boundary conditions have been applied and the mixed matrices correspond to free nodal deflections and moments.

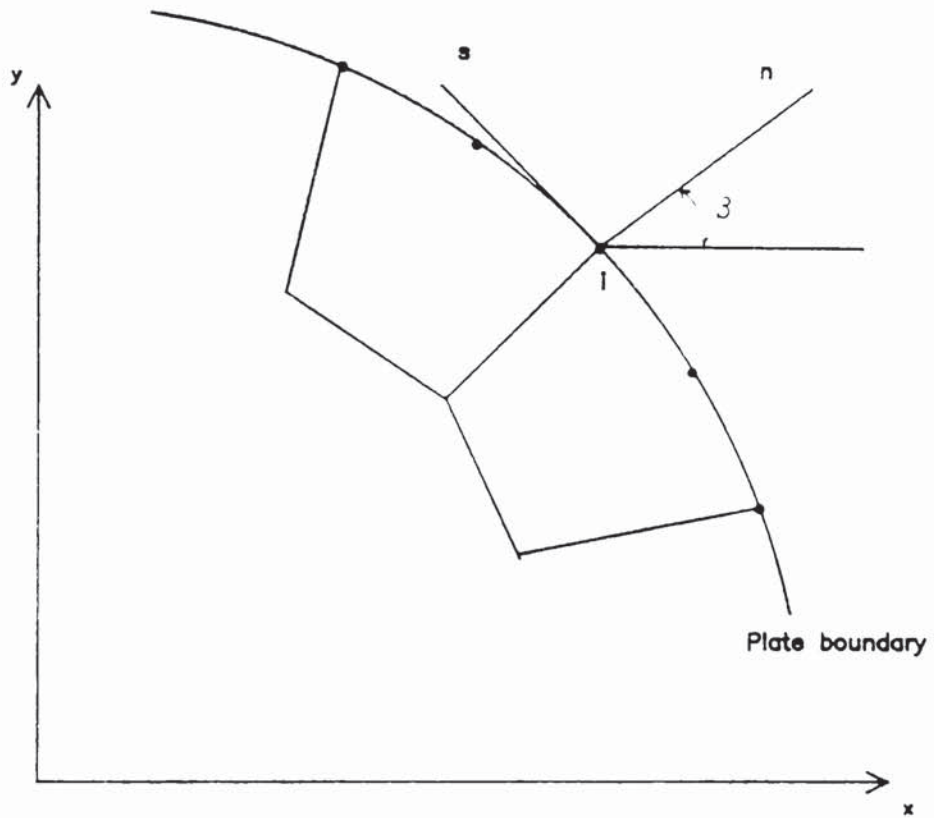


Fig 6.4 Typical boundary node.

6.8 MATRIX CONDENSATION OF THE MIXED GOVERNING EQUATIONS

The mixed matrix equations (6.60) should be transformed into an appropriate form prior to the solution procedure. In static analysis (7), the effect of inertia and damping is neglected and the following equation is obtained

$$\begin{bmatrix} -[G] & [H] \\ [H]^t & 0 \end{bmatrix} \begin{bmatrix} \{M^*\} \\ \{W^*\} \end{bmatrix} = \begin{bmatrix} \{0\} \\ \{R\} \end{bmatrix} \quad (6.64)$$

For an effective solution the nodal freedoms are rearranged and equation (6.64) is re-written as:

$$[K] \{\delta\} = \{F\} \quad (6.65)$$

in which

$$\{\delta\}^t = \left[(W^*, M_x^*, M_y^*, M_{xy}^*)_1, (W^*, M_x^*, M_y^*, M_{xy}^*)_2, \dots, (W^*, M_x^*, M_y^*, M_{xy}^*)_n \right] \quad (6.66)$$

$$\{F\}^t = \left[(R_1, 0, 0, 0), (R_2, 0, 0, 0), \dots, (R_n, 0, 0, 0) \right] \quad (6.67)$$

the mixed matrix $[K]$ is banded and non-positive definite. To avoid the zeros in the diagonal element, the Gauss elimination method, reference (65), with row interchanges is used in the solution of the equations. However, since the symmetry of the overall matrix is lost throughout the numerical process, it is required that the complete band form of the matrix $[K]$ to be stored as a two-dimensional array.

In dynamic problems, the matrix condensation is carried out as follows:

The first equation in equation (6.60) is solved for $\{M^*\}$ to give:

$$\{M^*\} = [G]^{-1} [H] \{W^*\} \quad (6.68)$$

and the result is substituted in the second of equation (6.60), thus:

$$[K^*] \{W^*\} + [C] \{\dot{W}^*\} + [M] \{\ddot{W}^*\} = \{R(t)\} \quad (6.69)$$

where

$$[K^*] = [H]^t [G]^{-1} [H] \quad (6.70)$$

is a real symmetric positive definite matrix. It should be noticed that the reduction of degrees of freedom (equation 6.68) to (6.70), is an exact operation and that the moments are calculated (equation 6.68) by a matrix transformation of the displacements. The solution of equation (6.69) is performed by one of the direct integration or mode superposition methods described in section (4.6).

For free harmonic vibrations (neglecting damping) equations (6.60) become:

$$-[G] \{\hat{M}^*\} + [H] \{\hat{W}^*\} = \{0\} \quad (a) \quad (6.71)$$

$$[H]^t \{\hat{M}^*\} - \omega^2 [M] \{\hat{W}^*\} = \{0\} \quad (b)$$

which can be easily transformed into the standard eigenvalue problems (see section 4.4.2). In terms of $\{\hat{W}^*\}$, the eigenvalue problem becomes:

$$[K^*] \{\hat{W}^*\} - \omega^2 [M] \{\hat{W}^*\} = \{0\} \quad (6.72)$$

and in terms of $\{\hat{M}^*\}$ eigenvectors, we will obtain the following equation:

$$[H] [M]^{-1} [H]^t \{\hat{M}^*\} - \omega^2 [G] \{\hat{M}^*\} = \{0\} \quad (6.73)$$

The natural frequencies (ω) and the mode shapes ($\{\hat{W}^*\}$ or $\{\hat{M}^*\}$) are determined by solving the corresponding eigenvalue problem. A standard subroutine is used which is described in Ref. (66).

CHAPTER 7

COMPUTER ALGORITHMS
AND
PROGRAM STRUCTURE

7.1 INTRODUCTION

Three finite element programs have been written which use the 8-node plate isoparametric element described in Chapter 6.

These programs are:

- (1) RFPLT1 For free vibration of thin plates.
- (2) RFPLT2 For forced vibration of plates using the mode superposition method.
- (3) RFPLT3 For forced vibration of plates using the direct integration method.

The memory capacity of the computer on which these programs have been implemented is 182 K. Due to a memory capacity constraint, the treatment of plate problems, using these programs is limited to systems having no more than (10-20) non-constrained nodes. This machine can be configured to have a maximum memory of .5M bytes. This would enable the maximum number of non-constrained nodes to be increased to (30-60) nodes.

The flowcharts for the three programs RFPLT1, RFPLT2 and RFPLT3 are presented in sections (7.3) to (7.14). The routines for the generation of element characteristics matrices are common to all three programs. These are presented in sections (7.7) to (7.10).

7.2 CLASSIFICATIONS OF THE SECTIONS OF THE PROGRAM

The program may be classified into the following main sections:

(i) Specification of the structural idealisation.

Data is input to the program in the following form:

- (a) Nodal coordinates and element topology - This data is prepared using a semi-automatic mesh generation program (Ref. (67)) where the structure is divided into a few large zones and the fineness of element subdivision within each is specified. The initial data is input in the normal way and the subdivision proceeds automatically.
- (b) Material properties
- (c) The boundary conditions
- (d) The loading to which the structure is subjected
- (e) Modal damping ratios, initial conditions, time varying forces, and time integration constants.

Data in parts a, b and c are common to all three programs dealt with in this section. This data is prepared by the mesh generation program and is input into the main program via data files (see Appendix B). Data in parts d and e are input at the keyboard by the operator in response to the appropriate programmed input prompts.

(ii) Evaluation of element characteristics.

The numerically integrated, mixed matrices $[g]$, $[h]$ and $[m]$ are formed for each element in turn with reference to the global coordinate system (x,y) . The load vector $\{r\}$ due to a distributed load,

matrix relation (6.48) is also evaluated numerically.

(iii) Assembly of the element matrices.

The element matrices are assembled into the overall structural matrices. The equivalent stiffness matrix is then calculated, from equation (6.70).

(iv) Solution of the eigenvalue-eigenvector problem.

The standard procedures Trans and Eigen in reference (66) yield the eigenvalues and eigenvectors which may be used for:

- (a) Free vibration analysis
- (b) Forced vibration analysis by mode superposition method.
- (c) Construction of a complete damping matrix in the forced vibration analysis by direct integration method.

(v) Steady state and transient response solutions.

Either a mode superposition (Duhammel integration) or a direct integration (Wilson θ) method is used to calculate the response of the plate subjected to time varying forces.

(vi) Output - The free vibration results are output as a table consisting of numbers for frequencies and mode shapes. The response output from programs RFPLT2 and RFPLT3 include time history plots for displacements and bending moments.

7.3 SUBPROGRAM Feinpt

This subprogram reads the input data file, generated by a pre-program for mesh generation. The variables are read in, in the following order:

(a) Control data

Njb : = Number of jobs
N1 : = Number of elements
N : = Number of nodes
Cw : = Number of nodes with constrained deflections
Cx : = Number of nodes with constrained M_x
Cy : = Number of nodes with constrained M_y
Cxy : = Number of nodes with constrained M_{xy}
Nmat : = Number of materials
Nskew : = Number of nodes with specified local coordinate direction

(b) Geometrical data

The subdivision of the structure into quadrilateral elements is defined by two sets of information:

(i) Nodal data - specifies the position of each node

$X_{(I)}$ x-coordinate of node I

$Y_{(I)}$ y-coordinate of node I

(ii) Element data - each element is identified by the nodal connection array and a material property set number. The nodal connections are represented by the array $N(I,J)$, for $I = 1, 2, \dots, N1$ and $J = 1, 2, 3, \dots, 9$.

(c) Specified boundary conditions

Any one or more degrees of freedom (W, M_x, M_y, M_{xy}) may be specified as zero at a nodal point. Data for this section is read in the following order:

- (i) Sequence of node numbers with specified W
- (ii) Sequence of node numbers with specified M_x
- (iii) Sequence of node numbers with specified M_y
- (iv) Sequence of node numbers with specified M_{xy}

By using the information in part (c), an array $Ndc(I,J)$, for $I = 1, 2, \dots, N$ and $J = 1, 2, 3, 4$ is constructed which specifies the free and restrained nodal degrees of freedom (moments, deflections). This array is used in the assembly process where the rows and columns corresponding to constrained degrees of freedom are determined and thus deleted. Figure (7.1) represents the nodal constraint array ($Ndc(*)$) for a quarter of a simply-supported plate. One element idealisation is used and zeros indicate the constrained degrees of freedom.

Node Number	M_x	M_y	M_{xy}	W
1	0	0	1	0
2	0	2	3	0
3	0	4	0	0
4	5	0	6	0
5	7	8	0	1
6	9	0	0	0
7	10	11	0	2
8	12	13	0	3

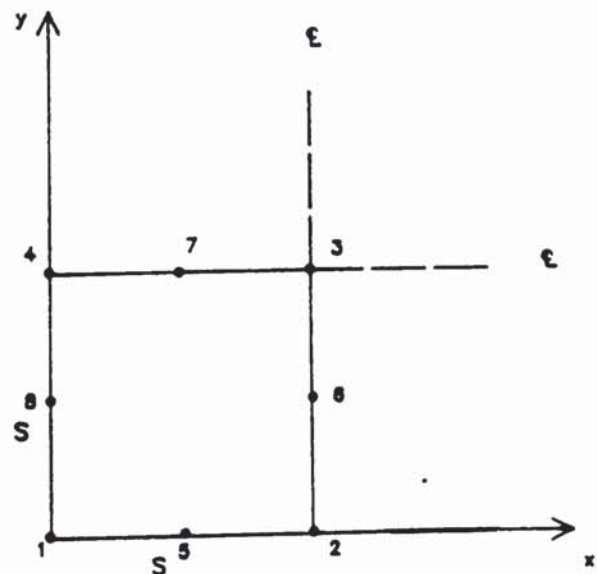


Fig. (7.1) Nodal connection array for a quarter of a SSSS plate.

Sequence of nodes with constrained W , 1, 2, 3, 4, 6
Sequence of nodes with constrained M_x , 1, 2, 3
Sequence of nodes with constrained M_y , 1, 4, 6
Sequence of nodes with constrained M_{xy} , 3, 5, 8, 7, 6

7.4 SUBPROGRAM Cmatrx

This subprogram reads the material properties of the structure from the input data file. The properties are specified for each set of elements of different materials. Each set is identified with a material property set number (Mat). Data is read in the following order:

- (i) Th (Mat) : = Group material thickness
- (ii) D (Mat) : = Group material density
- (iii) $E_x, \nu_{xy}, G_{xy}, E_y, \nu_{yx}$: = Group material constants

7.5 SUBPROGRAM Excitn

This subprogram permits the user to define the force function from the keyboard.

7.6 SUBPROGRAM Rspipt

This subprogram is used to input the data required for the response calculations. Data at this stage is input by the operator at the keyboard. The input variables are:

Time	Time required for the response calculations
T	The value of theta in Wilson integration scheme
Delta	Time incremental
A0 (*)	Integration constants used in Wilson θ method
D(*)	Vector of initial displacements
O f(*)	Vector of initial velocities
Nmod	Number of damped modes
Dr(*)	Array of damping ratios
Wp	Node number to calculate displacements for
Mp	Node number to calculate the moments for
J2	Code 1 - for M_x , 2 - for M_y , 3 - for M_{xy}

Subprograms Excitn and Rspipt are called in by programs RFPLT2 and RFPLT3.

7.7 SUBPROGRAM Qaux

Description: This subprogram is called in to perform the following operations:

- (a) Calculates the shape functions $N_1(\xi, \eta), \dots, N_8(\xi, \eta)$ at the Gauss point within an element.
- (b) Calculates the Jacobian J , its determinant and the inverse of the Jacobian, equation (6.30) at the Gauss point.
- (c) Calculates shape function derivatives $\frac{\partial N_1}{\partial \xi}, \dots, \frac{\partial N_8}{\partial \eta}$
- (d) Calculates the angle β in equation (6.41), and ds in equation (6.45) along each element side by calling four subroutines Side 1, Side 2, Side 3 and Side 4 respectively.

The subprogram Qaux can be considered as a standard routine, which with little change, may be used in developing of other two dimensional isoparametric elements.

Variables list:

L_1, L_2	Natural coordinates of the sampling point (ξ_p, η_p)
Sf(*)	Shape function array
Pm(*)	Shape function derivative array
X(*), Y(*)	Nodal cartesian coordinate array
Z	Current element number
U	Determinant of Jacobian J
N(*)	Nodal connection array
Be	Angle between normal to a boundary with the +ve x-axis direction

Ds Defined according to equation (6.45)
Jo Integer indicating which operations to
 be carried:

1 - step (d) on Side 1 of the element ($\eta = -1$)

2 - step (d) on Side 2 of the element ($\xi = -1$)

3 - step (d) on Side 3 of the element ($\eta = -1$)

4 - step (d) on Side 4 of the element ($\xi = -1$)

5 - steps (a) and (b)

6 - steps (a), (b) and (c)

The variables are passed to and from the subprogram via the parameter list. Fig (7.2) shows the flow diagram for subprogram Qaux.

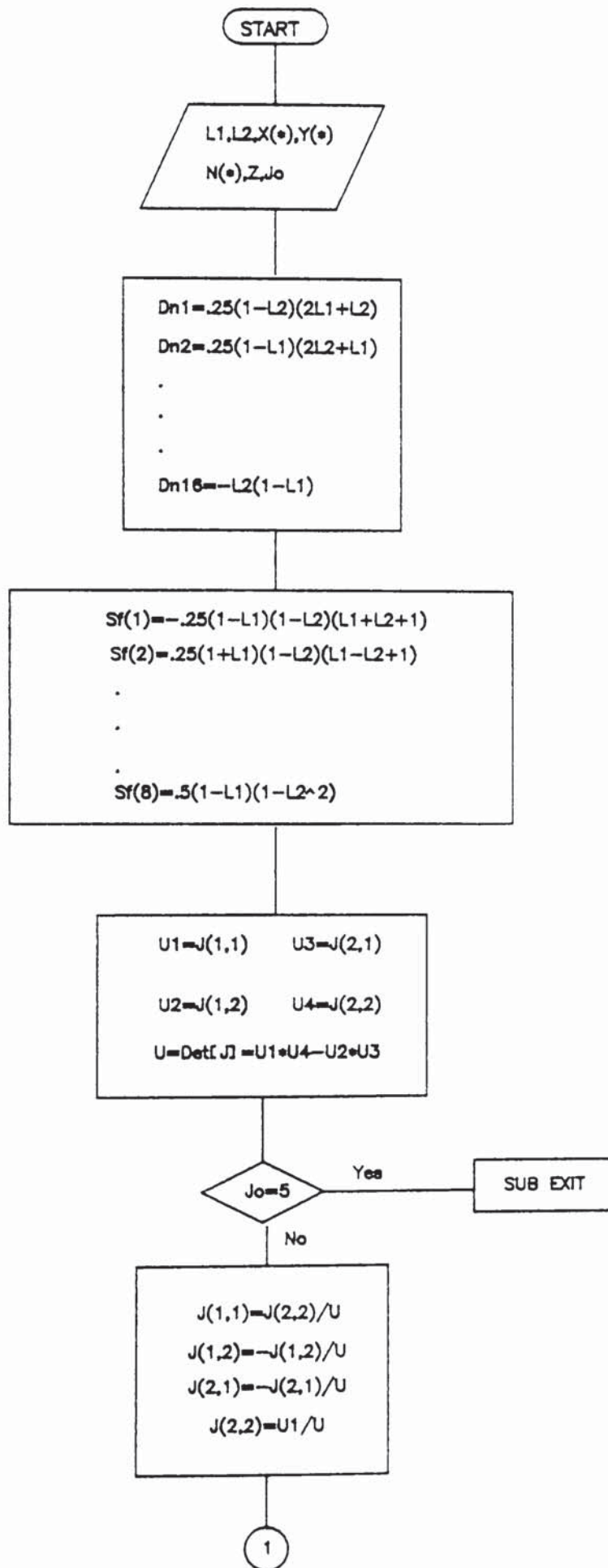
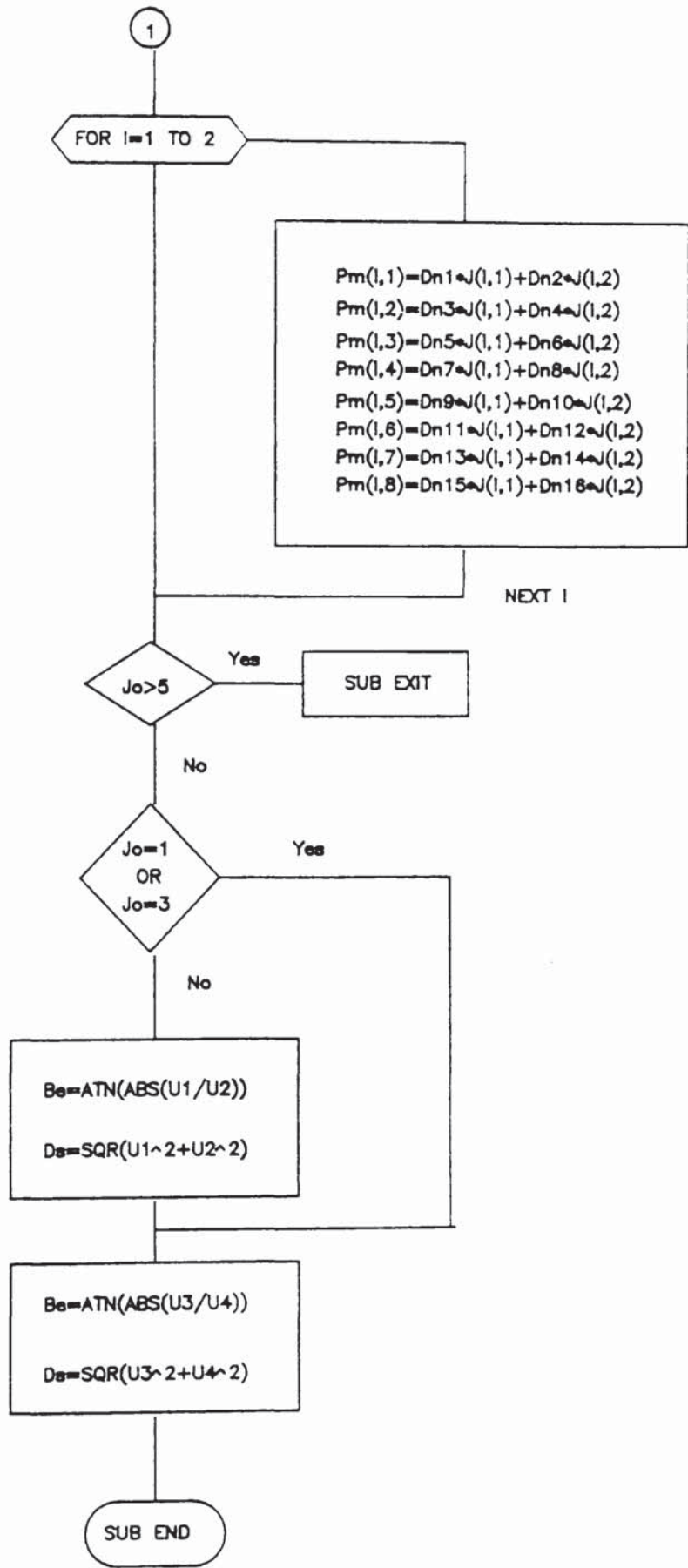


Fig 7.2 Flow diagram for SUB Qaux(L1,L2,X(*),Y(*),U,Pm(*),Sf(*),
Be,De,INTEGER Z,N(*),Jo)



7.8 ALGORITHMS FOR THE GENERATION OF ELEMENT MATRICES AND LOAD VECTOR

The coefficients of the element matrices $[h]$, $[g]$, $[m]$ and the equivalent nodal force vector $\{r\}$ due to a distributed load are evaluated numerically using the Gauss quadrature rule, see section (6.5.7).

The subprogram Qaux, described by the flow diagram of Fig. (7.2) is called up in the element loop of the program to evaluate the variables required in the numerical integration process. For the integration of the partitioning matrix $[g]$ equation (6.49), we only need to integrate 36 different coefficients, related by the array Sfm(*), see figure (7.7). The coefficients are later multiplied by the constant values of the compliance matrix, array Cons(*), and located in $[g]$ in accordance with equation (6.50) by the subprogram Geform. The contributions of the double integral in equation (6.52) to the mixed matrix $[h]$ are evaluated by calling up subprogram Heform. The line integral contributions are calculated in the subprogram Mnsws and added to construct the complete $[h]$ matrix. Subprograms Meform and Loadap are called up to calculate the element mass matrix and load vector respectively.

7.8.1 Subprogram Mnsws

This subprogram evaluates the contributions of the line integral $\int_{-1}^1 [L_{ns}]^t [Y] ds$, to element mixed matrix $[h]$ (equation 6.52).

Variables list:

Zn(*) Gauss points & weights array

C(*)	L_{ns} array in Eqn. (6.42)
D(*)	Y array in Eqn. (6.38)
He(*)	Element mixed array [h]
X(*), Y(*)	Cartesian coordinates arrays
Bm(*)	Shape function derivative array
N(*)	Nodal connection array
Sf(*)	Shape function array
Z	Element counter
K	Element Side number (1,2,3 or 4)
Be	Angle
Ds	$(\frac{\partial S}{\partial \xi} d\xi)$ or $(\frac{\partial S}{\partial \eta} d\eta)$

Figure (7.3) shows the flow diagram for subprogram Mnsws.

7.8.2 Subprogram Heform

This subprogram calculates the coefficients of the mixed array [h] due to double integral in equation (6.52).

Variable list:

T_1, T_2	weight coefficients
He(*)	Element mixed array [h]

Other variables are as defined in section 7.8.1.

Figure (7.4) shows the flow diagram for subprogram Heform.

7.8.3 Subprogram Geform

The coefficients of the submatrix $[g_{ij}]$ are multiplied by the constant values of the compliance matrix, array $C(*)$ and located in $[g]$ in accordance with Equation (6.50).

Variables list:

Ge(*)	Element mixed array $[g]$
A(*)	Array of shape function products
C(*)	Array of material constants
Matno	Number of material

Fig. (7.5) shows the flow diagram for this subprogram.

7.8.4 Subprogram Transf.

Description: This subprogram modifies the element mixed matrices $[g]$ and $[h]$ for those nodes on the boundary which require a coordinate transformation from the global x,y to a local n,s axes. Thus the boundary conditions for the bending and twisting moments may be applied directly in terms of normal and tangential components. The modification is carried out at element level. If for instance node 6 of element e requires modification then we have: (see section 6.7)

$$\begin{aligned} \begin{bmatrix} g'_{ij} \end{bmatrix} &= \begin{bmatrix} g_{ij} \end{bmatrix} \begin{bmatrix} 1 \end{bmatrix} && \text{for } \begin{matrix} i = 1,2,3,4,5 \\ j = 6 \end{matrix} \\ \begin{bmatrix} g'_{ij} \end{bmatrix} &= \begin{bmatrix} 1 \end{bmatrix}^t \begin{bmatrix} g_{ij} \end{bmatrix} && \text{for } \begin{matrix} i = 6 \\ j = 7,8 \end{matrix} \\ \begin{bmatrix} g'_{66} \end{bmatrix} &= \begin{bmatrix} 1 \end{bmatrix}^t \begin{bmatrix} g_{66} \end{bmatrix} \begin{bmatrix} 1 \end{bmatrix} \\ \text{and} \\ \begin{bmatrix} h'_{ij} \end{bmatrix} &= \begin{bmatrix} 1 \end{bmatrix}^t \begin{bmatrix} h_{ij} \end{bmatrix} && \text{for } \begin{matrix} i = 6 \\ j = 1, \dots, 8 \end{matrix} \end{aligned}$$

$\begin{bmatrix} 1 \end{bmatrix}$ is the direction cosine matrix given by equation (3.26), evaluated from the value of the angle which the normal n makes with the x axis. The matrices g_{ij} and h_{ij} are the partitioning matrices of element mixed matrices $\begin{bmatrix} g \end{bmatrix}$ and $\begin{bmatrix} h \end{bmatrix}$.

Figure (7.6) shows the flow diagram for this subprogram. Subroutine Cosd is called to calculate the direction cosine matrix $\begin{bmatrix} 1 \end{bmatrix}$. The four subprograms Matmult, Matmult1, Matmult2 and Matmult3 are called up to evaluate the products $\begin{bmatrix} 1 \end{bmatrix}^t \begin{bmatrix} g_{ij} \end{bmatrix} \begin{bmatrix} 1 \end{bmatrix}$, $\begin{bmatrix} 1 \end{bmatrix}^t \begin{bmatrix} g_{ij} \end{bmatrix}$, $\begin{bmatrix} g_{ij} \end{bmatrix} \begin{bmatrix} 1 \end{bmatrix}$ and $\begin{bmatrix} 1 \end{bmatrix}^t \begin{bmatrix} h_{ij} \end{bmatrix}$ respectively.

Variables list:

Ge(*)	Element array [g]
He(*)	Element mixed array [h]
Be	Angle (DEGREE)
W	Node number (1,2,3,4,5,6,7 or 8)

7.8.5 Subprogram Meform

The element consistent mass matrix equation (6.53), is formed by calling up subprogram Meform.

Variables list:

D(*)	Array of material densities
Th(*)	Material thicknesses
X(*), Y(*)	Nodal coordinates array
N(*)	Nodal connection array
Z	Element counter
Me(*)	Element mass matrix
U	Counter for numerical integration

Figure (7.8) shows the flow diagram for subprogram Meform.

7.8.6 Subprogram Loadap

Description: This subprogram evaluates the element load vector and adds contributions to global load vector from element load vector. Two types of loading may be accommodated. Firstly at each node a load in the z direction may be input. Secondly, a distributed load acting normal to the plate (i.e. in the z direction) may be applied. Such a loading is converted into equivalent nodal forces by use of the expression (6.55). Data is input at the keyboard.

Variables list:

Type	Specifies type of loading:	1 - for concentrated loads
		2 - for uniformly distributed
		3 - for general distributed loading
N(*)	Nodal connection array	
Ndc(*)	Nodal constraint array - specifies free & constrained nodes	

Nelemt	Number of elements
Sf(*)	Shape function array
U	Counter round the integration points
W(*)	Gauss points & weight factors
Re(*)	Element load vector
R(*)	Global load vector
N	Number of nodes with concentrated loading
S1	Node number
Val	Value of the concentrated loads
Ne1	Number of elements with distributed loads
P	Load per unit area
E1(*)	Array of element numbers with distributed loading
P(*)	Nodal pressure intensities array

Figure (7.9) shows the flow diagram for subprogram Loadap.

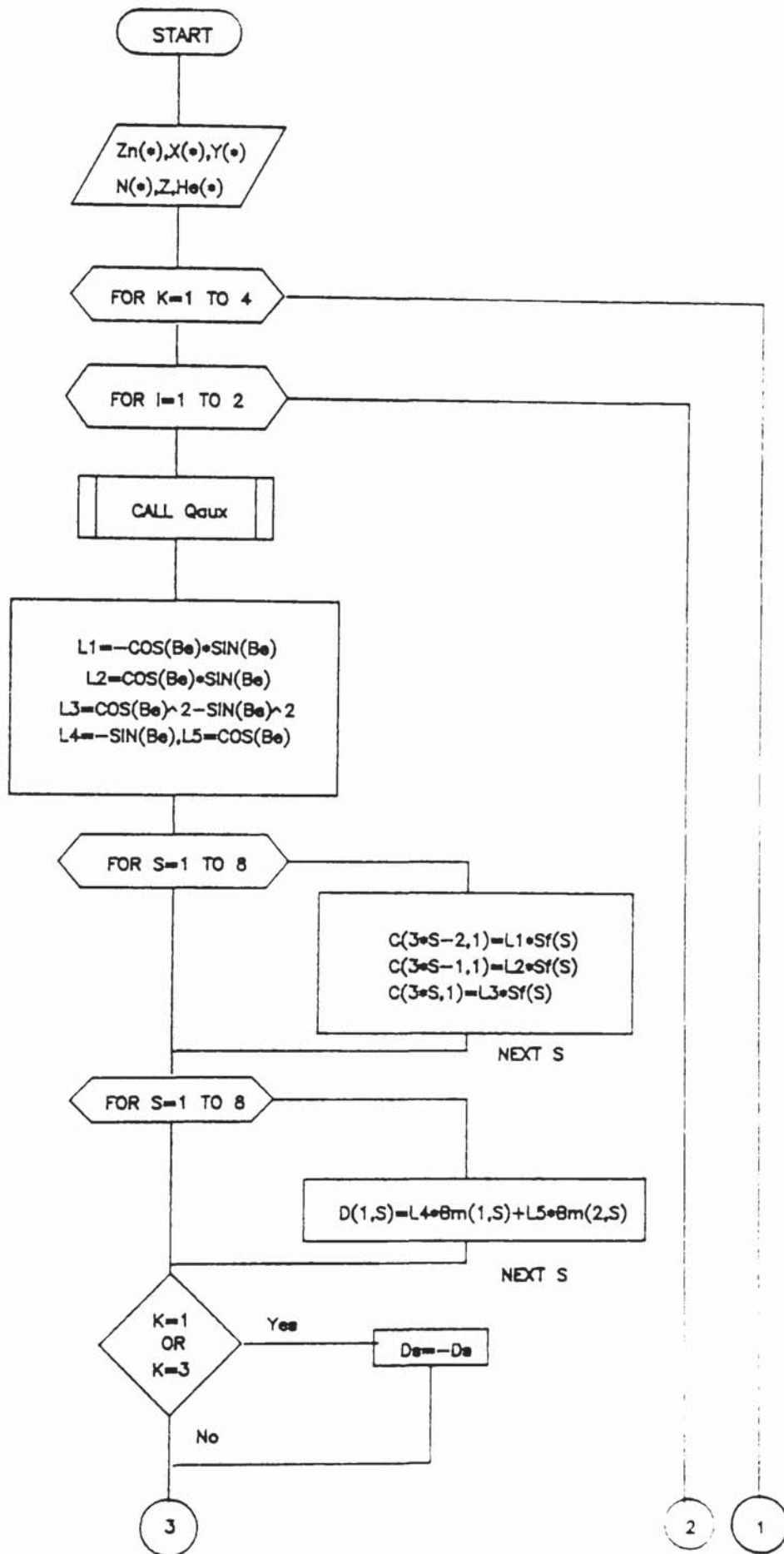
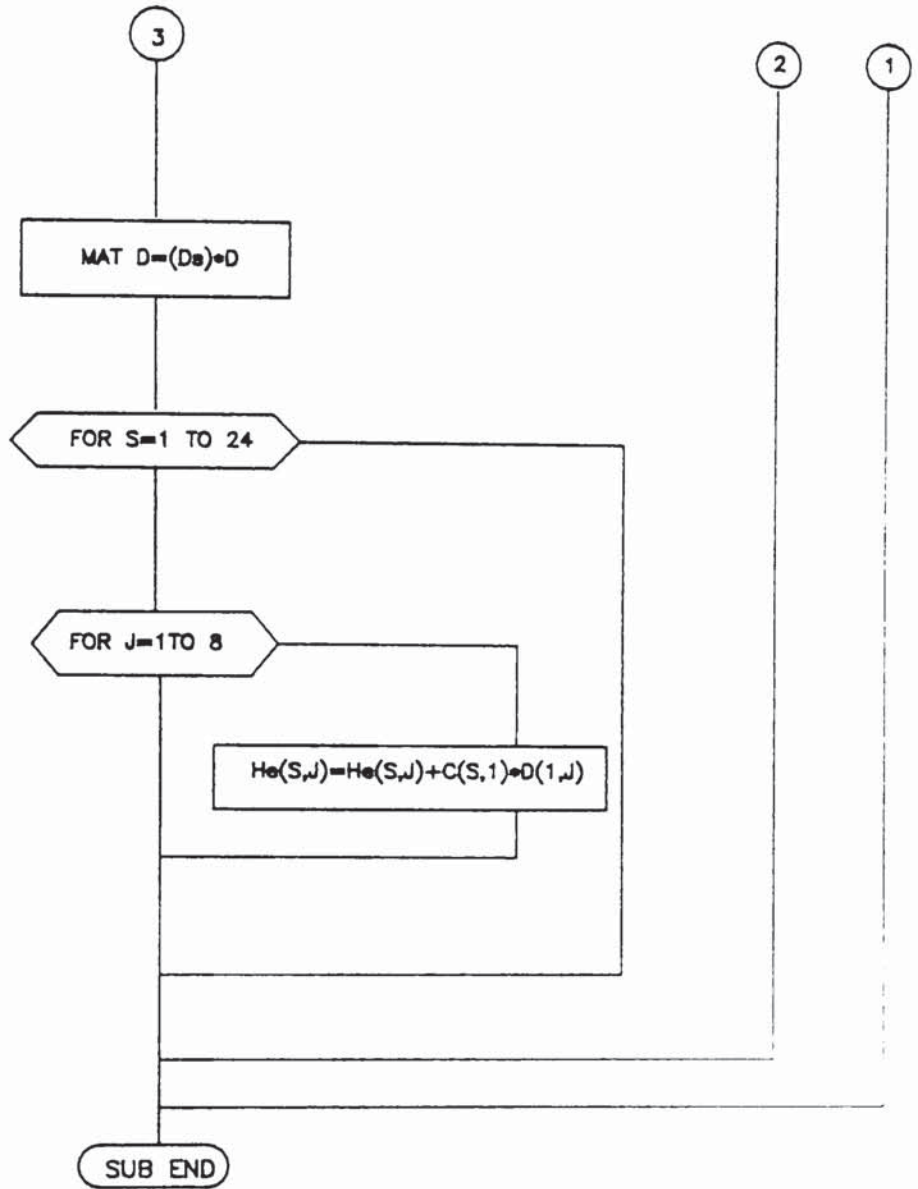


Fig 7.3 Flow diagram for SUB Mnews(He(*),X(*),Y(*),Bm(*),St(*),Be

De, INTEGER N(*),Z,K)



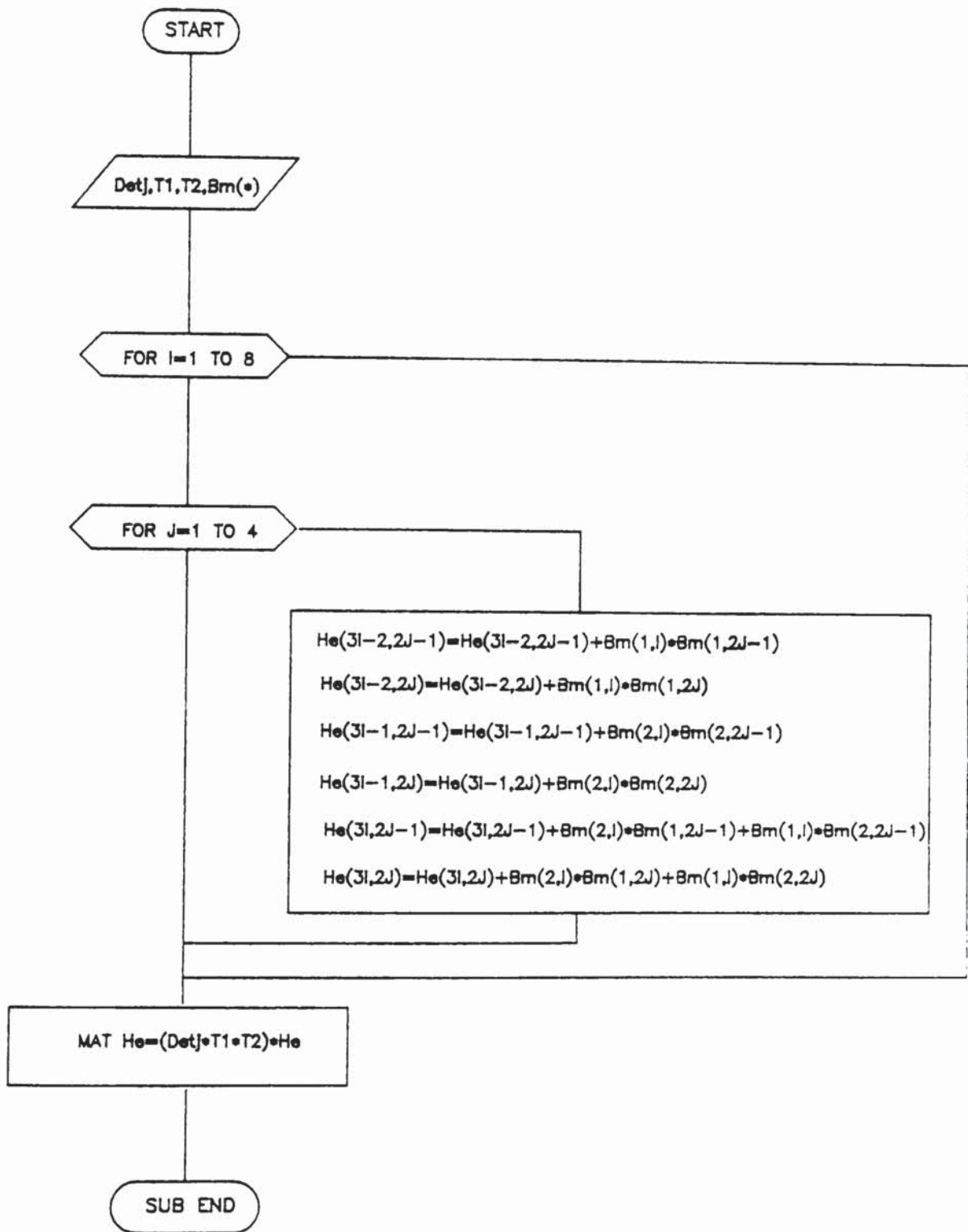


Fig 7.4 Flow diagram for SUB Heform(He(*),Bm(*),DetJ,T1,T2)

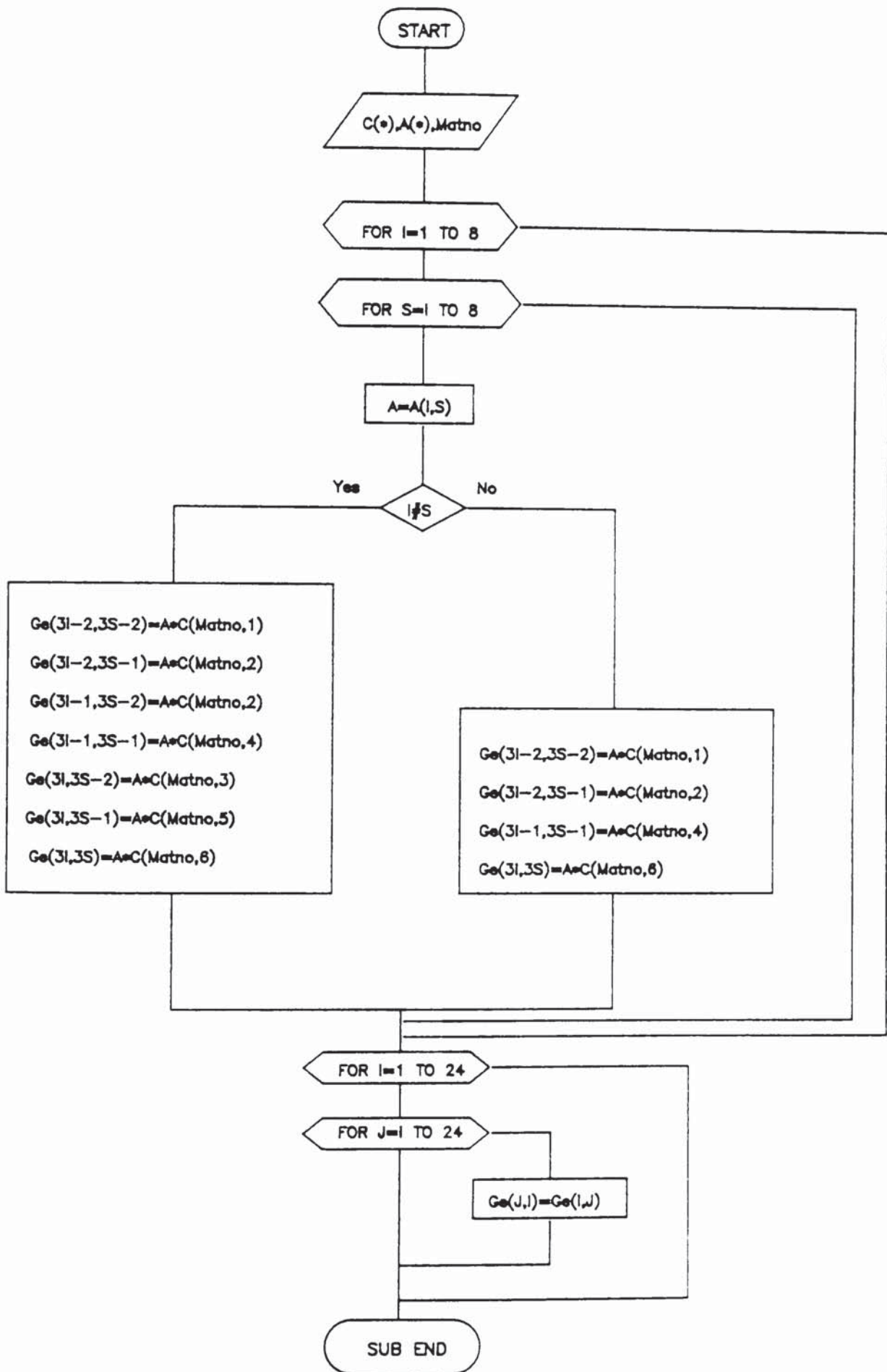


Fig 7.5 Flow diagram for SUB Geform(Ge(*),A(*),C(*),INTEGERMatno)

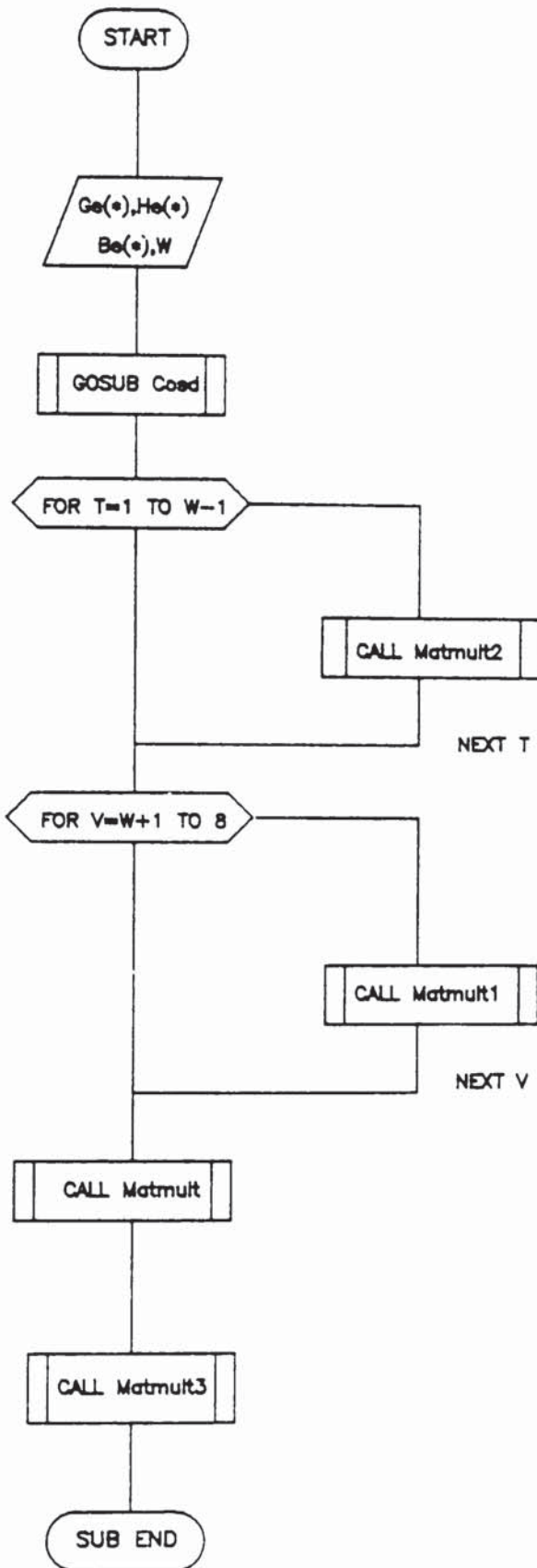


Fig 7.6 Flow diagram for SUB Transf(Ge(*),He(*),Be(*),W)

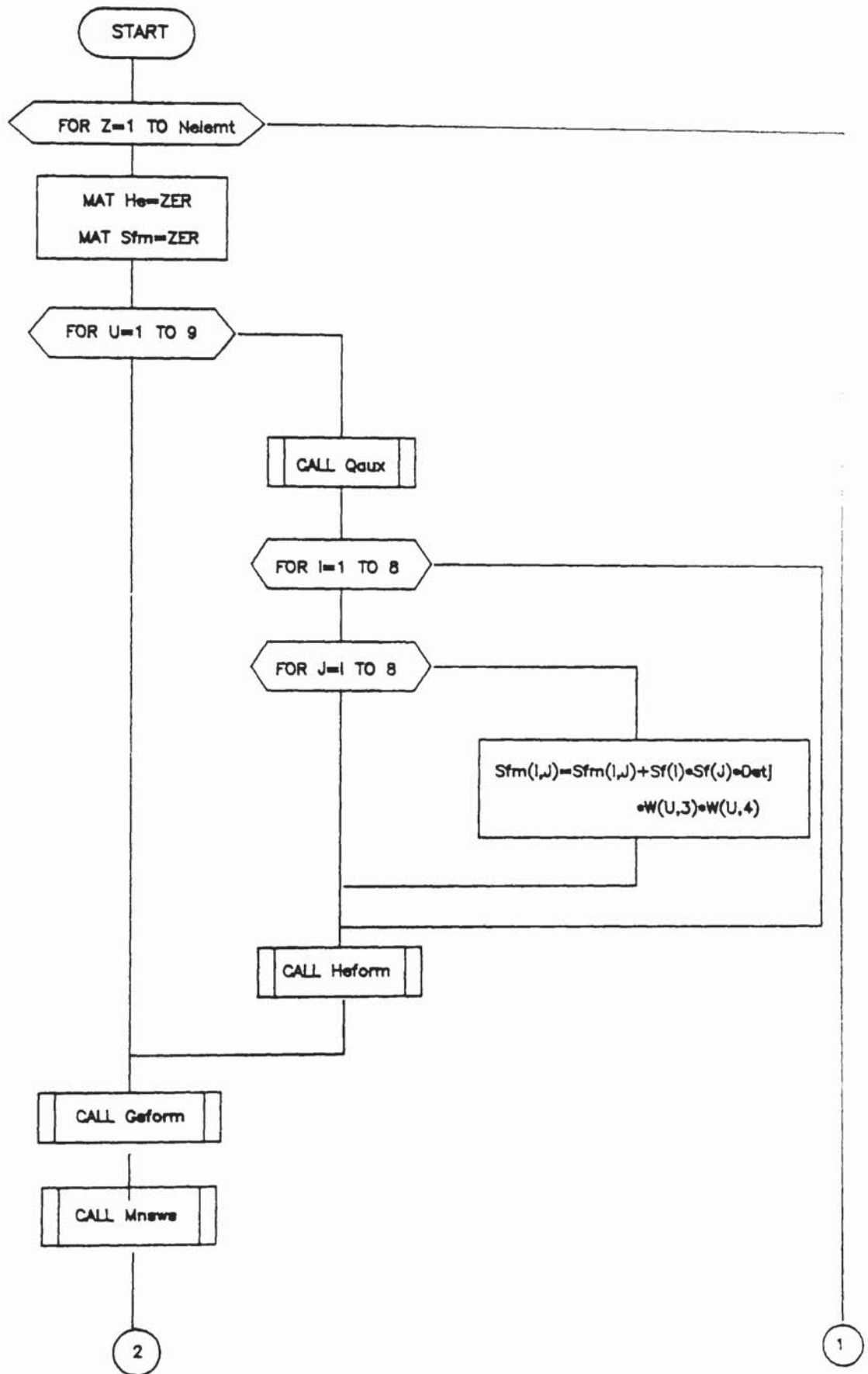
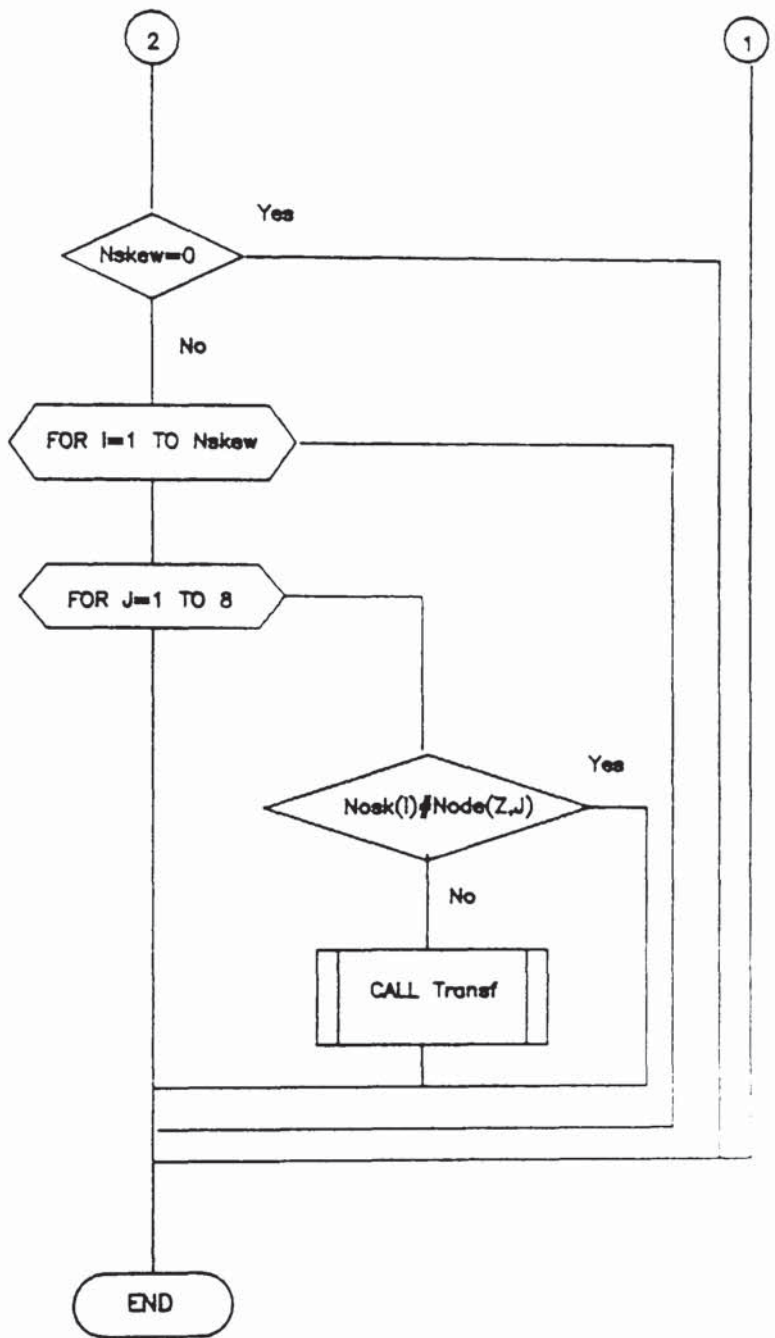


Fig 7.7 Flow diagram for the construction of element matrices:
[g] and [h]



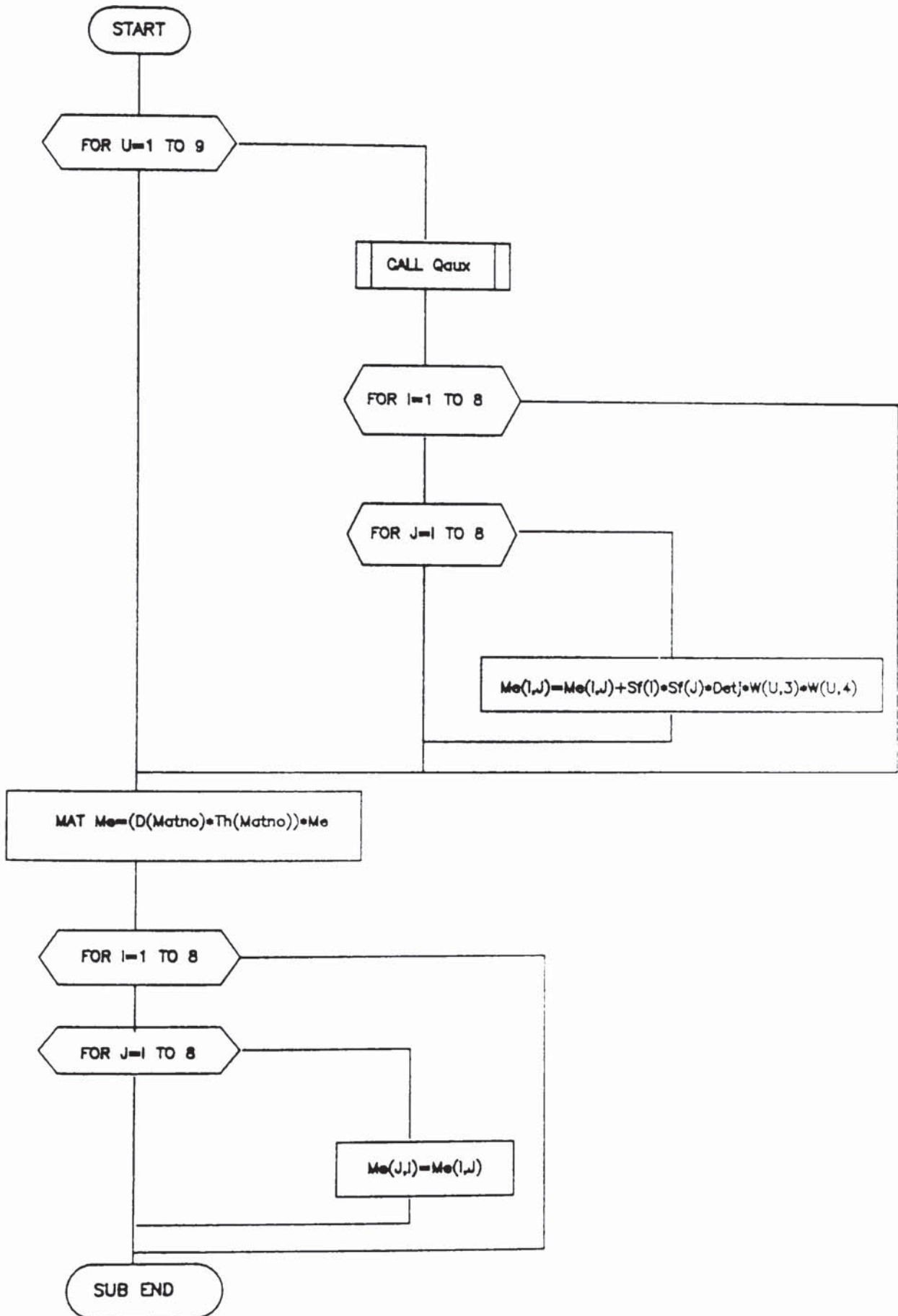


Fig 7.8 Flow diagram for SUB Meform(D(*),Th(*),Me(*),X(*),Y(*),
W(*),Detj,Sf(*),Bm(*),INTEGER N(*),Matno,Z)

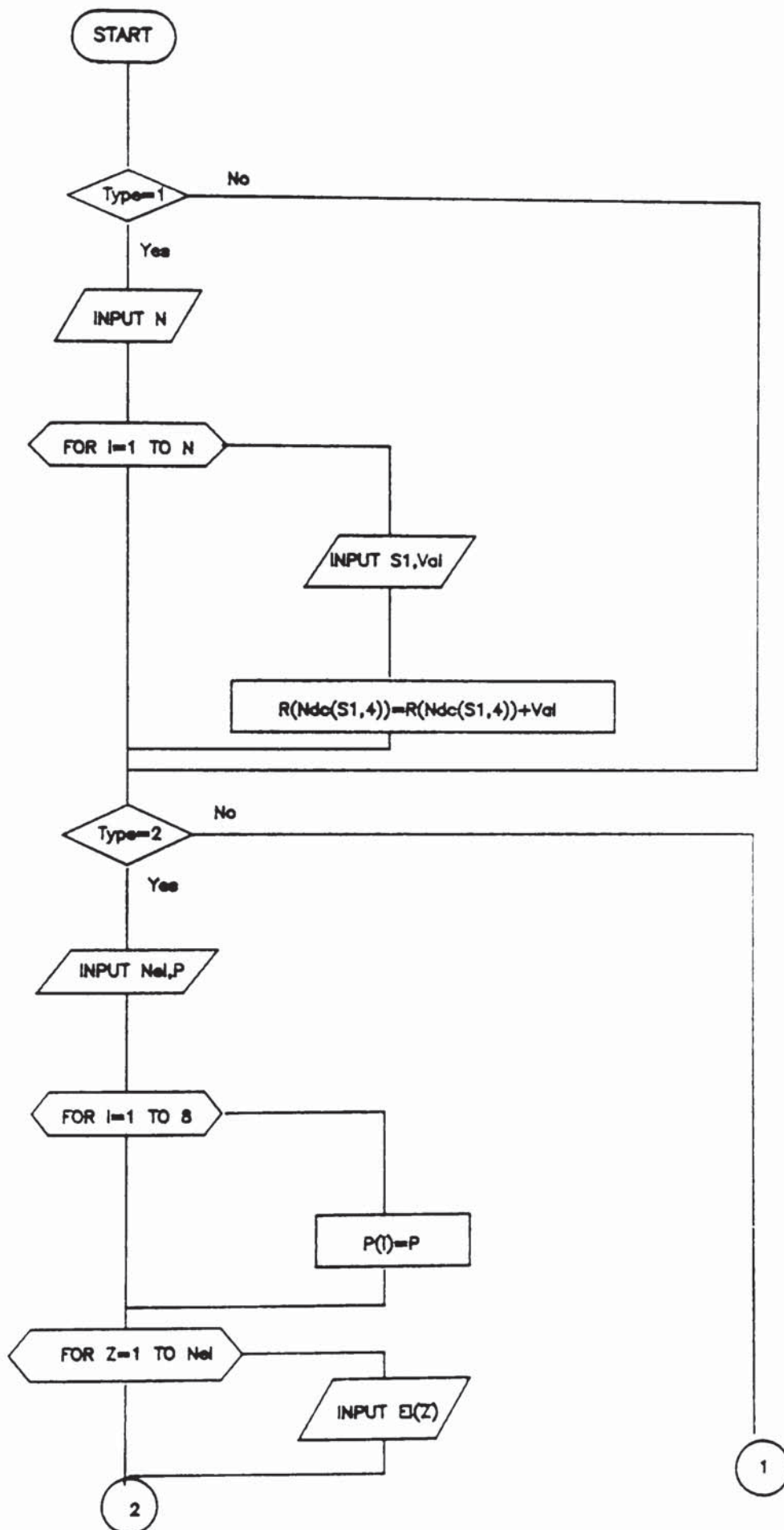
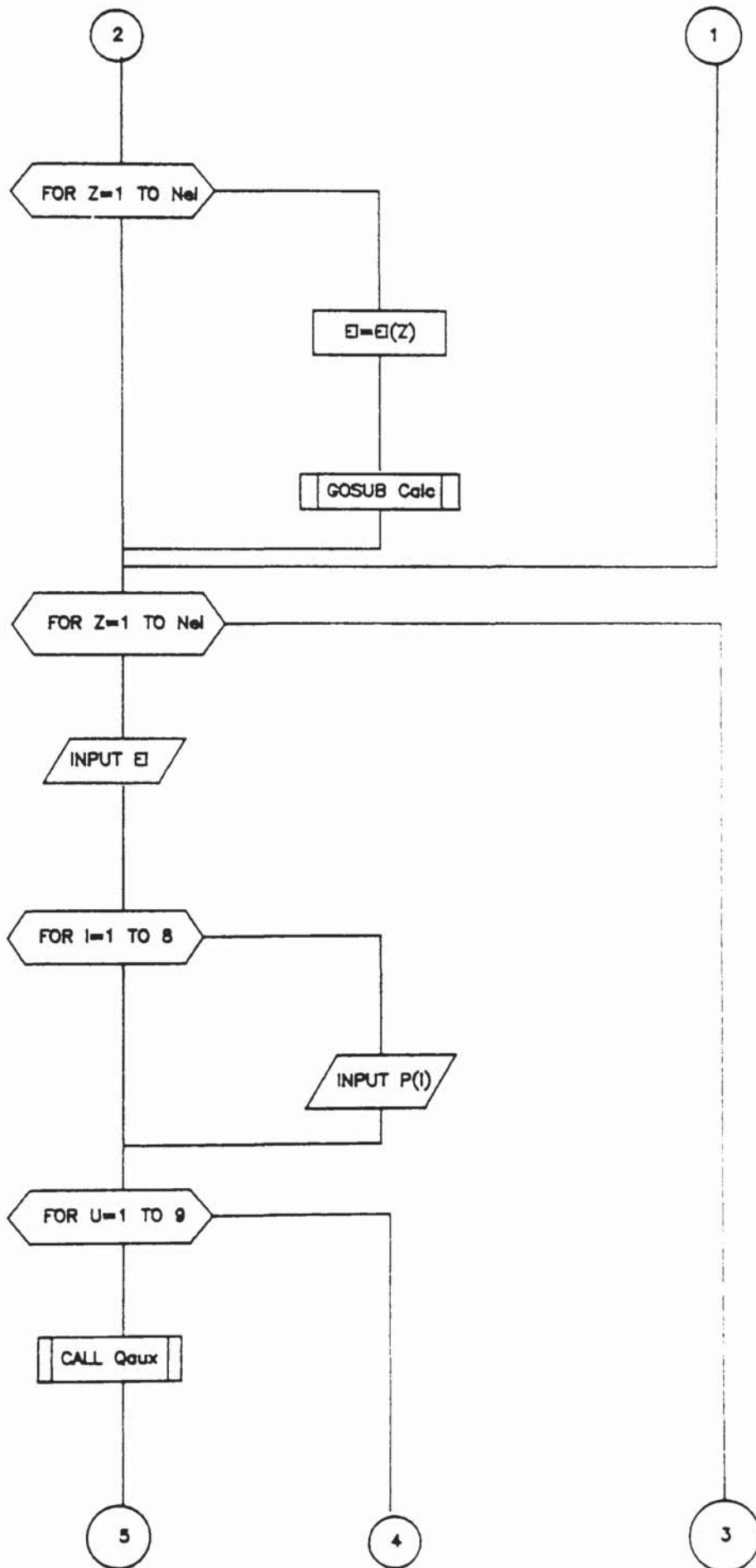
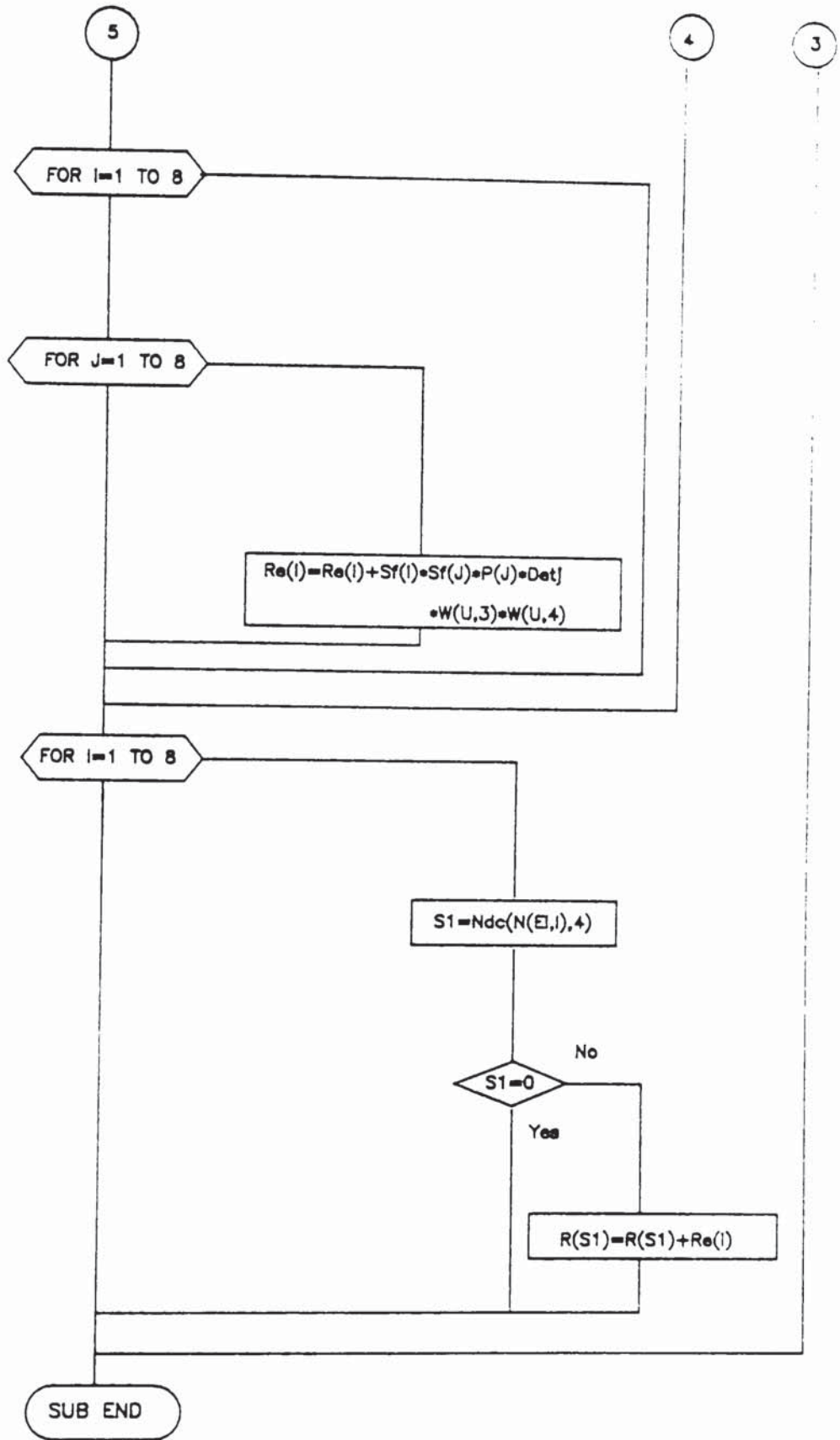


Fig7.9 SUB Loadap(R(*),W(*),X(*),Y(*),DetJ,Bm(*),Sf(*),:NTEGER
N(*),Ndc(*),Nelemt,Nnode)





7.9 ALGORITHMS FOR THE ASSEMBLY OF THE OVERALL MATRICES

The overall matrices $[G]$, $[H]$ and $[M]$ are assembled in full matrices by calling up the subprograms Ghasemb and Masemb respectively. Due to symmetry of coefficient matrices $[M]$ and $[G]$, only the lower half is used in the assembly process.

The variables involved in these subprograms are defined as follows:

K(*)	overall mixed matrix [G]
Ke(*)	element mixed matrix [g]
H(*)	overall mixed matrix [H]
He(*)	element mixed matrix [h]
Fm	number of stress degrees of freedom
Z	element counter
N(*)	nodal connection array
Ndc(*)	nodal constraint array
M(*)	element consistent mass matrix
Fw	number of displacement degrees of freedom

Figures (7.10) and (7.11) show the flow diagrams for subprograms Ghasemb and Masemb respectively.

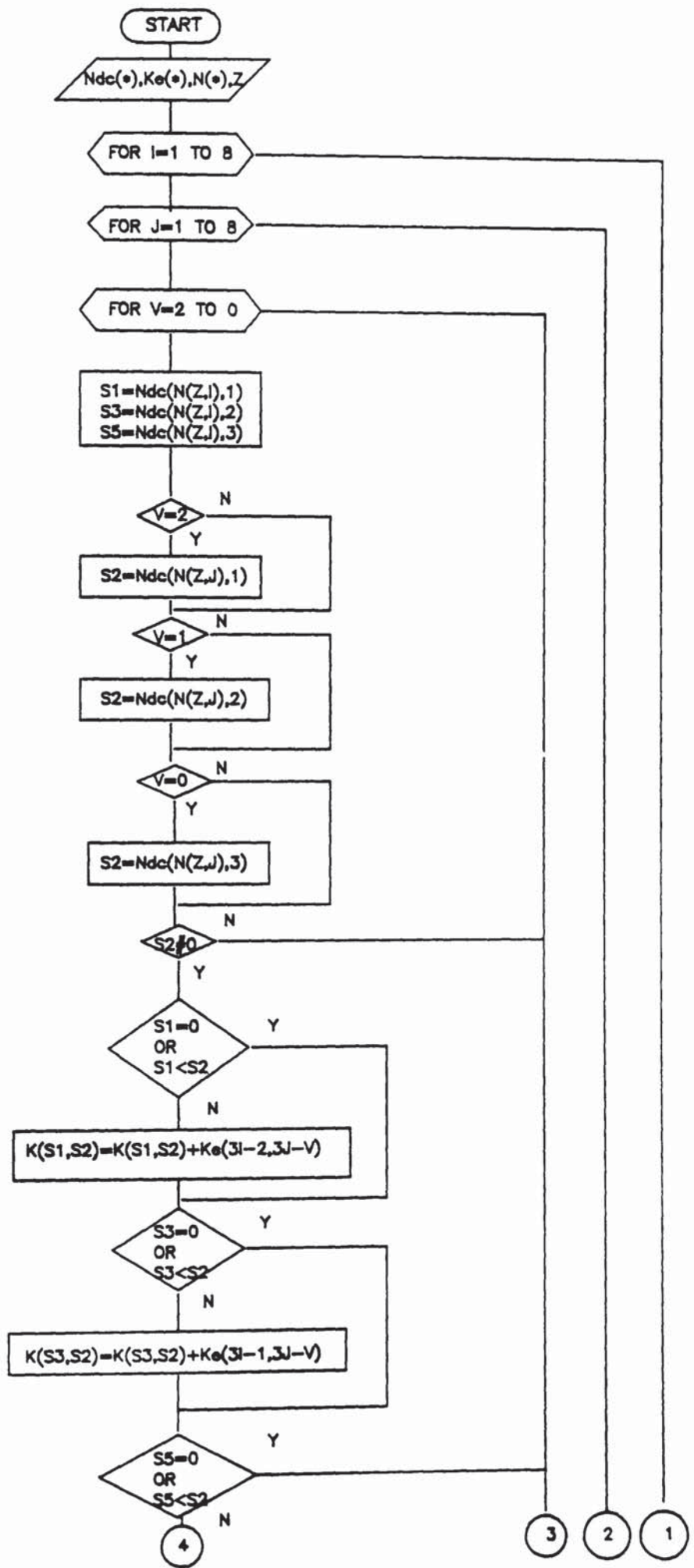
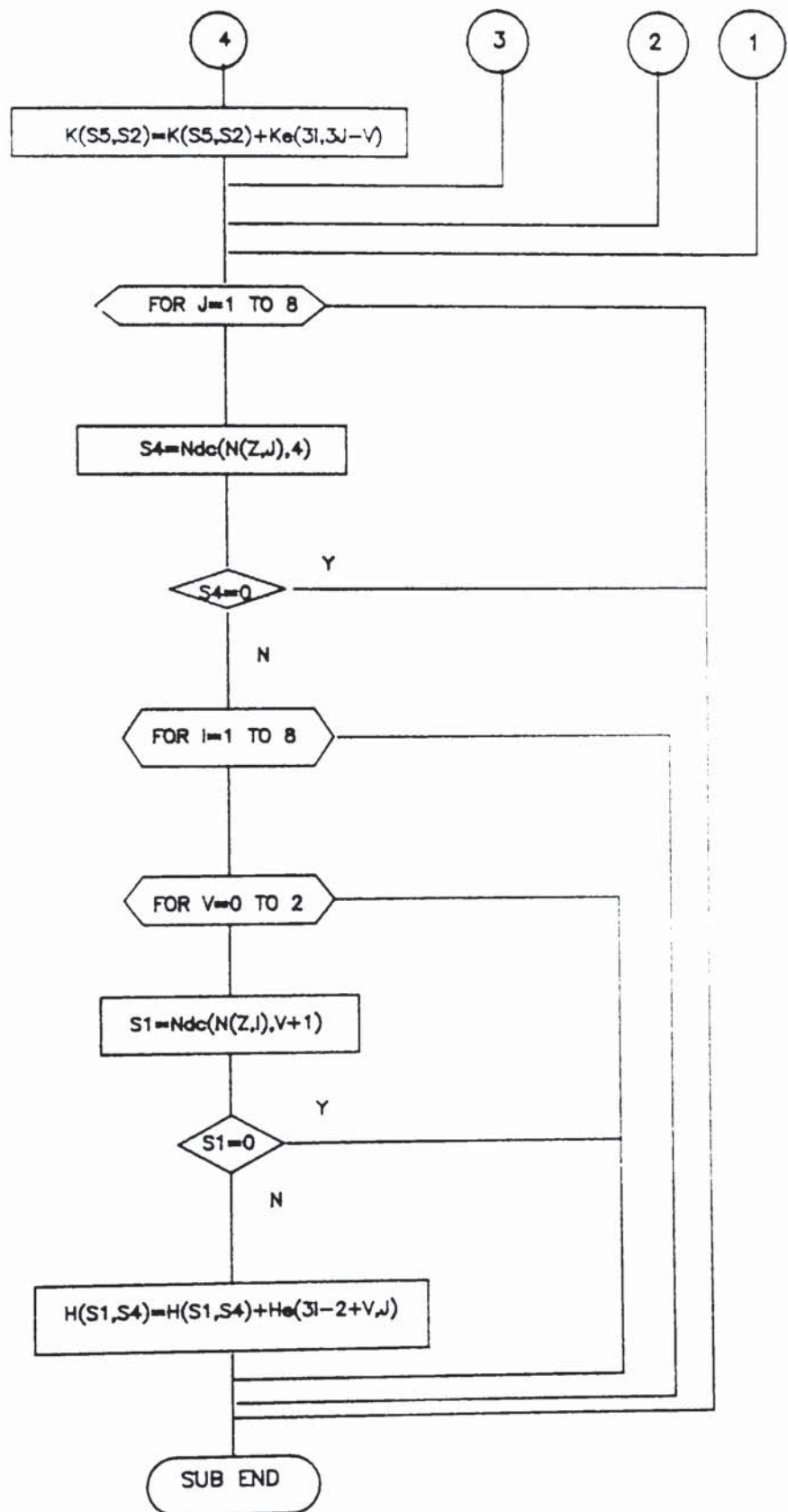


Fig 7.10 Flow diagram for SUB Ghasemb(K(*),Ke(*),H(*),He(*))
 INTEGER Fm,Z,N(*),Ndc(*)



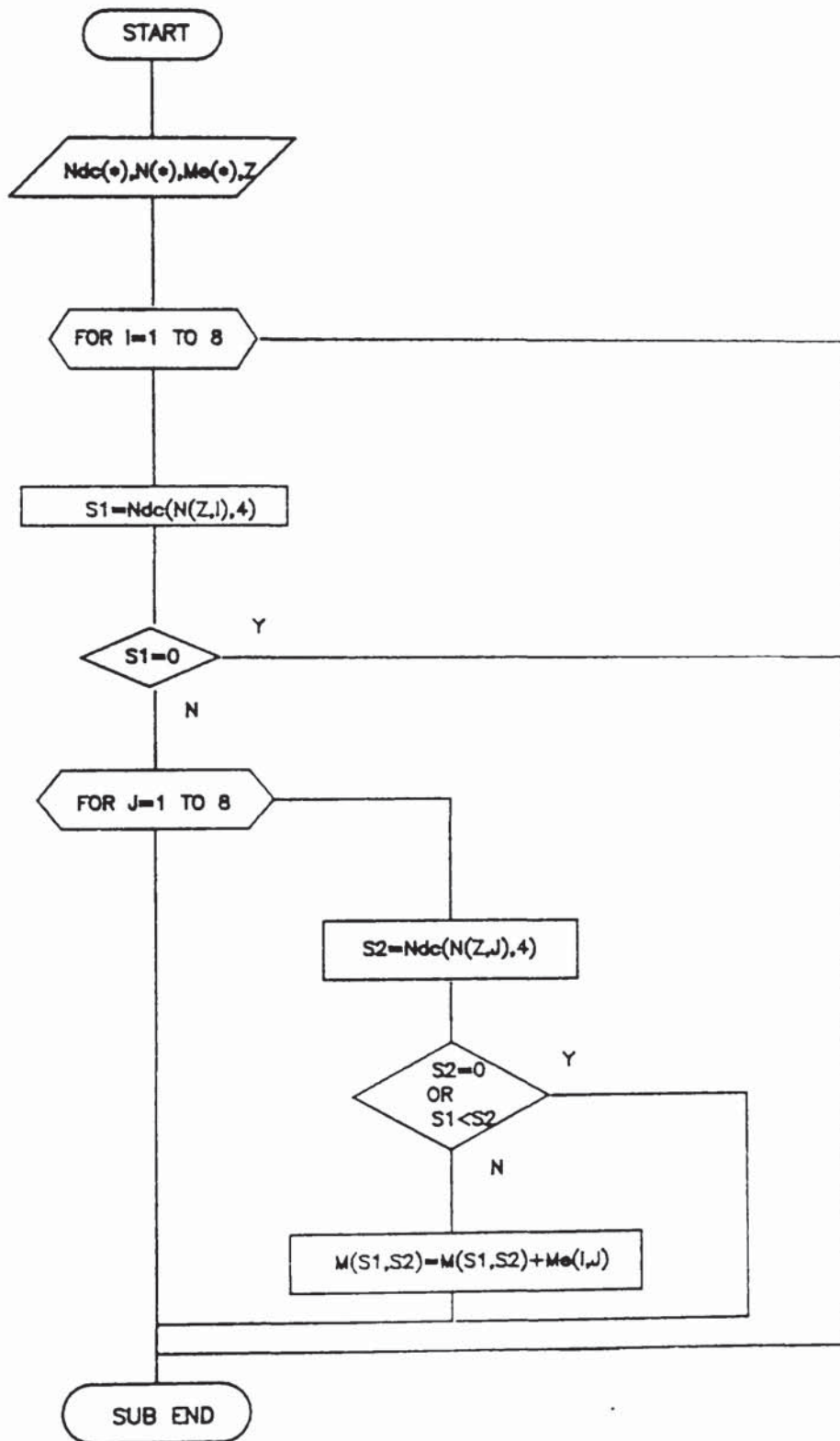


Fig 7.11 Flow diagram for SUB Masemb($M(\bullet)$), $Me(\bullet)$),INTEGER $Fw, Z, N(\bullet)$
 $Ndc(\bullet)$)

7.10 ELIMINATION OF THE NODAL MOMENT DEGREES OF FREEDOM

The fully populated symmetric positive definite stiffness matrix K^* , ($[K^*] = [H]^t [G]^{-1} [H]$) is obtained prior to the solution process. The product $[G]^{-1} [H]$ is calculated by calling up subprogram Eqsolv. This procedure was developed by Wilkinson (68) for the solution of symmetric positive definite equations by Choleski factorization method. The algorithm solves the system of equations $[A][X] = [B]$ where $[A]$ is a symmetric positive definite matrix of order $N \times N$, and $[B]$ is a $N \times R$ matrix of R right end sides. The solution $[X]$ overwrites $[B]$. The stiffness matrix $[K^*]$ is then obtained by executing the product $[H]^t [X]$ i.e.

$$[K^*] = [H]^t [X]$$

7.11 SUBPROGRAM Dampmat

This subprogram computes an orthogonal damping matrix for the structure based on known modal damping ratios. Subprograms Trans and Eigen are called by Dampmat to evaluate the structure's normal modes and frequencies. The construction of the damping matrix is then carried out using a procedure described in Appendix A.

Variables list:

C(*)	Damping matrix
M(*)	Mass matrix
K(*)	Stiffness matrix
Vec(*)	Array of eigenvectors
Eval(*)	Array of eigenvalues
Zeta(*)	Array of damping ratios
P	Number of damped modes

Subprogram Dampmat is called by Program RFPLT3. Flow chart for this subprogram is shown in Fig. (7.12).

7.12 SUBPROGRAM Init1

This subprogram computes the initial acceleration vector from a knowledge of initial velocities and displacements. The initial acceleration vector is required when numerical integration is performed by Wilson θ method.

7.13 SUBPROGRAM Wilsnsol

This subprogram uses the Wilson method for numerical integration, described in section (4.6.1), to calculate the displacements at equal time intervals. Matrix inversion is carried out by Choleski factorization method (68). The subprogram Eqsolv1 is called before the solution procedure to triangularize the stiffness matrix according to $[K] = [L][D][L]^t$. The subprogram Eqsolv2 performs the back substitution process to calculate displacements at each time interval.

The variables in this subprogram are:

K(*), M(*), C(*)	Structural stiffness, mass and damping matrices
F0 (*)	Load vector
Ndc(*)	Nodal constraint array
N	Number of displacement degrees of freedom.
Npts	Number of time steps
H(*)	Mixed array $[G]^{-1}[H]$
P(*)	Vector of bending moments calculated from equation (6.68)
A0 (*)	Integration constants
D(*), D1(*), D2(*)	Vector of initial displacements velocities and accelerations

Fig. (7.13) shows the flow diagram for subprogram Wilsnsol.

7.14 SUBPROGRAM Duhamel

This subprogram is called by Program RFPLT2 to perform the numerical integration of the Duhamel integral (Eqn. 4.46). The order of the integration approximation being used is 2 (Trapezoidal rule). This procedure is explained in reference (42).

Listings of programs RFPLT1, RFPLT2 and RFPLT3 including the subprograms presented in this section are given in Appendix C.

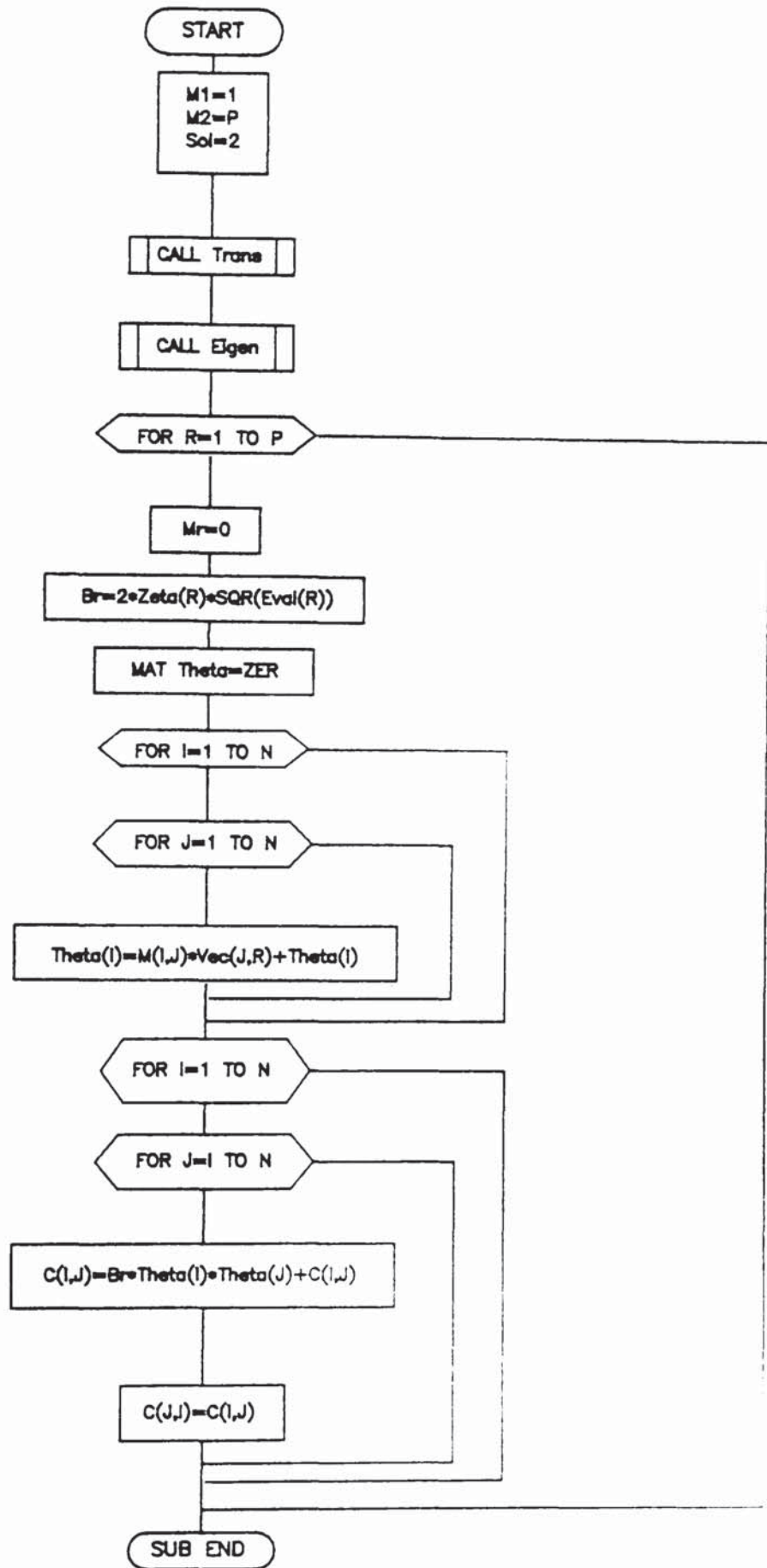


Fig 7.12 Flow diagram for SUB Dampmat(C(*),Vec(*),Eval(*),M(*),
K(*),Zeta(*),D(*),Offd(*),Offd2(*),DI(*),INTEGER P,N,Type,Sol)

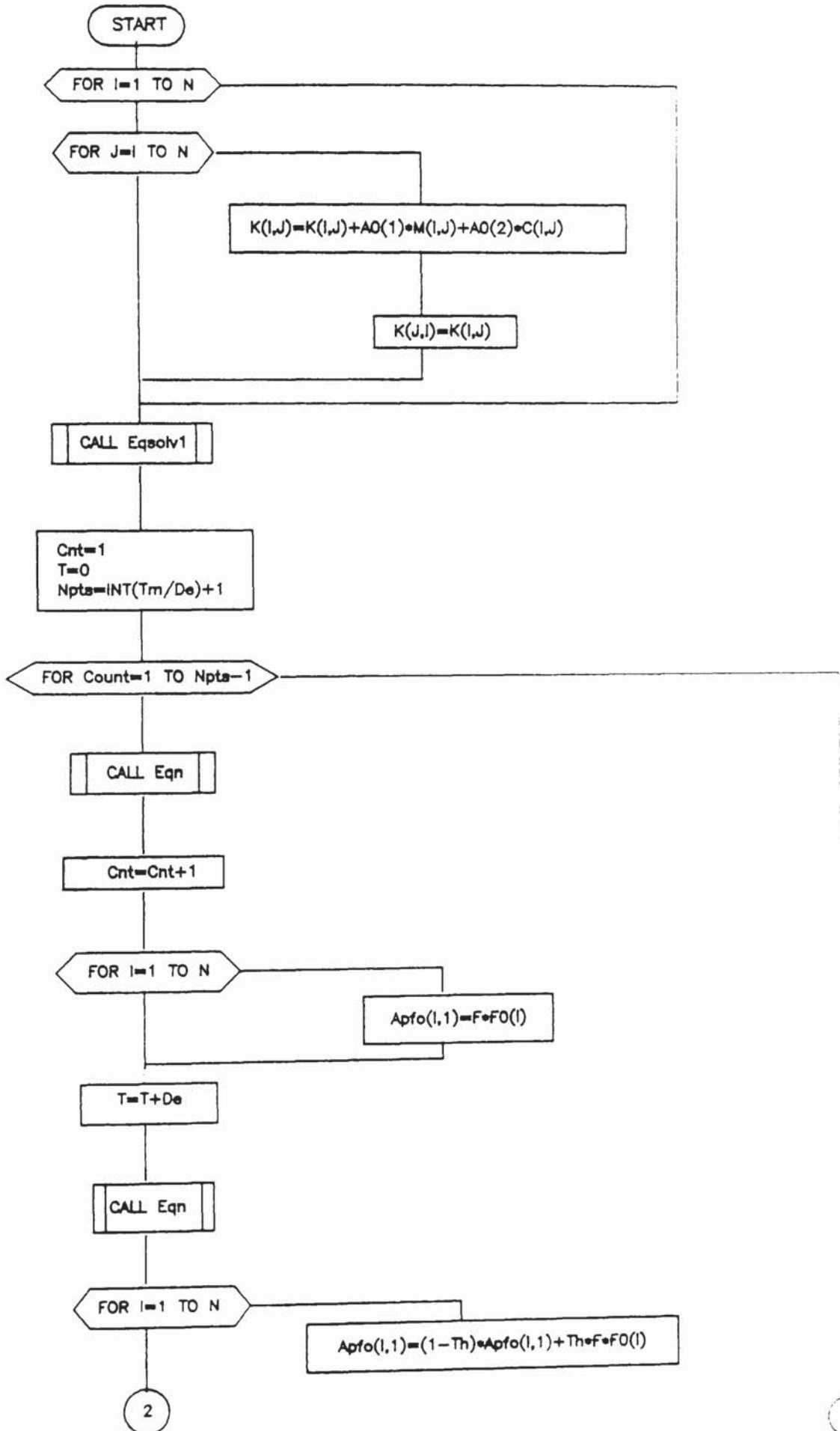
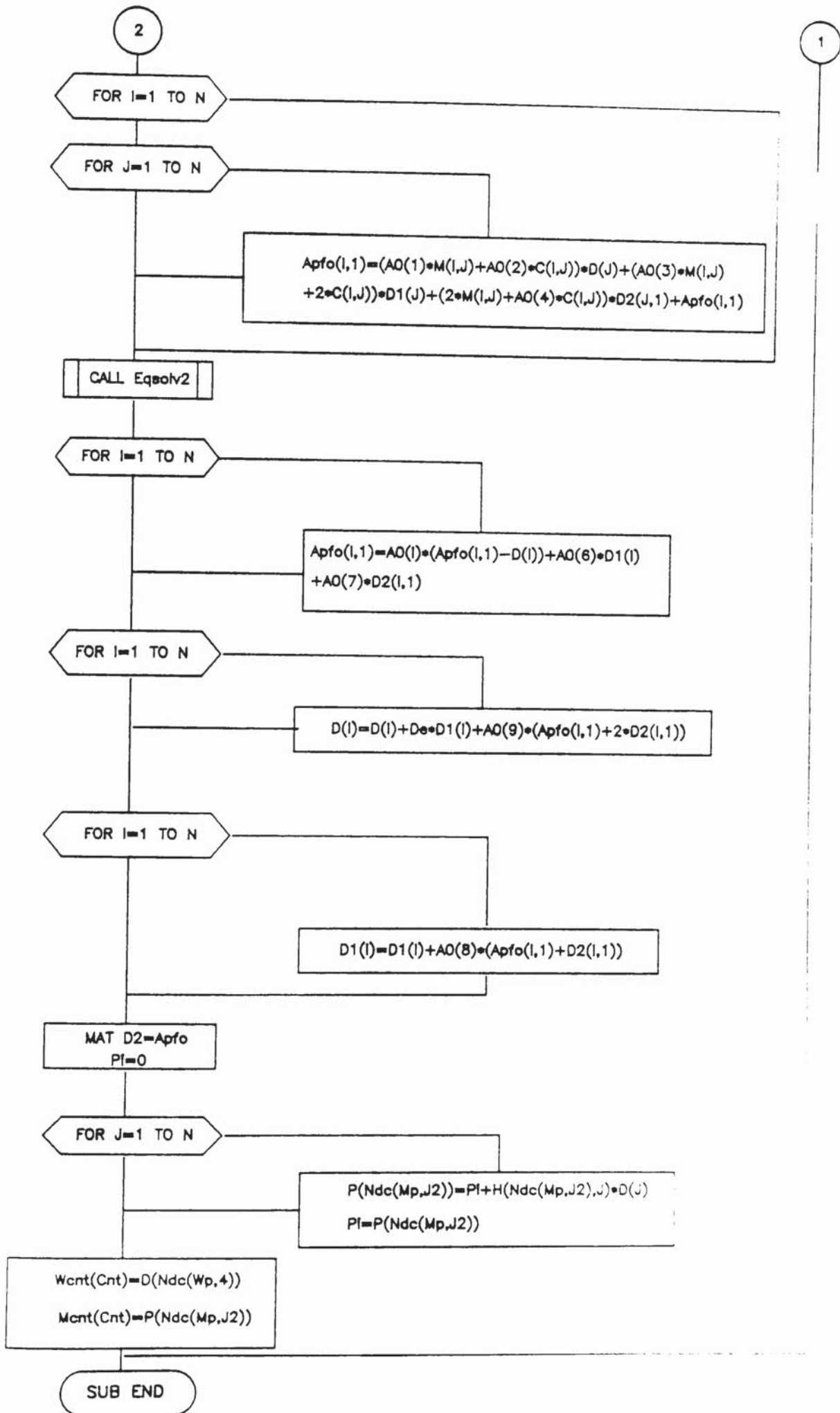


Fig 7.13 Flow diagram for SUB Wlansol(K(*),M(*),C(*),Apfo(*), F0(*),D(*),D1(*),D2(*),DI(*),A0(*),Tm,De,Th,K1,P(*),H(*),Wcnt(*), Mcnt(*),INTEGER Ndc(*),Mp,Wp,N,R,U2)



CHAPTER 8

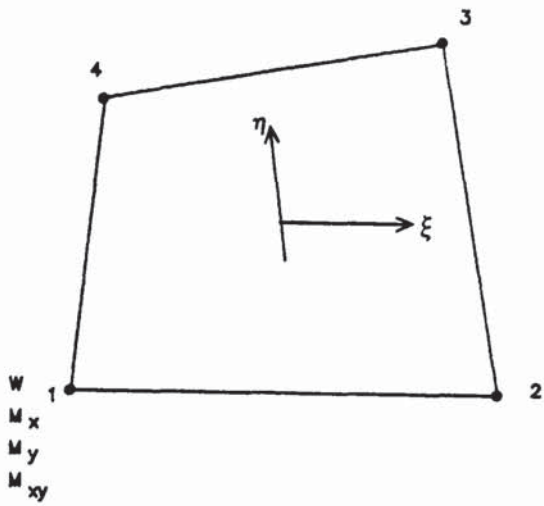
APPLICATIONS OF MIXED BEAM & PLATE
FINITE ELEMENTS IN
FREE AND FORCED VIBRATION PROBLEMS

8.1 INTRODUCTION

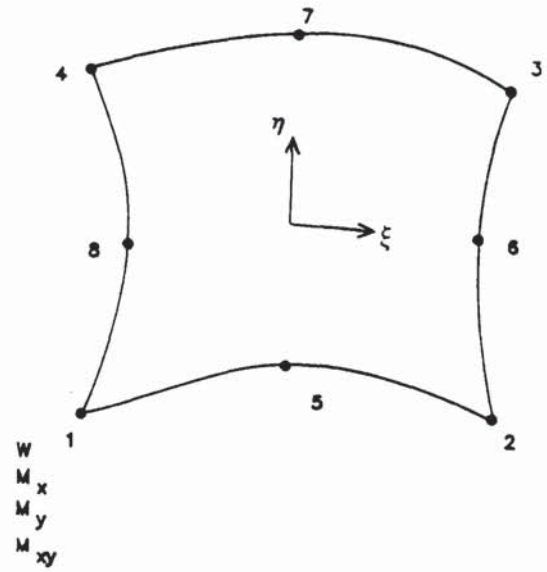
In order to determine the convergence and accuracy of the developed finite element models, the numerical solutions so derived are compared with the available analytical and, other accepted, finite element model solutions. This comparison has been made with reference to displacement type finite element models for the following groups of problems:

1. Free vibration of beams.
2. Forced vibration of beams.
3. Free vibration of thin plates.
4. Forced vibration of thin plates.

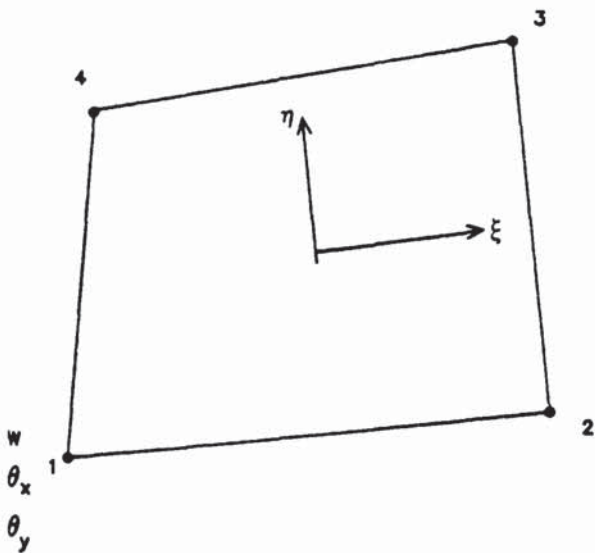
Beam elements were shown in Table (6.1). Figure (8.1) shows the types of elements used in the solution of plate problems. QR4 and QR8 elements, represent the linear and quadratic mixed plate elements. QD4 and QD8 are the non-conforming displacement type element, using 12 and 24 term polynomials as the assumed displacement functions, (Ref (9)).



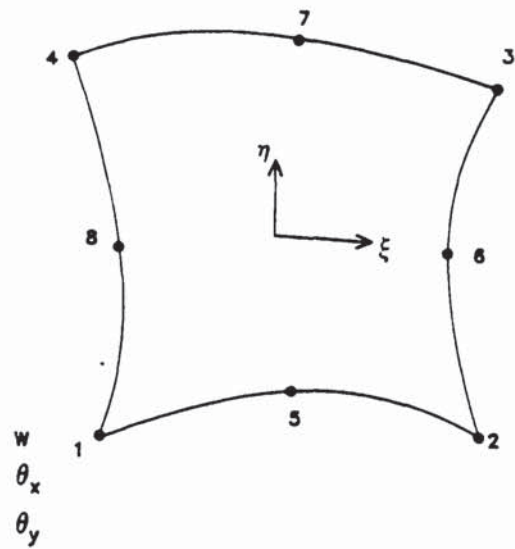
(a) QR4 element



(b) QR8 element



(c) QD4 element



(d) QD8 element

Fig 8.1 Types of plate bending elements.(a,b)—mixed elements
(c,d)—non conforming displacement elements.

8.2 NUMERICAL EXAMPLES ON FREE VIBRATION OF BEAMS

Several mixed beam elements were presented in Section 6.2 with various combinations of interpolations for the deflection w and bending moment M_x . In applying the elements to free vibration problems, it was found that the two elements MB7 and MB8 (defined in Section 6.2) produce erroneous results, and failed the convergency test. For these elements, the element mixed matrix $[h]$ in equation (6.10b) is found to be of the form

$$[h]_{MB7} = \begin{bmatrix} \frac{1}{I} & 0 & -\frac{1}{I} \\ -\frac{1}{I} & 0 & \frac{1}{I} \end{bmatrix} \quad (a)$$

and (8.1)

$$[h]_{MB8} = \begin{bmatrix} \frac{1}{I} & -\frac{1}{I} \\ 0 & 0 \\ -\frac{1}{I} & \frac{1}{I} \end{bmatrix} \quad (b)$$

The zero column and the zero row in the element matrices $[h]_{MB7}$ and $[h]_{MB8}$ reduce the rank of these matrices. Thus the element stiffness matrix derived from equation (8.2) will become deficient in rank.

$$[k] = [h]^t [g]^{-1} [h] \quad (8.2)$$

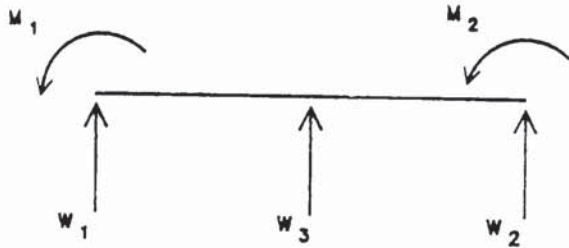
The cause of failure can be attributed to the existence of the zero energy modes which do not correspond to the expected rigid body

motion. The characteristics of such unwanted modes may be determined by carrying out an eigenvalue-eigenvector analysis on an individual unconstrained element.

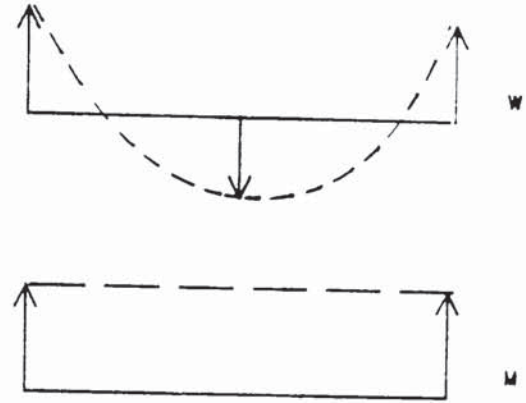
The incorrect zero eigenvalue modes for element MB7 is shown in Figure (8.2a). For this mode the bending moment is constant throughout the element, whereas the displacement is varying.

Figure (8.2b) shows that a constant displacement and variable moment distributions are obtained for the zero eigenvalue mode of element MB8. It is anticipated that these modes can not be removed by applying the kinematic boundary conditions and therefore contribute to the misbehaviour of the aforementioned elements. The correct zero eigenvalues for the expected rigid body modes were obtained for other displacement-stress combinations. The zero energy mode for the element MB5 is shown in Figure (8.2c).

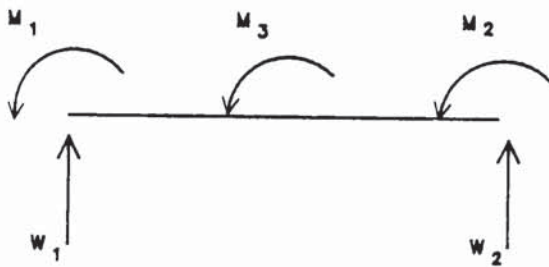
The results for elements other than MB7 and MB8 compare favourably with displacement type element. Figures (8.4) to (8.9) compare the accuracy of the mixed elements with the displacement element in predicting the fundamental natural frequency of the cantilever beam shown in Figure (8.3). The convergence curves correspond to degrees of freedom of the final eigenvalue problem and the total number of degrees of freedom of the models. It can be concluded that the natural frequencies predicted by the mixed element models are converging to the exact values. Also from tables (8.1) and (8.2), it is observed that better accuracy in predicting the first 3 natural frequencies of the cantilever beam can be achieved by using fewer higher order elements than lower order elements.



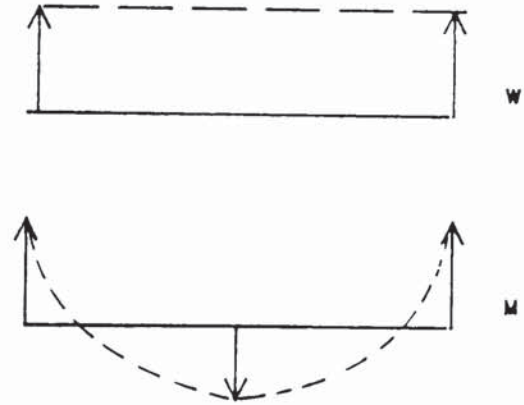
(MB7)



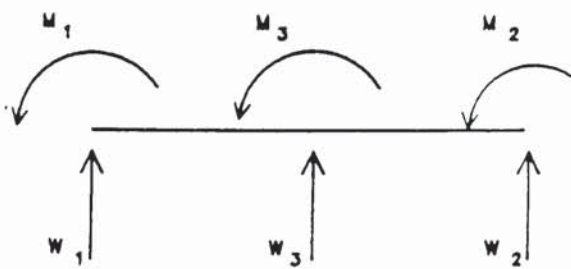
(a) Incorrect rigid body mode



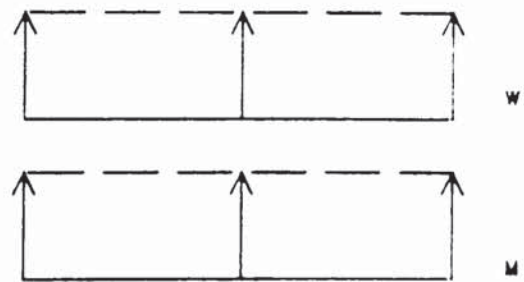
(MB8)



(b) Incorrect rigid body mode.

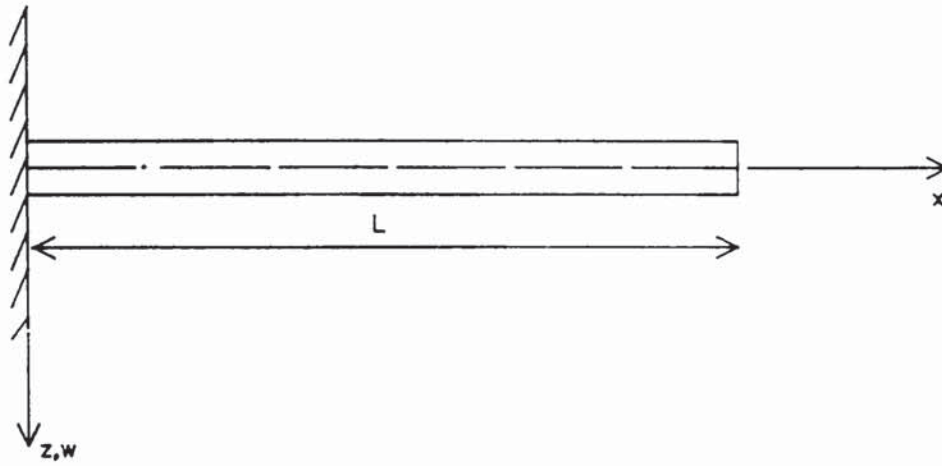


(MB5)



(c) Correct rigid body mode.

Fig 8.2 Zero energy modes in elements MB7(a),MB8(b) and MB5(c)



Beam properties:

$$L=80 \text{ Cm}$$

$$\rho=7.8 \times 10^{-3} \text{ Kg/Cm}^3$$

$$E=2.07 \times 10^7 \text{ N/Cm}^2$$

$$A=1 \text{ Cm}^2$$

$$I=1/12 \text{ Cm}^4$$

Exact natural frequencies(Rad/Sec):

$$\omega_1=8.1689$$

$$\omega_2=51.1979$$

$$\omega_3=143.37$$

Fig 8.3 Cantilever beam used in free vibration tests.

Mixed/Displacement F.E Models

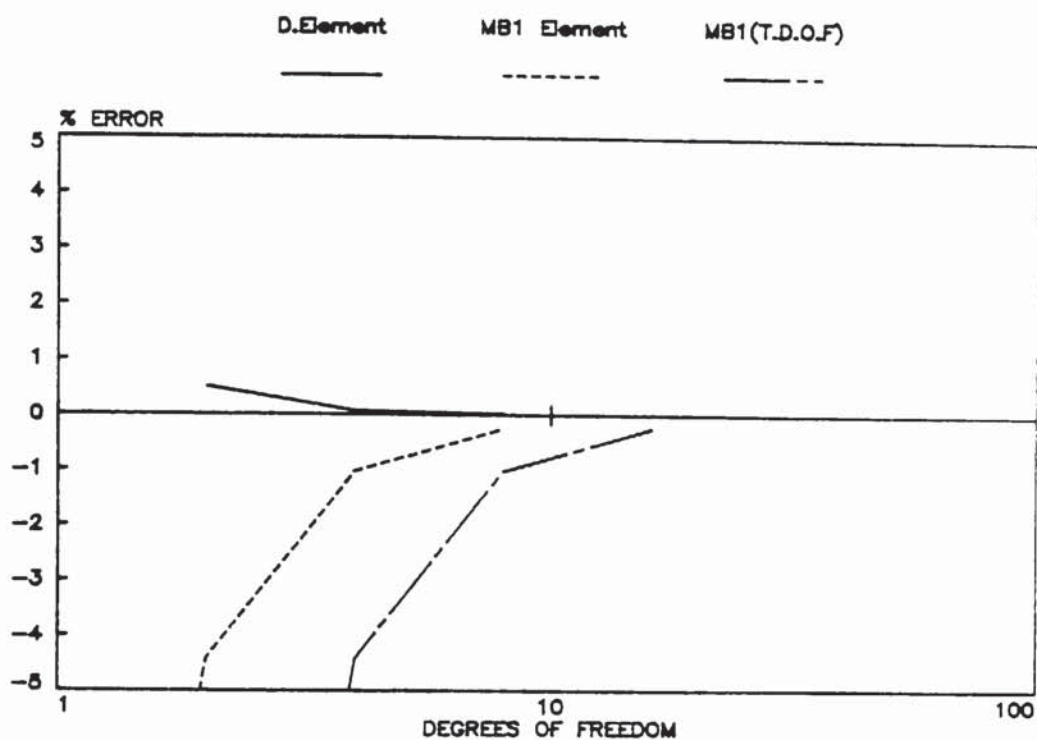


Fig 8.4 Prediction of 1st nat. freq. of CF beam :Elements D & MB1

Mixed/Displacement F.E Models

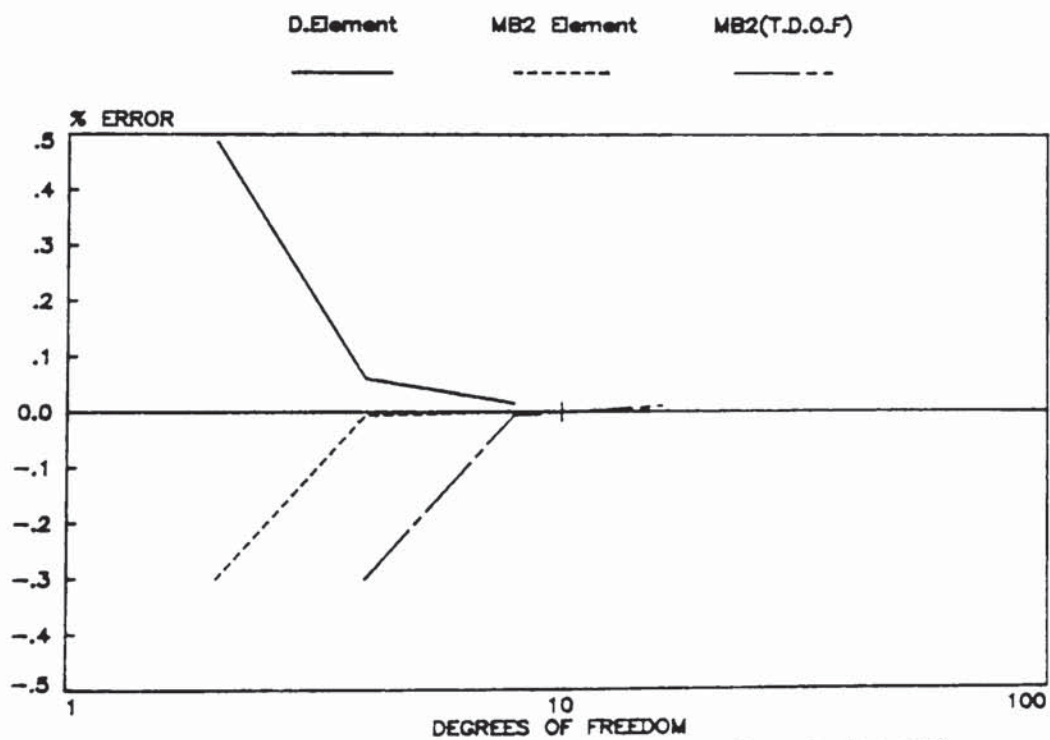


Fig 8.5 Prediction of 1st nat. freq. of CF beam:Elements D & MB2

Mixed/Displacement F.E Models

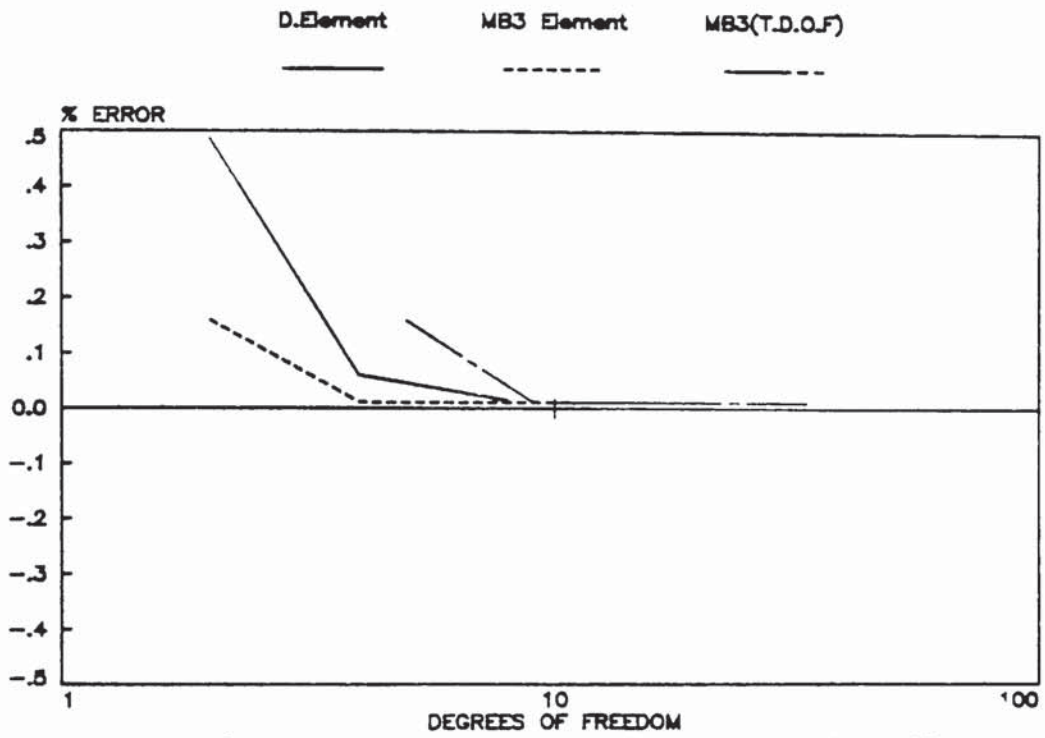


Fig8.6 Prediction of 1st nat. freq. of CF beam:Elements D & MB3

Mixed/Displacement F.E Models

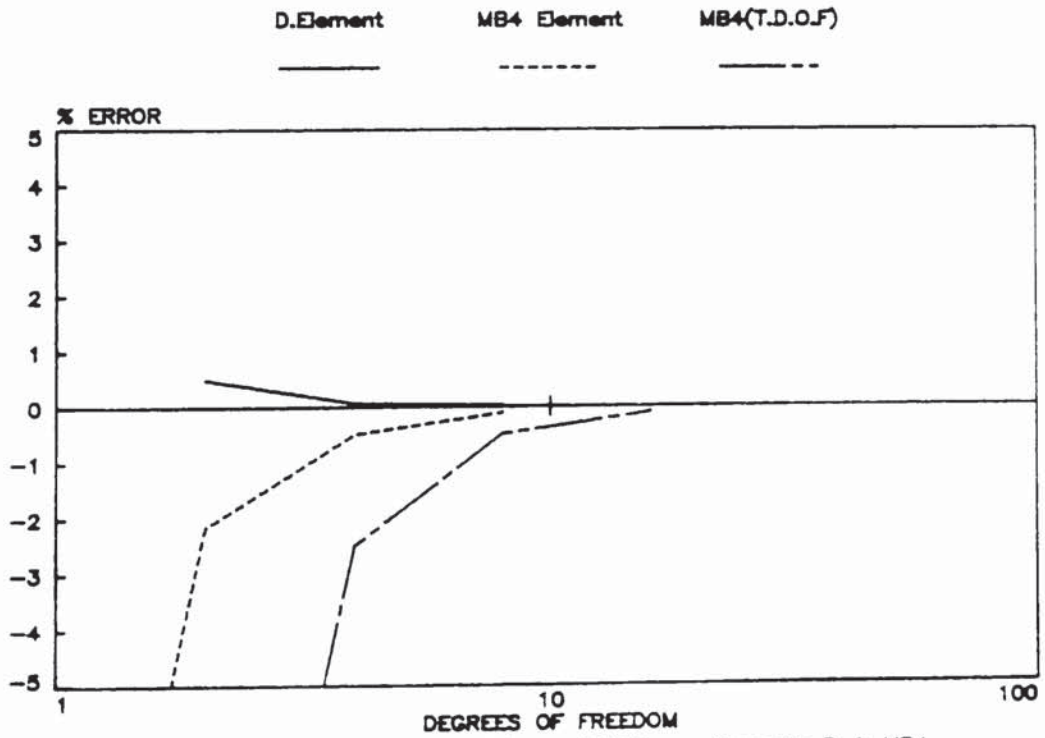


Fig8.7 Prediction of 1st nat.freq. of CF beam:Elements D & MB4

Mixed/Displacement F.E Models

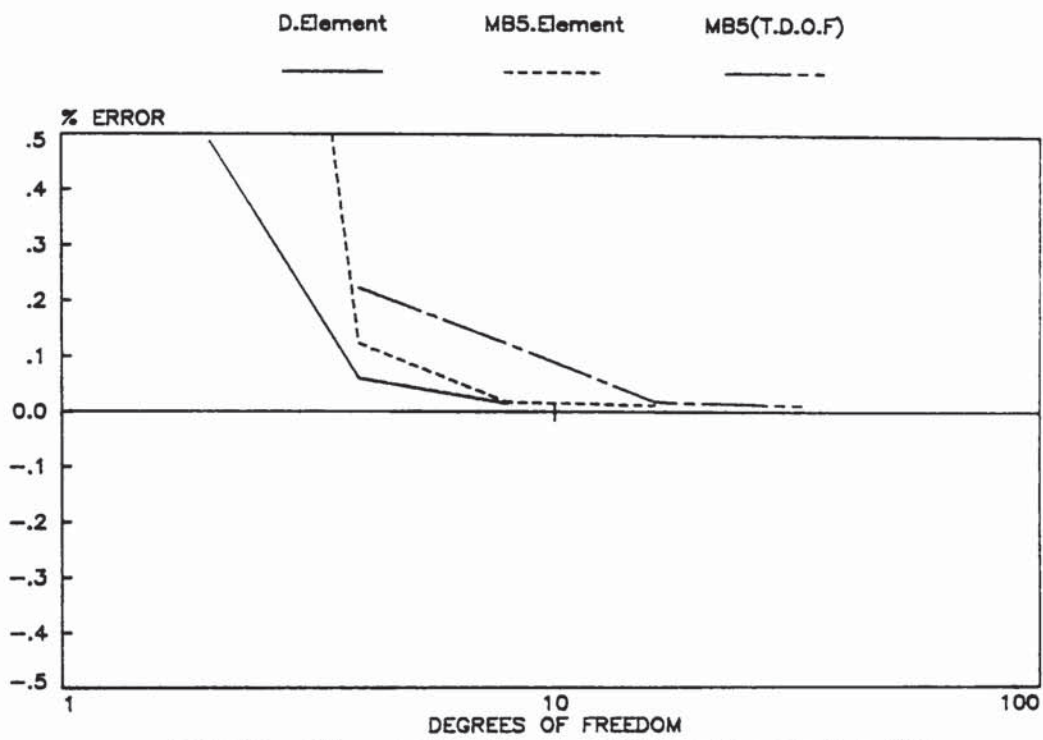


Fig 8.8 Prediction of 1st nat.freq. of CF beam:Elements D & MB5

Mixed/Displacement F.E Models

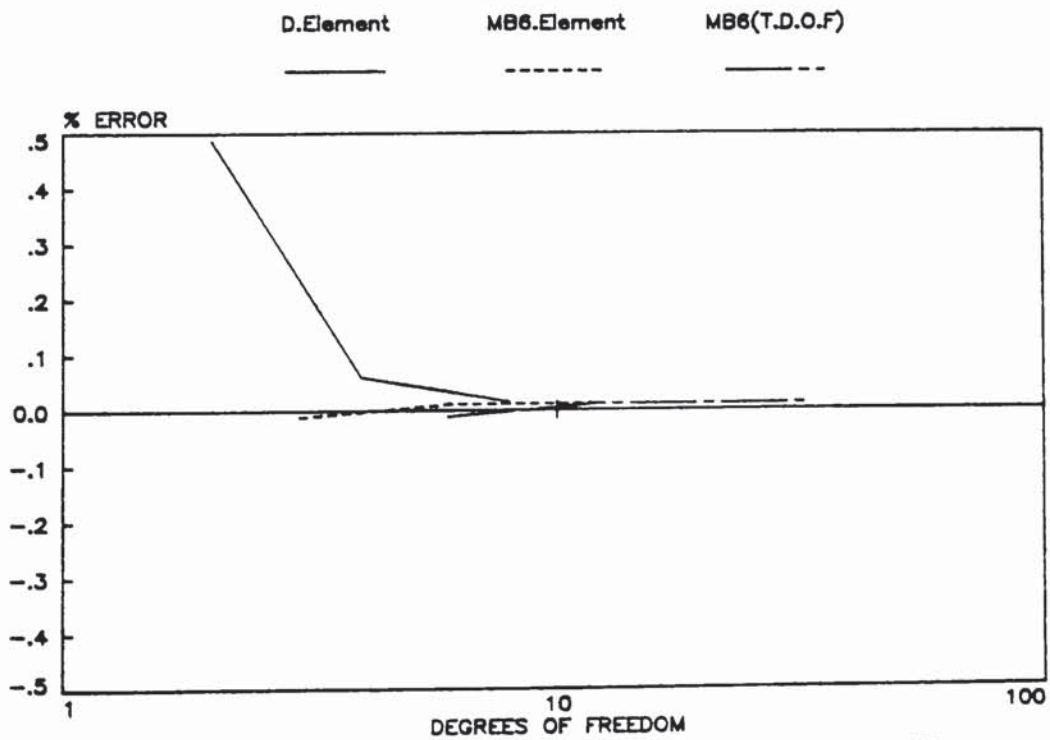


Fig 8.9 Prediction of 1st nat.freq. of CF beam:Elements D & MB6

Table 8.1
 % Error in the first 3 natural frequencies of cantilever beam.
 C1 elements

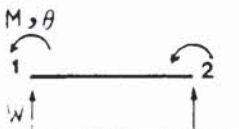
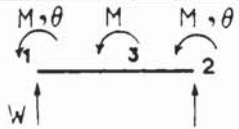
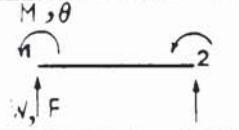
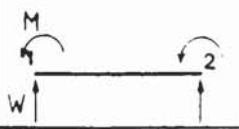
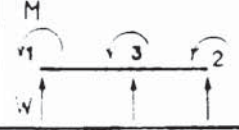
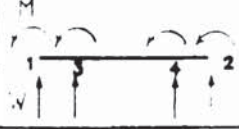
Type of Element	Number of Elements	Total Degrees of Freedom	Mode 1	Mode2	Mode3
	8	16	-.241	.70	3.291
	4	16	.01	.0626	-.079
	3	13	-.011	.0589	.06

Table 8.2
 % Error in the first 3 natural frequencies of cantilever beam.
 C0 elements

Type of Element	Number of Elements	Total Degrees of Freedom	Mode1	Mode2	Mode3
	8	16	-.1037	1.880	5.76
	4	16	.0177	.265	2.012
	2	12	.0107	.0328	2.1

8.3 NUMERICAL EXAMPLES ON FORCED VIBRATION OF BEAMS

In this section several examples of beam bending problems are solved using the developed finite element computer programs. These tests are aimed at illustrating the behaviour of mixed type beam elements in the solution of forced vibration problems.

The results are compared with the analytical and displacement element solutions. Table (8.3) shows the types of problems which have been tackled. Unless otherwise specified, the constants used in these solutions are:

$$\begin{aligned} \text{Beam: } E &= 2.07 \times 10^7 \text{ N/cm}^2, \quad \nu = 0.3, \quad \rho = 7.8 \times 10^{-3} \text{ Kg/cm}^3 \\ A &= 100 \text{ cm}^2, \quad I = \frac{1}{12} \text{ cm}^4, \quad L = 80 \text{ cm} \end{aligned}$$

The numerical integration of the equations of motion is performed by Wilson θ method using a time step size of $\Delta t = .001$ sec.

8.3.1 Response of a cantilever to a transient force (half-sine pulse input)

The tip deflection and maximum bending moment at the root section of a uniform cantilever beam subjected, at the tip, to the transient force, shown in Table (8.3), are calculated. (T is the period of the fundamental mode of vibration of the cantilever). Figures (8.10) and (8.11) show the tip deflection and the root bending moment responses for models with two degrees of freedom. A two element idealisation is used for element MB4 and one element idealisation for the rest of the elements (D, MB5, MB2 and MB3). The

results show that the displacements are predicted with good accuracy and the bending moments predicted by mixed elements are generally superior to those obtained from the displacement element (for the same number of degrees of freedom). However, for one mixed element, MB3, the displacement and moment predictions are similar to the displacement element, D, predictions.

The convergence of the results is studied by increasing the number of degrees of freedom. Figures (8.12) and (8.13) show the deflection and bending moment responses for the same cantilever with 4 degrees of freedom idealisations (only displacement d.o.f.). It is seen that the predictions from mixed elements (MB2) and MB3, converge more rapidly than those from MB4 and MB5. In this case, the total number of degrees of freedom (displacements and moments) used in the idealisations with mixed elements is 8.

8.3.2 Response of a cantilever to a ramp force input at the tip

The cantilever beam of the previous example is tested for a ramp force input at the tip. Bending moment response at the root of the beam and the tip deflection response are calculated for various finite element models with 2, 4 and 6 degrees of freedom. The results are shown in Figures (8.14) to (8.18). It is observed that the displacement solutions converge very rapidly towards the exact solution, for all types of finite element models (D, MB4, MB5, MB2 and MB3). In particular, Figure (8.14) shows that the displacement response prediction obtained by using element MB5 is much more accurate than those obtained by using other models including the displacement type element.

Figures 8.15, 8.17 and 8.18 show the bending moment response for finite element models with 2, 4 and 6 degrees of freedom respectively. It is interesting to notice that, for idealisations with 2 degrees of freedom, the predictions from mixed elements MB4 and MB5 (from C0 continuity class) are superior to solutions from other types of elements (Figure 8.15).

8.3.3 Response of a clamped-clamped beam to a step force input

Figures (8.19) to (8.21) show the deflection and bending moment responses of a clamped-clamped beam to a step force input applied at the middle of the beam. It is observed that the models exhibit good accuracy even with the lowest number of degrees of freedom. Besides, elements MB2 and MB3 of the C1 continuous class show similar accuracy to the displacement type element .

8.3.4 Response of a clamped-simply supported beam to half sine pulse input

Mid point deflection and bending moment responses for a CS beam subjected to half sine pulse input are shown in Figures (8.22) to (8.25). The convergence characteristics of various finite elements are studied by increasing the number of degrees of freedom from 3 in Figures (8.22), (8.23) to 7 in Figures (8.24) and (8.25). The results for the displacements show that for the same number of unknowns, the accuracy of the mixed elements matches that of the displacement type element. Bending moments, however, are calculated more accurately using the C1 continuous mixed elements (MB2, MB3). In addition, C0 continuous mixed elements are found to perform just as well, with the parabolic, MB5 element being superior to the

linear MB4 element.

8.3.5 Response of a clamped-simply supported beam to a ramp force input. (Damping included)

Figures (8.26) and (8.27) show the mid point deflection and bending moment responses, respectively, for a damped CS beam of length, $L = 40$ cm. The results are obtained for idealisations with 3 degrees of freedom. Damping is introduced in mode 1 with $\zeta = .05$, modes 2 and 3 with $\zeta = .02$.

Both displacement and bending moment results show that very good accuracy has been obtained.

8.3.6 Response of a cantilever to a step moment input at the tip

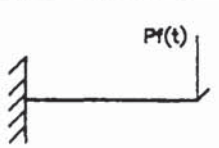
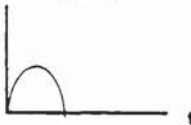
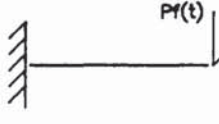
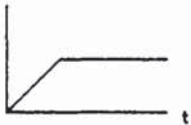
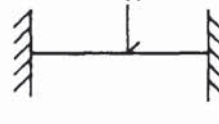
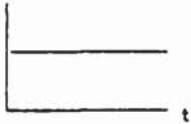
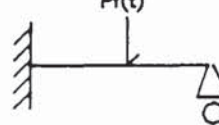

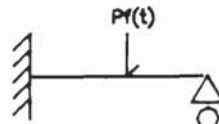
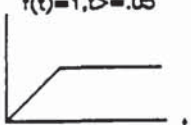

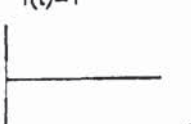
Figures (8.28) to (8.33) show the deflection and bending moment responses of a cantilever subjected to a step moment input. The tests are performed in order to demonstrate the convergence of the results as the beam sub-divisions increases. The elements used in this example are from C1 continuous class (D, MB1, MB2, MB3). With these elements, the slope continuity between elements' joints is satisfied.

It can be seen that the mixed element MB1 has a weaker convergence rate than the rest of the elements used in this test.

From these applications, it is concluded that, in general, the elements developed for dynamic analysis of beams are capable of predicting the structure response to various force inputs with good

accuracy. The rate of convergence in C^0 continuous elements (MB4, MB5) is lower than C^1 elements (MB2, MB3). Nevertheless, in view of the simplicity in formulation and programming, these elements offer some advantages over the more complex C^1 continuous elements.

Table 8.3 Beam forced vibration problems.

Beam type	Type of force inputs.	Type of elements	Figure numbers
	$f(t) = \sin(\pi t/T), t \leq T$ $f(t) = 0, t > T$ 	D, MB2 MB3, MB4 MB5	(8.10) to (8.13)
	$f(t) = 20t, t < .05$ $f(t) = 1, t \geq .05$ 	D, MB2 MB3, MB4 MB5	(8.14) to (8.18)
	$f(t) = 1$ 	D, MB2 MB3, MB4 MB5	(8.19) to (8.21)
	$f(t) = \sin(\pi t/T), t \leq T$ $f(t) = 0, t > T$ 	D, MB2 MB3, MB4 MB5	(8.22) to (8.25)
	$f(t) = 20t, t < .05$ $f(t) = 1, t \geq .05$ 	D, MB2 MB3, MB4 MB5	(8.26) to (8.27)
	$f(t) = 1$ 	D, MB1 MB2, MB3	(8.28) to (8.33)

Addendum

Type of boundary cond'n	Type of element	Number of elements	Number of deg.of.freedom (displacement)	Number of deg.of.freedom (moments)
CLAMPED, FREE Figs 8.10,8.11, 8.14,8.15, 8.28,8.29	D	1	2	
	MB2	1	2	2
	MB3	1	2	2
	MB4	2	2	2
	MB5	1	2	2
CLAMPED, CLAMPED Figs 8.19,8.20	D	2	2	
	MB2	2	2	5
	MB3	2	2	6
	MB4	4	3	5
	MB5	2	3	5
CLAMPED, SIMPLY SUPP'TD Figs 8.22,8.23, 8.26,8.27	D	2	3	
	MB2	2	3	4
	MB3	2	3	4
	MB4	4	3	4
	MB5	2	3	4

BEAM ELEMENT CONFIGURATIONS IN FORCED VIBRATION PROBLEMS.

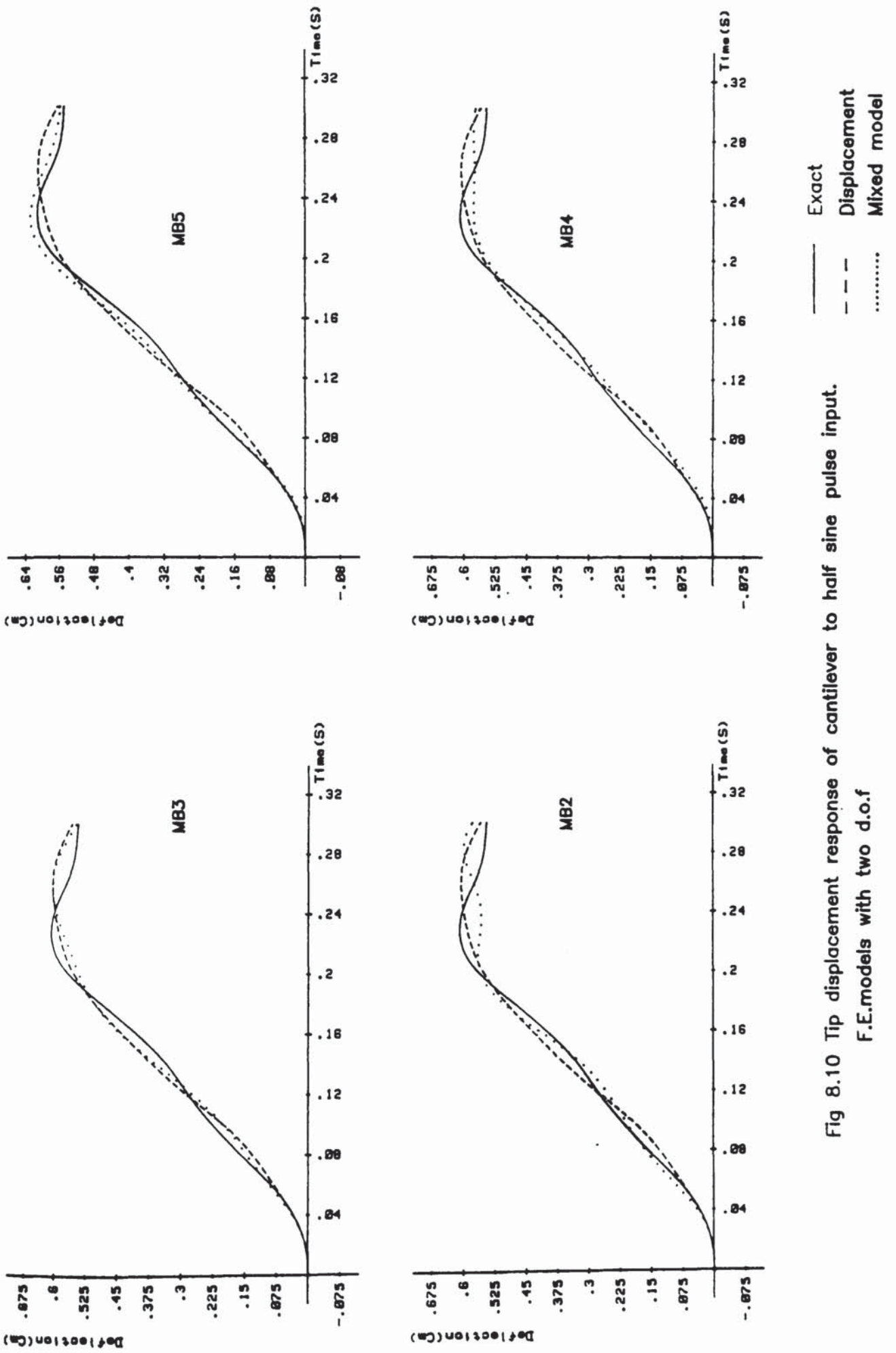


Fig 8.10 Tip displacement response of cantilever to half sine pulse input.
F.E.models with two d.o.f

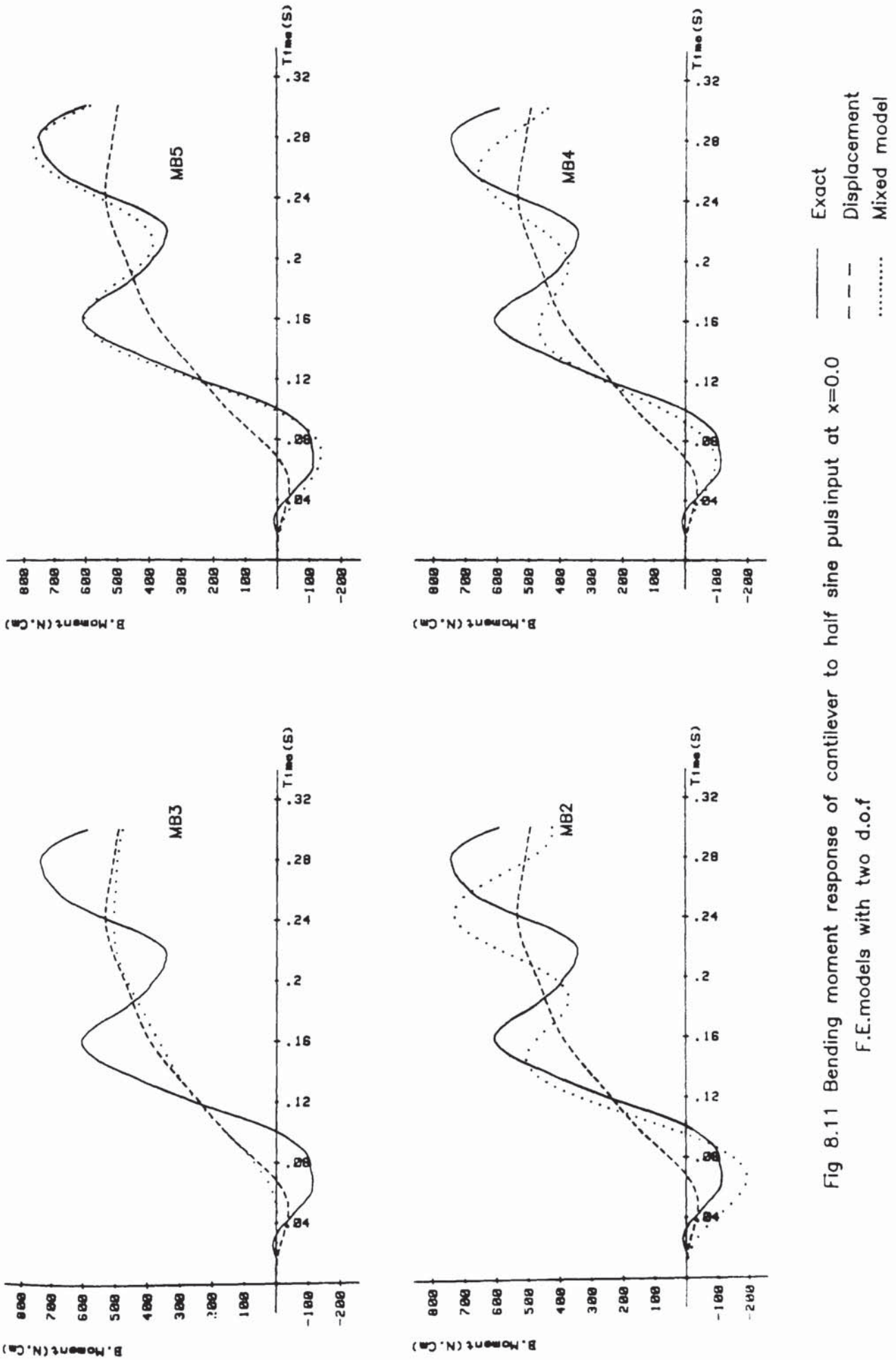


Fig 8.11 Bending moment response of cantilever to half sine pulsinput at $x=0.0$
 F.E.models with two d.o.f

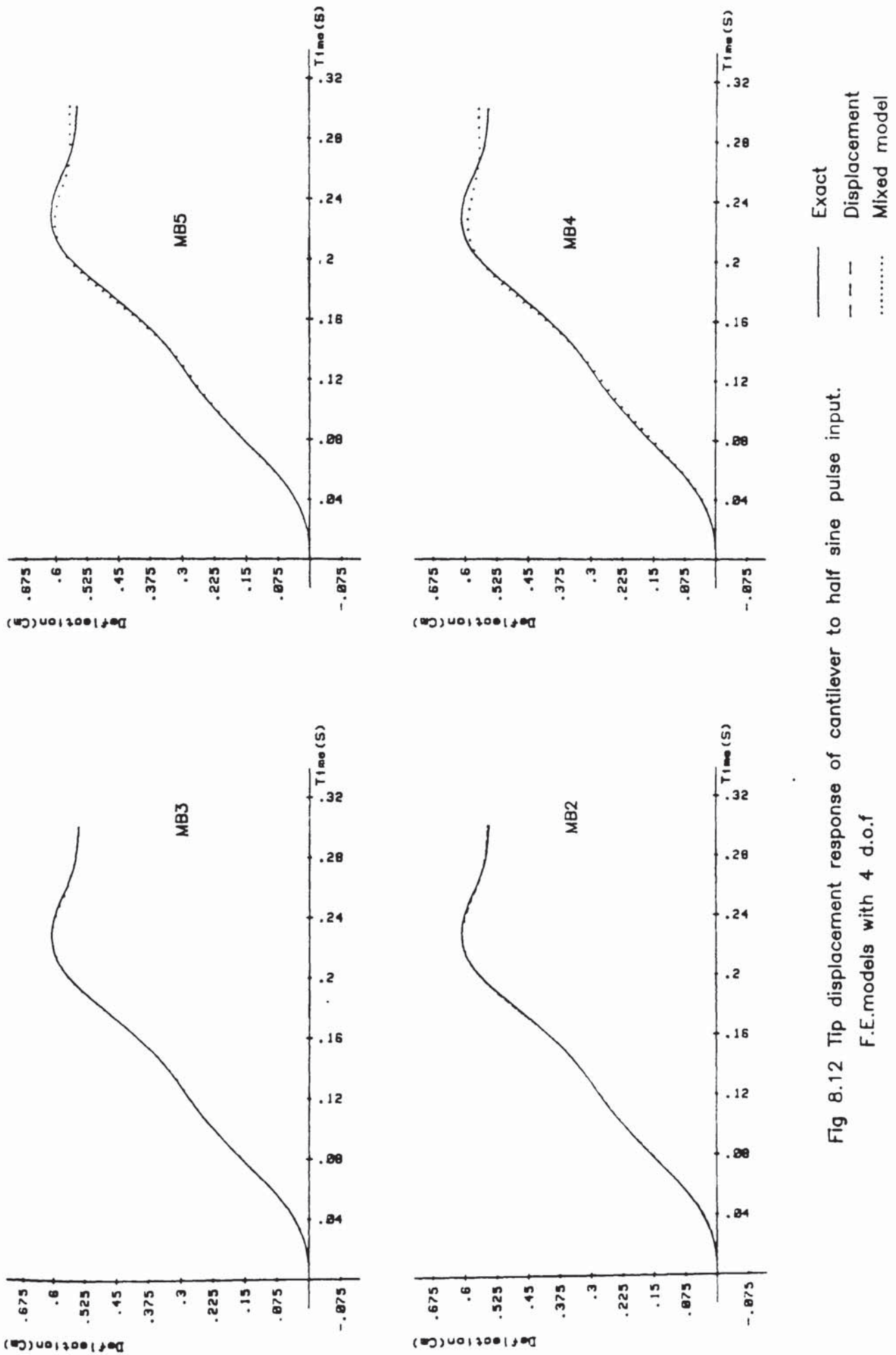
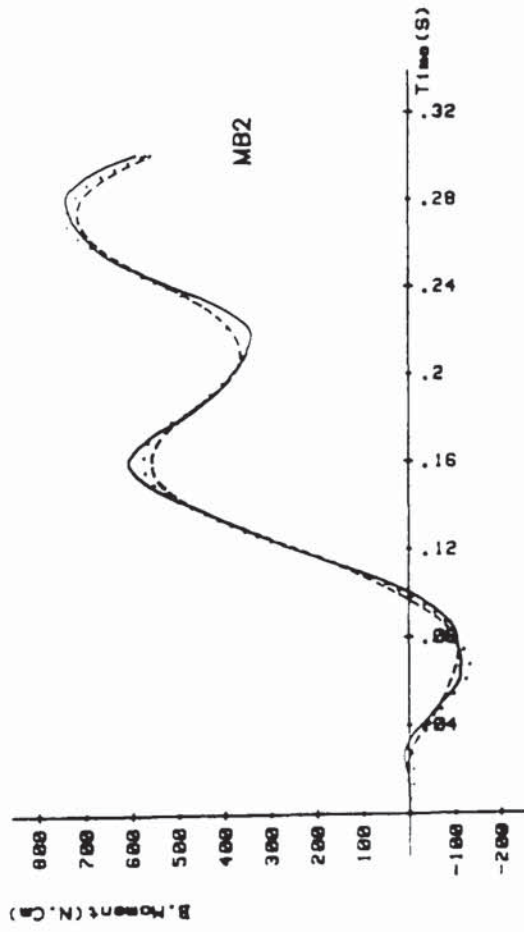
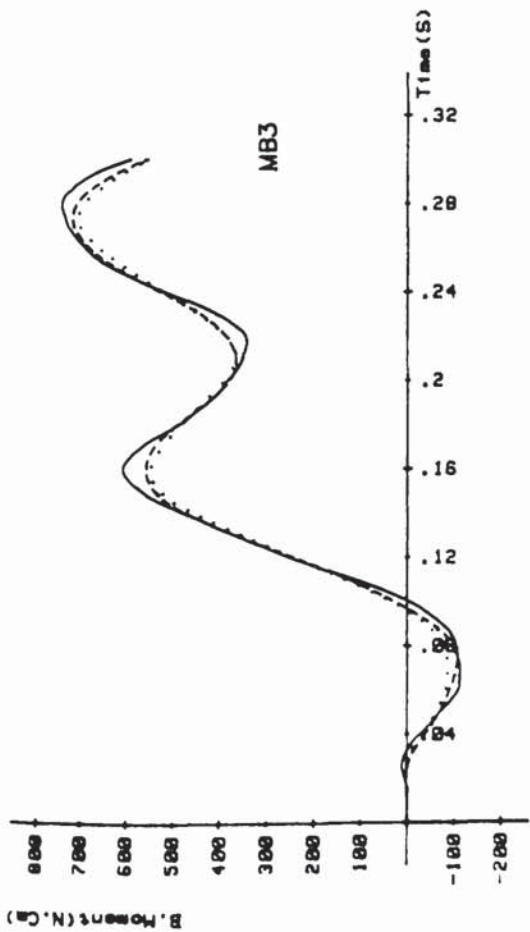
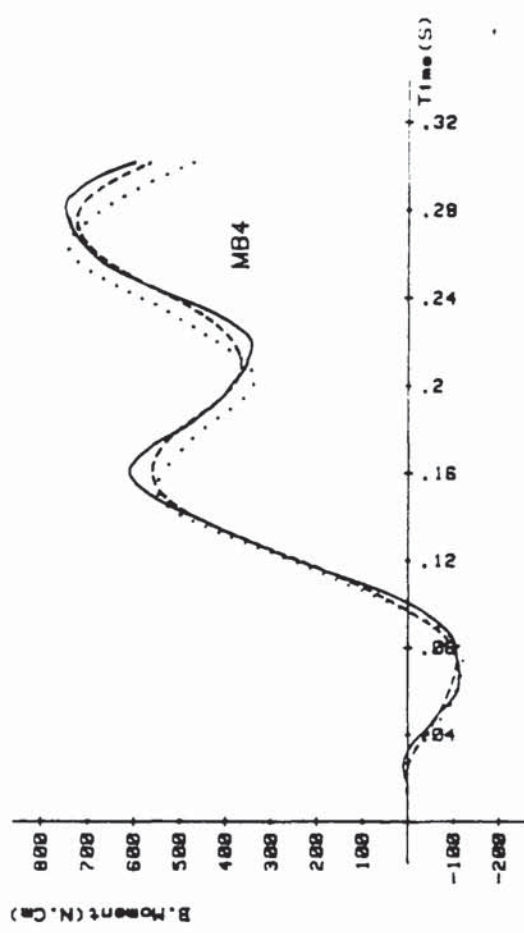
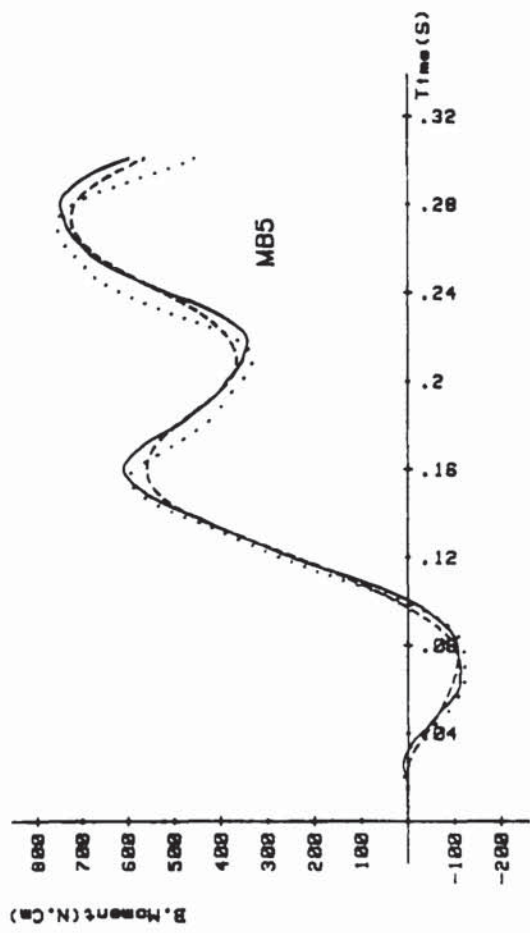
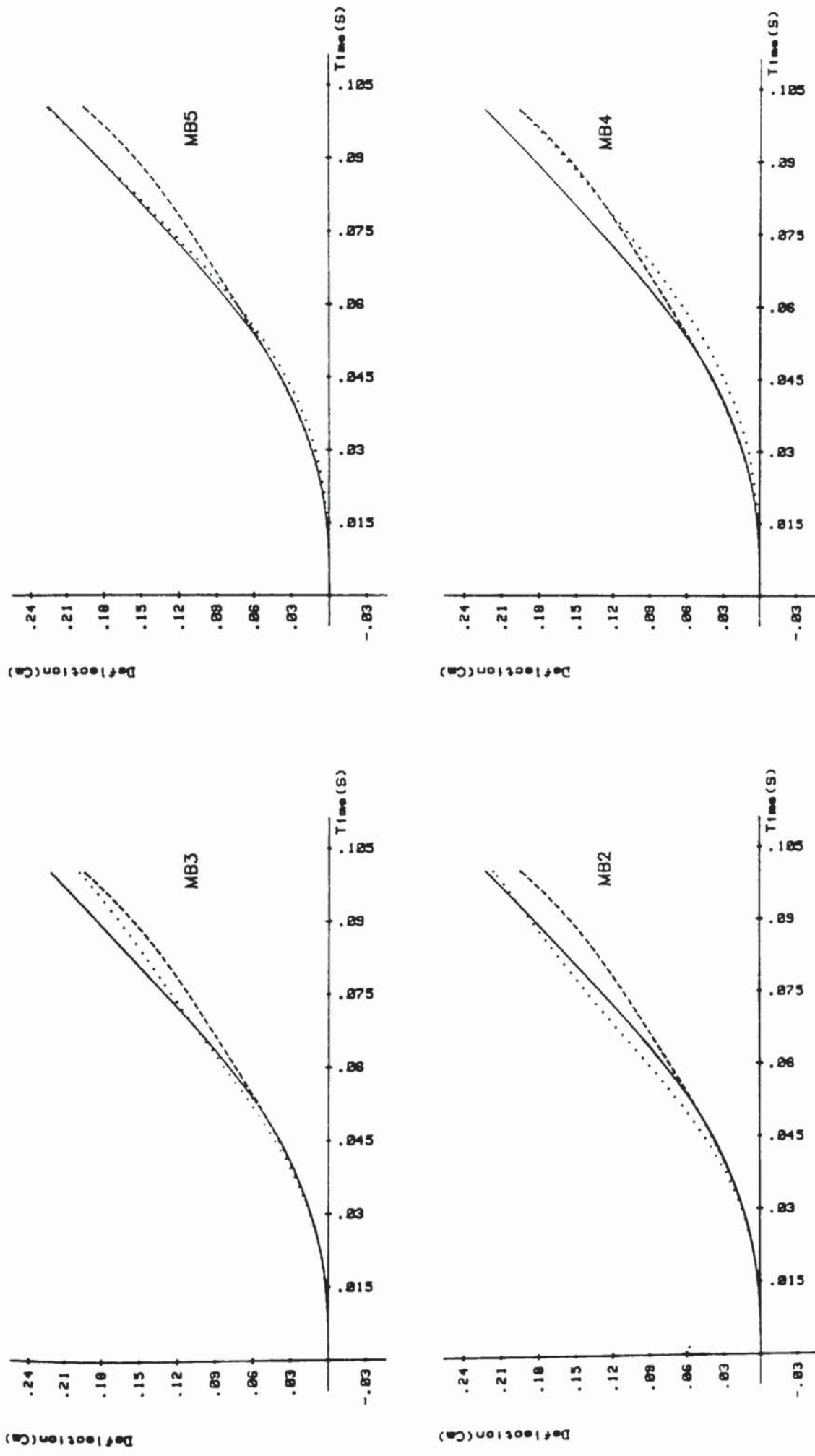


Fig 8.12 Tip displacement response of cantilever to half sine pulse input.
F.E.models with 4 d.o.f



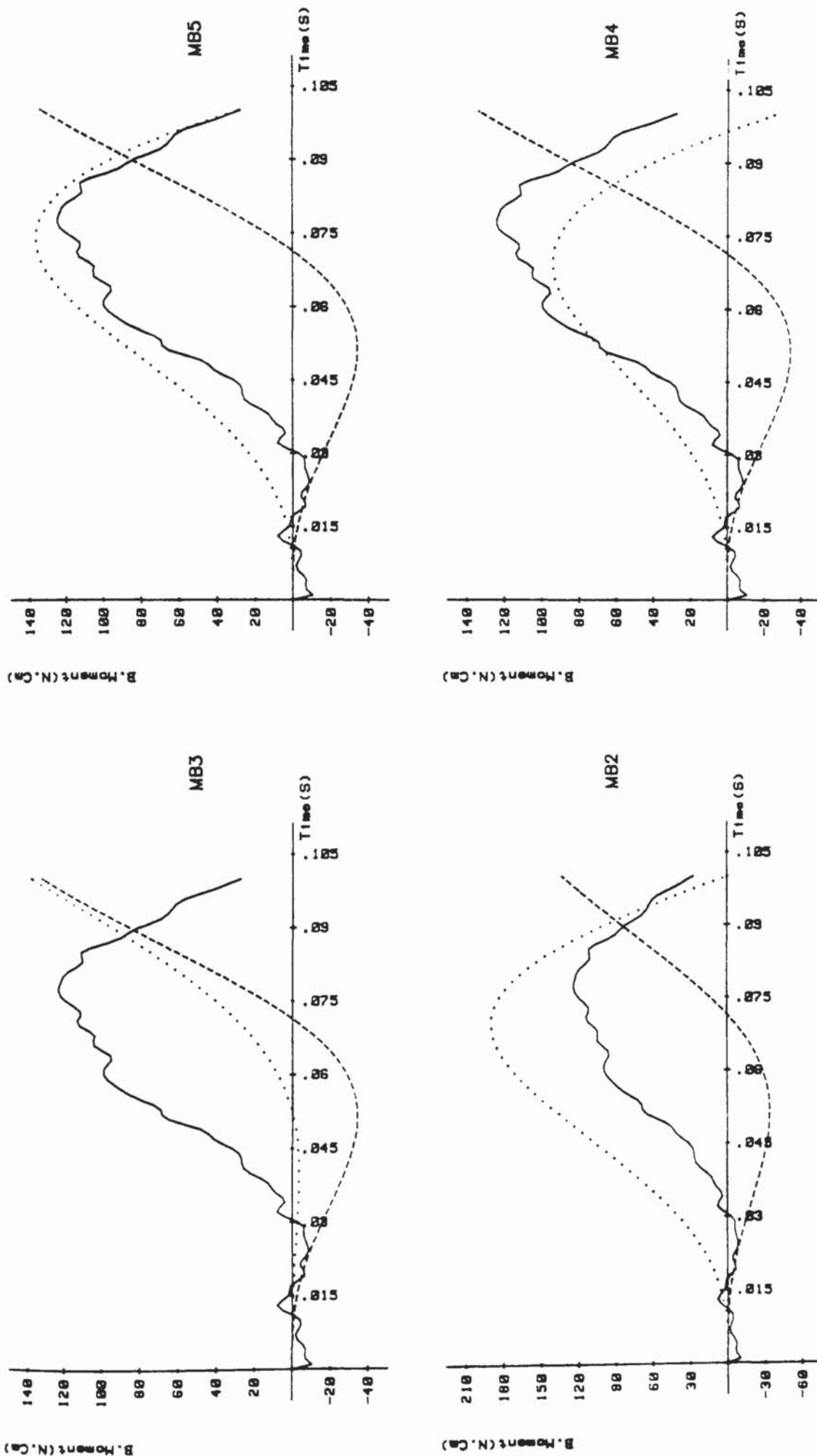
— Exact
 - - - Displacement
 Mixed model

Fig 8.13 Bending moment response of cantilever to half sine pulsinput at $x=0.0$
F.E.models with 4 d.o.f



— Exact
 - - - Displacement
 Mixed model

Fig 8.14 Tip displacement response of cantilever to ramp input
 F.E.models with two d.o.f



Exact
 Displacement
 Mixed model

Fig 8.15 Bending moment response of cantilever to ramp force input , $x=0.0$
 F.E.models with 2 d.o.f

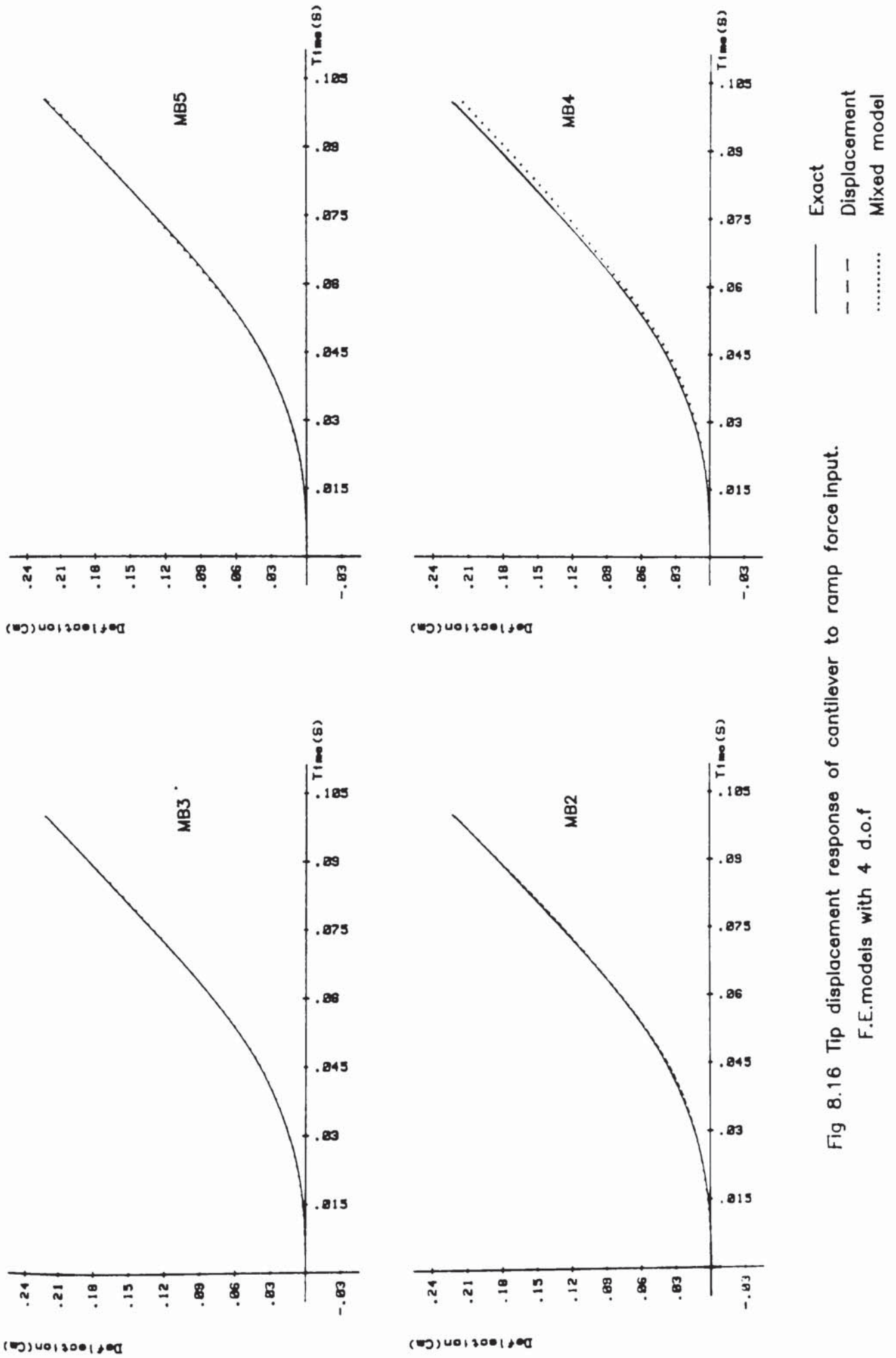


Fig 8.16 Tip displacement response of cantilever to ramp force input.
F.E.models with 4 d.o.f

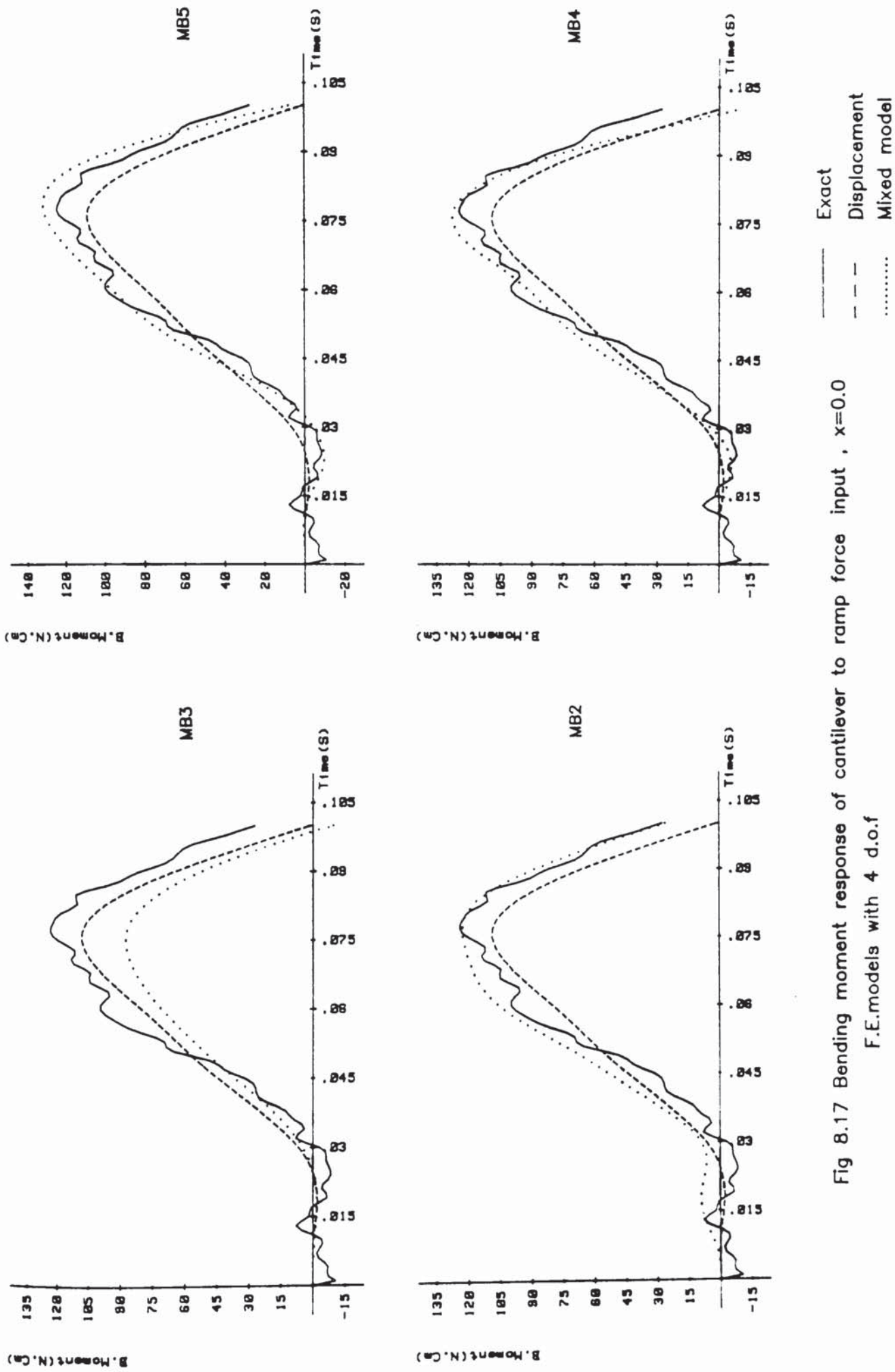


Fig 8.17 Bending moment response of cantilever to ramp force input , $x=0.0$
 F.E.models with 4 d.o.f

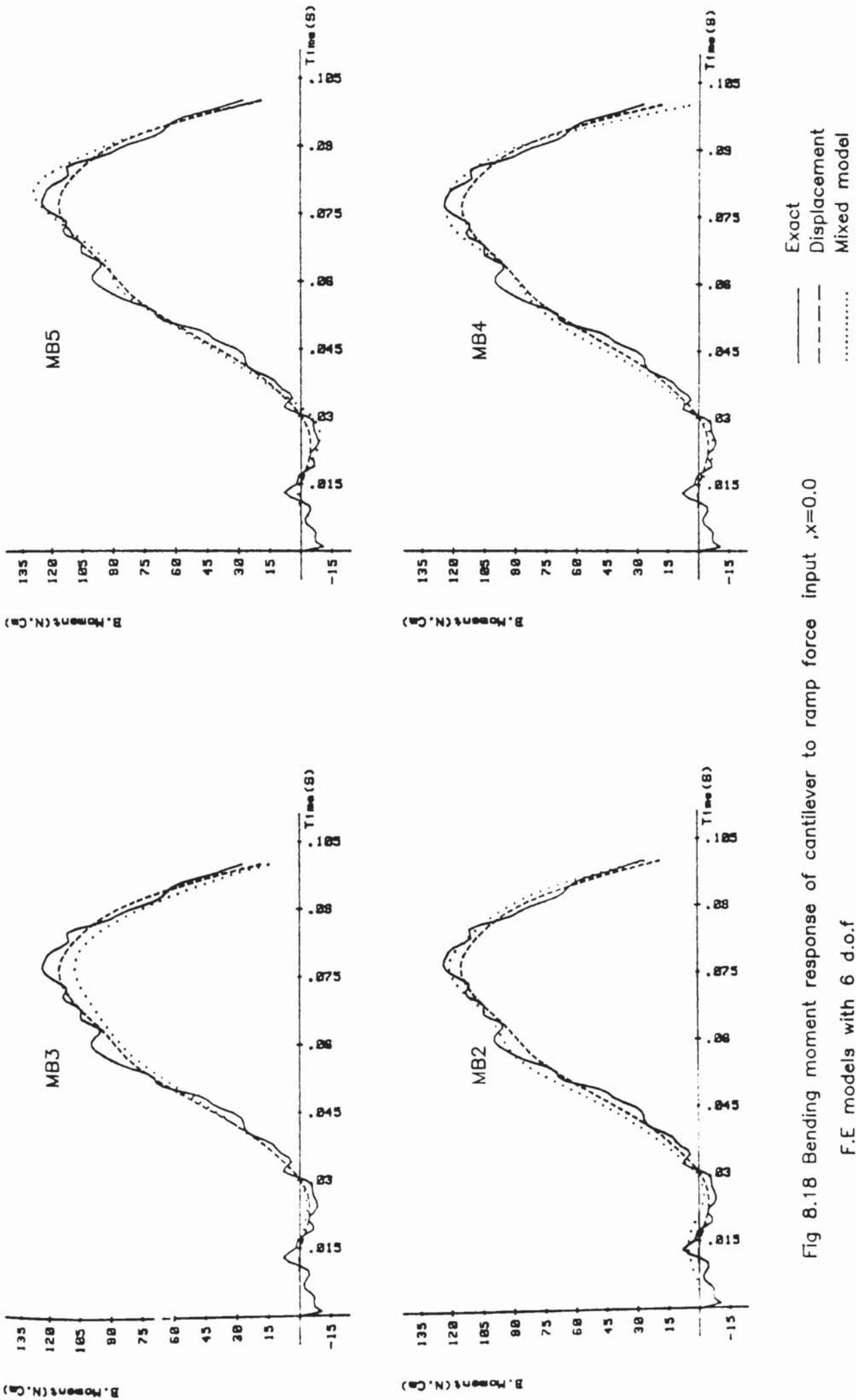


Fig 8.18 Bending moment response of cantilever to ramp force input , $x=0.0$
F.E models with 6 d.o.f

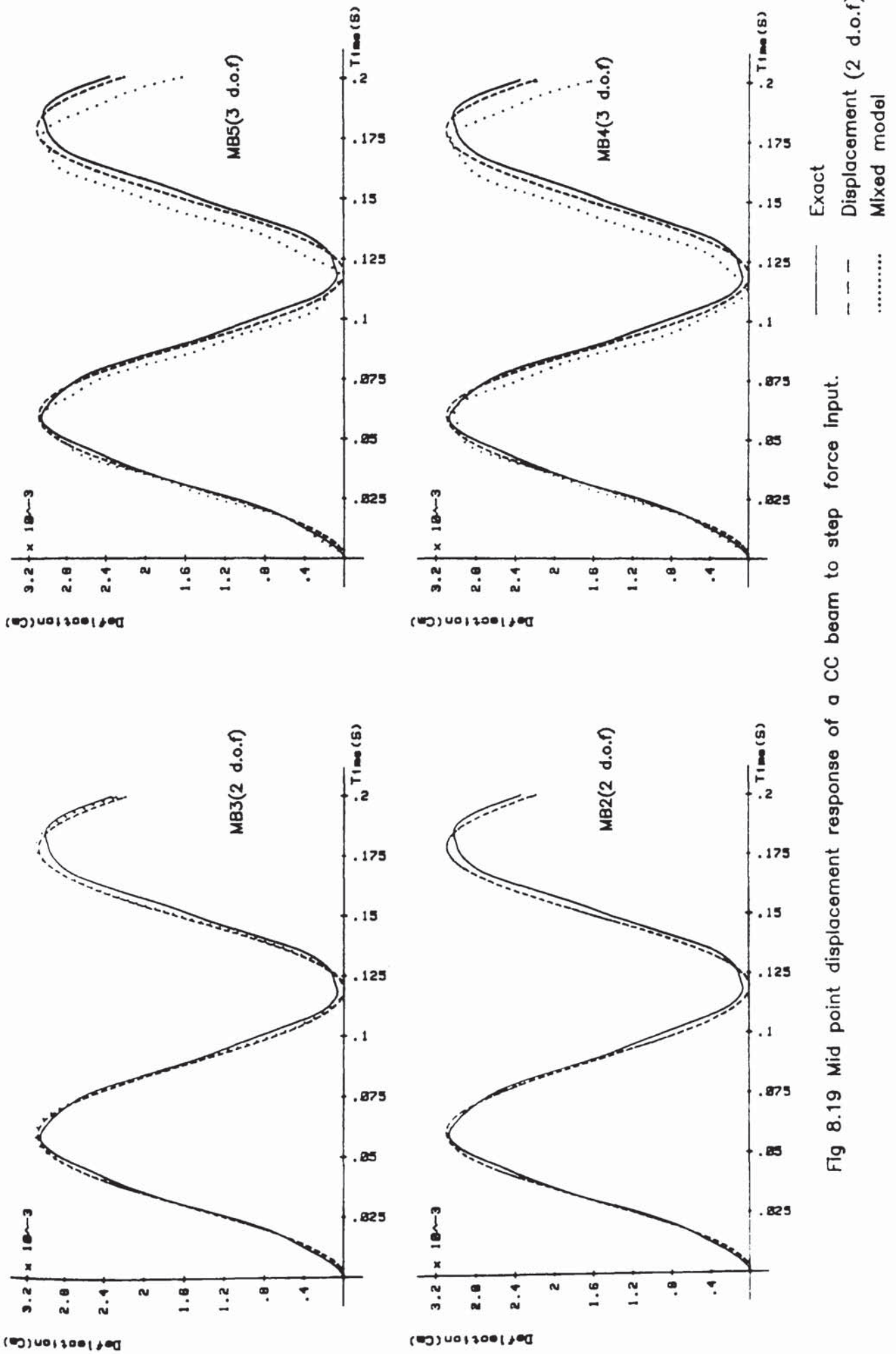


Fig 8.19 Mid point displacement response of a CC beam to step force input.

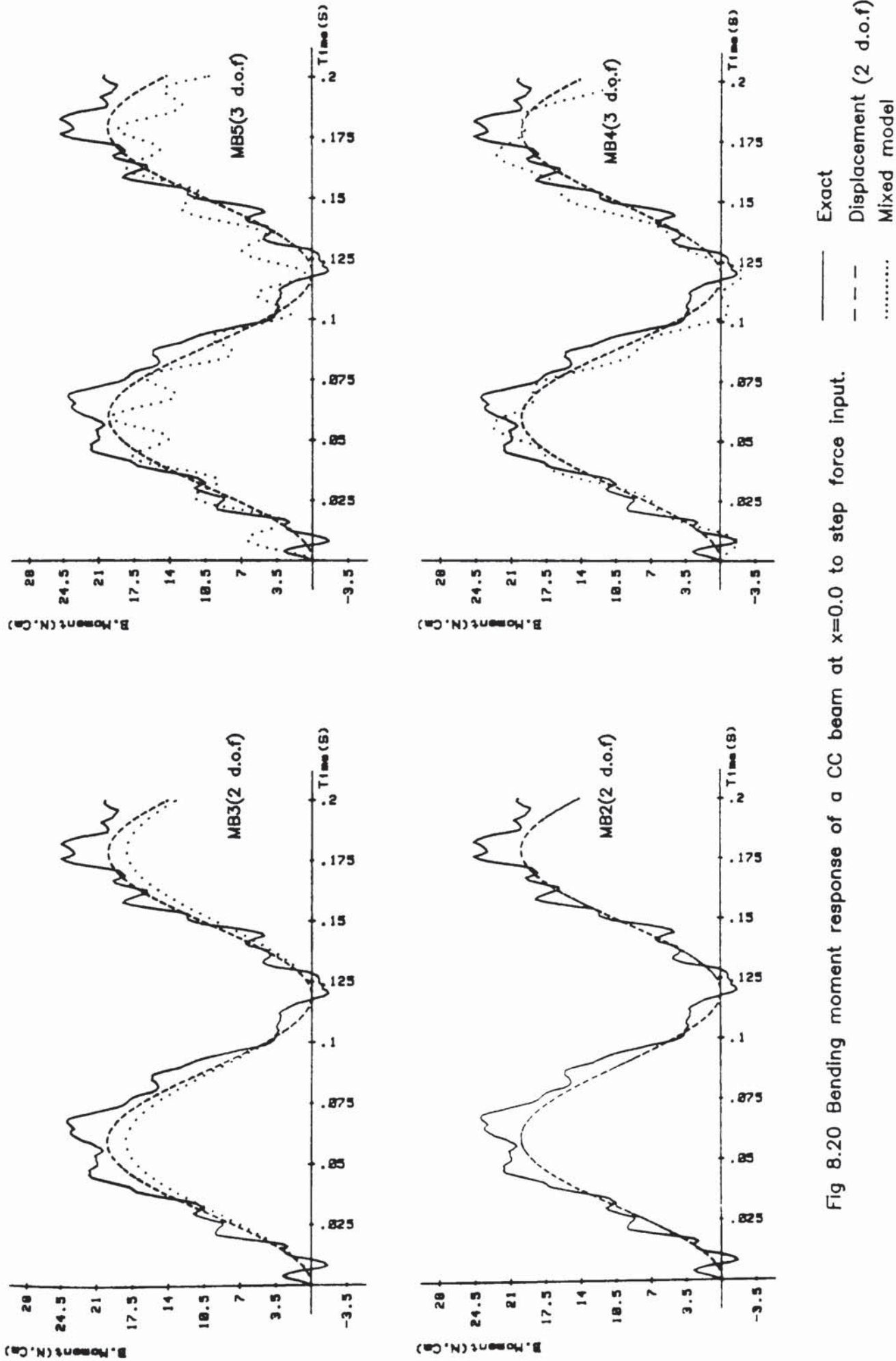
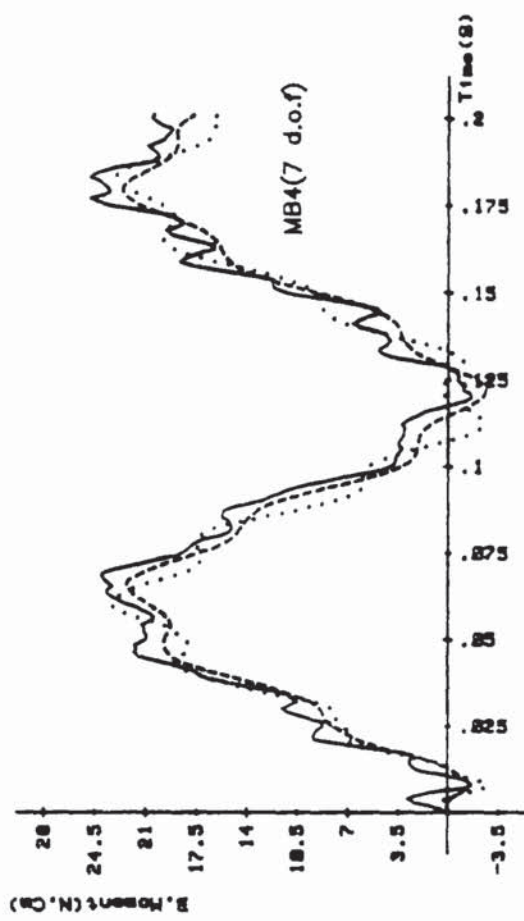
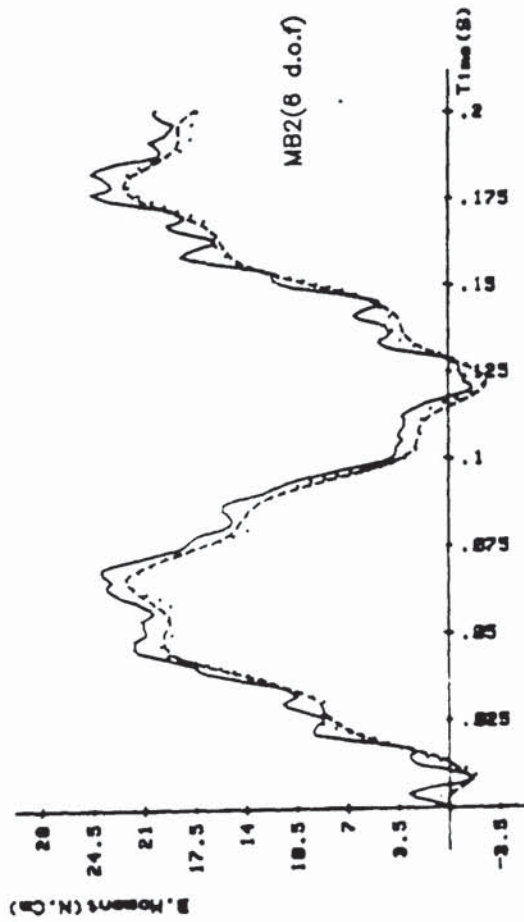
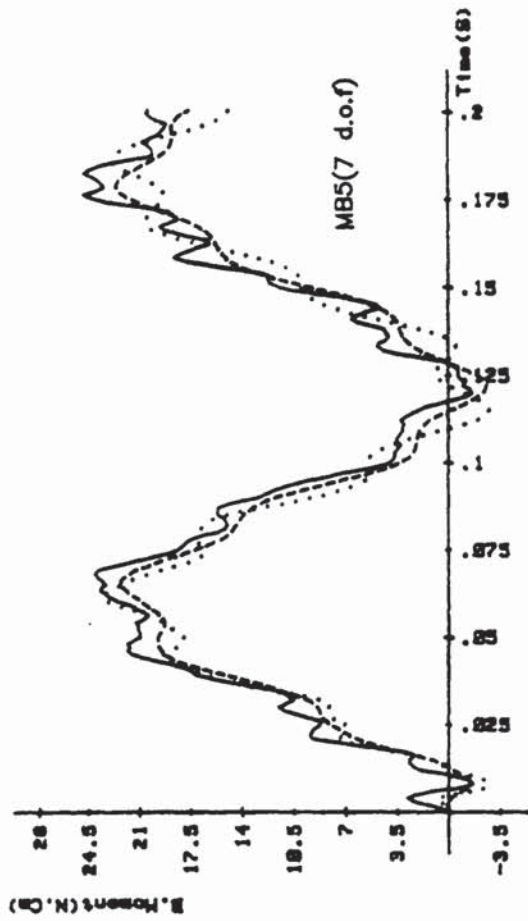
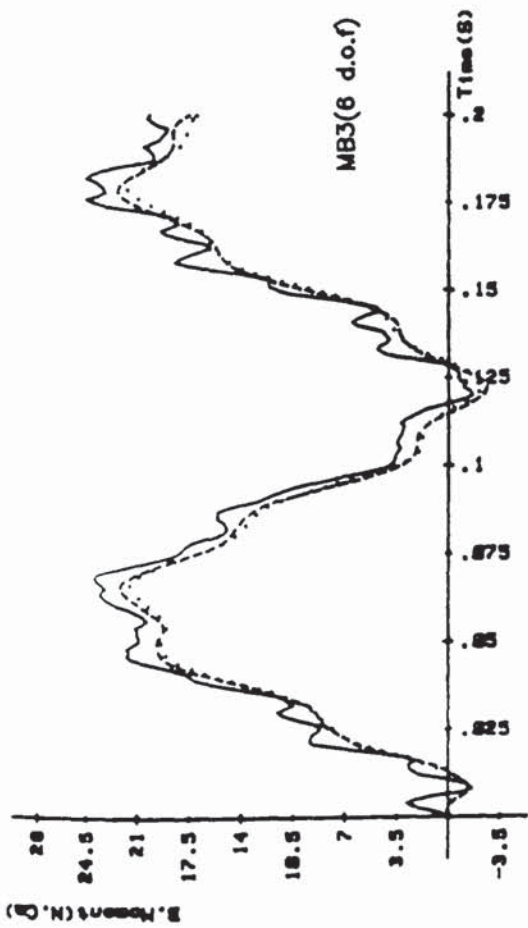


Fig 8.20 Bending moment response of a CC beam at $x=0.0$ to step force input.



Exact
 Displacement (6 d.o.f)
 Mixed model

Fig 8.21 Bending moment response of a CC beam at x=0.0 to step force input.

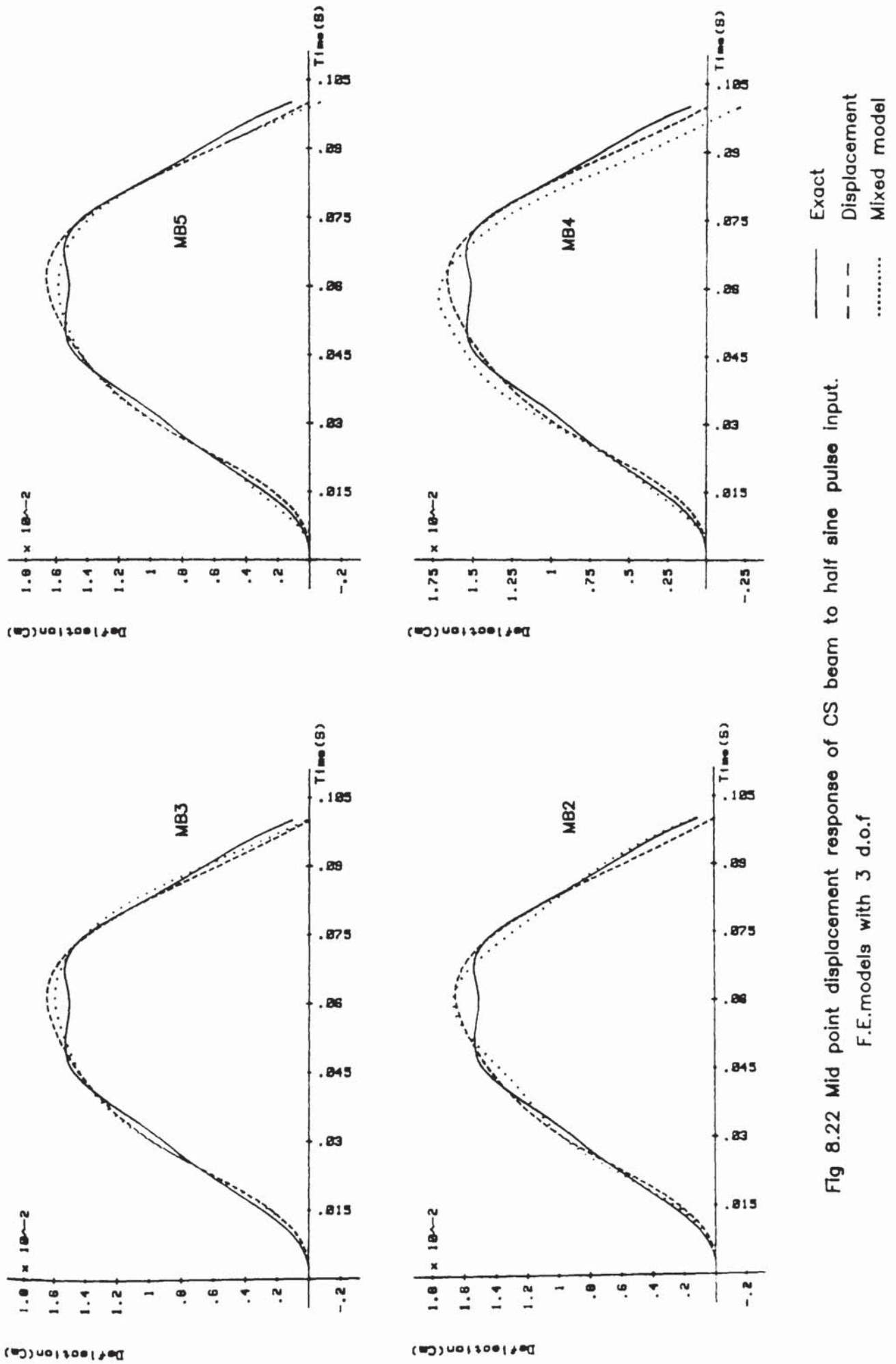
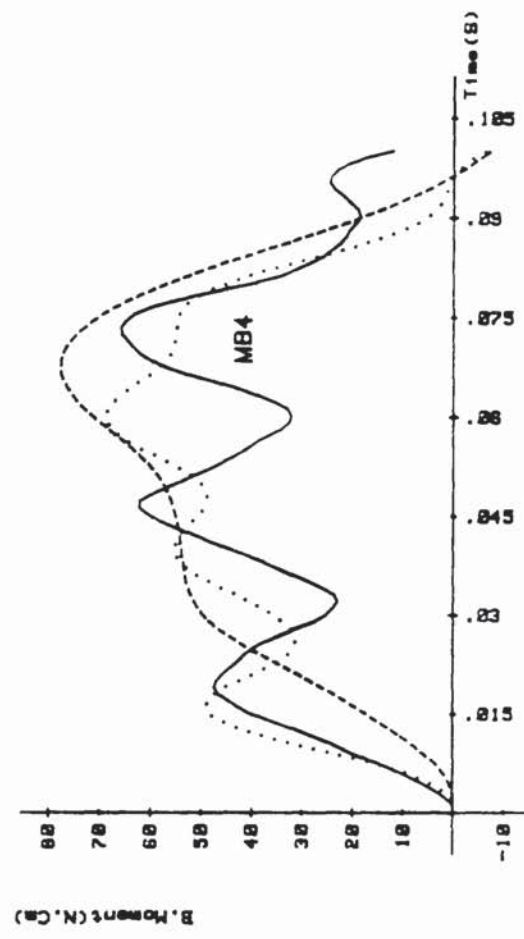
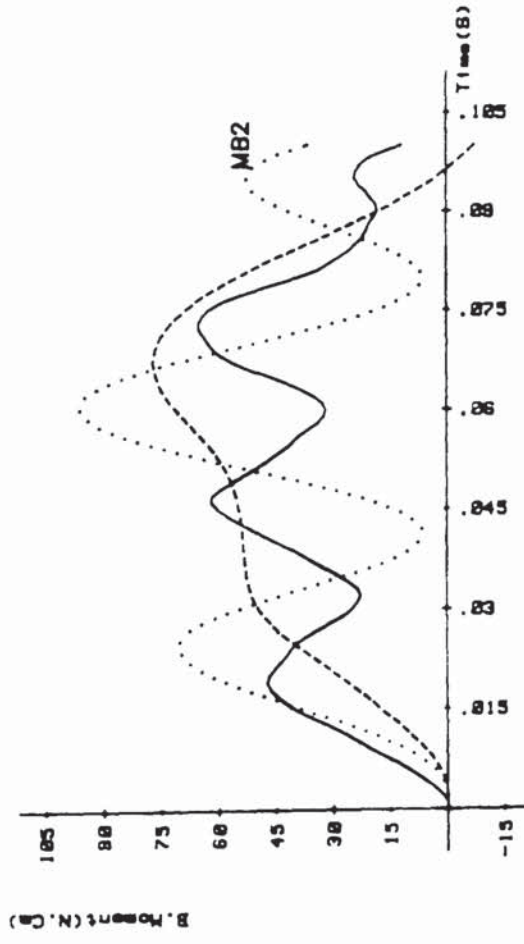
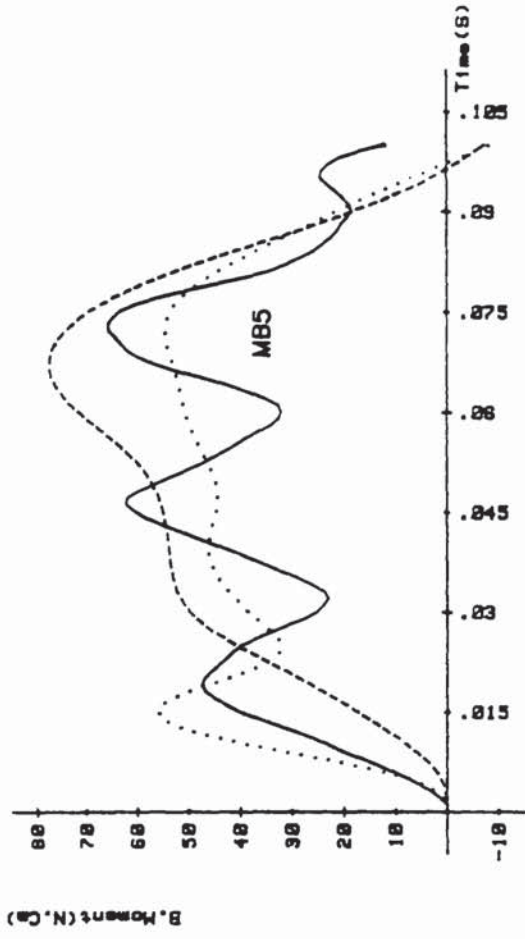
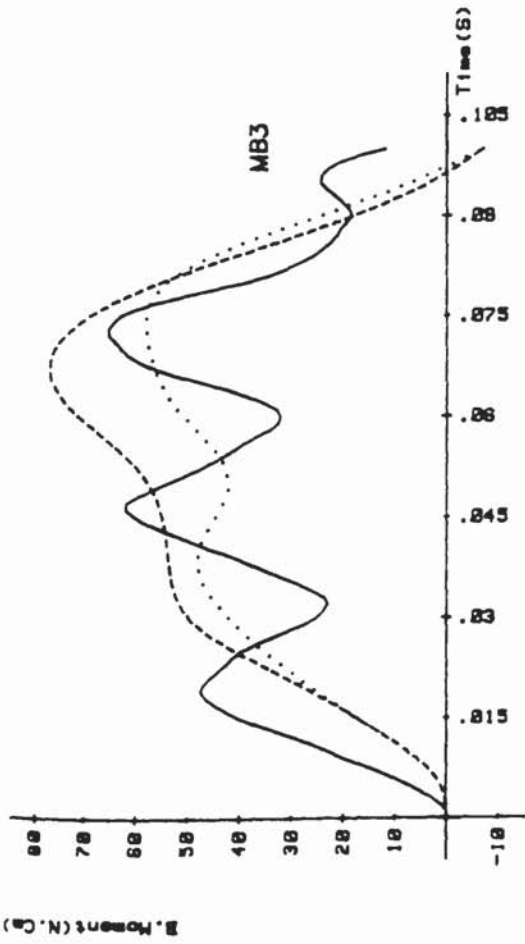


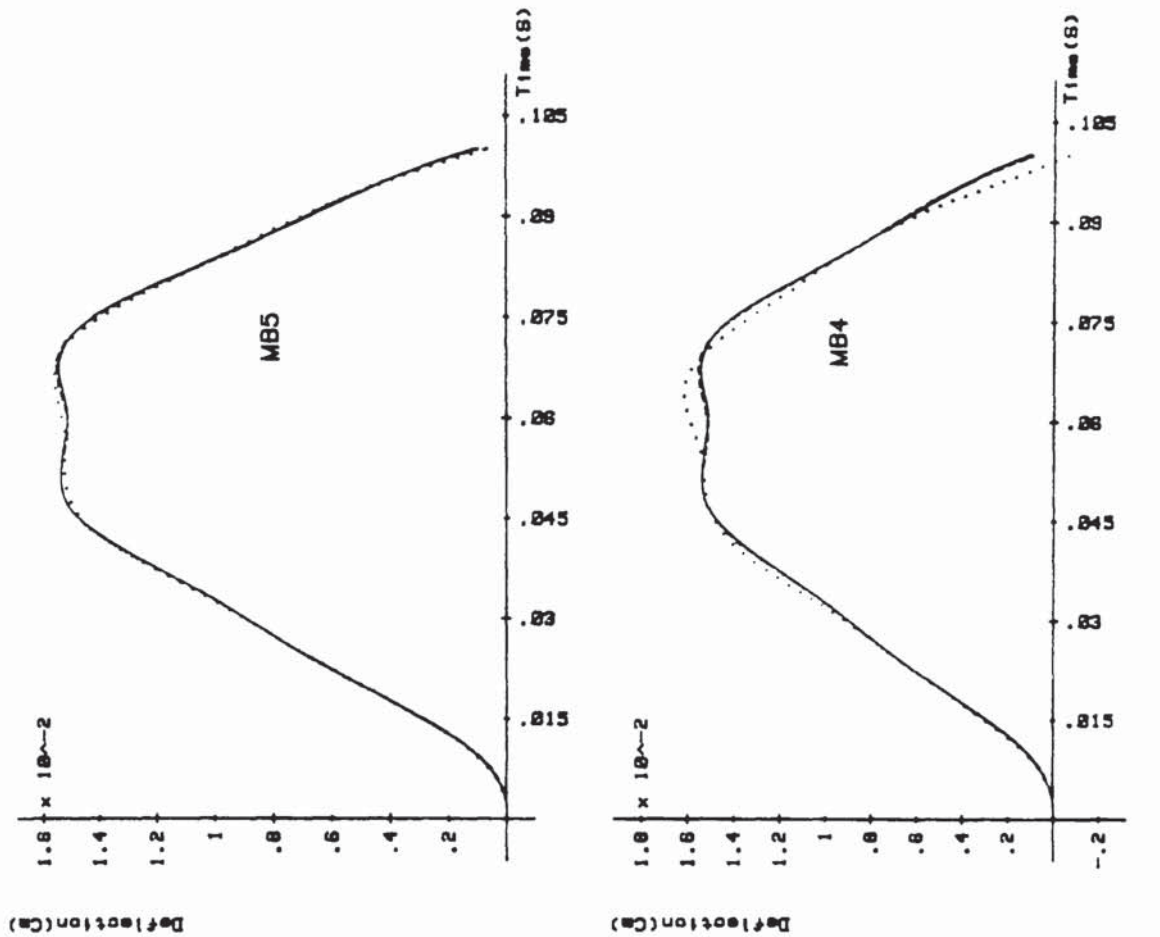
Fig 8.22 Mid point displacement response of CS beam to half sine pulse input.

F.E.models with 3 d.o.f



— Exact
 - - - Displacement
 Mixed model

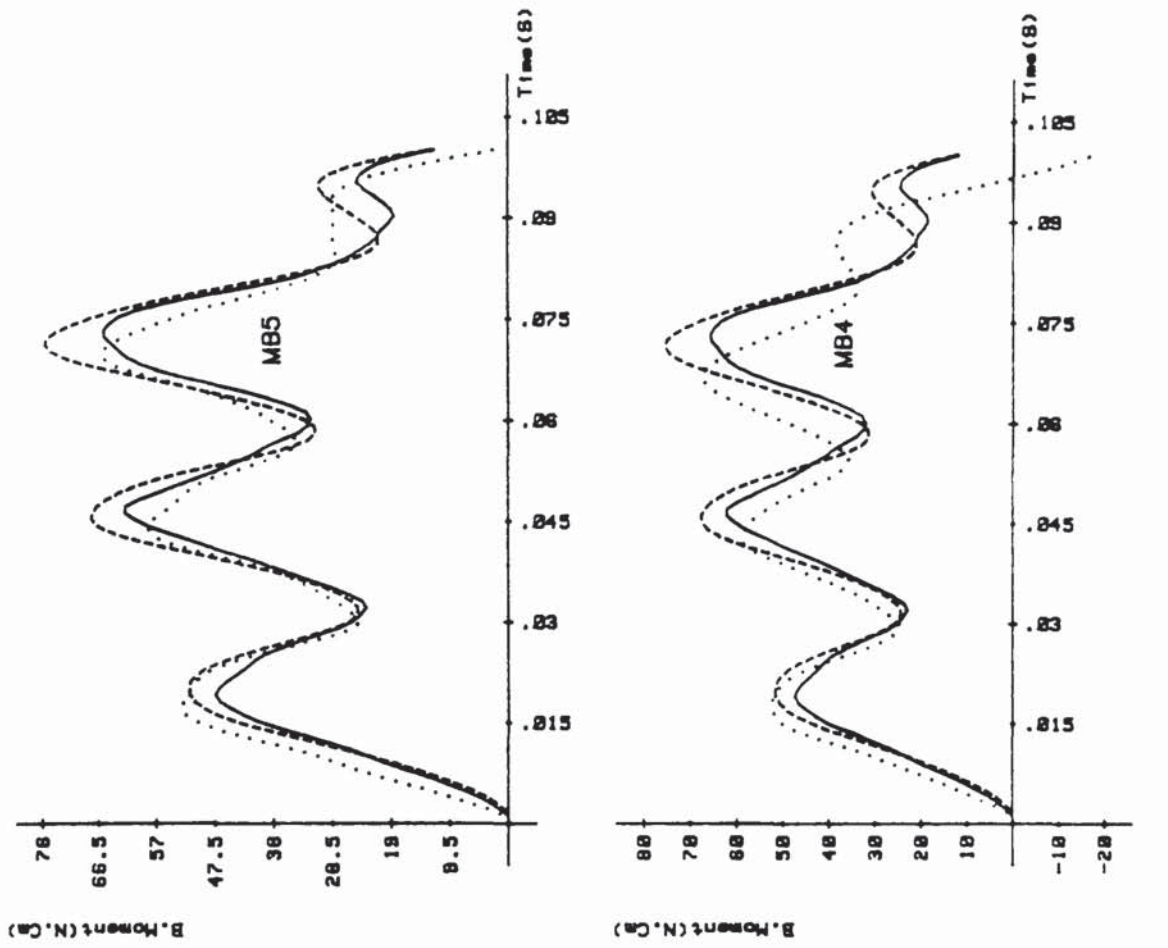
Fig 8.23 Mid point bending moment response of CS beam to sine pulse input. F.E.models with 3 d.o.f



Exact
 Displacement
 Mixed model

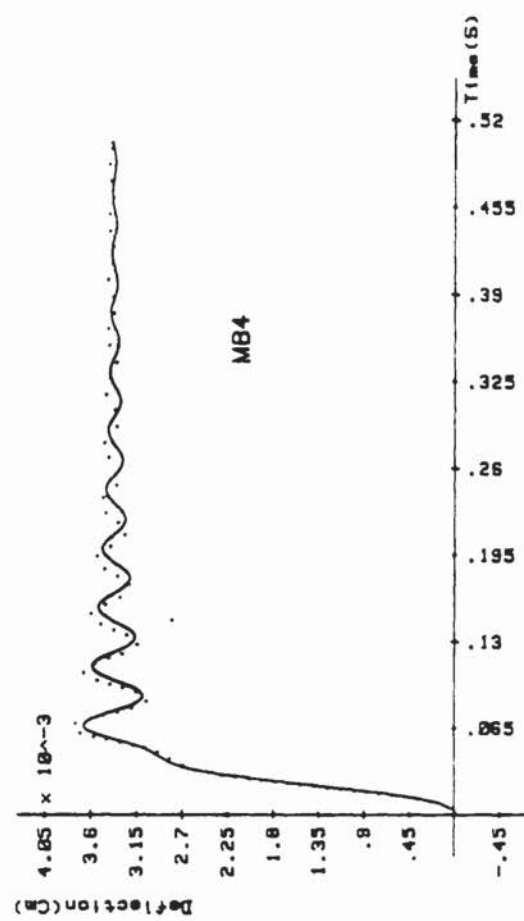
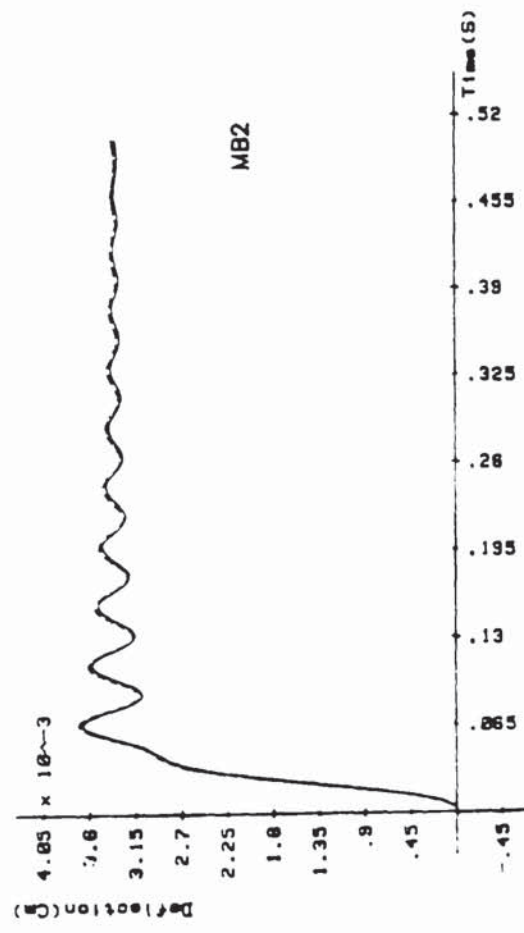
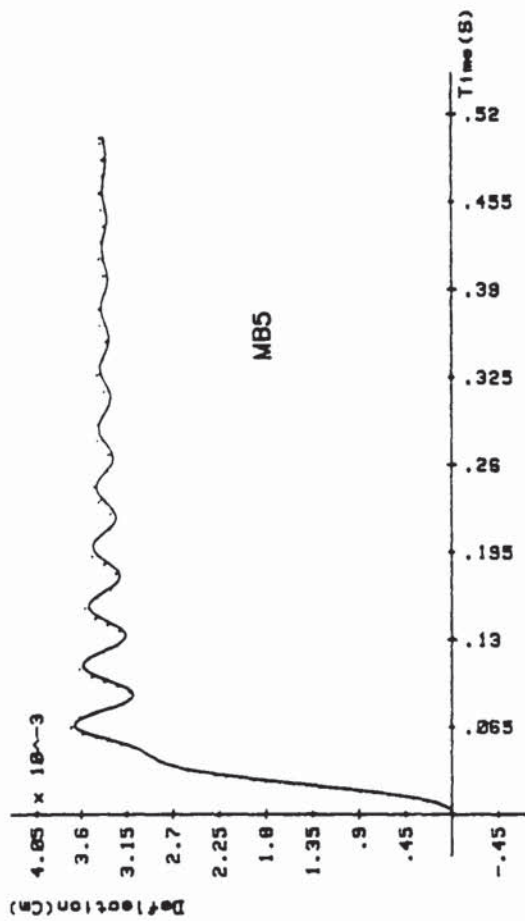
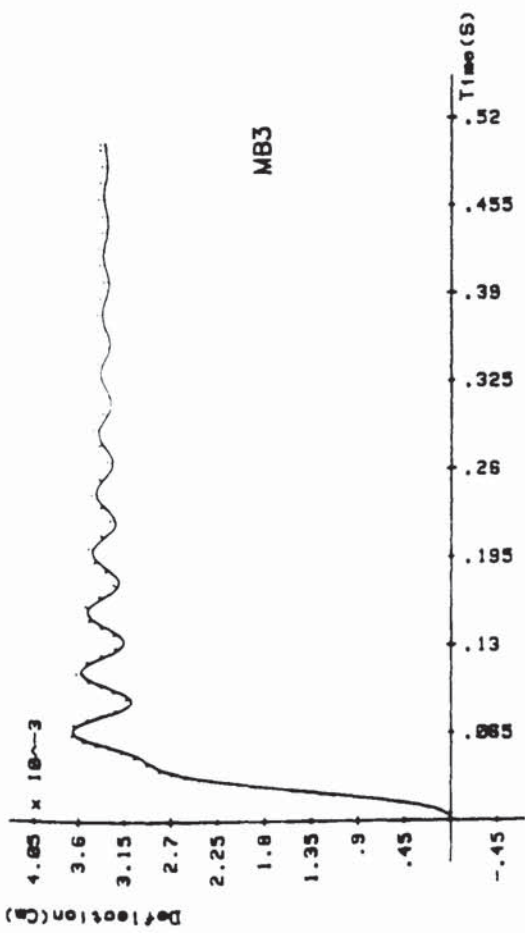
Fig 8.24 Mid point displacement response of CS beam to half sine pulse input.

F.E.models with 7 d.o.f



Exact
 Displacement
 Mixed model

Fig 8.25 Mld point bending moment response of CS beam to sine pulse input.
 F.E.models with 7 d.o.f



— Exact
 - - - Displacement
 Mixed model

Fig 8.26 Mid displacement response of a damped CS beam to ramp force input.
F.E.models with 3 d.o.f

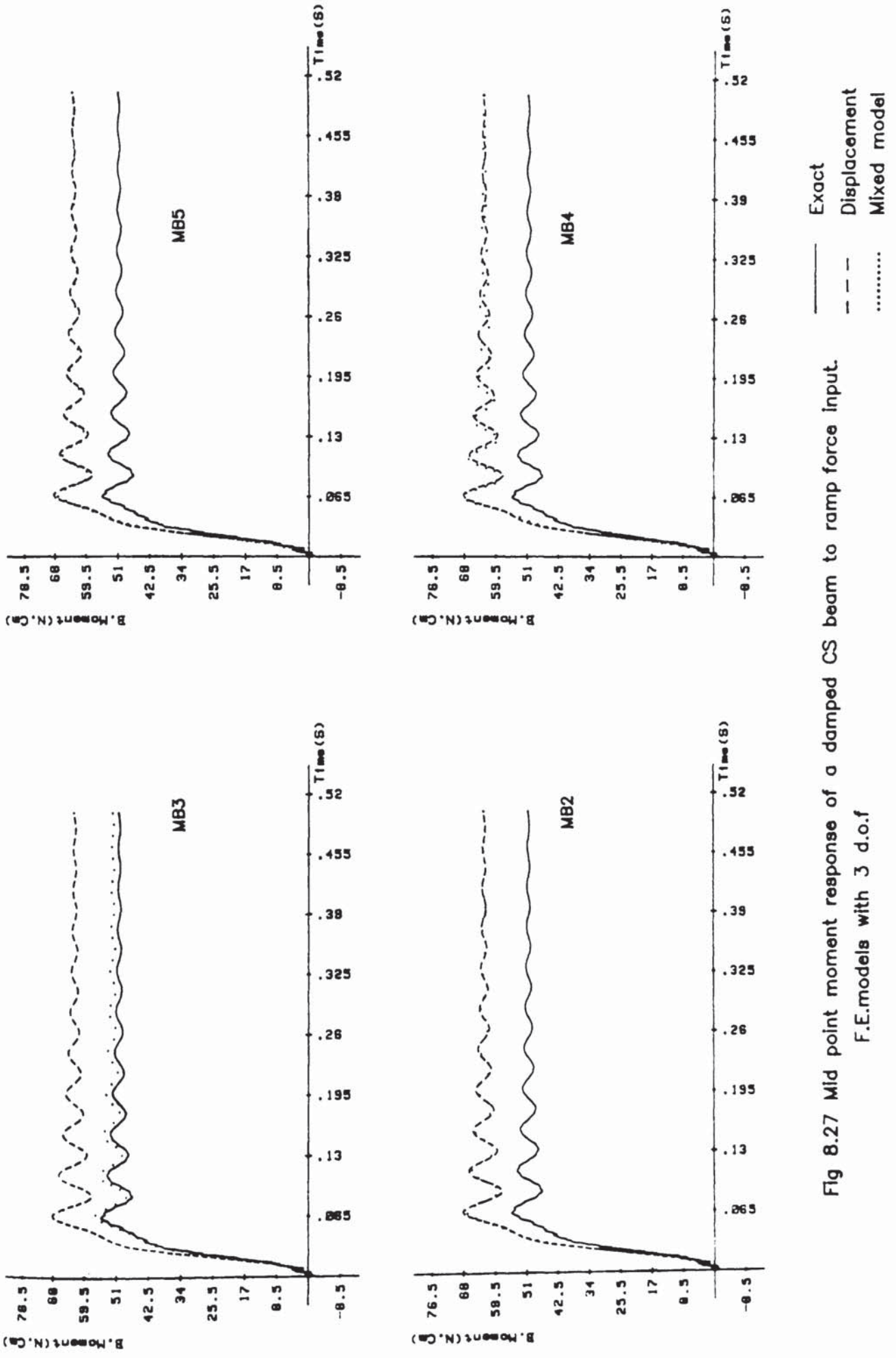


Fig 8.27 Mid point moment response of a damped CS beam to ramp force input.
 F.E.models with 3 d.o.f

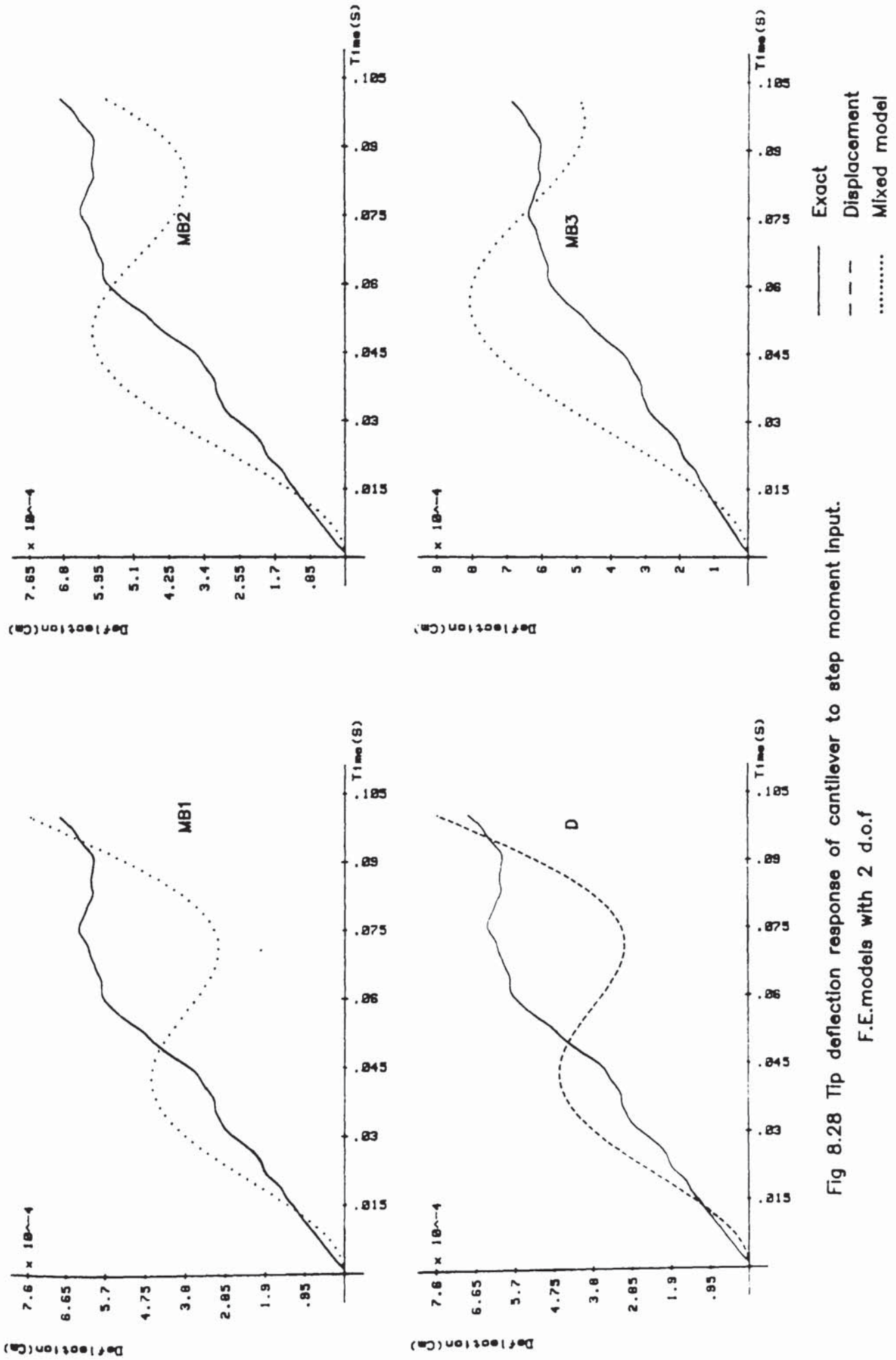
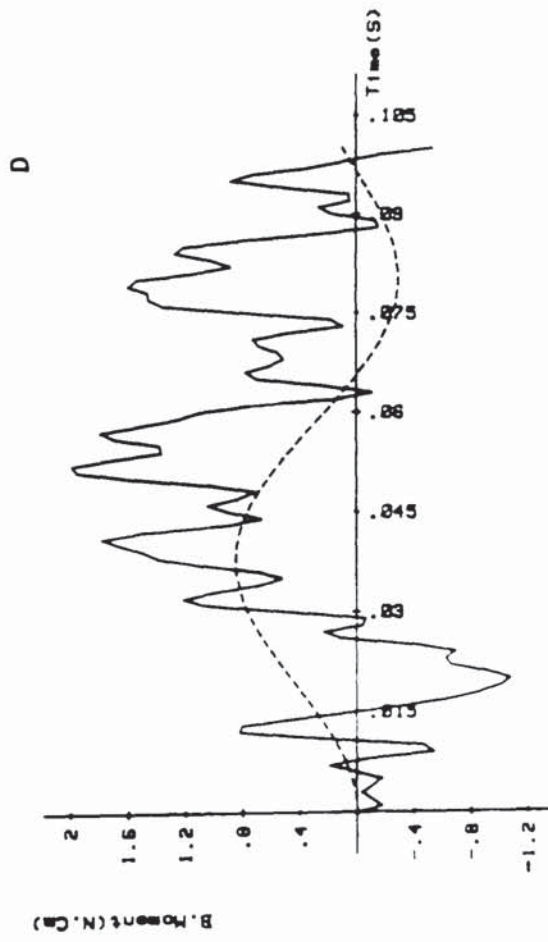
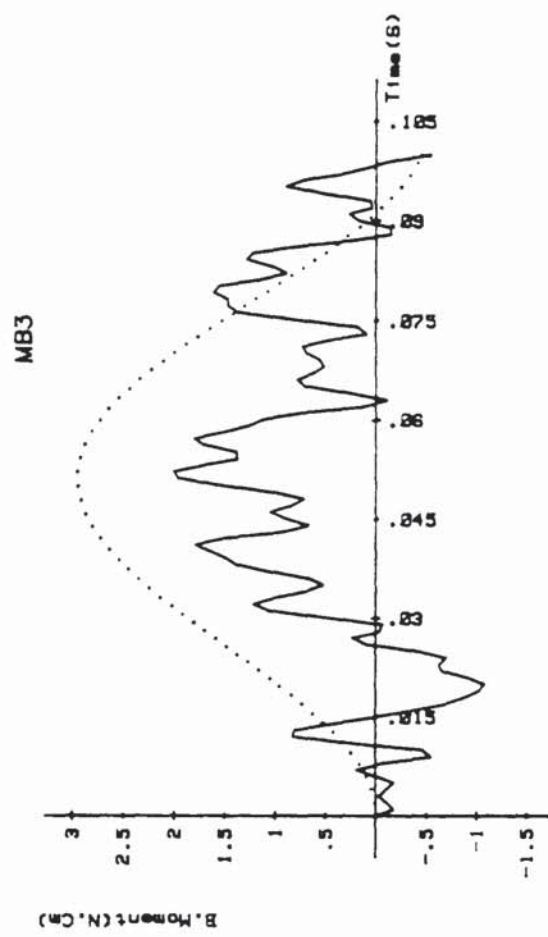
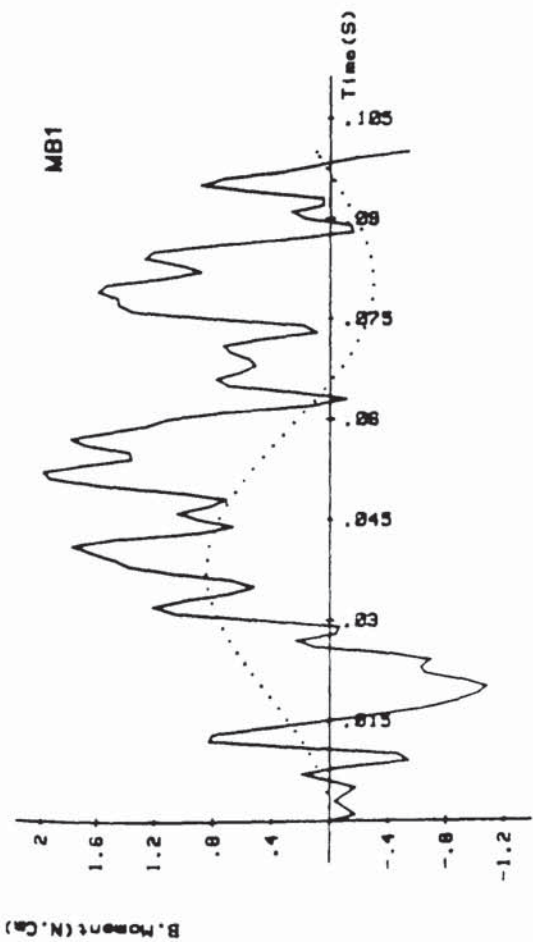
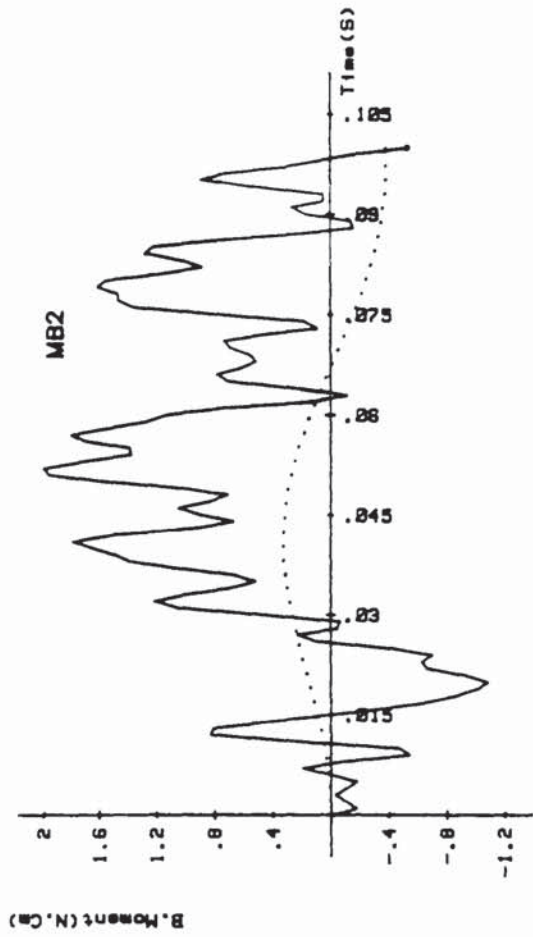


Fig 8.28 Tip deflection response of cantilever to step moment input.
F.E.models with 2 d.o.f



— Exact
 - - - Displacement
 Mixed model

Fig 8.29 Bending moment response of cantilever at $x=0.0$ to step moment input.

F.E.models with 2 d.o.f

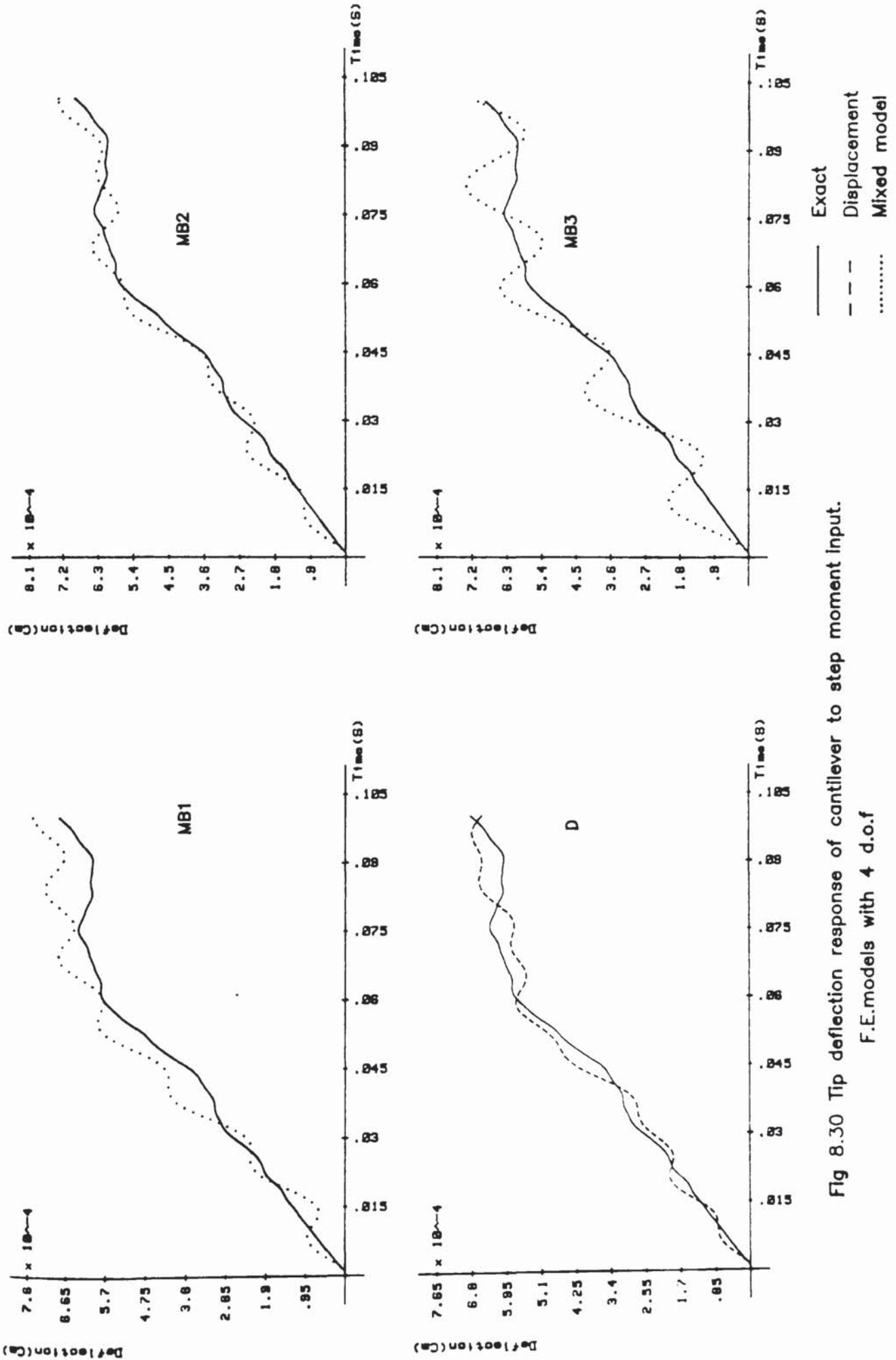
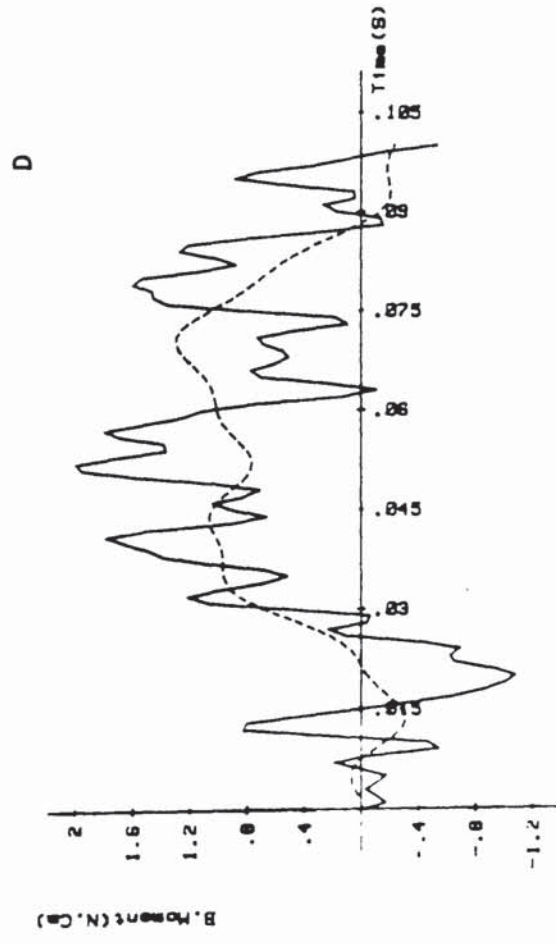
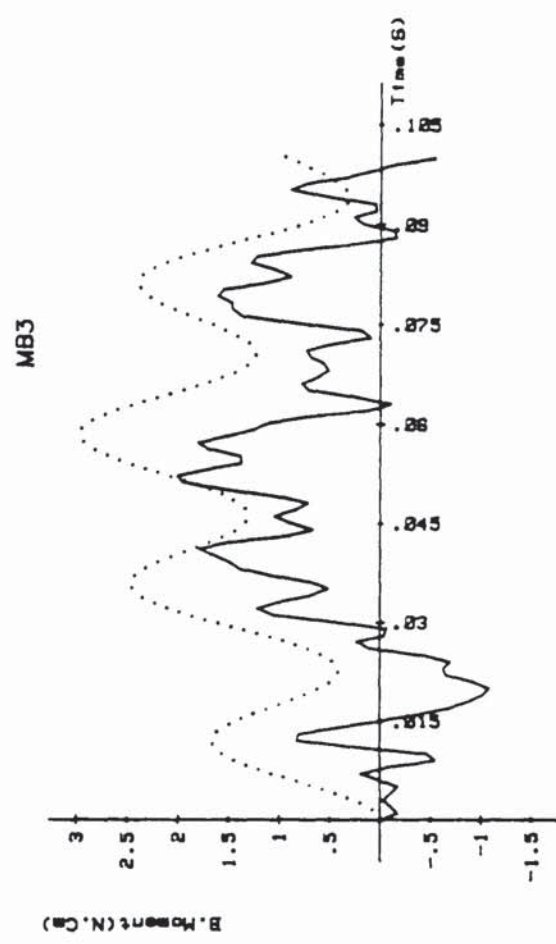
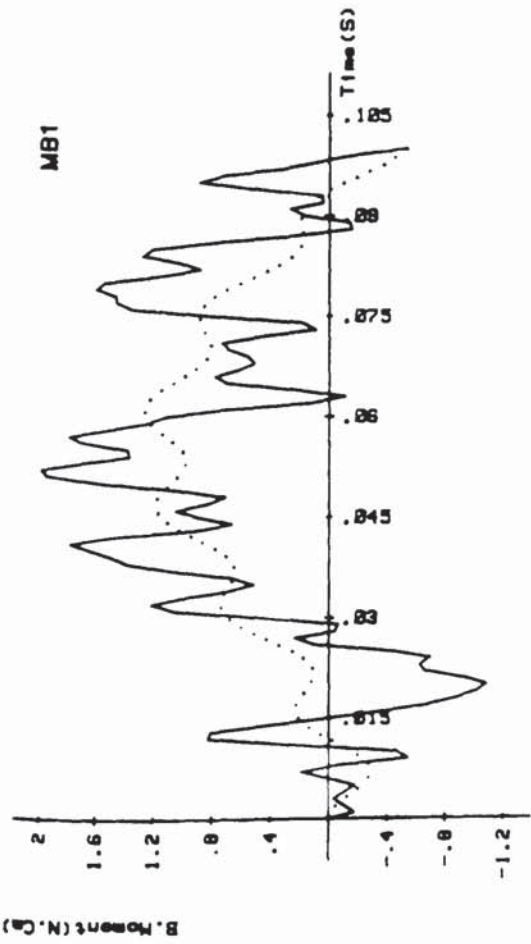
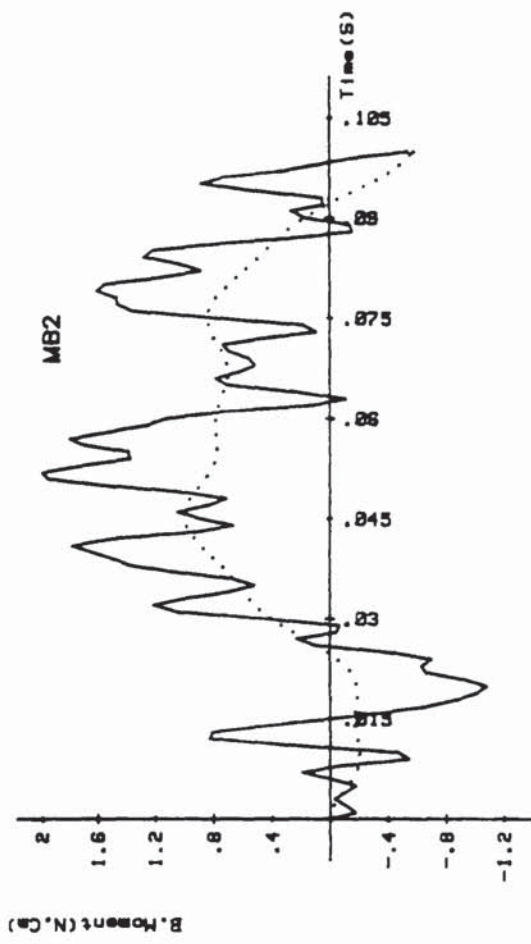


Fig 8.30 Tip deflection response of cantilever to step moment input.
F.E.models with 4 d.o.f



— Exact
 - - - Displacement
 Mixed model

Fig 8.31 Bending moment response of cantilever at $x=0.0$ to step moment input. F.E.models with 4 d.o.f

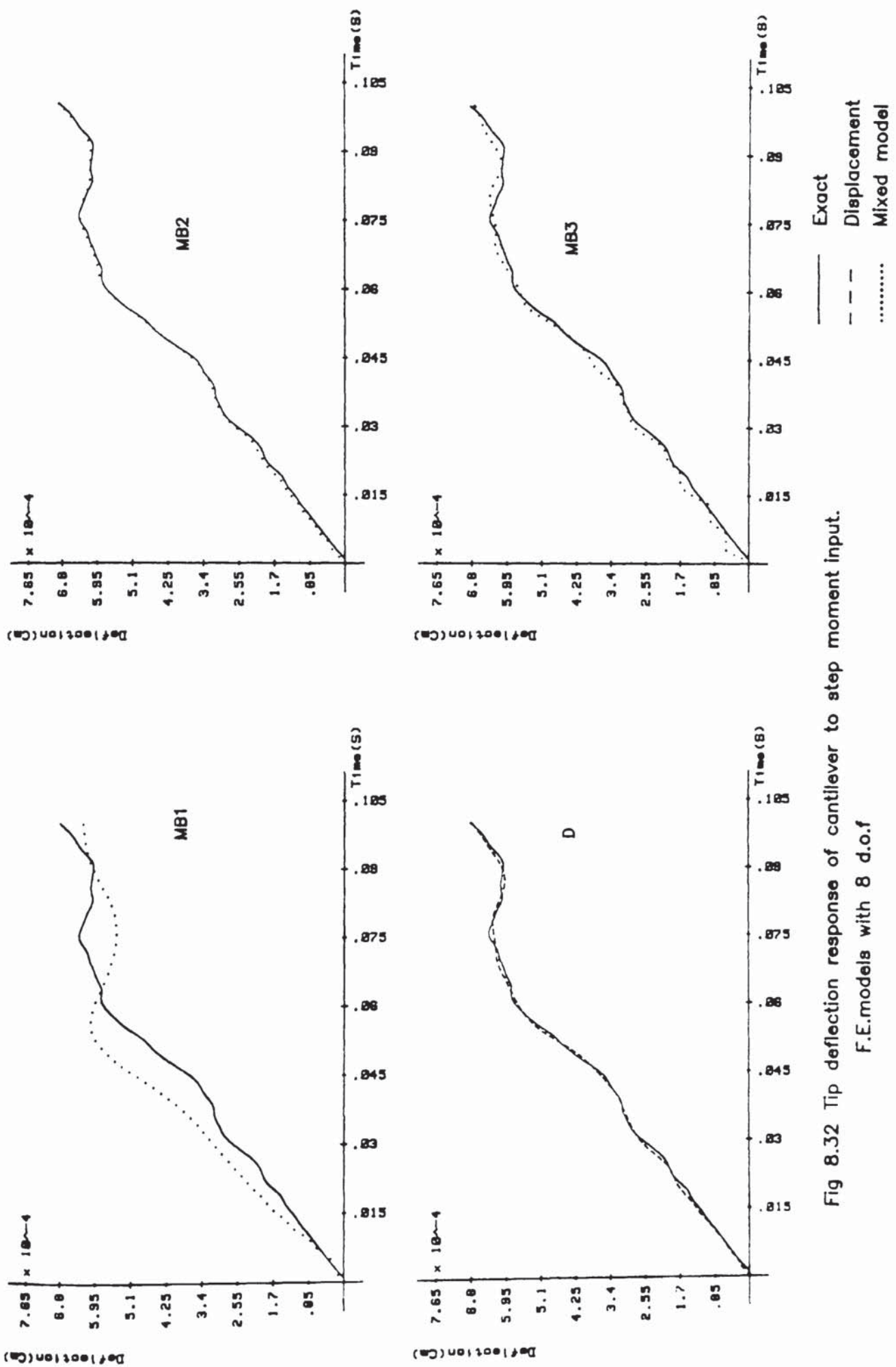
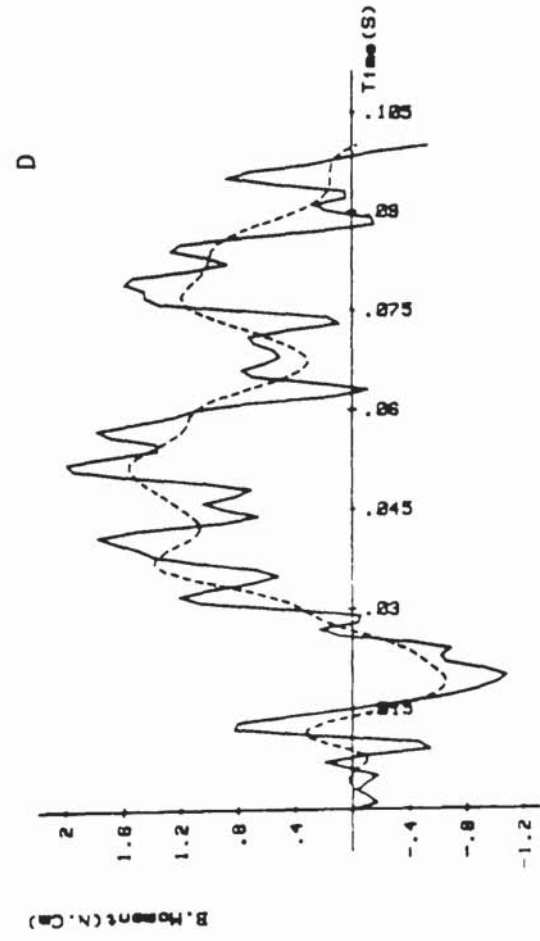
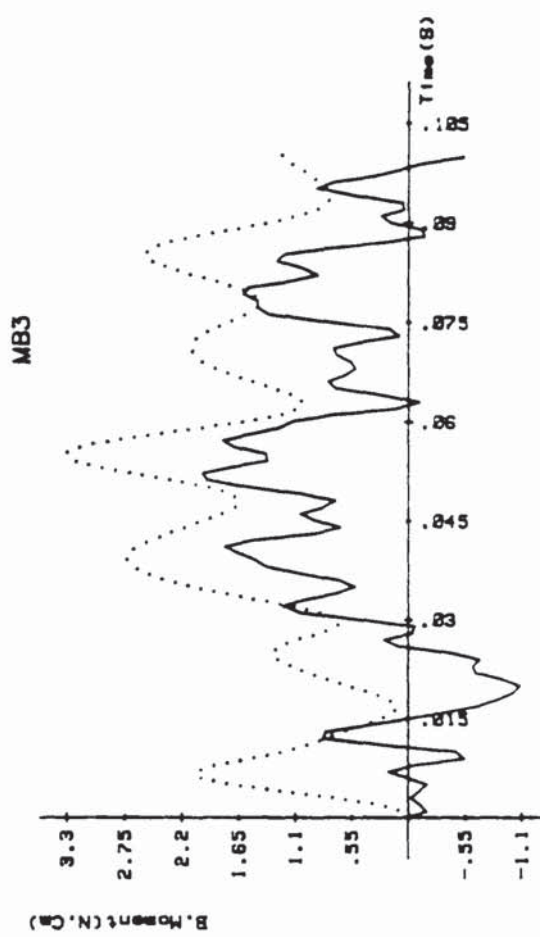
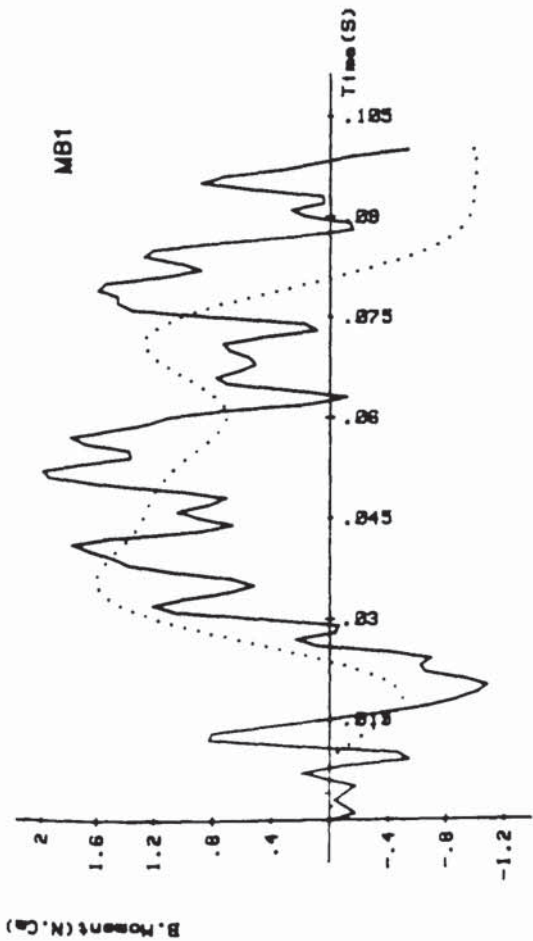
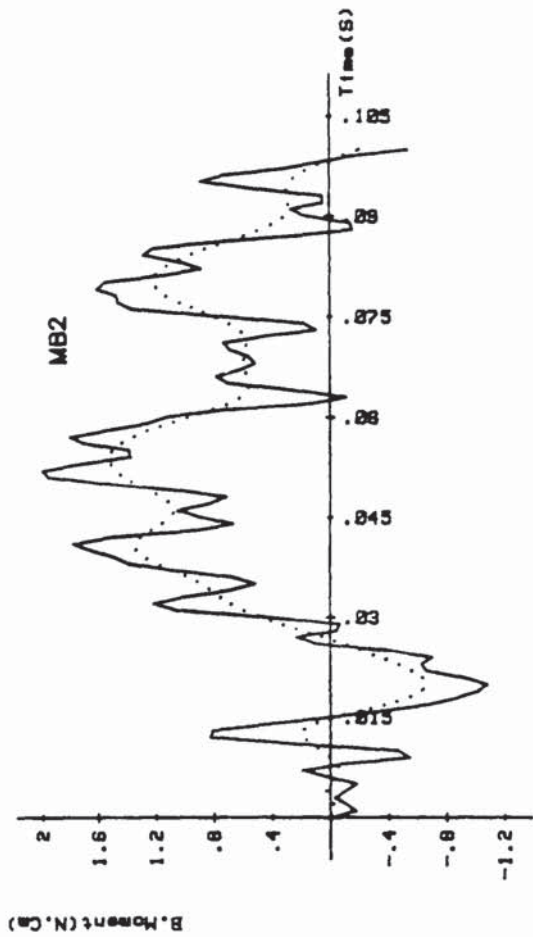


Fig 8.32 Tip deflection response of cantilever to step moment input.

F.E.models with 8 d.o.f



Exact
 Displacement
 Mixed model

Fig 8.33 Bending moment response of cantilever at $x=0.0$ to step moment input.
 F.E.models with 8 d.o.f

8.4 NUMERICAL EXAMPLES ON FREE VIBRATION OF PLATES

A number of free vibration problems of square plates with various boundary conditions are solved using the mixed quadratic element of Figure (8.1b). The predicted results are compared with the analytical solutions and those obtained from other finite element models (Figs. 8.1a, 8.1c, 8.1d). Frequencies are computed for the following three cases:

- (i) Simply supported square plate.
- (ii) Square plate simply supported on two opposite edges and clamped on the other two edges.
- (iii) Cantilevered square plate.

The constants used in these solutions are:

$$\text{Plate: } E = 2.07 \times 10^7 \text{ N/cm}^2, \quad \nu = 0.3, \quad \rho = 7.8 \times 10^{-3} \text{ Kg/cm}^3$$
$$h = 1 \text{ cm}, \quad a = b = 120 \text{ cm.}$$

8.4.1 Simply-supported plate

The natural frequencies of the simply supported square plate shown in Figure (8.34) were predicted by the mixed quadratic element QR8, using (2 x 2), (3 x 3) and (6 x 6) finite element meshes. The results for the (6 x 6) mesh are obtained by solving a (3 x 3) mesh representation of one quarter of the plate, taking advantage of the symmetry of the problem. In this case only the symmetric modes are obtained.

Table (8.4) contains computed frequencies for various meshes. The accuracy of the fundamental frequency predicted by (2 x 2), (3 x 3) and (6 x 6) meshes are within 1.47, 0.15 and .005% of the analytical value. It should be noted that for the (2 x 2), (3 x 3) and (6 x 6) meshes, the final eigenvalue problem has 5, 16 and 85 degrees of freedom respectively. Figures (8.35) and (8.36) compare the accuracy of the developed mixed element, QR8, with the linear, QR4, element when predicting the first and second natural frequencies of the SS plate. It is seen that the mixed quadratic element is more efficient than the corresponding linear one. Also Figures (8.37) and (8.38) show the convergence curves for different types of elements when predicting the first and fifth natural frequencies. It is observed that the mixed 4 node and 8 node elements provide better results than the corresponding displacement type elements.

8.4.2 Clamped-simply supported square plate

The natural frequencies for a clamped simply supported square plate are obtained by using the mixed quadratic element with various meshes. These results are presented in table (8.5). It shows that a (4 x 6) mesh is capable of predicting the first natural frequency within 0.138%. The coarsest mesh used in this example is (2 x 2) and is capable of predicting this frequency to within 1.54%.

Figures (8.39) to (8.42) compare the performance of mixed quadratic element with the linear one in predicting the lowest four natural frequencies. The comparison with other types of elements are presented in Figures (8.43) and (8.44), corresponding to the second and third natural frequencies of the CSCS plate. It is seen that QR8 element has a much better performance than the 4-

noded QR4, and QD4 elements and is comparable with the 8-noded QD8 element.

8.4.3 Cantilevered square plate

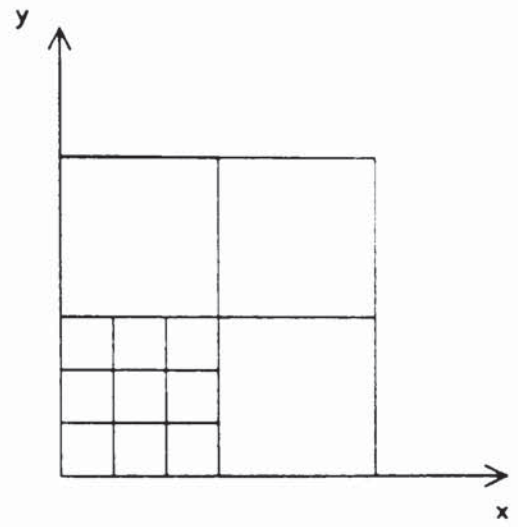
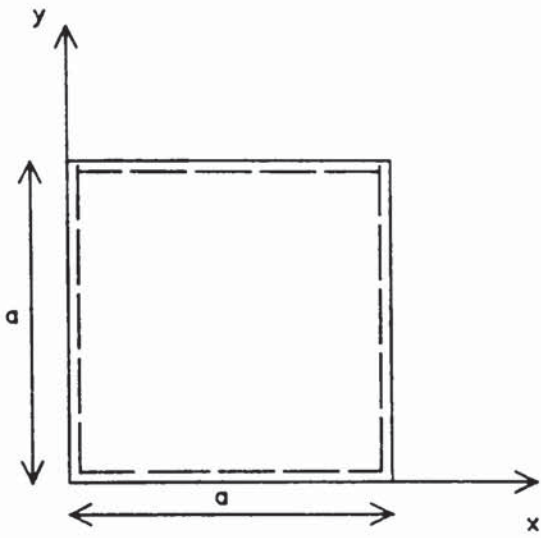
Natural frequencies for a cantilever square plate are computed by using different types of elements presented in section 8.1. No exact solution exists for this problem and therefore the results are compared with the experimental (69) and other types of numerical solutions. These are shown in Table (8.6).

It can be seen that the mixed models using element QR8, have computed the first 5 natural frequencies with good accuracy, but the convergence to the experimental values is not necessarily monotonic. For a (2 x 2) mesh of QR8 element which leads to the final eigen problem of 16 degrees of freedom, the discrepancies of the values of the first five frequencies with reference to the Ritz solution (10) are 0.621, 5.86, - 2.9, 0.962 and 5.924%.

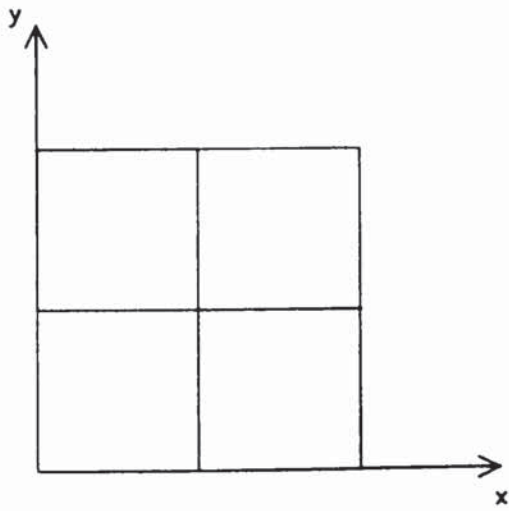
The equivalent discrepancies of a (2 x 2) mesh of displacement element QD8 with 48 degrees of freedom are 1.795, - 1.717, 1.068, - .54 and -1.7%. IN this case, the mixed model discrepancies are larger than the displacement models. It should however be noted that these are obtained using a much smaller eigenvalue problem than the displacement problem.

In application to eigenvalue problems, mixed models possess an important advantage over the conventional displacement models. This is because the reduction of degrees of freedom from total (displacements plus stresses) to the final having either displacements

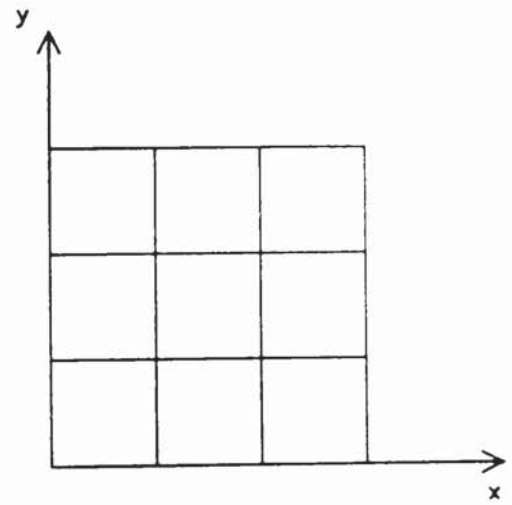
or stresses alone, is an exact operation. In the displacement models, the eigenvalue problem can be reduced by means of the so-called "eigenvalue economizer" method. In this operation, however, the accuracy of the computed eigenvalues decreases.



(a)



(b)



(c)

Fig 8.34 Finite element idealisations for a simply supported square plate.

Mixed Finite Element Models

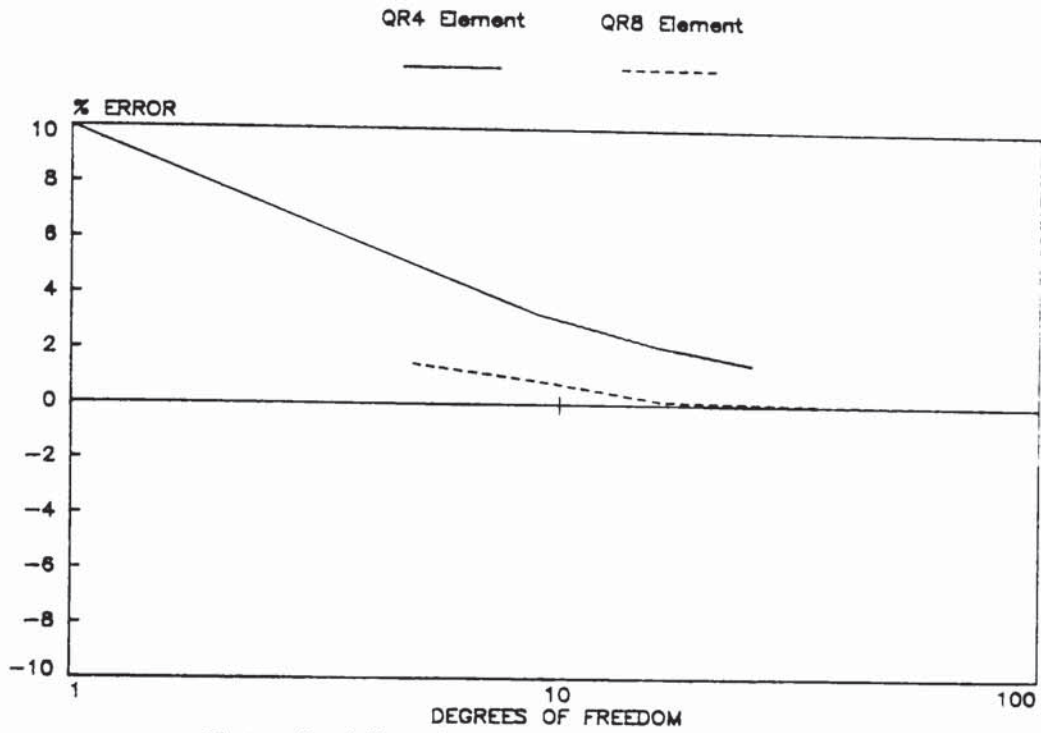


Fig 8-35 Prediction of lowest natural frequency of SSSS plate

Mixed Finite Element Models

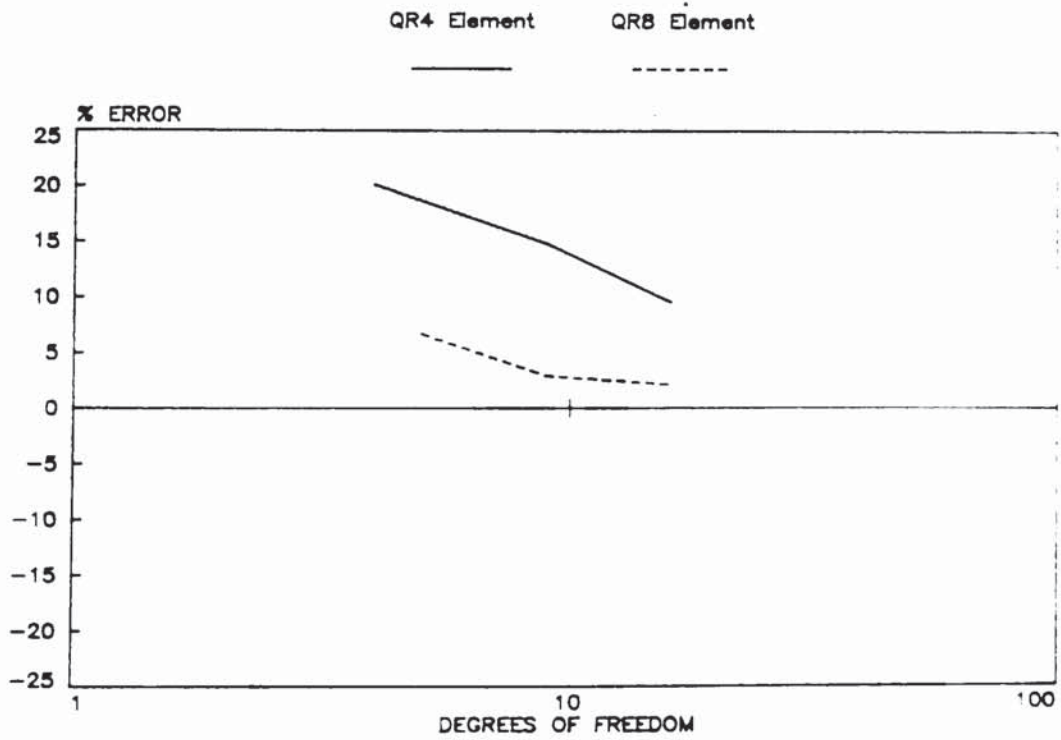


Fig 8-36 Prediction of second natural frequency of SSSS plate

Mixed/Displacement Finite Element Models

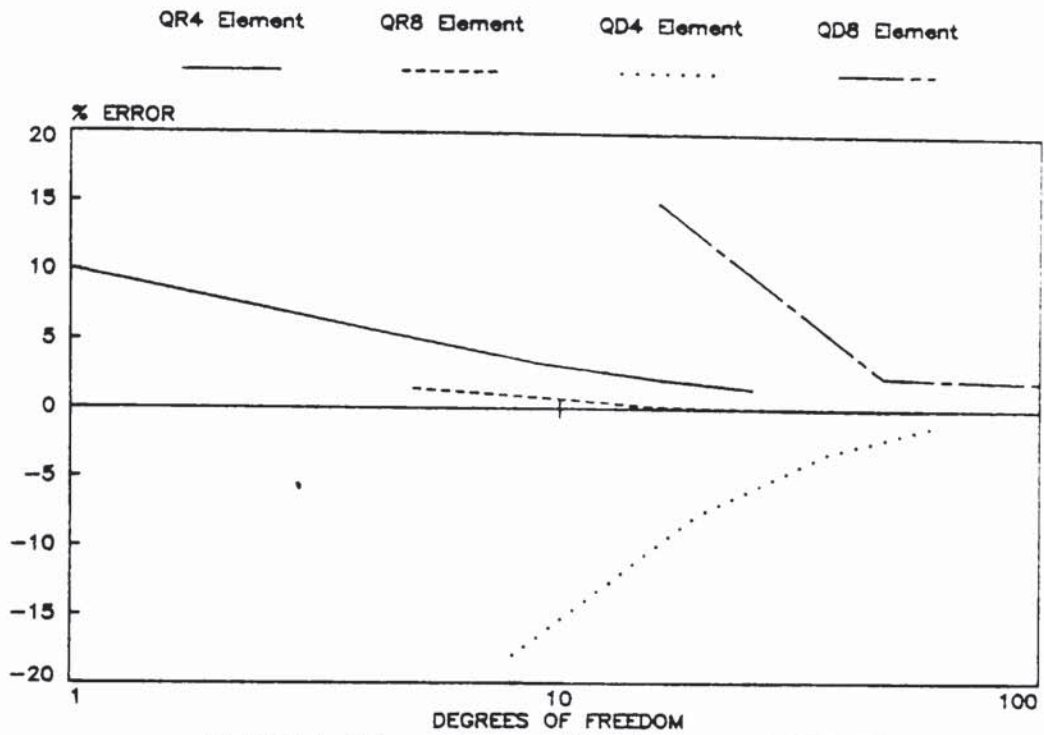


Fig 8-37 Prediction of lowest natural frequency of SSSS plate

Mixed/Displacement Finite Element Models

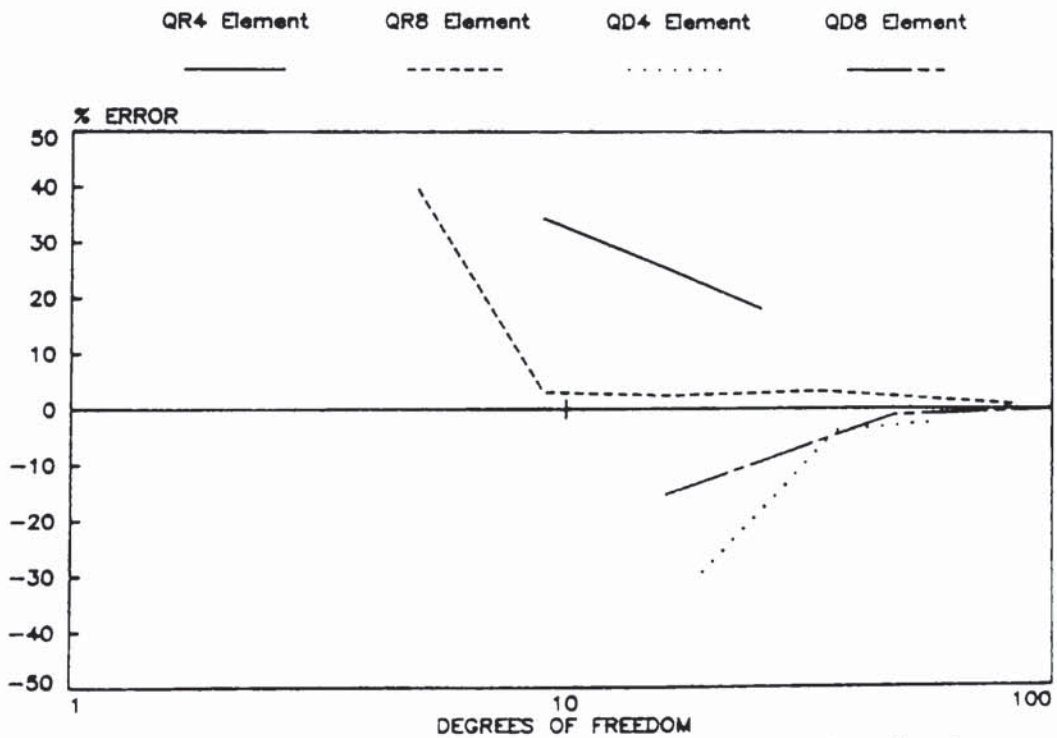


Fig 8-38 Prediction of fifth natural frequency of SSSS plate. $m=3, n=1$

Mixed Finite Element Models

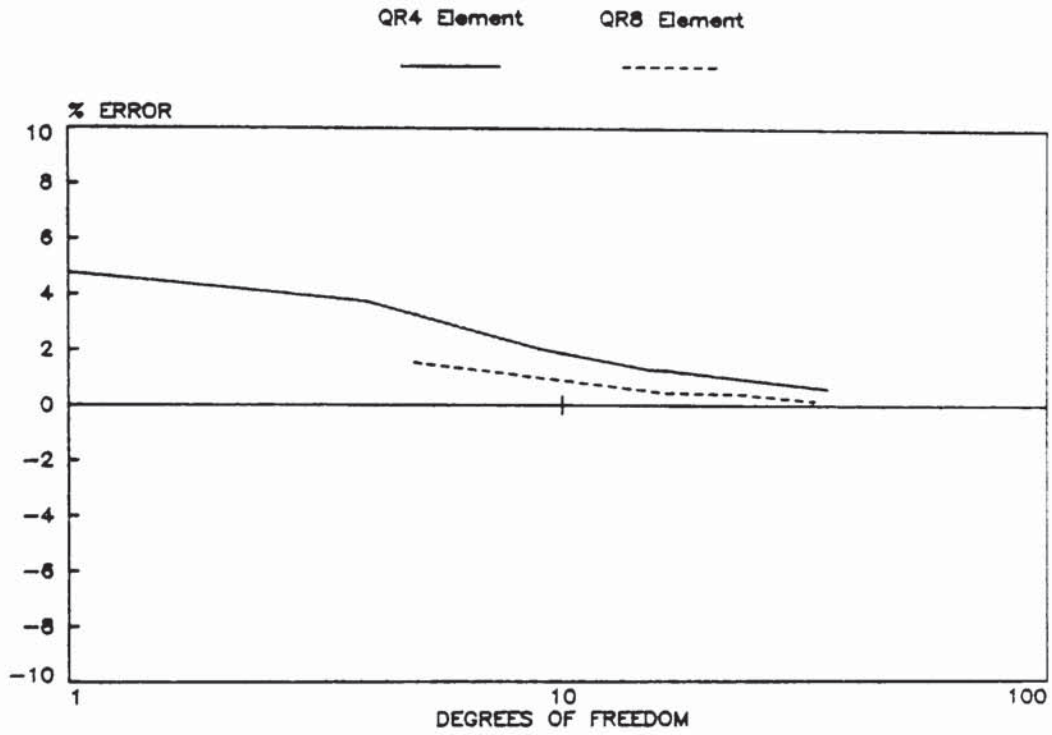


Fig 8.39 Prediction of lowest natural frequency of C/SCS plate

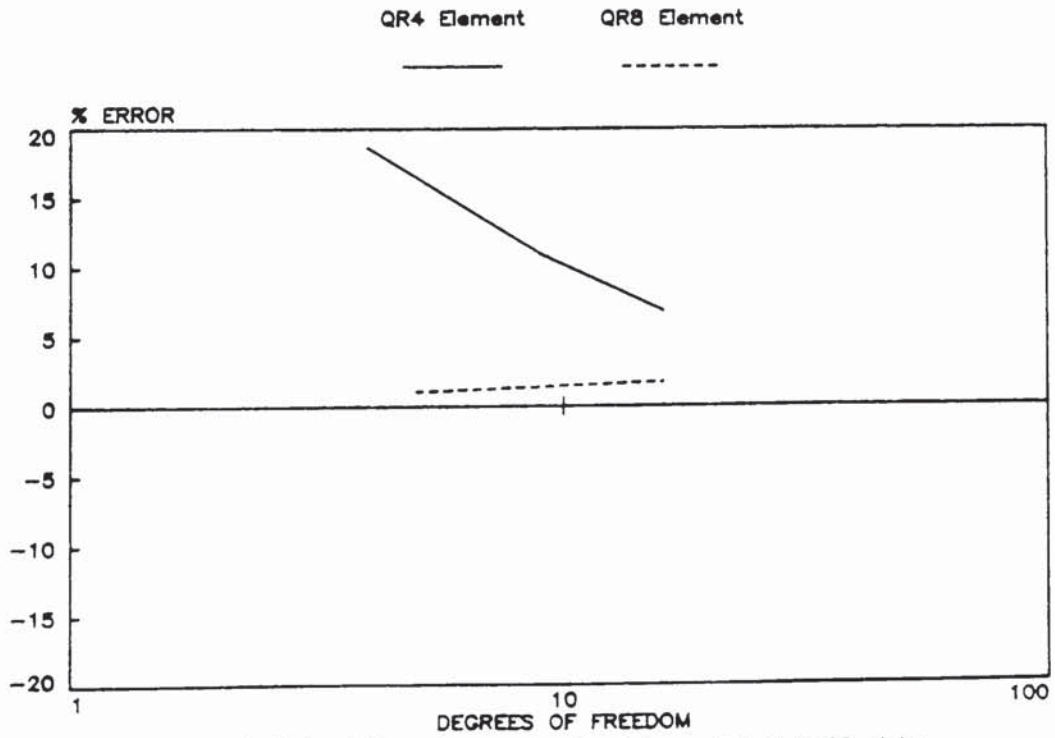


Fig 8.40 Prediction of second natural frequency of C/SCS plate

Mixed Finite Element Models

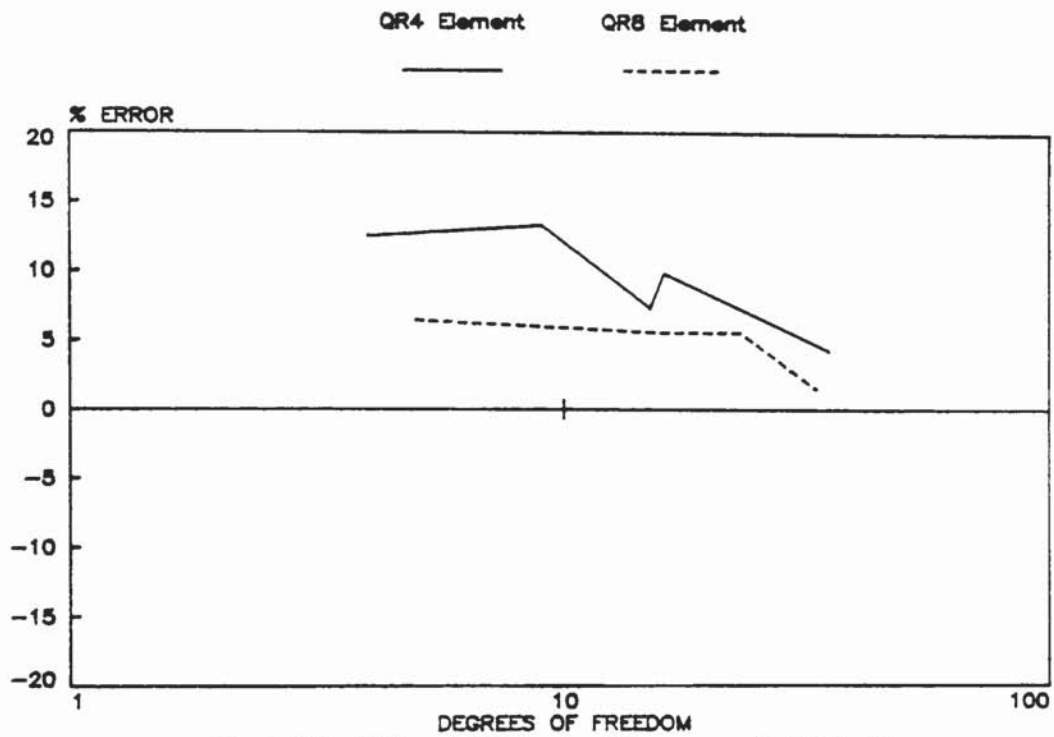


Fig 8.41 Prediction of third natural frequency of CSCS plate

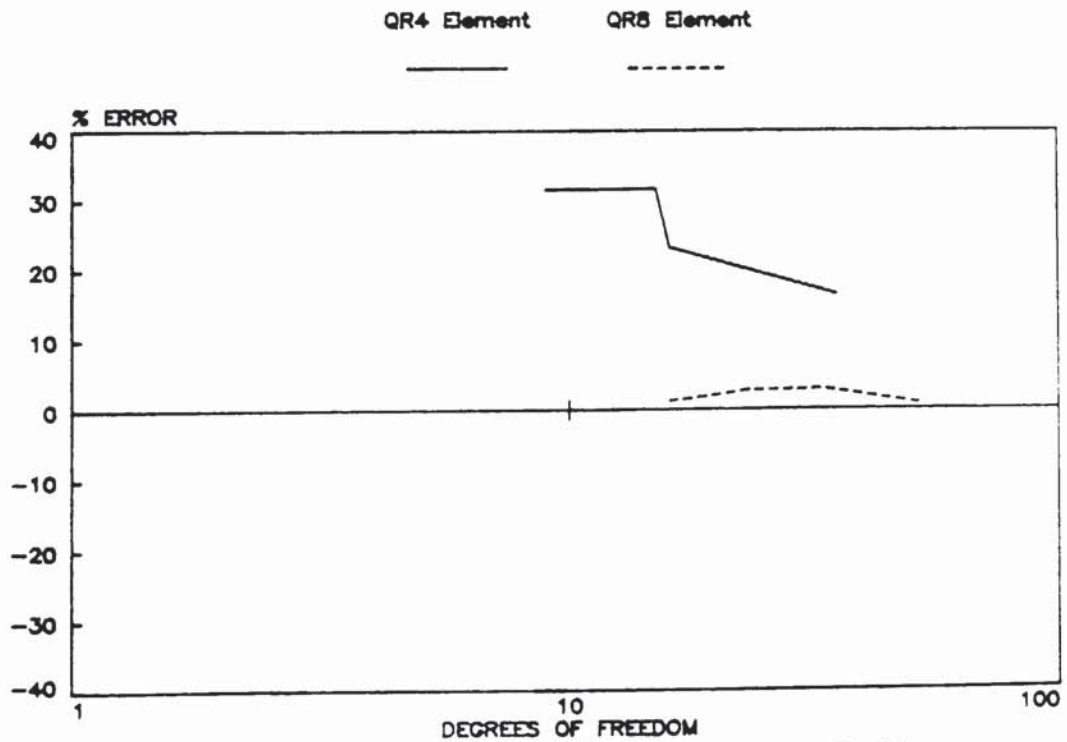


Fig 8.42 Prediction of fourth natural frequency of CSCS plate

Mixed/Displacement Finite Element Models

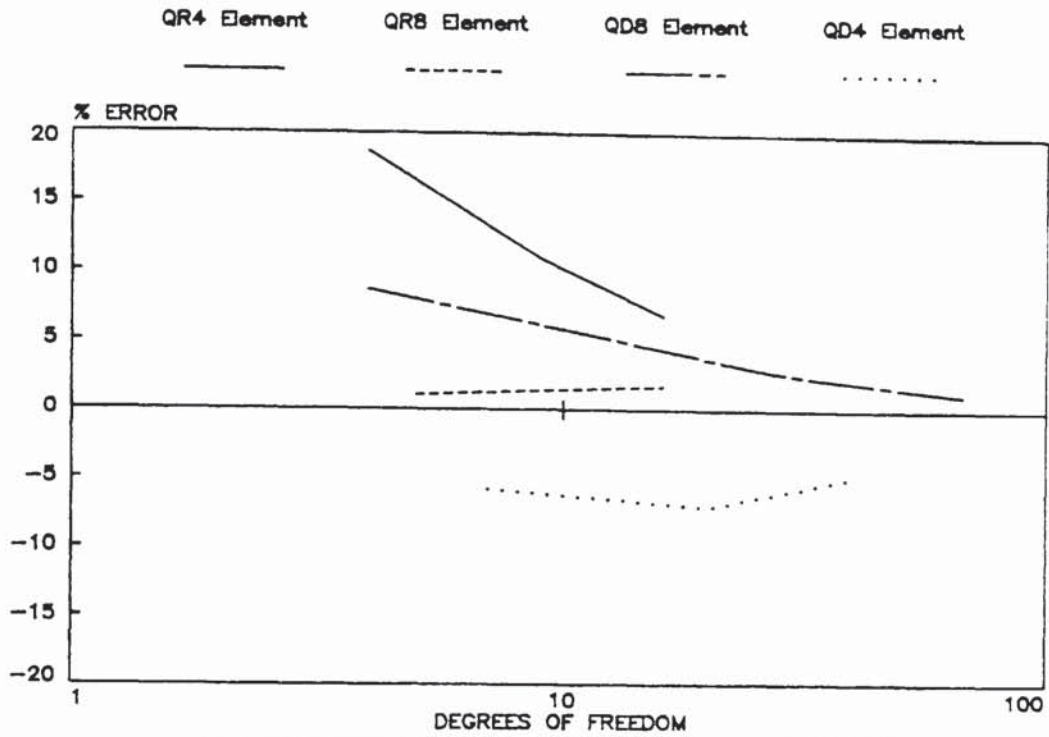


Fig 8.43 Prediction of second natural frequency of CSCS plate

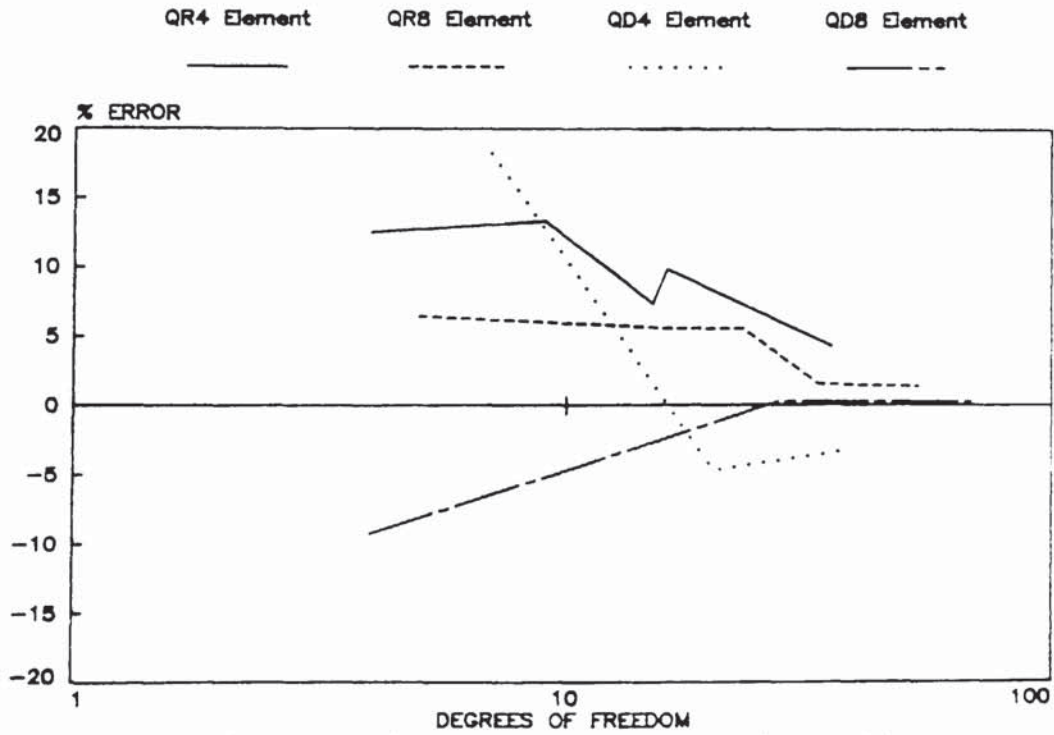


Fig 8.44 Prediction of third natural frequency of CSCS plate

Table 8.4 Eigenvalues of a simply supported plate.

Square Plate	$\lambda = \omega a^2 \sqrt{\frac{\rho h}{D}}$			
Number of half waves in x & y directions	Exact Ref(10)	Mesh(QR8)		
		2x2	3x3	6x6
m=1,n=1	19.74	20.03	19.77	19.741
m=2,n=1	49.35	52.63	50.393	
m=2,n=2	78.96	135.53	83.122	
m=3,n=1	98.70	137.74	101.06	99.36

Table 8.5 Eigenvalues of a clamped-simply supported plate.

Square Plate	$\lambda = \omega a^2 \sqrt{\frac{\rho h}{D}}$			
Mode Number	Exact Ref(10)	Mesh(QR8)		
		2x2	4x4	4x6
1	28.95	29.397	29.07	28.99
2	54.74	55.333		
3	69.32	73.803	73.163	70.36
4	94.59	137.76		
5	102.2	169.372	105.966	102.877

Table 8.6 Vibration eigenvalues of square cantilever plate

Square Plate		$\lambda = \omega a^2 \sqrt{\frac{\rho h}{D}}$				
Number of degrees of freedom	Vibration Mode					
	Source	1	2	3	4	5
6	QR4	3.364	7.067	22.047	24.853	25.947
12		3.426	7.575	22.607	27.37	28.254
30		3.454	7.986	21.856	27.152	29.681
5	QR8	3.545	6.993	20.53	26.055	26.388
16		3.470	8.025	22.049	27.068	29.268
33		3.467	8.205	21.36	26.8	29.87
6	QD4	3.329	9.256	30.632	35.934	47.452
12		3.296	8.865	17.137	31.267	31.939
18		3.458	8.849	21.796	26.686	30.951
36		3.468	8.825	21.709	27.185	31.5
15	QD8	3.442	8.782	21.60	28.192	31.397
48		3.458	8.785	21.28	27.47	31.795
99		3.429	8.671	21.20	27.48	31.64
Experimental	Ref(69)	3.37	8.26	20.55	27.15	29.75
Energy solution	Ref(70)	3.494	8.547	21.44	27.46	31.17
Ritz Method	Ref(10)	3.4917	8.5246	21.429	27.331	31.111

8.5 NUMERICAL EXAMPLES ON FORCED VIBRATION OF PLATES

In this section some numerical tests for the solution of problems concerned with the forced vibration of plates are presented. The tests are aimed at illustrating the performance of mixed quadrilateral elements (QR4, QR8) in the solution of dynamic transient problems. The results are compared with the solutions from analytical and from displacement type formulations. The convergence and accuracy of the results are determined as the element sub-division of the plate is refined. In these examples, the solution of the dynamic equilibrium equations are obtained using the unconditionally stable direct integration of Wilson θ with a time step size of $\Delta t = .001$ sec.

Some numerical tests are given at the end of this section to show the effect of time-step size on the stability and accuracy of the solution. It is also possible to use the mode superposition approach to solve the equilibrium equations. Two further examples are given to show the effect of number of modes, included in a mode superposition analysis, on the accuracy of the solution.

8.5.1 Simply-supported square plate under uniform loading, varying sinusoidally with time

This example is chosen to show the accuracy and convergence rate of the present finite element models by comparing the results with the exact solution given in Ref. (32). The finite element meshes used for this example are shown in Figure (8.45) together with the loading condition. Using symmetry, only a quarter of the plate is analysed. From equation (3.81), it can be easily checked that under these conditions, asymmetric modes can not be excited and

therefore need not be included in the response calculations. The convergence of the centre deflection of the plate with mesh refinement is presented in Figures (8.46) and (8.47). The moment response M_x is plotted in Figures (8.48) and (8.49) for the (1 x 1) and (2 x 2) meshes respectively.

The results show that they converge rapidly towards the correct solution as the mesh is refined. It is also observed that mixed models have predicted more accurate results than the displacement models. This is despite the fact that mixed models involve fewer number of degrees of freedom than the displacement models.

Figure (8.50) shows the bending moment response M_x obtained by using the 8-noded quadrilateral elements of QR8 and QD8. The finite element idealisation using the QD8 element is (2 x 2) and has 44 degrees of freedom whereas the same mesh with QR8 element has only 12 degrees of freedom. It is seen that the results predicted with use of QR8 element are more accurate than those from QD8 element.

8.5.2 Simply supported square plate under point load, step force input

The purpose of this example is once again to show the accuracy and convergence of the predicted results when the structure is under the severe condition of point loading. The finite element grids used in this test together with the forcing function are shown in Figure (8.51). Due to symmetry only $\frac{1}{4}$ of the plate is analyzed.

The lateral deflection under the point of application of the load and bending moment M_x are plotted in Figures (8.52) to (8.57) together with the exact results.

From these figures, it is obvious that mixed models based on elements QR4 and QR8 have predicted the transient deflection and bending moment with good accuracy and that the solutions improve as the mesh is refined. Figures (8.54) and (8.57) show the results for deflection and bending moment respectively, obtained by using the displacement type elements of QD4 and QD8. Considering the fact that the number of degrees of freedom used in these models is almost three times that of corresponding mixed models, we can conclude that mixed type elements can be much more efficient than the corresponding displacement elements. For example, the results obtained from a (2×2) mesh of QR8 elements with 12 degrees of freedom are comparable with those obtained using the (2×2) mesh of QD8 elements having 44 degrees of freedom.

8.5.3 Clamped square plate under point load, step force input

In this example the performance of the mixed linear and quadratic elements (QR4 and QR8) are assessed by comparing with the results obtained from a (2×2) finite element idealisation based on the 8-noded displacement element with 28 degrees of freedom.[‡] The plate structure and the forcing function are shown in Figure (8.51). In figures (8.58) and (8.59) the central deflection and bending moment, M_x obtained from various meshes of QD4 element are presented. It is seen that results converge to those predicted from QD8 element, as the element sub-division increases. The same test has been carried out with finite element models using the mixed element QR4 and QR8. Figures (8.60) and (8.61) show the convergence of the mid-point deflection and bending moment for models using QR4 element.

‡ The accuracy of the solution obtained using this element has been demonstrated in sections (8.5.1) and (8.5.2) for the solution of simply supported plate.

The corresponding solutions based on QR8 element are presented in Figures (8.62) and (8.63). It is seen that mixed models can favourably predict the plate response and the solutions are comparable with those from displacement models.

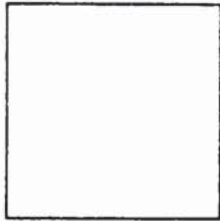
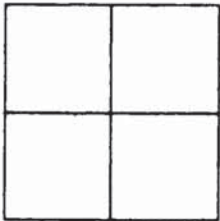
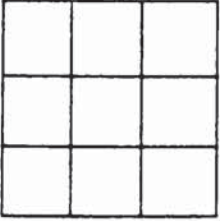
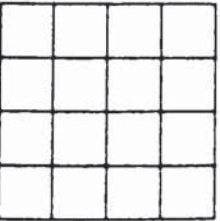
In the numerical tests reported in this section, several convergence plots were obtained indicating that in general, the appropriate order of convergence is obtained with mesh refinement. One important point should however be noted which is related to the computational time for the response calculations. Using the displacement type formulation, the bending moment response at a specific node is to be calculated at each increment of time through differentiating the pre-determined nodal displacements.

This procedure is repeated for all the elements sharing the specific node and the bending moment is determined by averaging the values from each element. This is a time-consuming process and consequently requires much more computational time than in the mixed models where nodal bending moments are calculated through a simple matrix transformation procedure. In table (8.7) the computational time spent at the response stage for various finite element models is indicated.

8.5.4 The effect of time step size, Δt on the numerical stability and accuracy of the solution

In the numerical tests presented in sections 8.5.1 to 8.5.3, integration of the equations of motion of the finite element assemblage was carried out using the Wilson θ method which is an unconditionally stable integration scheme. To test the stability and

Table 8.7 Computer execution time at the response analysis process by Wilson theta method. *

Finite Element Model	Element Type	Number Of Degrees Of Freedom	Time for response calculations(sec)
	QD4	1	240
	QR4	1	5
	QD8	5	600
	QR8	3	18
	QD4	8	300
	QR4	4	20
	QD8	28	840
	QR8	12	60
	QD4	21	420
	QR4	9	30
	QD4	40	660
	QR4	16	50

* Processed with HP 9845B desk top with enhanced processor.

accuracy of the solution as the time step size increases, two cases are studied. Figure (8.64) shows a square simply supported plate which is discretized by a (2 x 2) mesh of QR8 elements. The plate is subjected to either one of the two types of loading shown in Figure (8.64). The time step sizes used in the solutions are $\Delta t = .0001$, $\Delta t = .001$, $\Delta t = .005$ and $\Delta t = .01$.

Figures (8.65) to (8.68) show the deflection and bending moment responses of the SS plate under the two conditions of loading. It is interesting to notice that the accuracy of the solution is significantly reduced only for the largest time step size, that is for $\Delta t = .01$. For the other three time-step sizes, the solutions remain bounded and the accuracy of the results is acceptable. In particular, Figure (8.65) shows that the displacement response predicted by a time step size of $\Delta t = .001$ is more accurate than the one from $\Delta t = .0001$. This can be attributed to the fact that with $\Delta t = .0001$, the response will be affected by the contributions from higher, inaccurate modes of the finite element assemblage.

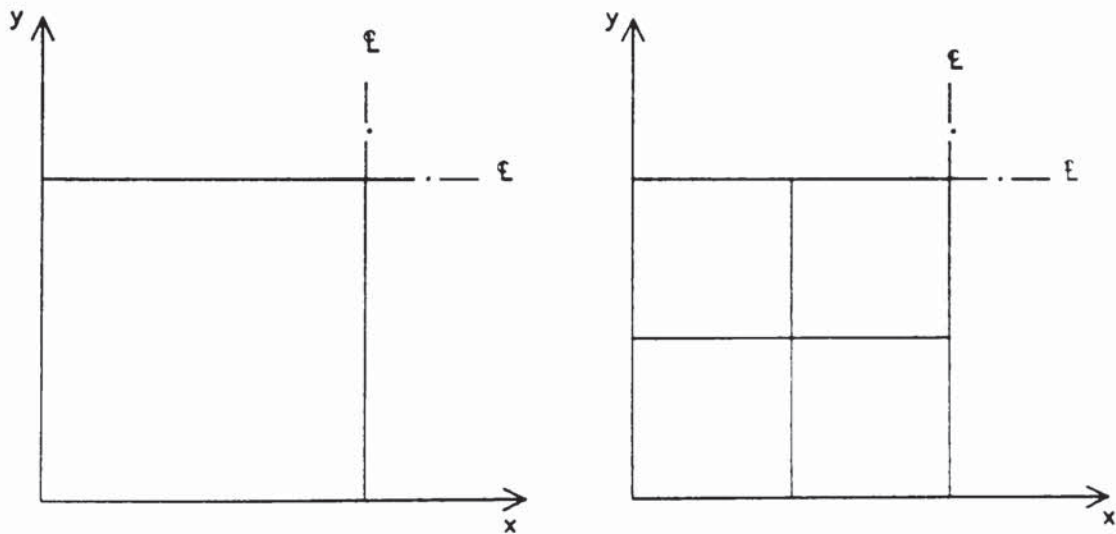
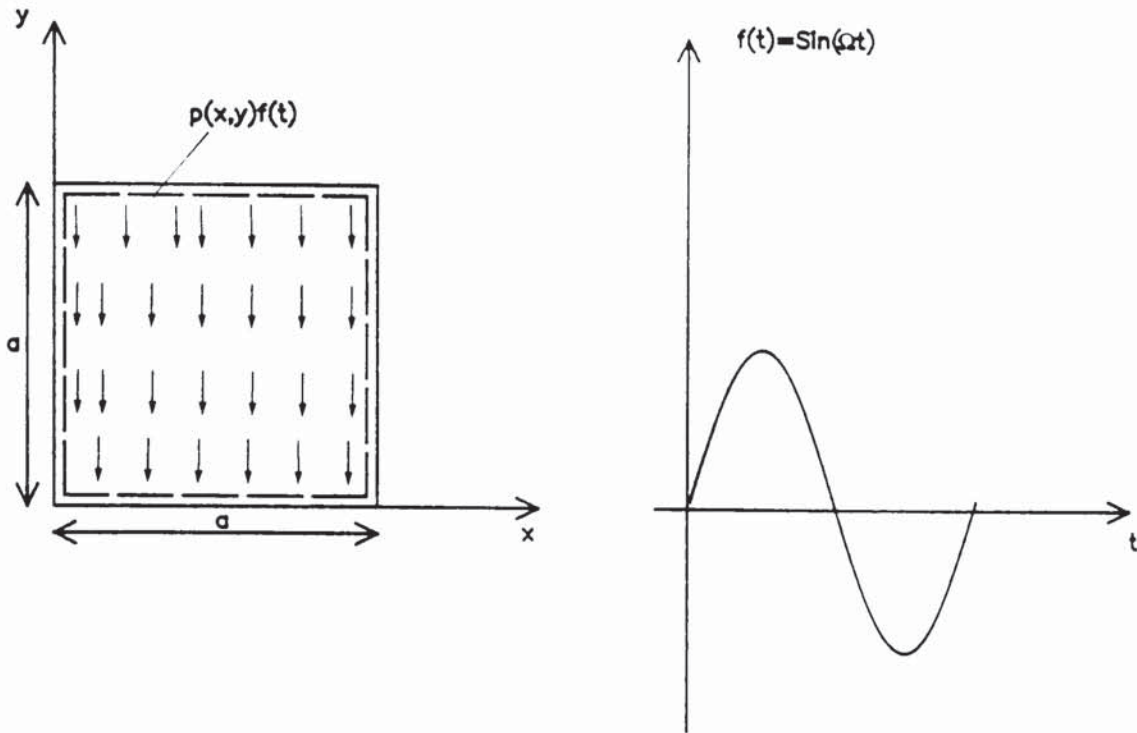
8.5.5 The effect of number of modes on the accuracy of the solution from mode-superposition method

The mode superposition procedure can in some practical problems be more efficient than a direct step by step integration method. To demonstrate this, the simply supported plate of the previous example under the impulsive load ($f(t) = 1 \quad .01 \leq t \leq .015$) is analyzed. The finite element model being used is once again a (2 x 2) mesh of QR8 elements.

Figures (8.69) to (8.71) show the deflection and bending

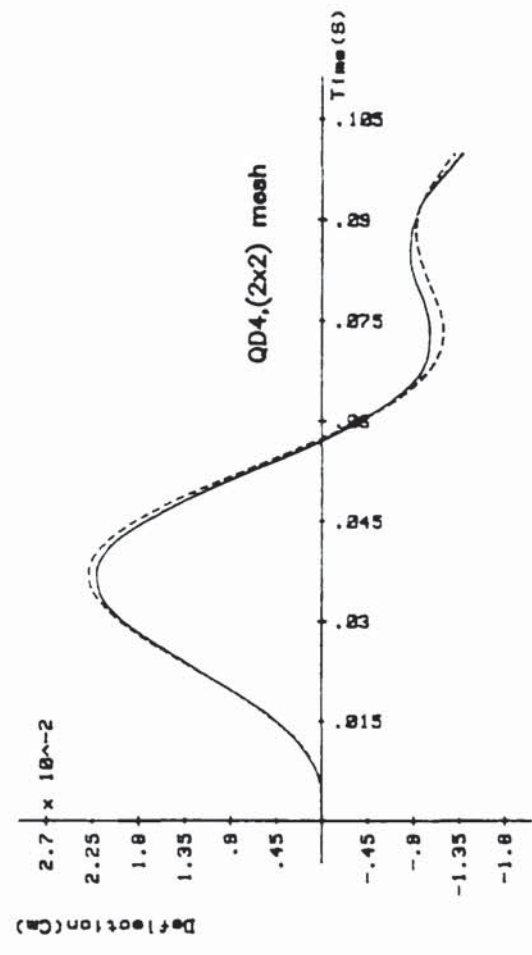
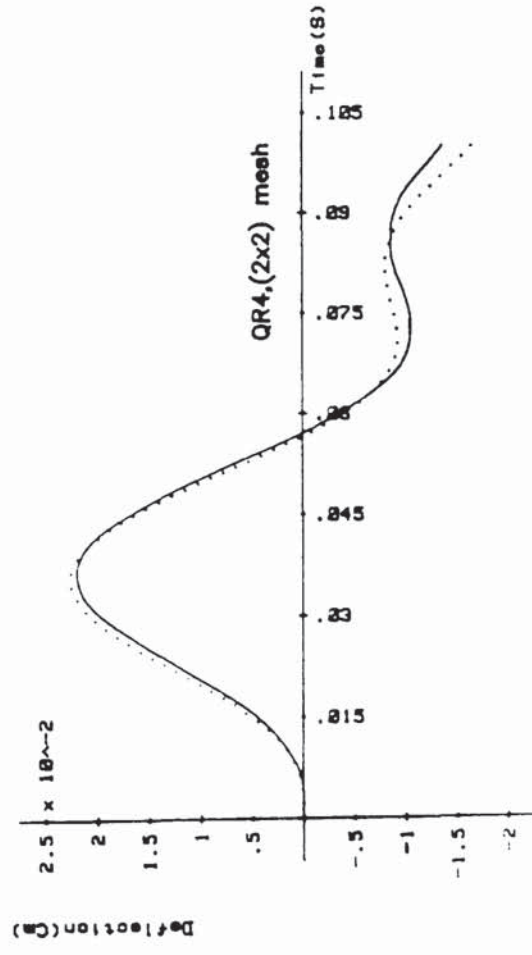
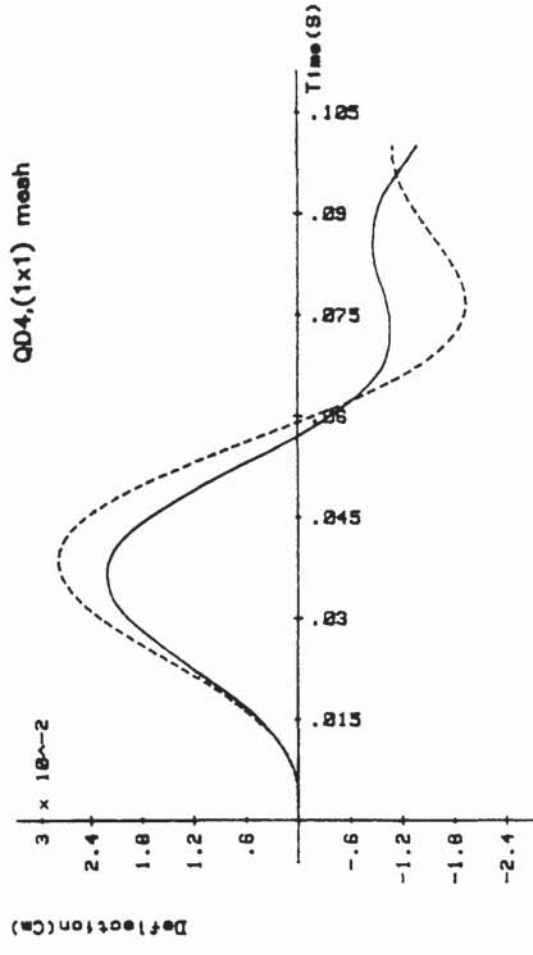
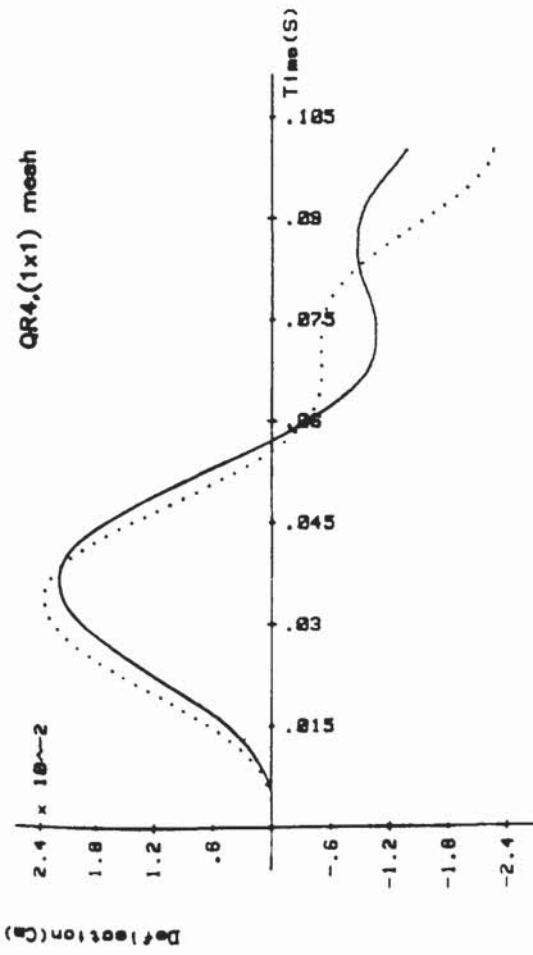
moment responses at the middle of the plate for different number of modes. The total number of modes present in the finite element assemblage is 12.

It is observed that the displacement obtained by using only 1 mode (Fig. 8.69a) is calculated with reasonable accuracy whereas the bending moment is not as good (Fig. 8.70a). On the other hand, the analysis with 3 modes has predicted excellent results for both displacement and bending moment (Figs. (8.69b), (8.70b)). Figures (8.71a) and (8.71b) show the displacement and bending moment responses, respectively, obtained by using the total number of modes in the analysis. It is observed that the solution obtained by using 3-modes compares favourably with the 12-mode solution and no particular accuracy has been gained by increasing the number of modes in the analysis.



$\nu = .3$ $E = 2.07 \times 10^7 \text{ N/Cm}^2$
 $h = 1 \text{ Cm}$ $\rho = 7.8 \times 10^{-3} \text{ Kg/Cm}^3$
 $a = 50 \text{ Cm}$ $\Omega = 50 \text{ Hz}$
 $p(x,y) = 1 \text{ N/Cm}^2$

Fig 8.45 Finite element meshes used for the analysis of a thin simply supported plate under steady state loading.



Exact
 Displacement
 Mixed model

Fig 8.46 Deflection W , vs time; t at the centre of a simply supported plate under uniform loading varying sinusoidally with time.

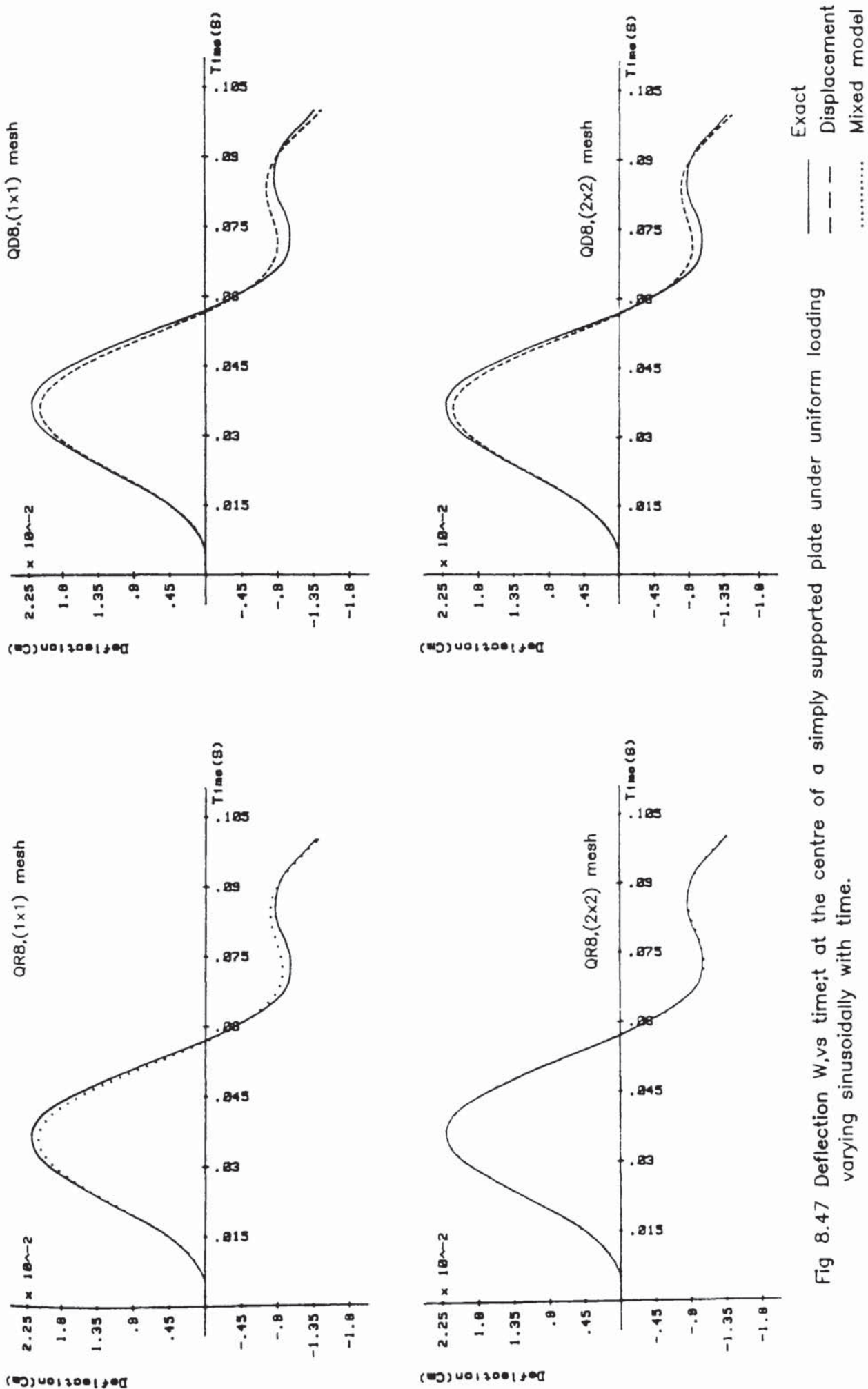


Fig 8.47 Deflection W , vs time; t at the centre of a simply supported plate under uniform loading varying sinusoidally with time.

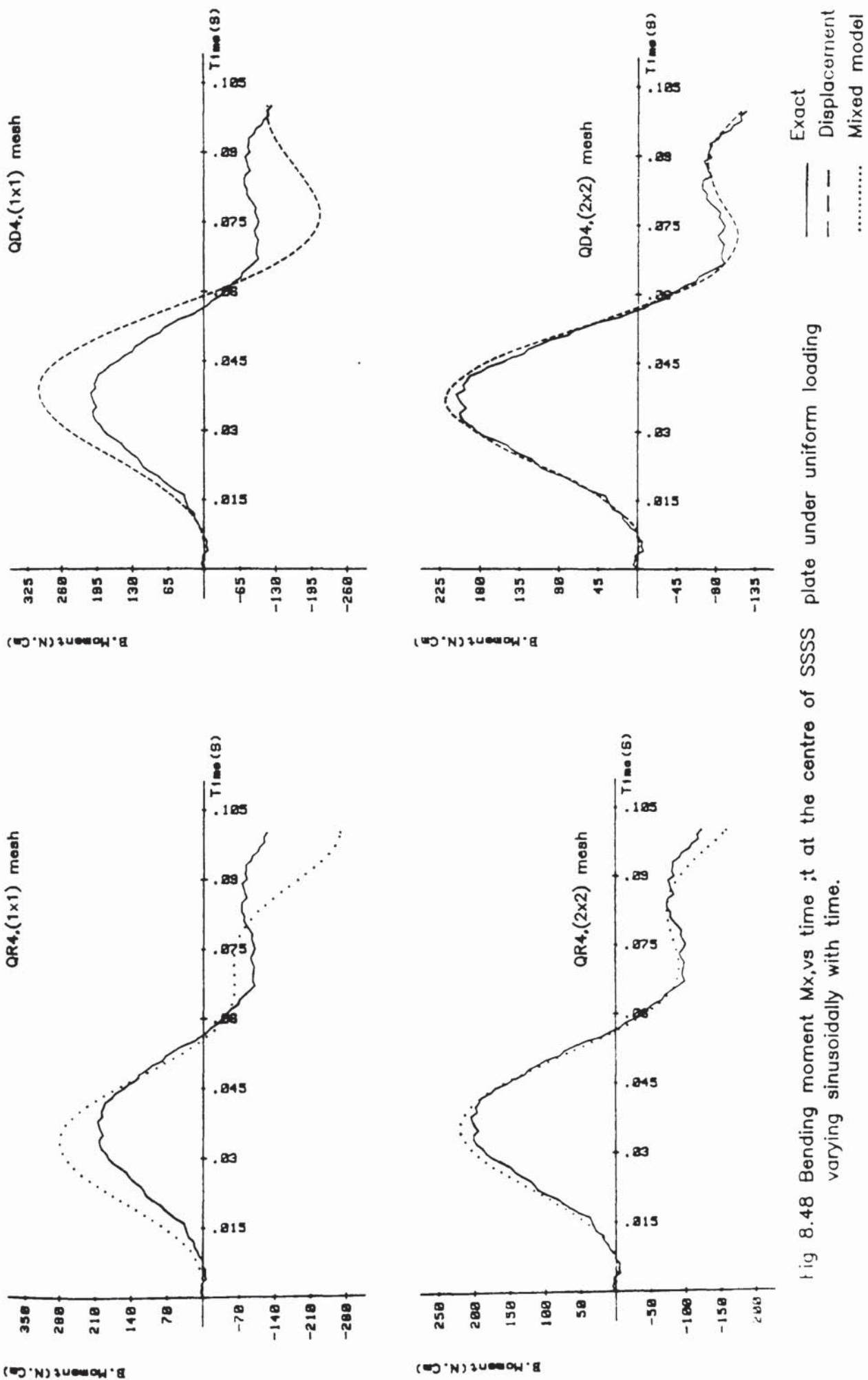
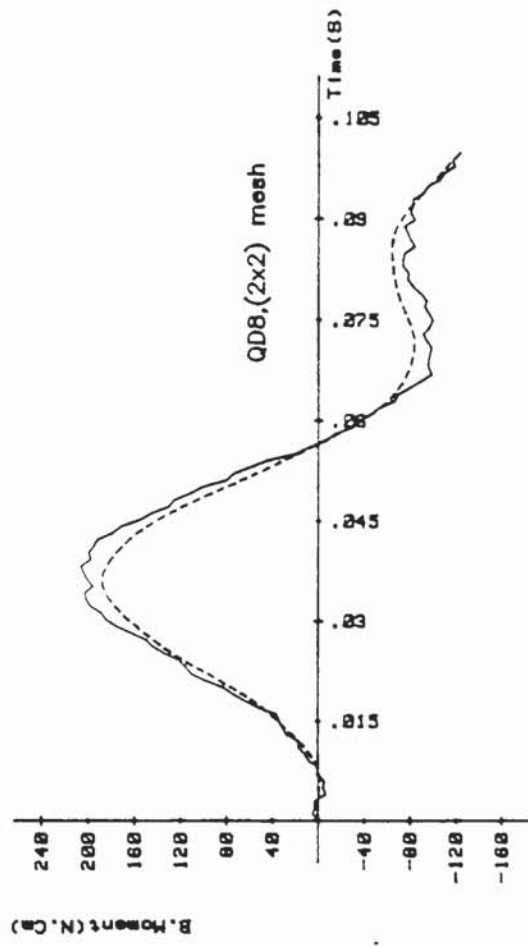
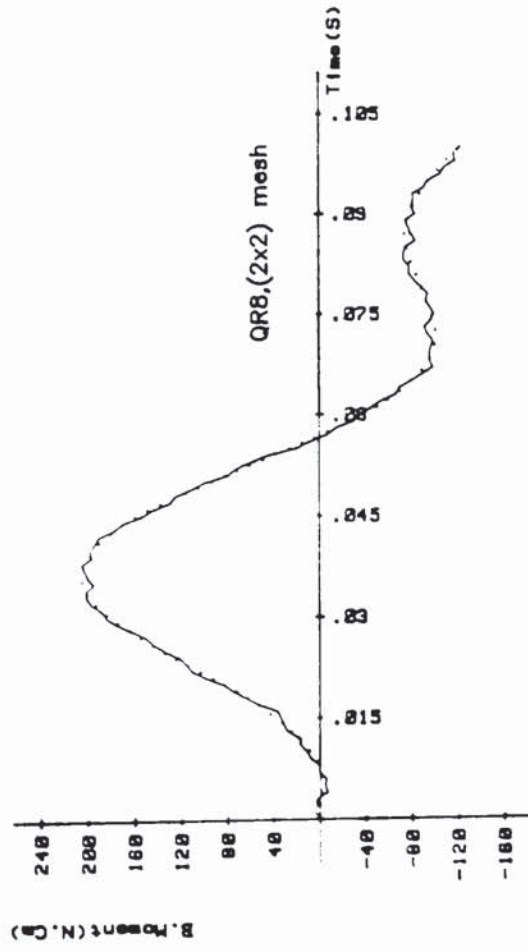
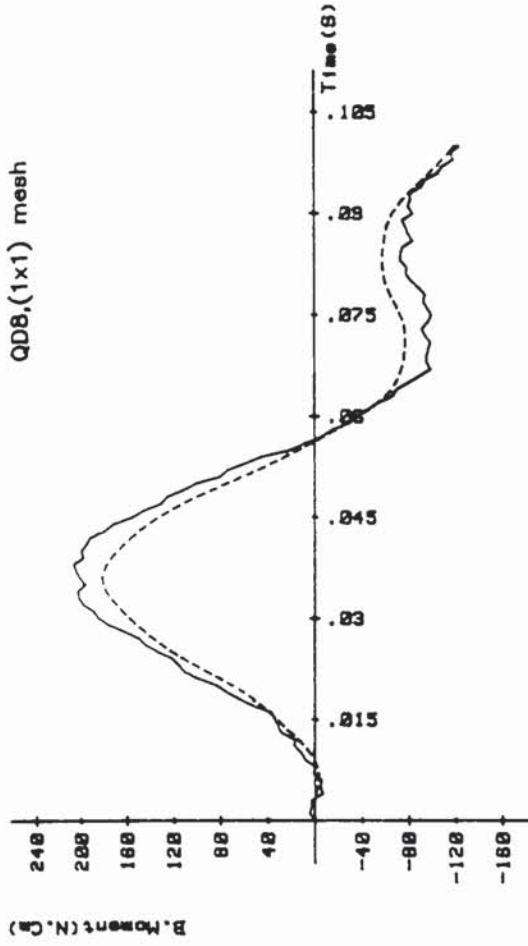
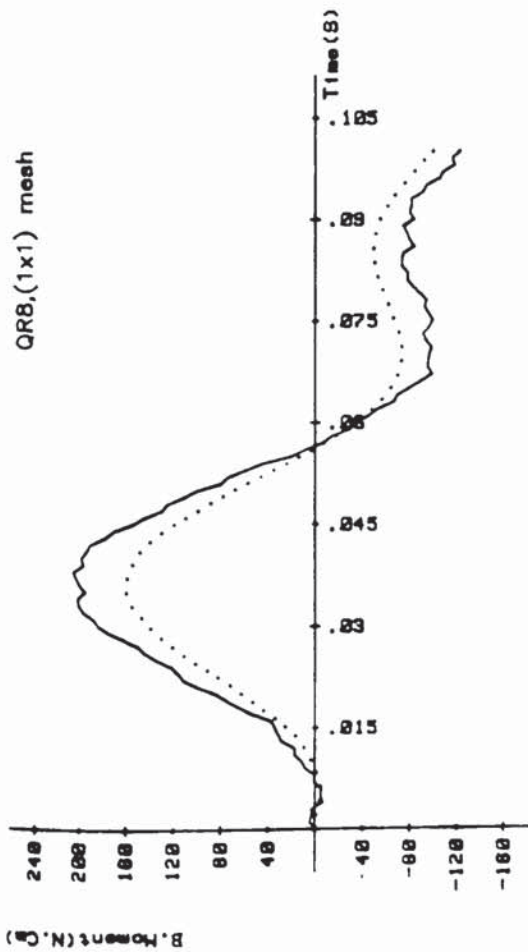


Fig 8.48 Bending moment M_x vs time t at the centre of SSSS plate under uniform loading varying sinusoidally with time.



Exact
 Displacement
 Mixed model

Fig 8.49 Bending moment M_x vs time t at the centre of SSSS plate under uniform loading varying sinusoidally with time.

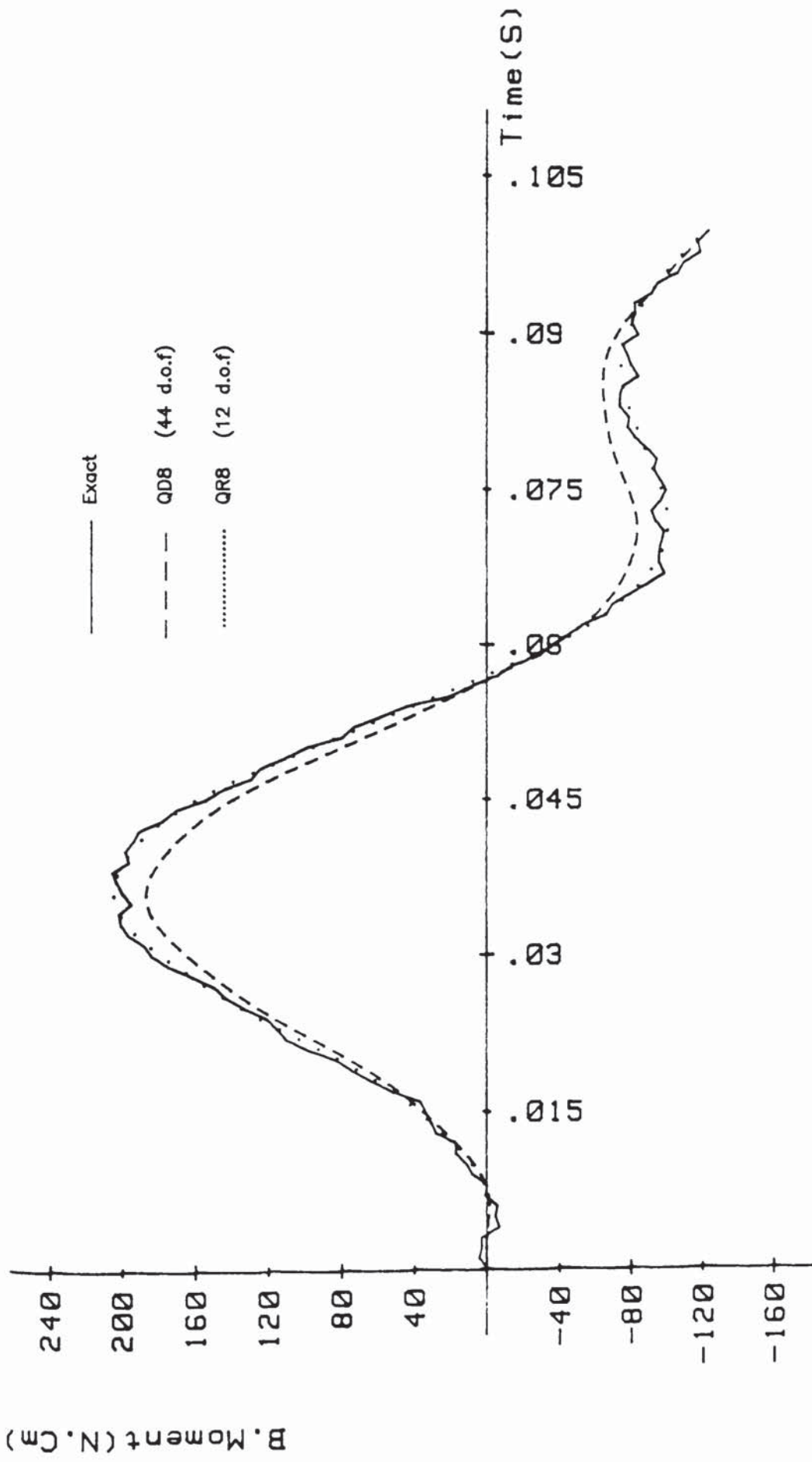


Fig 8.50 Bending moment M_x , vs time, at the centre of SSSS plate.
Uniform loading, varying sinusoidally with time.

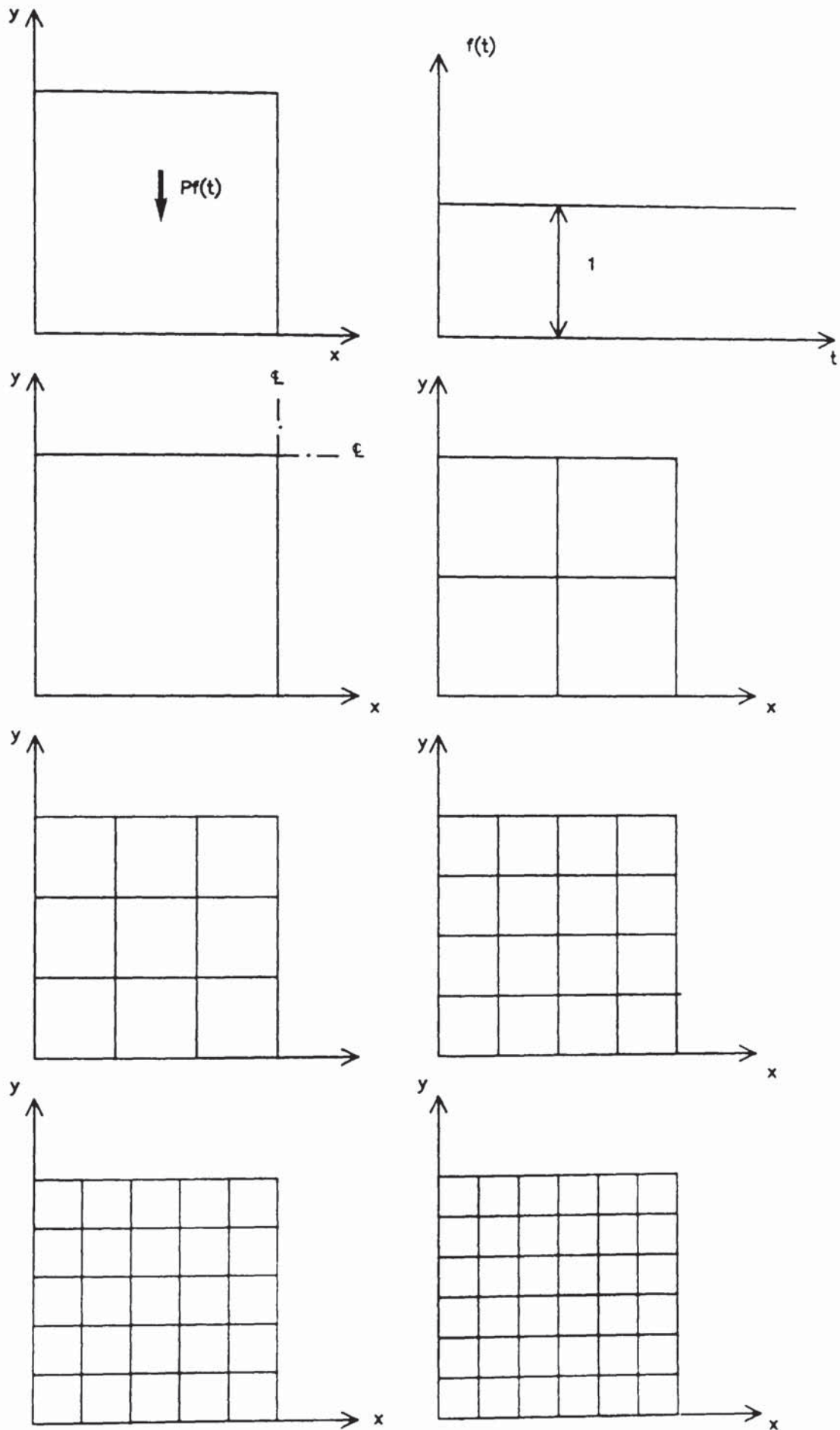


Fig 8.51 Finite element meshes used for the analysis of a square plate under transient point loading.

$a=120\text{Cm}, h=1\text{Cm}, P=100\text{N}$

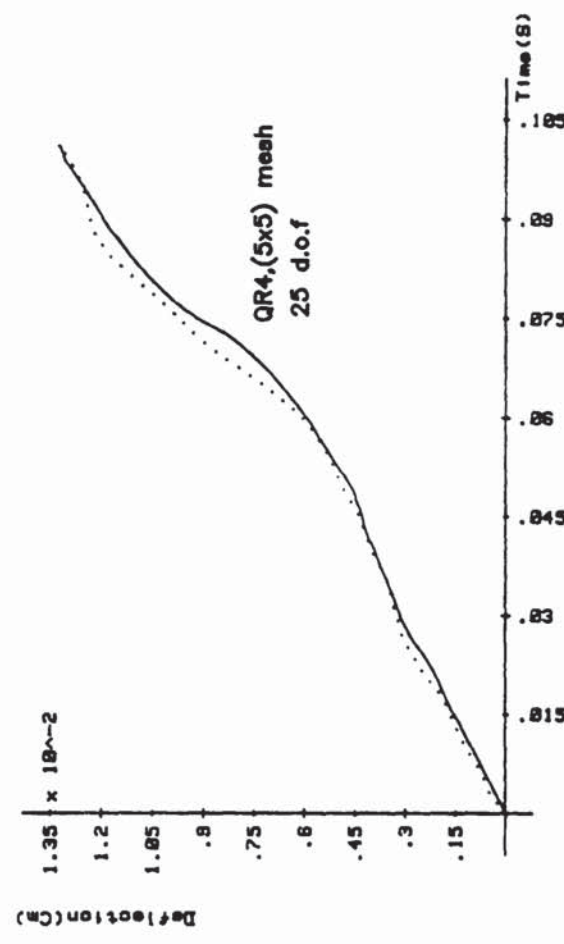
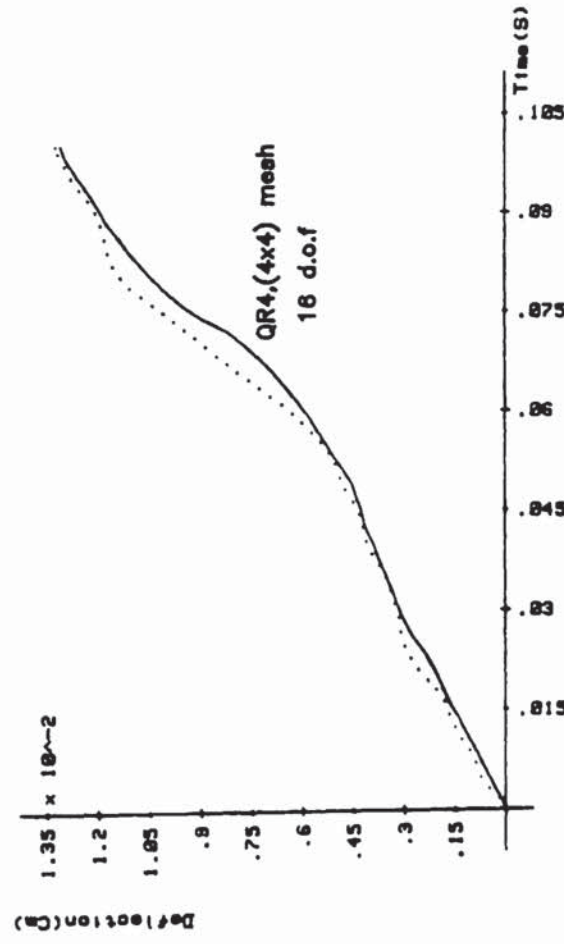
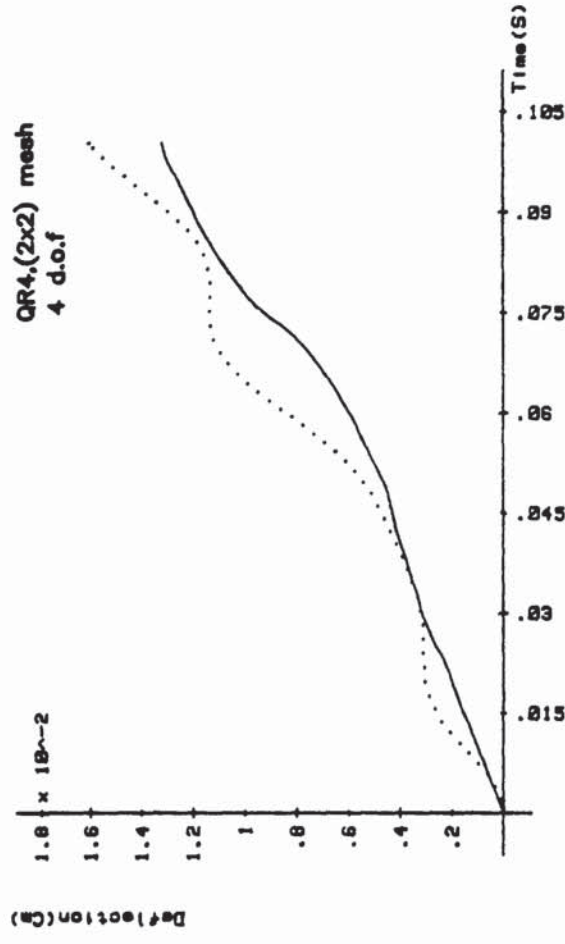
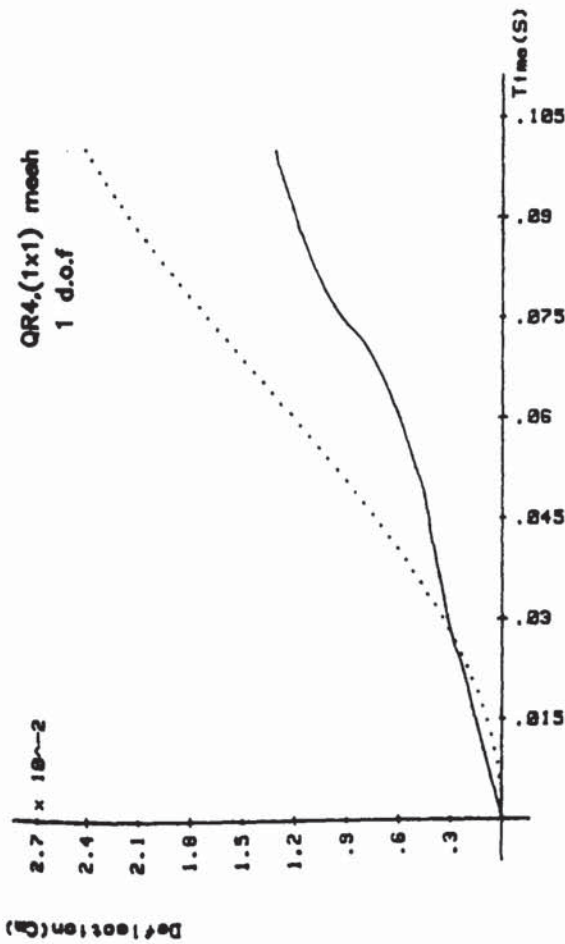


Fig 8.52 Deflection W , vs time t at the centre of SSSS plate under transient point load. (QR4 element)

— Exact
..... Mixed model

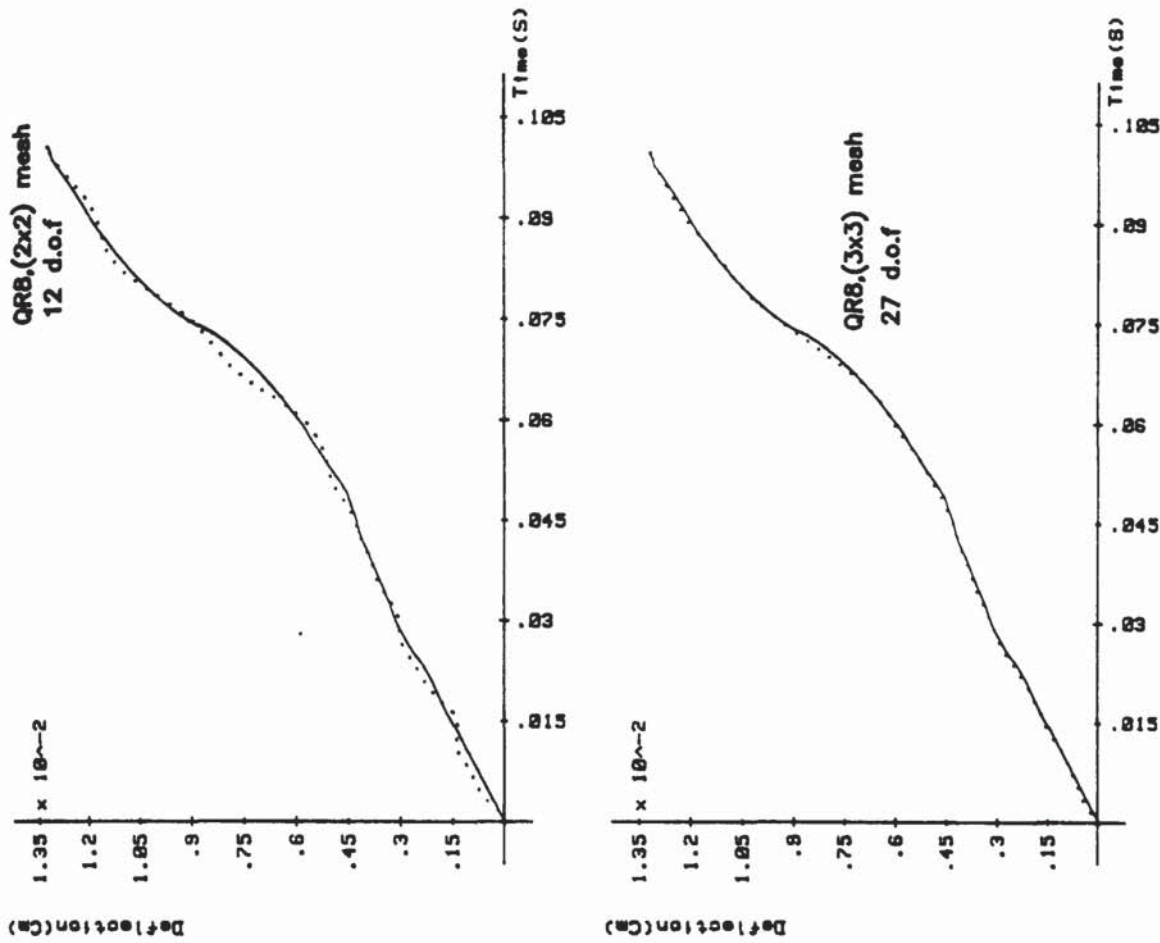


Fig 8.53 Deflection W, vs time ; t at the centre of SSSS plate under transient point load. (QR8 element)

— Exact
 Mixed model

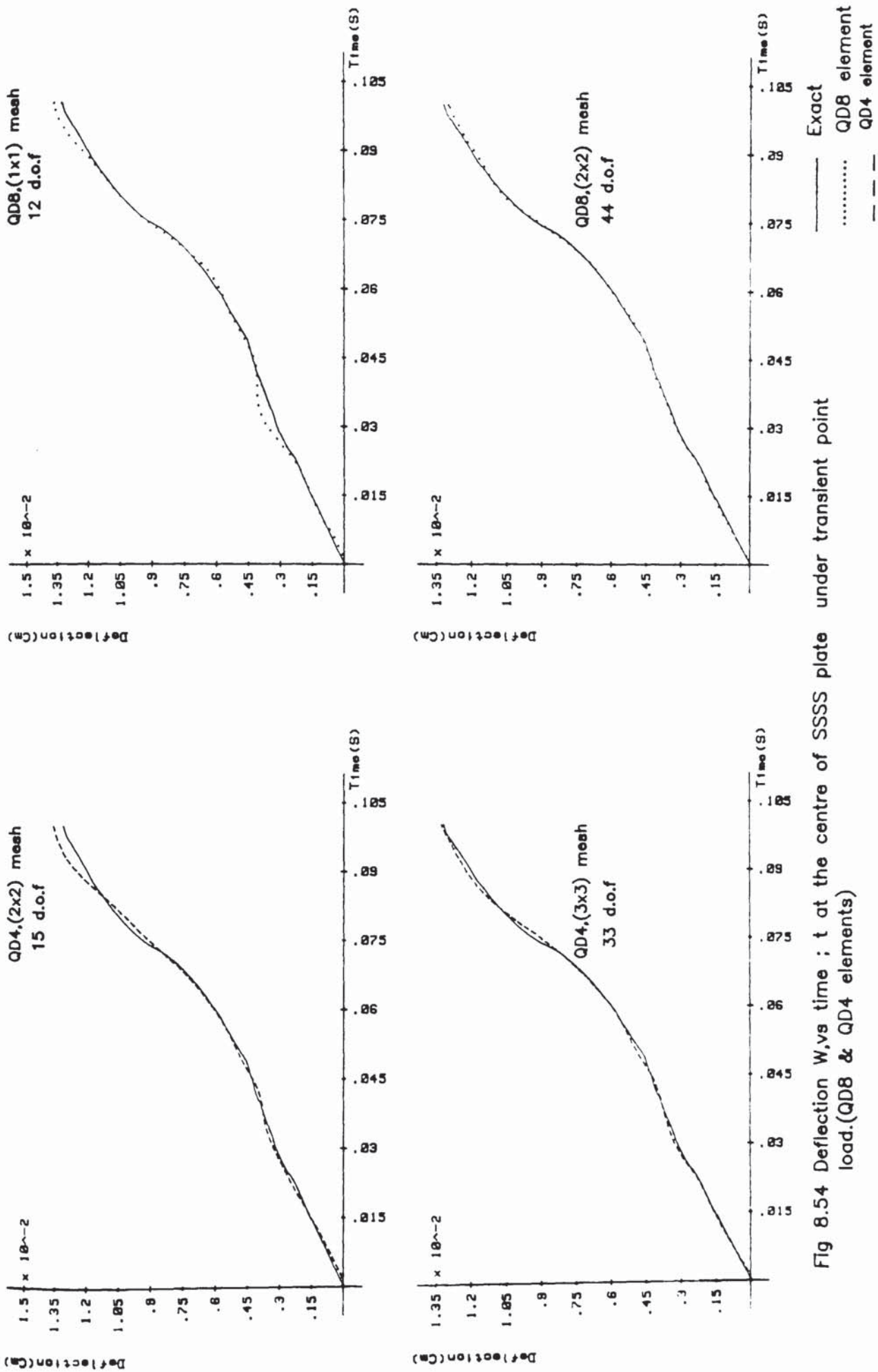


Fig 8.54 Deflection W , vs time t at the centre of SSSS plate under transient point load, (QD8 & QD4 elements)

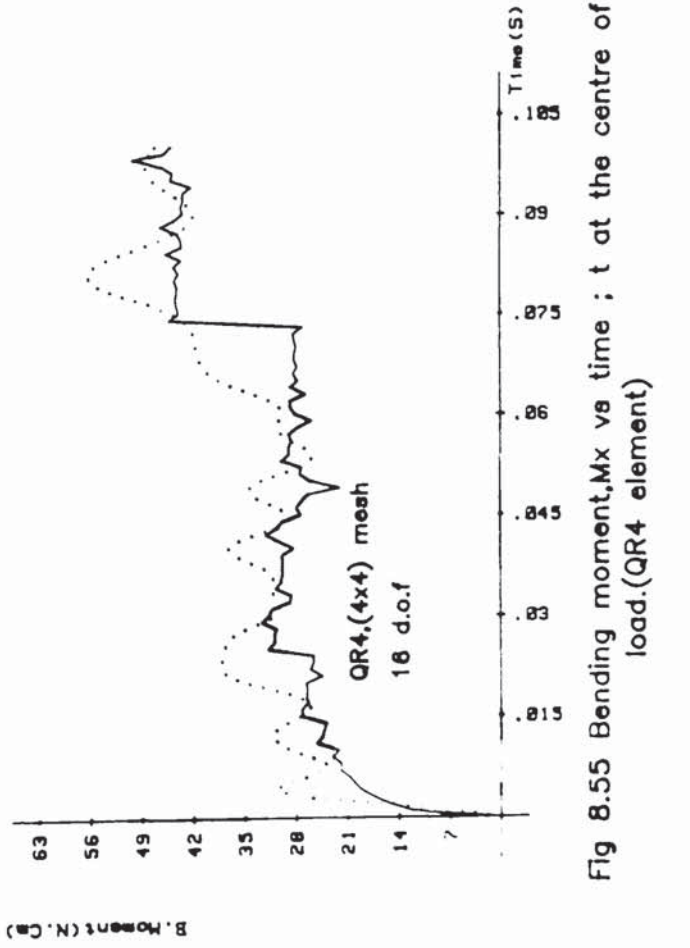
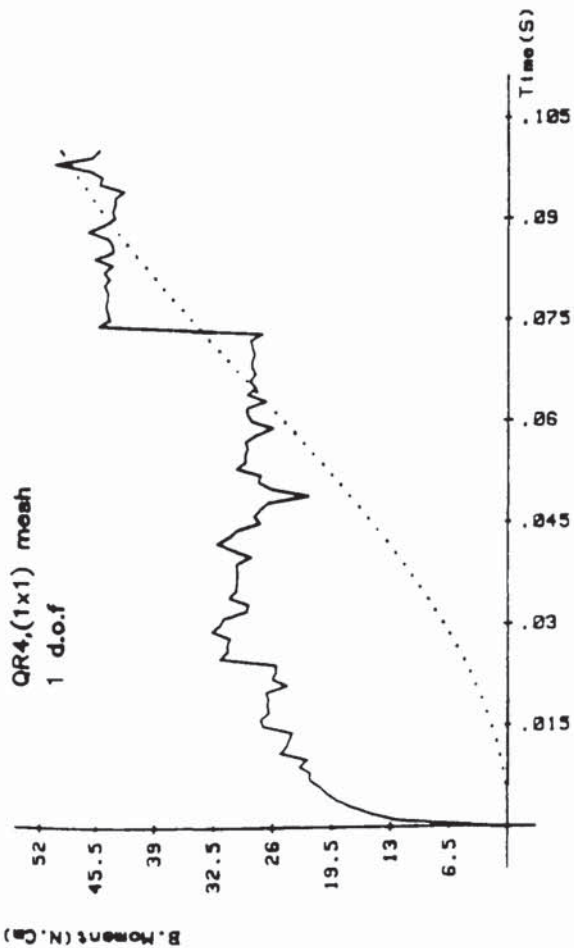
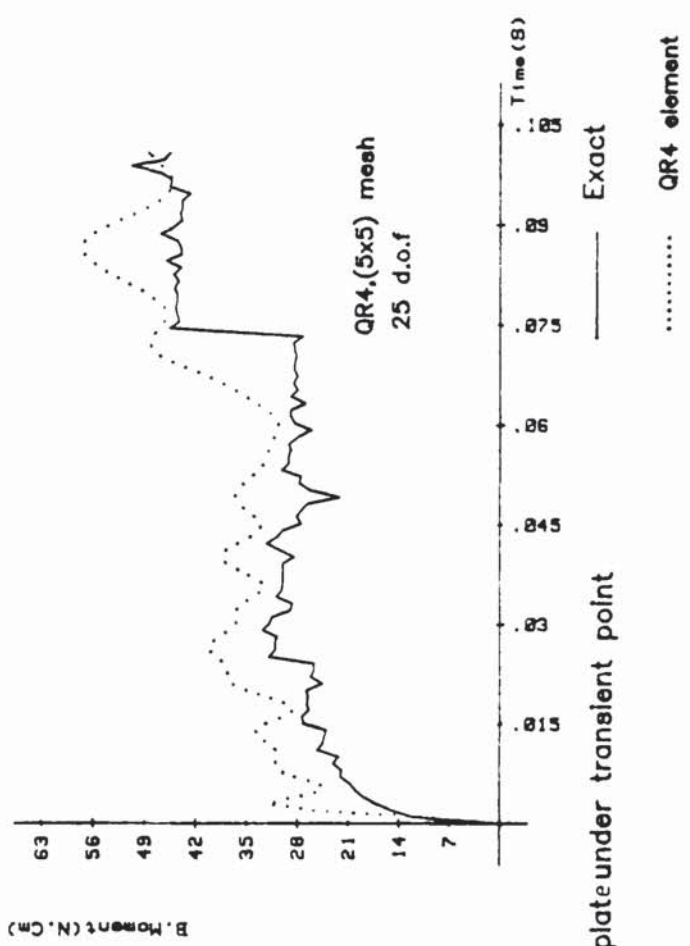
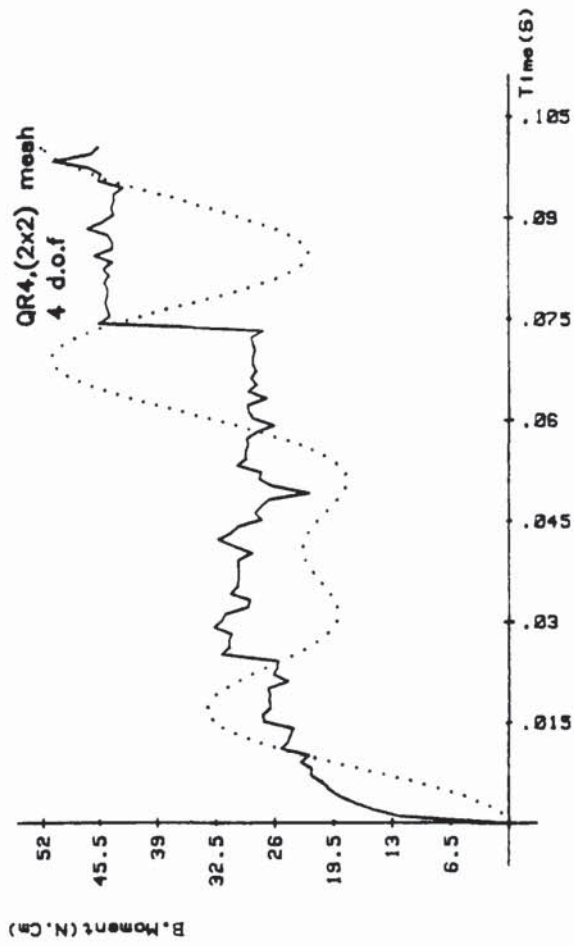


Fig 8.55 Bending moment, M_x vs time ; t at the centre of SSSS plate under transient point load. (QR4 element)

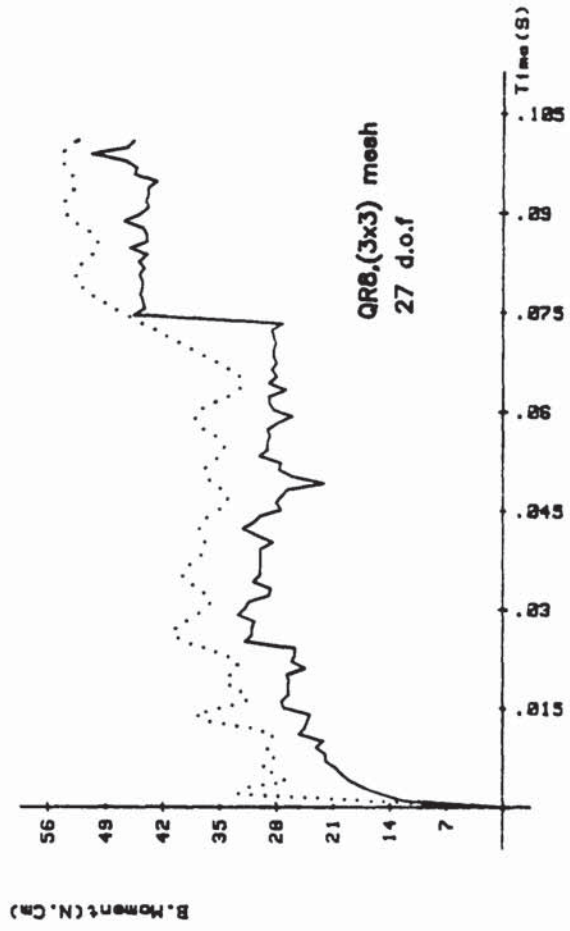
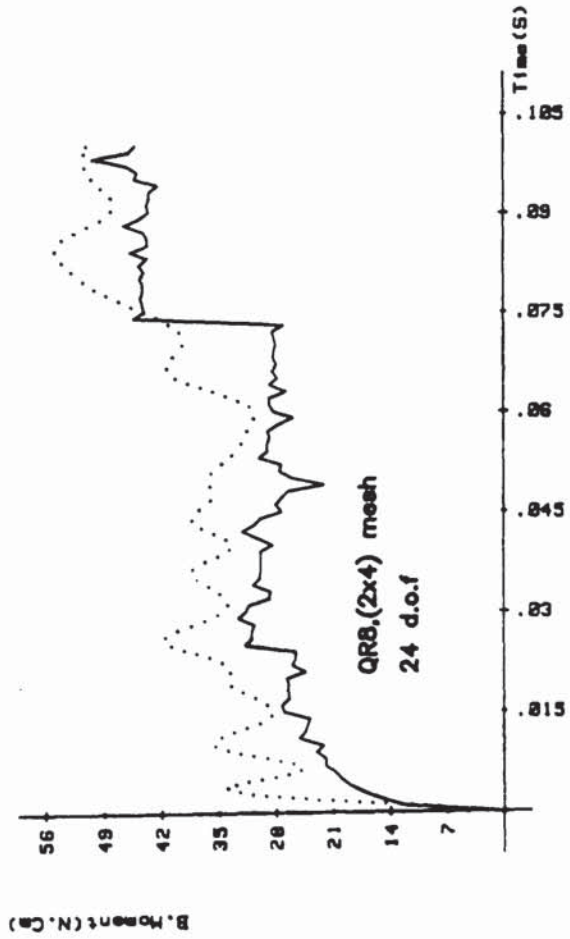
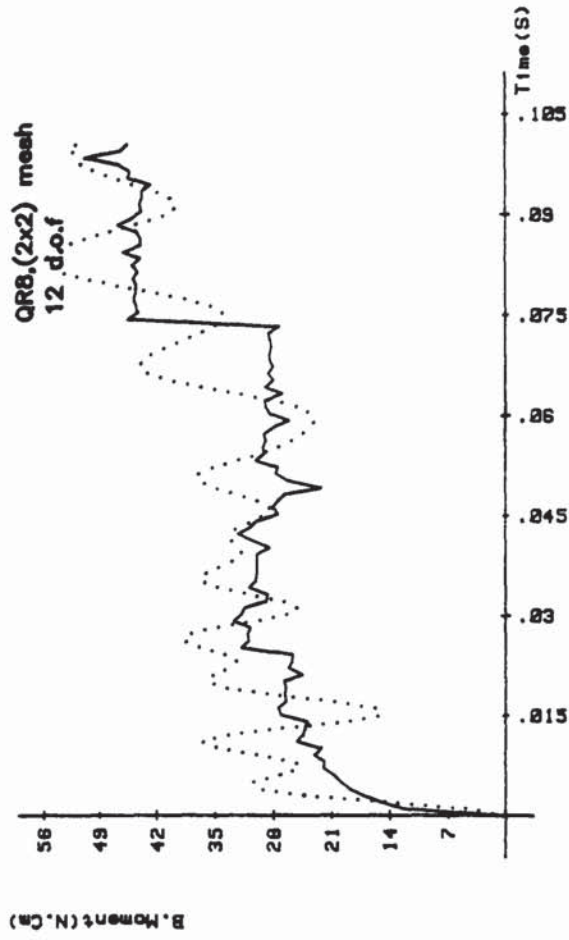
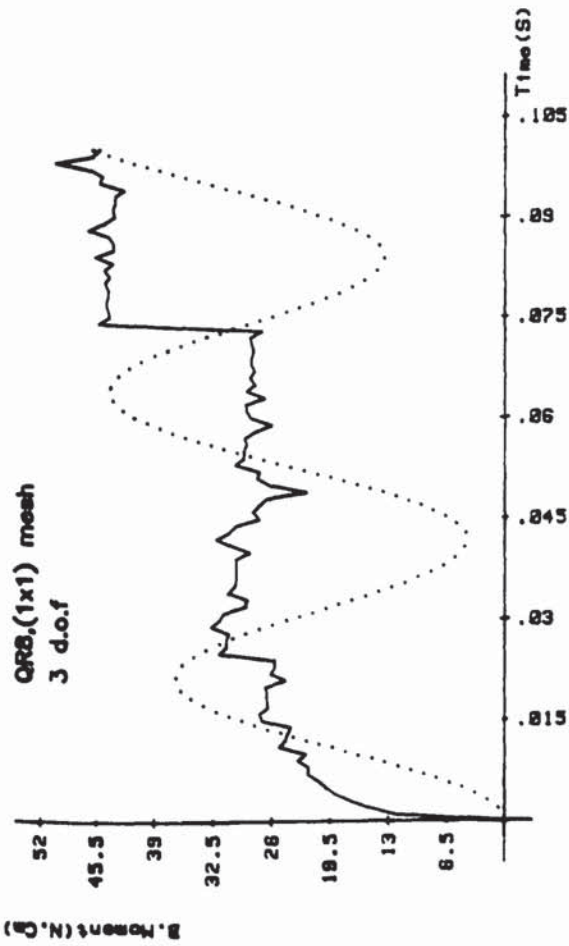


Fig 8.56 Bending moment, M_x vs time ; t at the centre of SSSS plate under transient point load. (QR8 element)

Exact

..... QR8 element

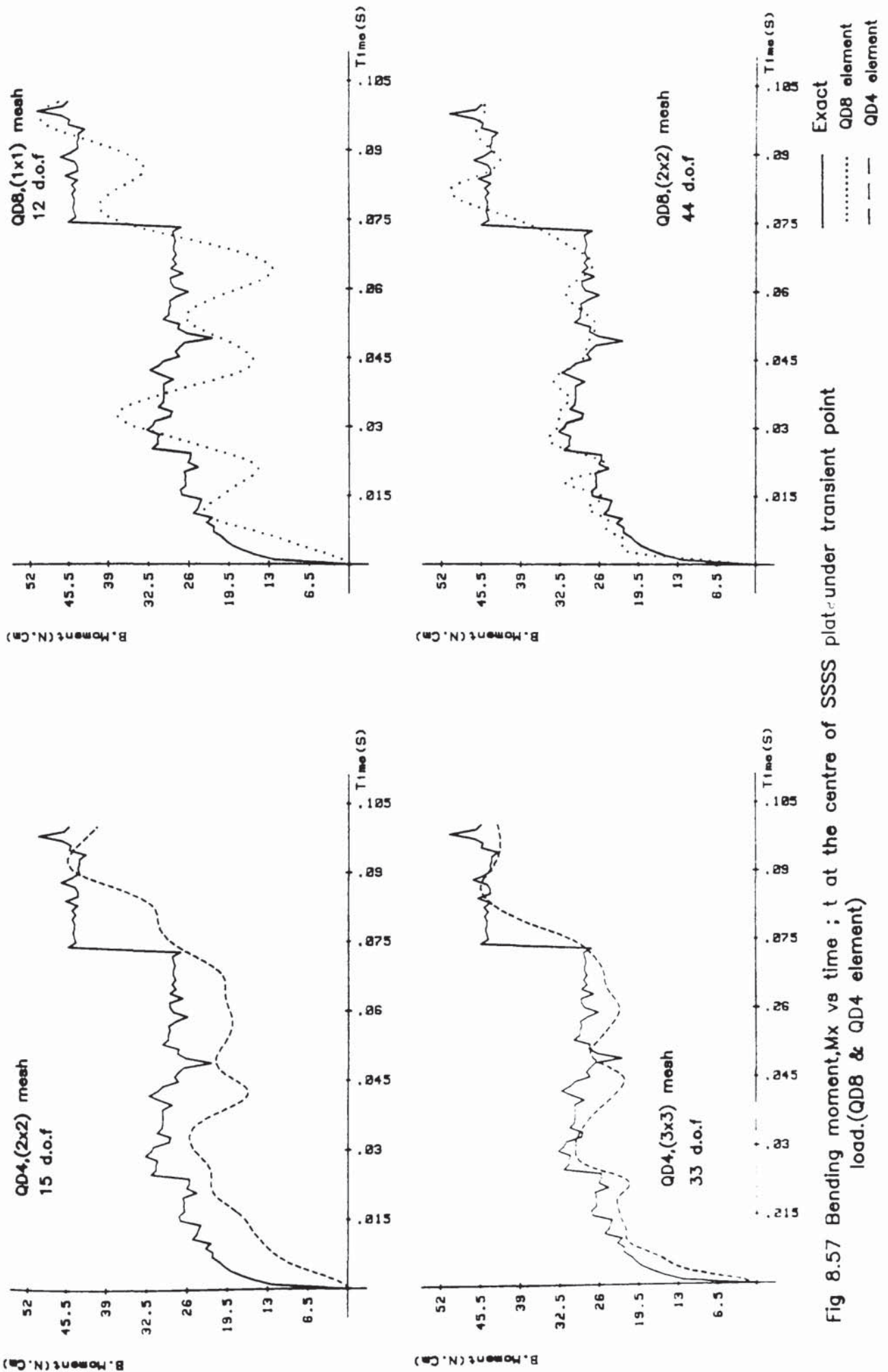


Fig 8.57 Bending moment, M_x vs time ; t at the centre of SSSS plate under transient point load. (QD8 & QD4 element)

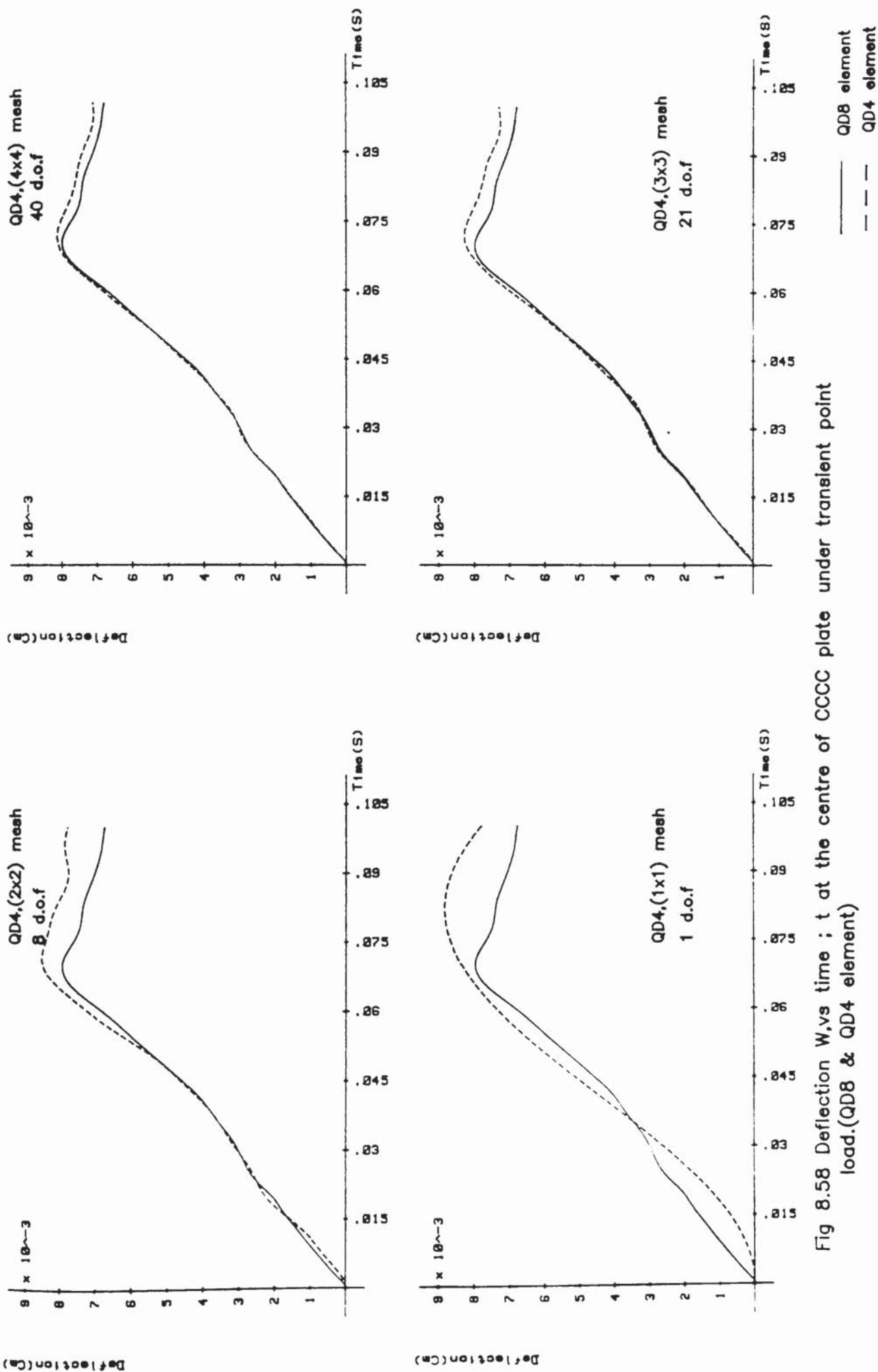
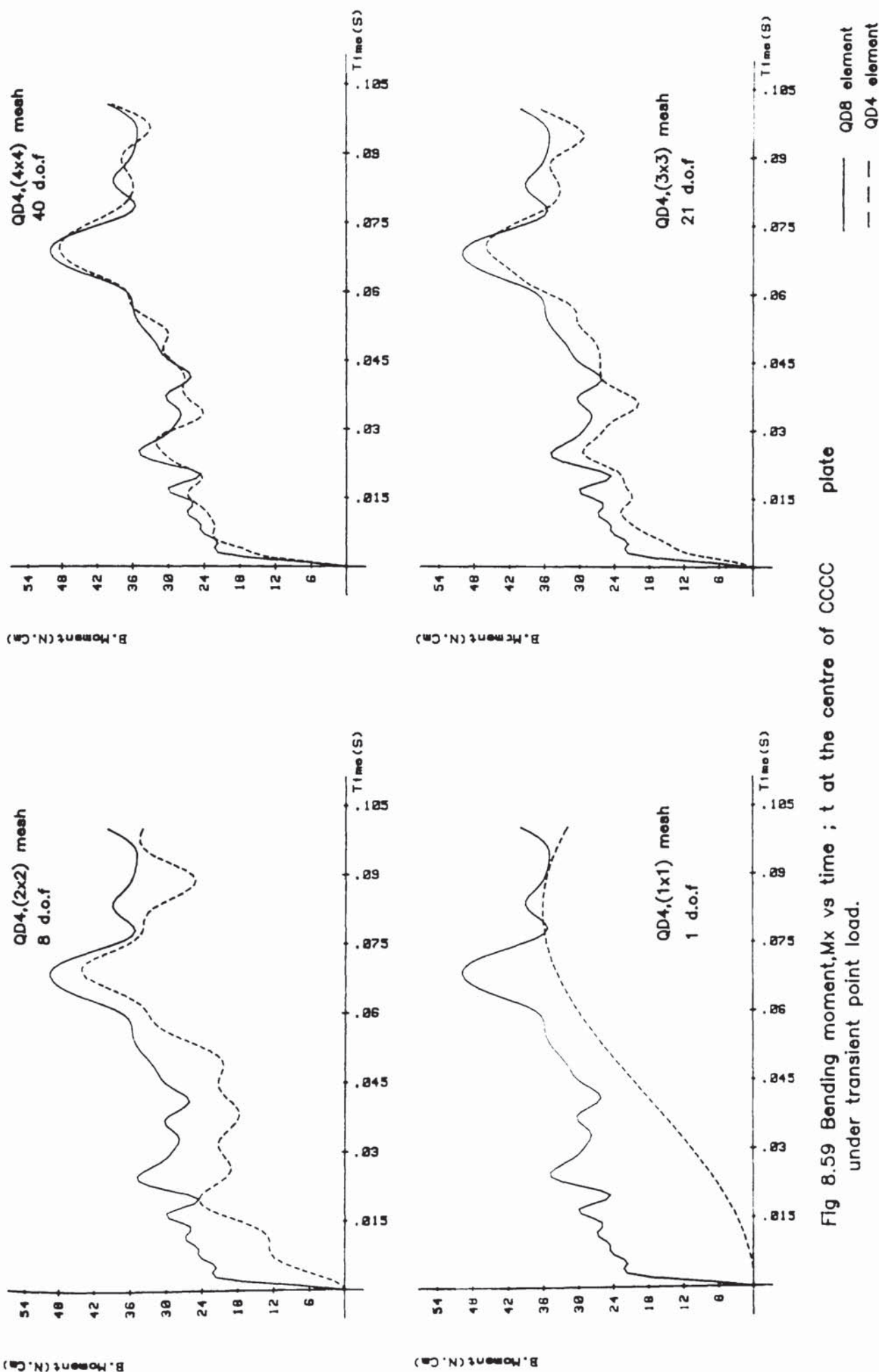


Fig 8.58 Deflection W, vs time ; t at the centre of CCCC plate under transient point load. (QD8 & QD4 element)



plate

Fig 8.59 Bending moment, M_x vs time ; t at the centre of CCCC under transient point load.

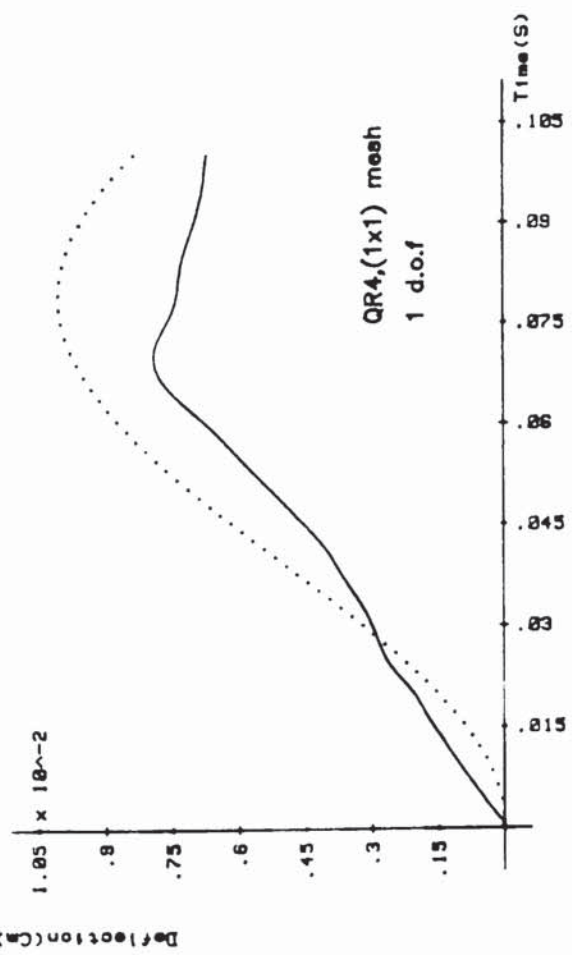
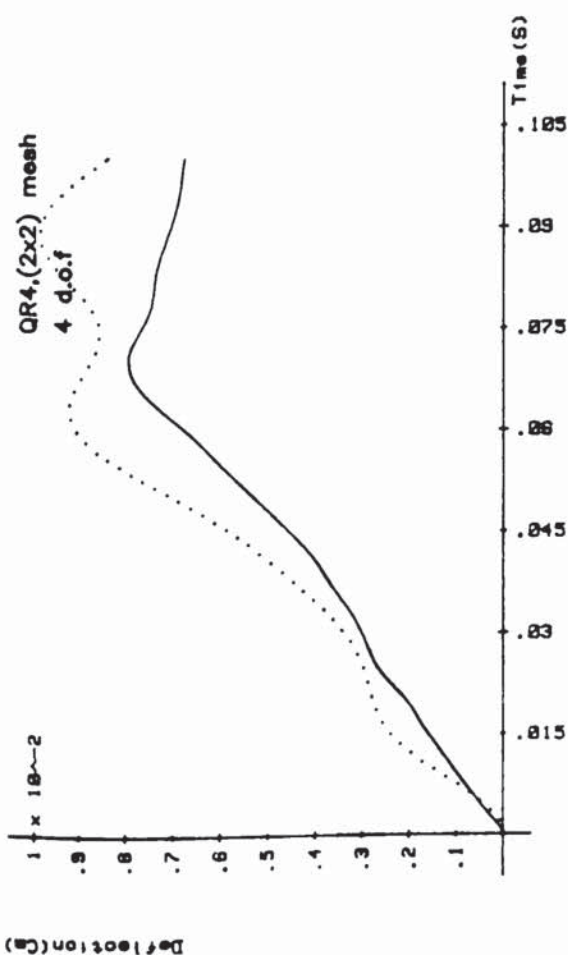
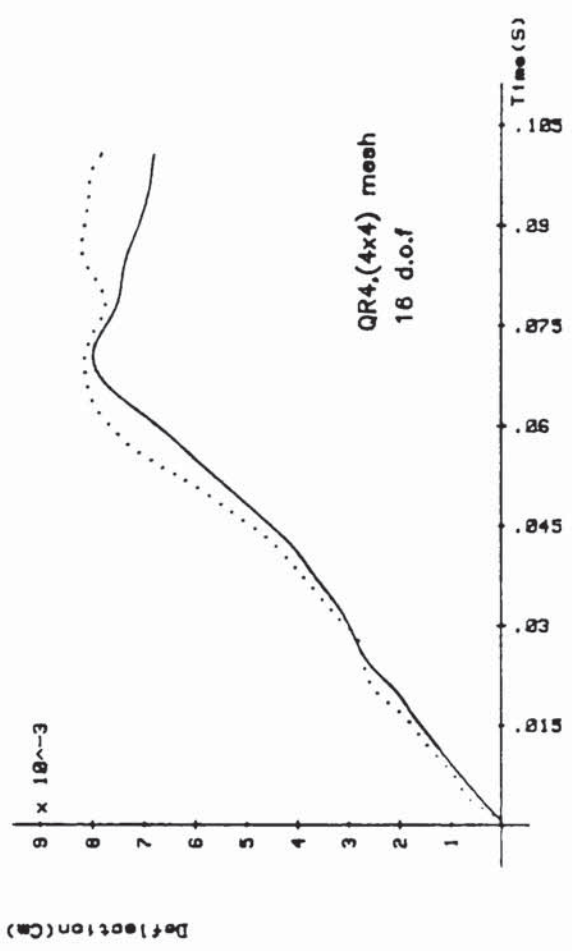
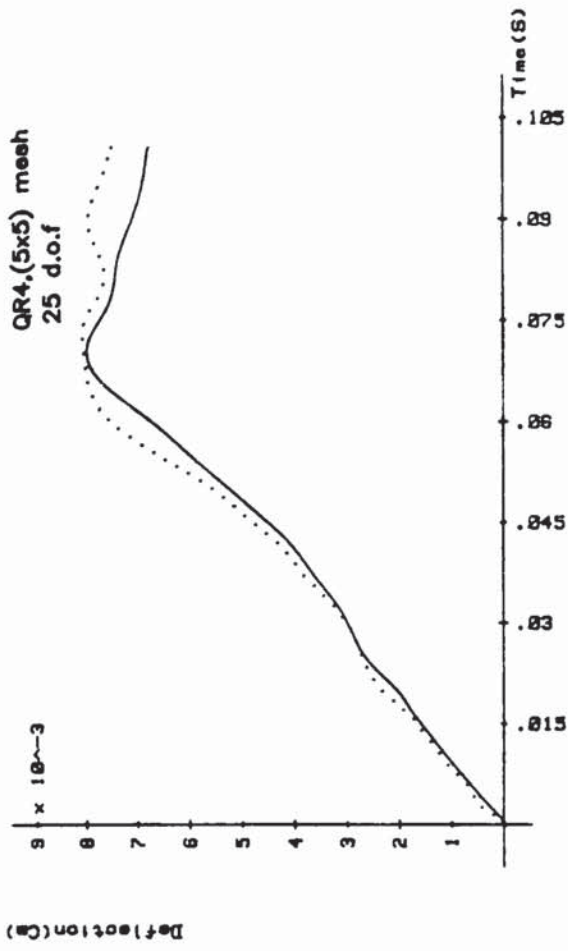


Fig 8.60 Deflection W , vs time : t at the centre of CCCC plate under transient point load

— QD8 element
..... QR4 element

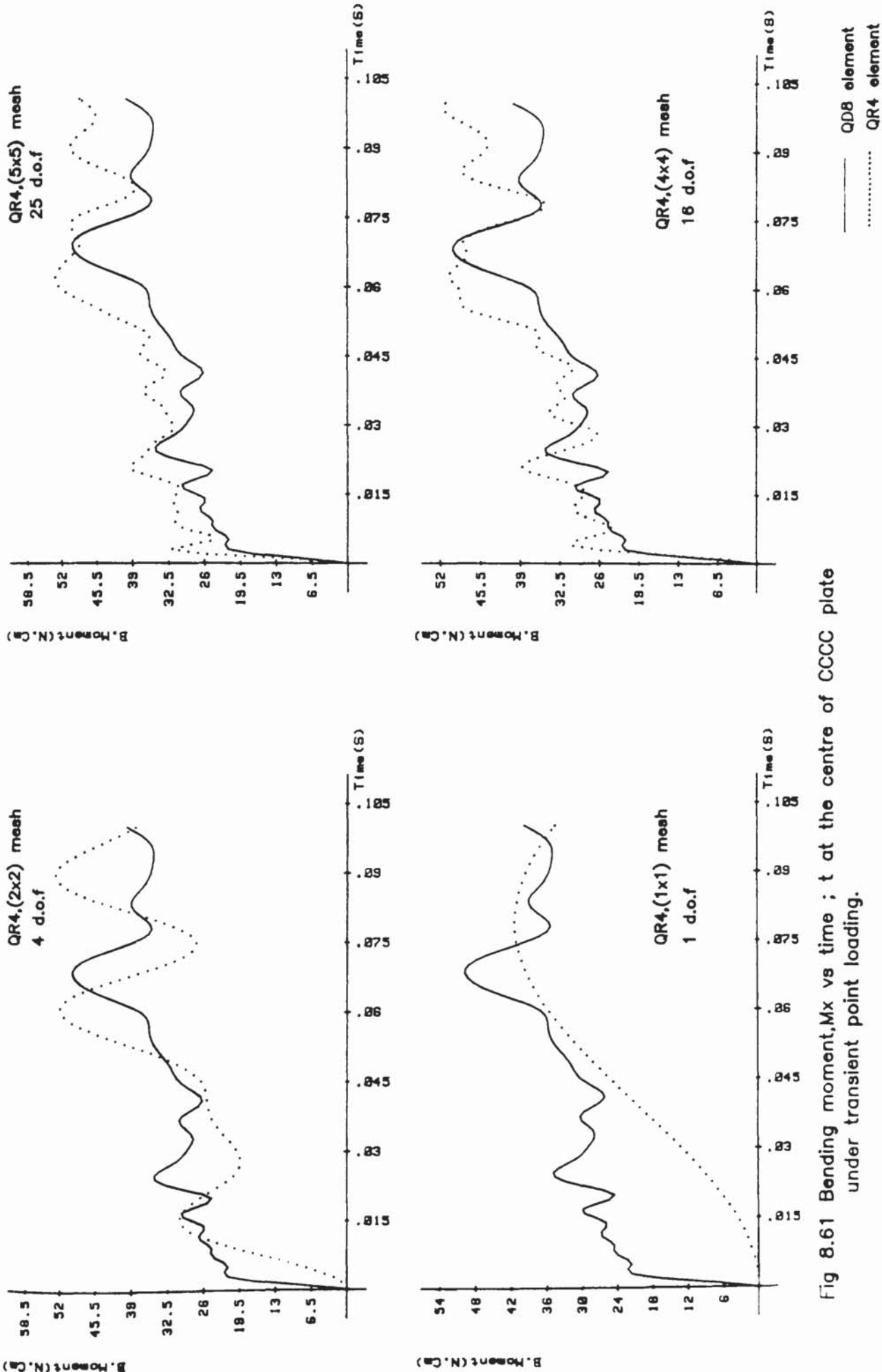


Fig 8.61 Bending moment, M_x vs time ; t at the centre of CCCC plate under transient point loading.

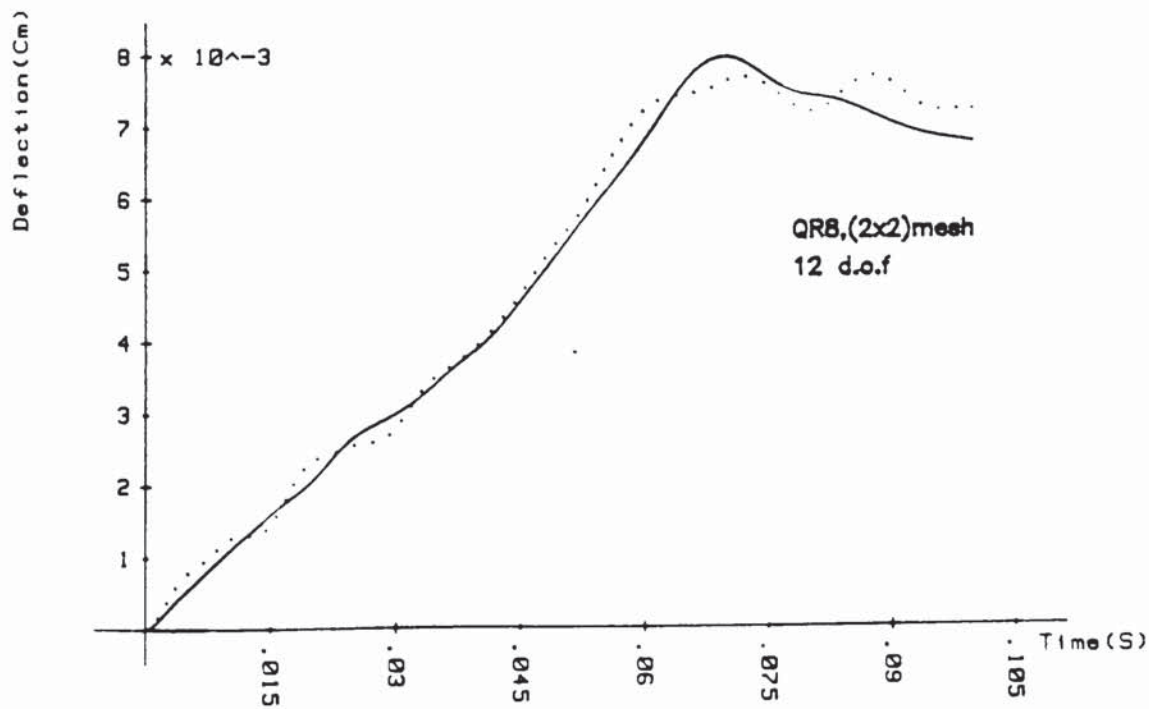
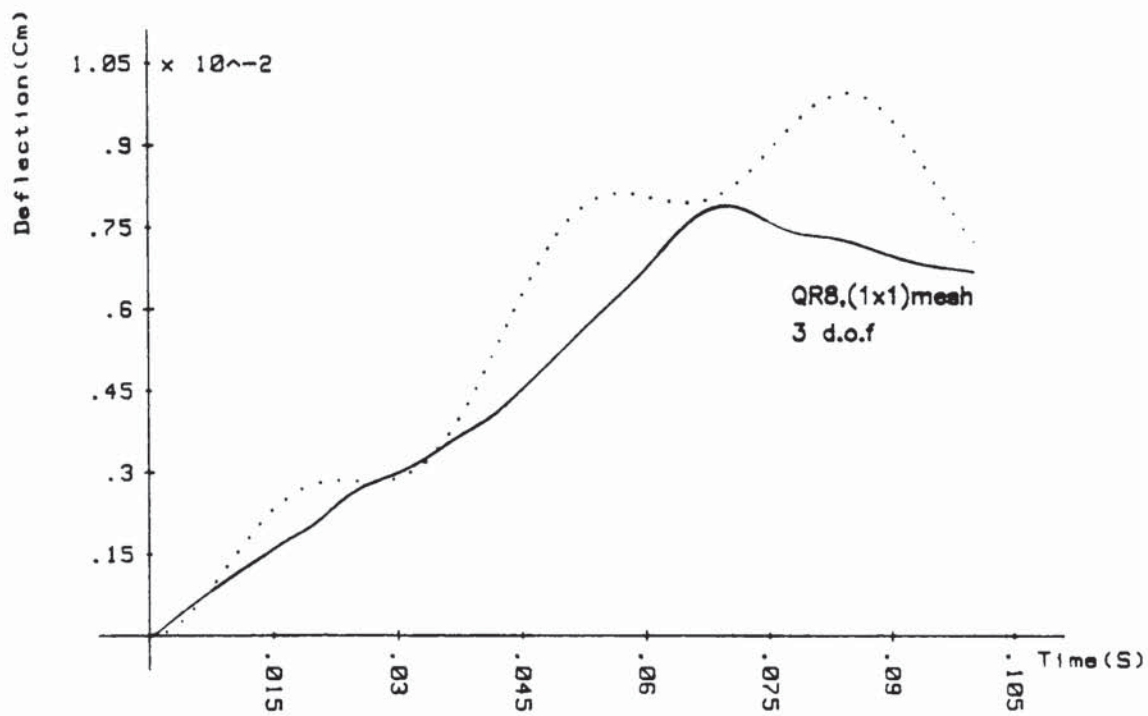


Fig 8.62 Deflection W vs time; t at the centre of clamped plate under transient point load.

———— QD8 element
 QR8 element

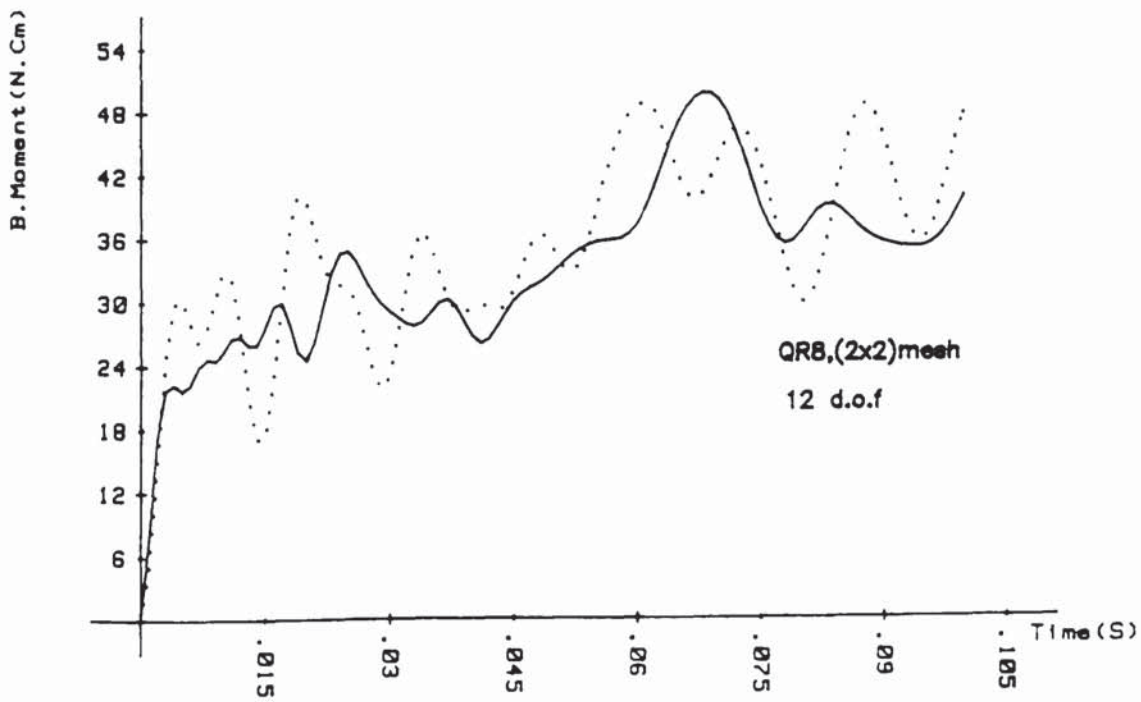
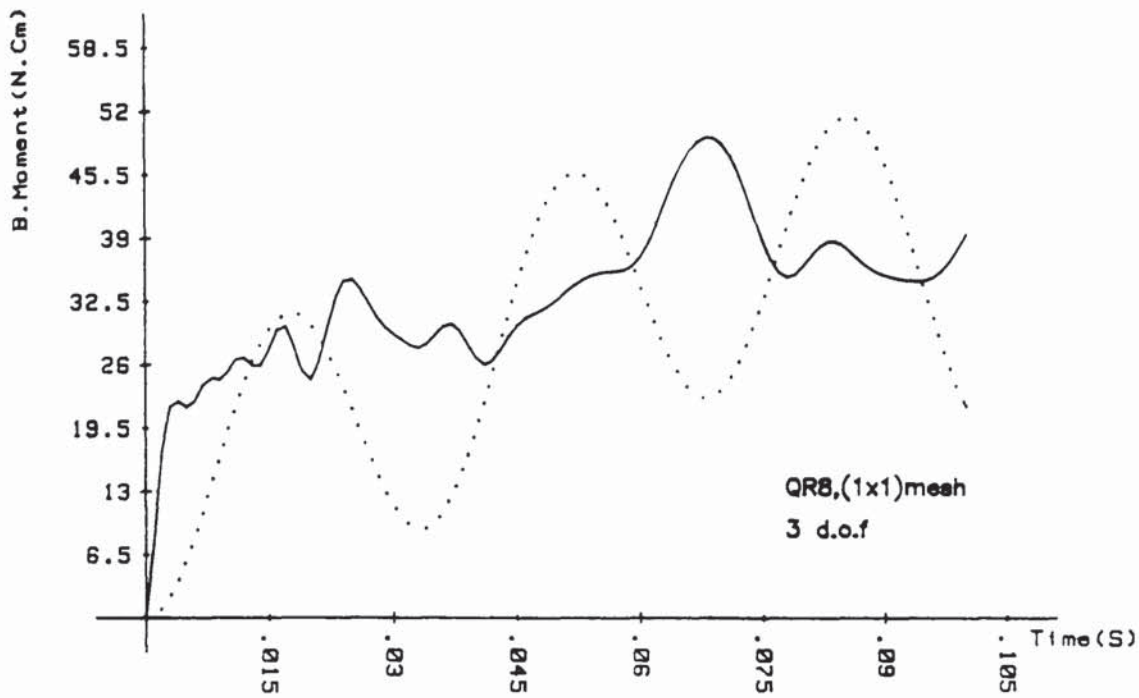
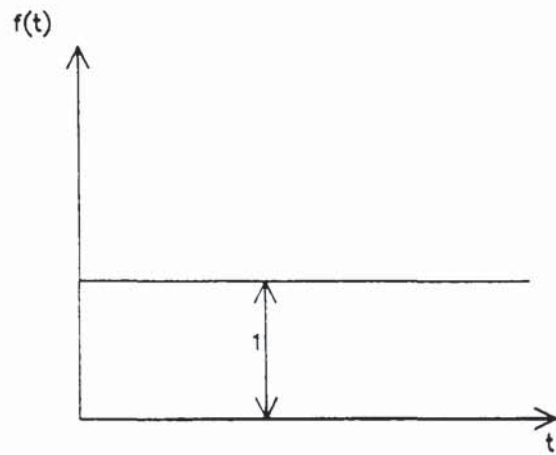
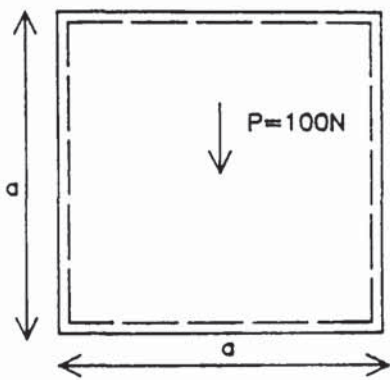
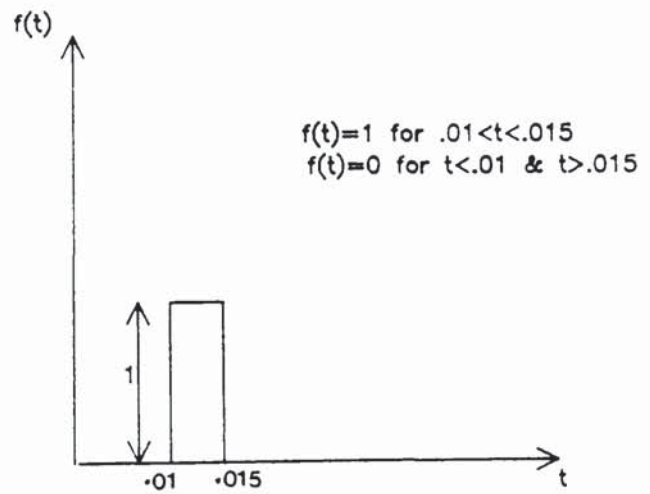


Fig 8.63 Bending moment M_x vs time; t at the centre of clamped plate under transient point load. ——— QD8 element
..... QR8 element



Case(a)–Step function input.



Case(b)–Impulsive input

Fig 8.64 Simply supported square plate subjected to:
 (a)Step function input,(b)Impulsive input.

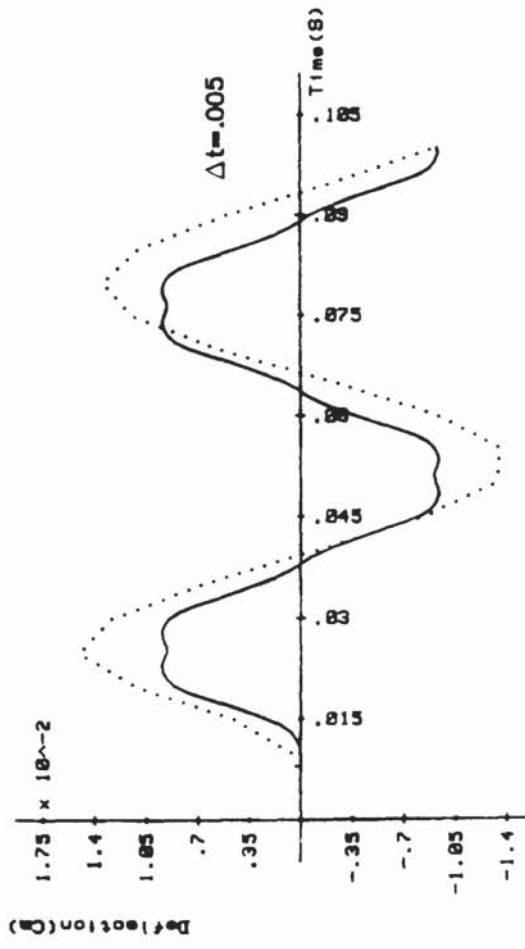
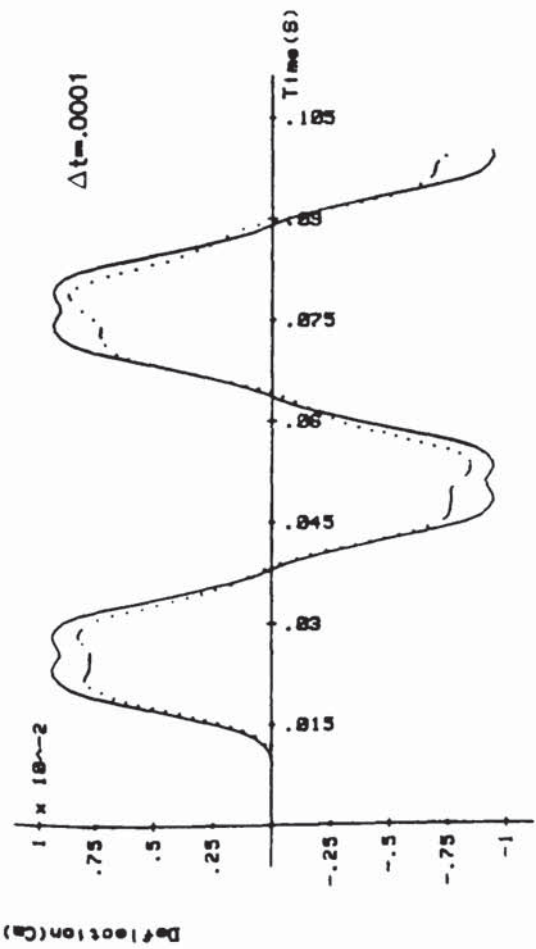
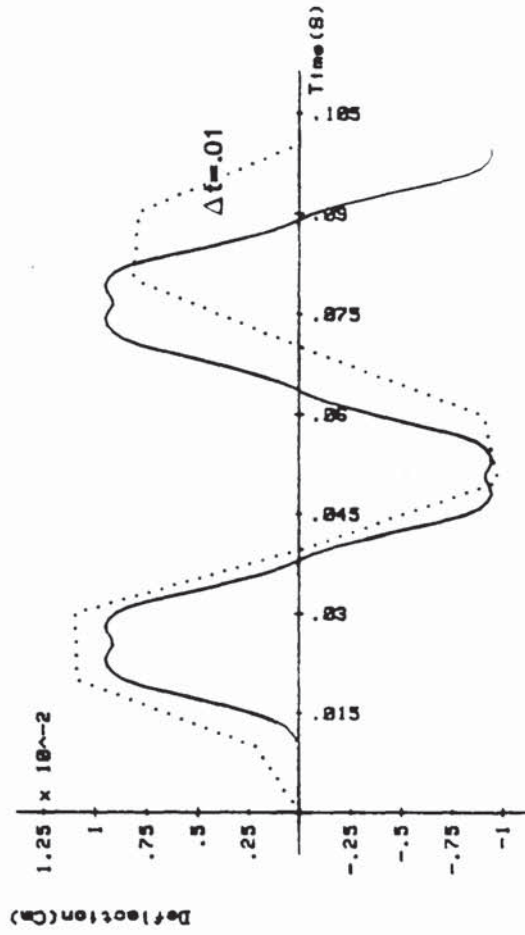
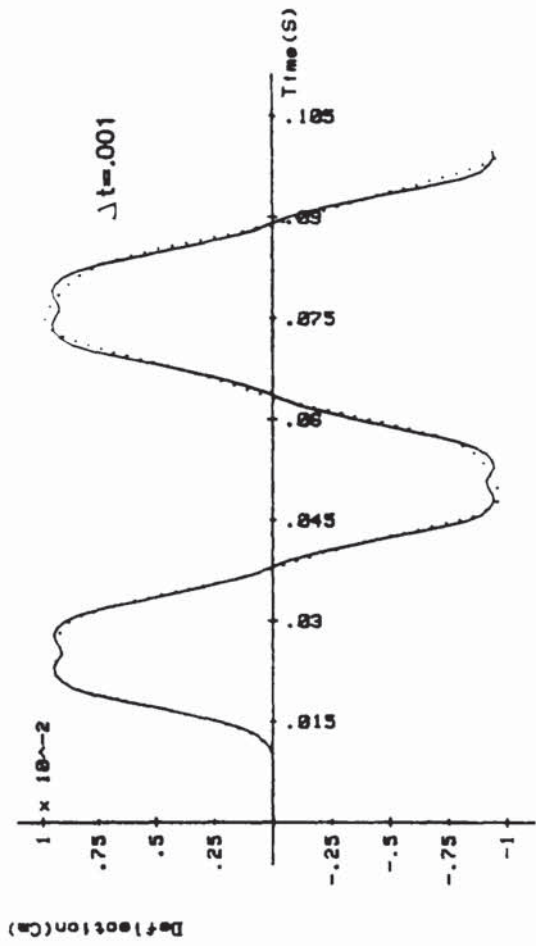


Fig 8.65 Displacement response predicted with increasing time step size Δt ; Wilson ($\theta=1.4$) (case a)

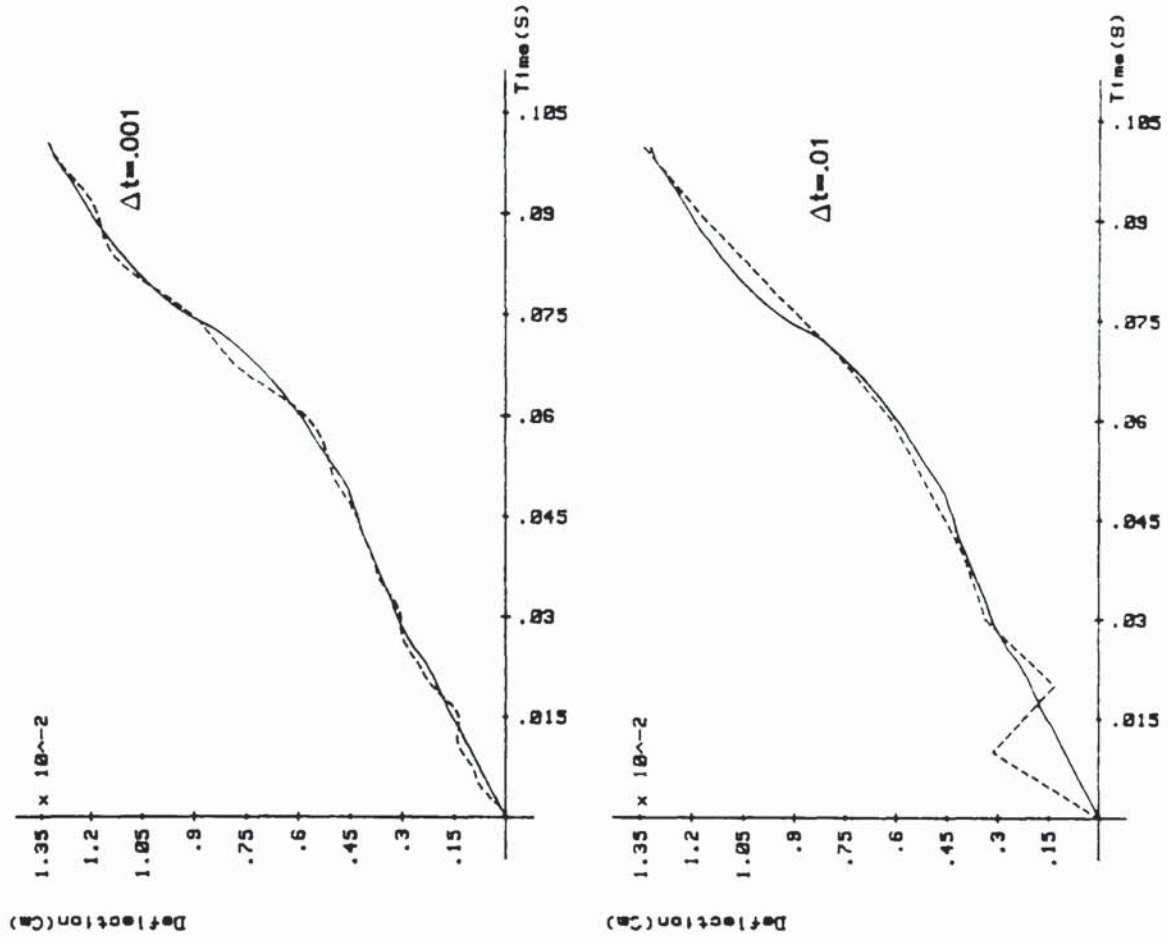
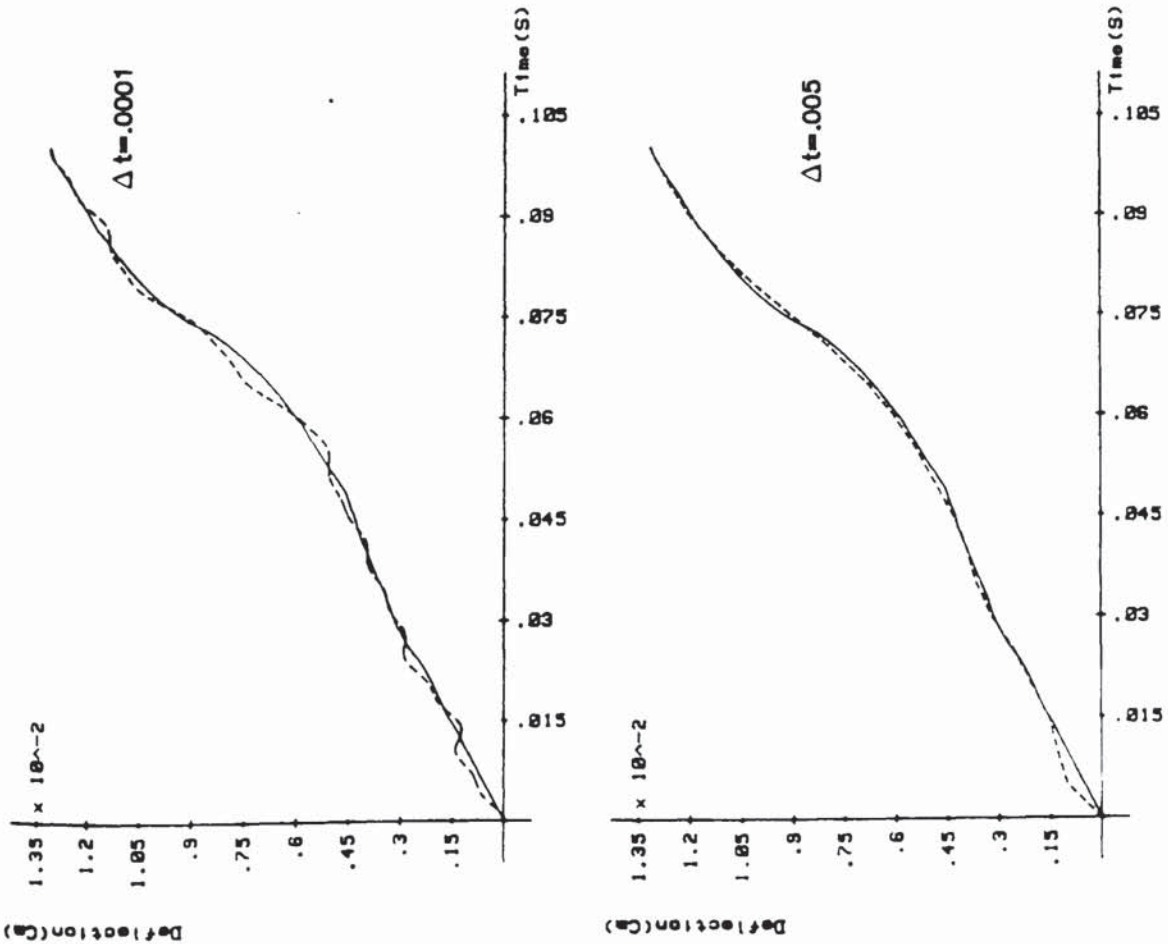


Fig 8.66 Displacement response predicted with increasing time step size Δt ; Wilson () method, $\Delta t=1.4$ (case b)



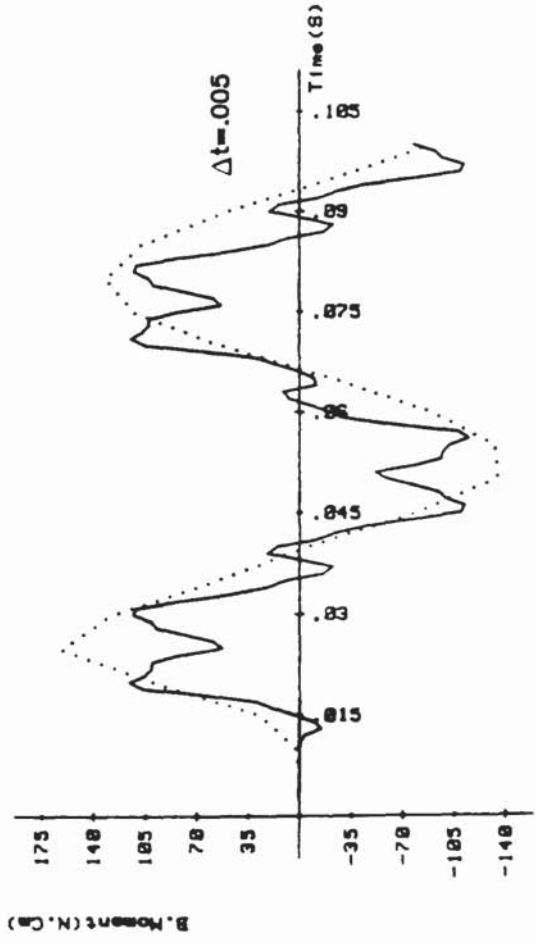
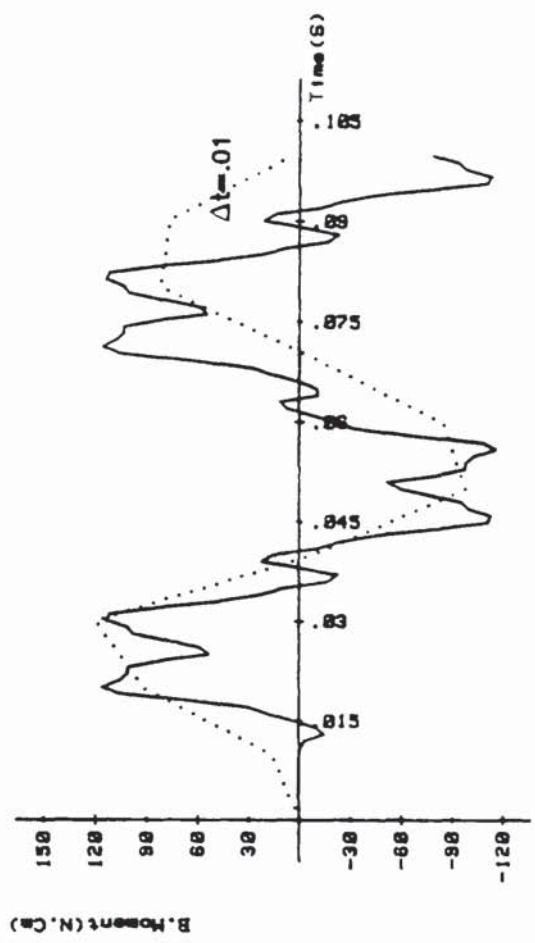
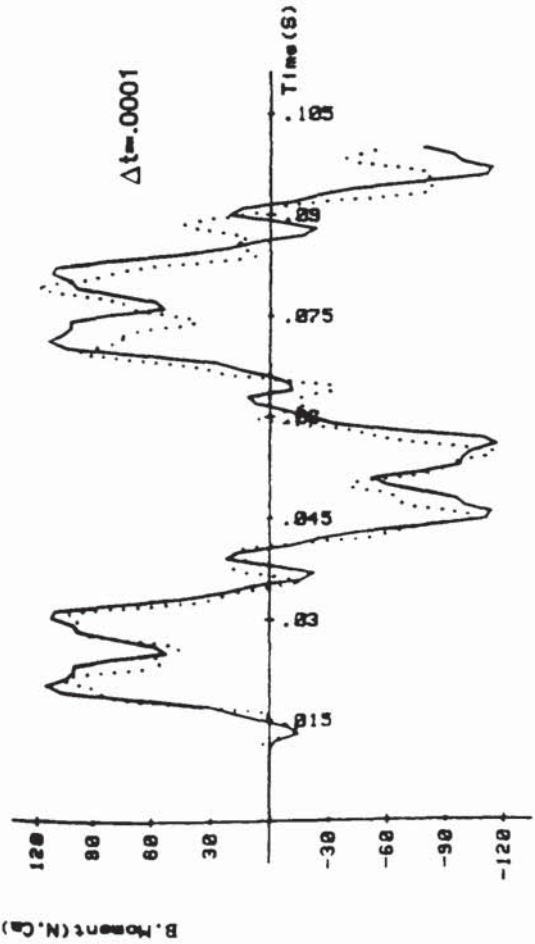
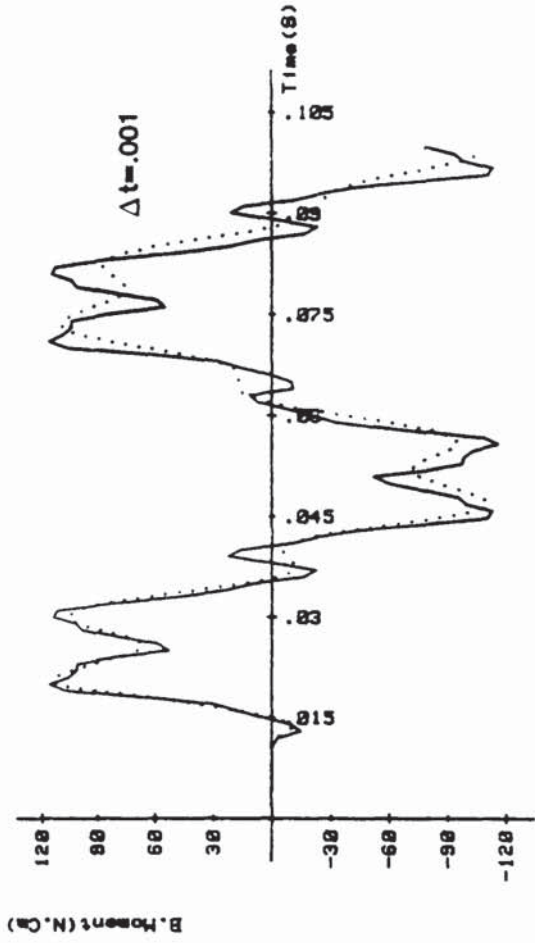


Fig 8.67 Bending moment response predicted with increasing time step size Δt ; Wilson () method, $\rho=1.4$ (case a)

Exact

.....

F.E model

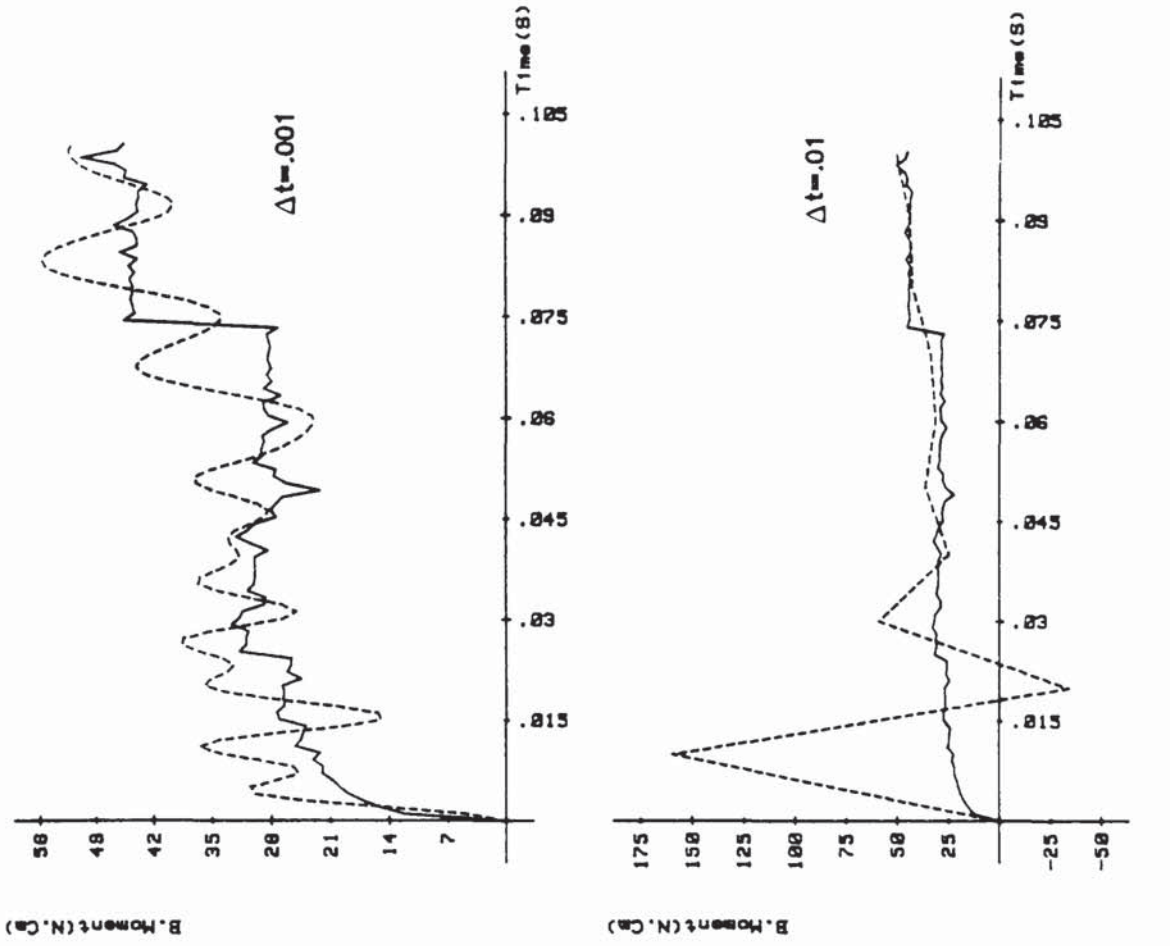
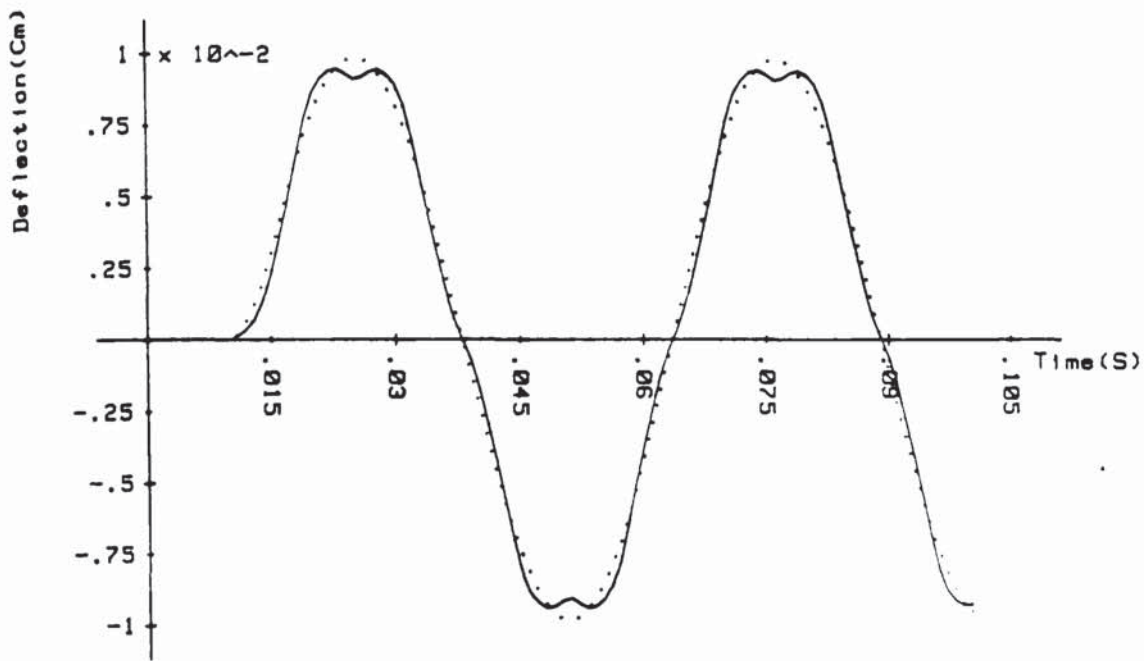
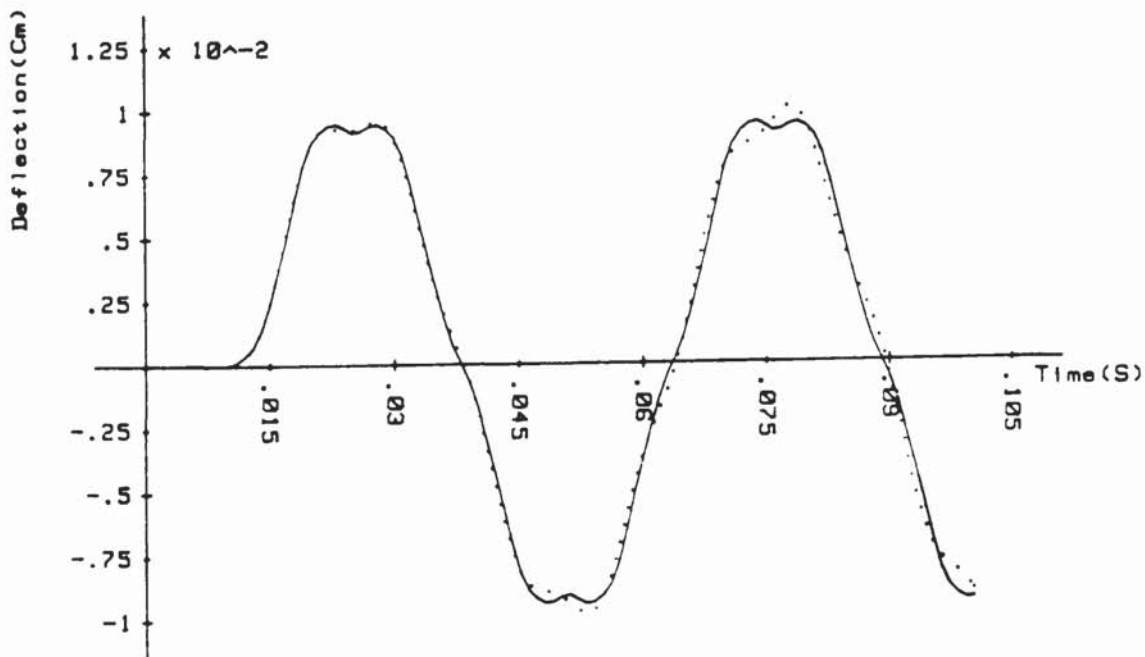


Fig 8.68 Bending moment response predicted with increasing time step size Δt ; Wilson θ method, $\theta=1.4$ (case b)

Exact
F.E model



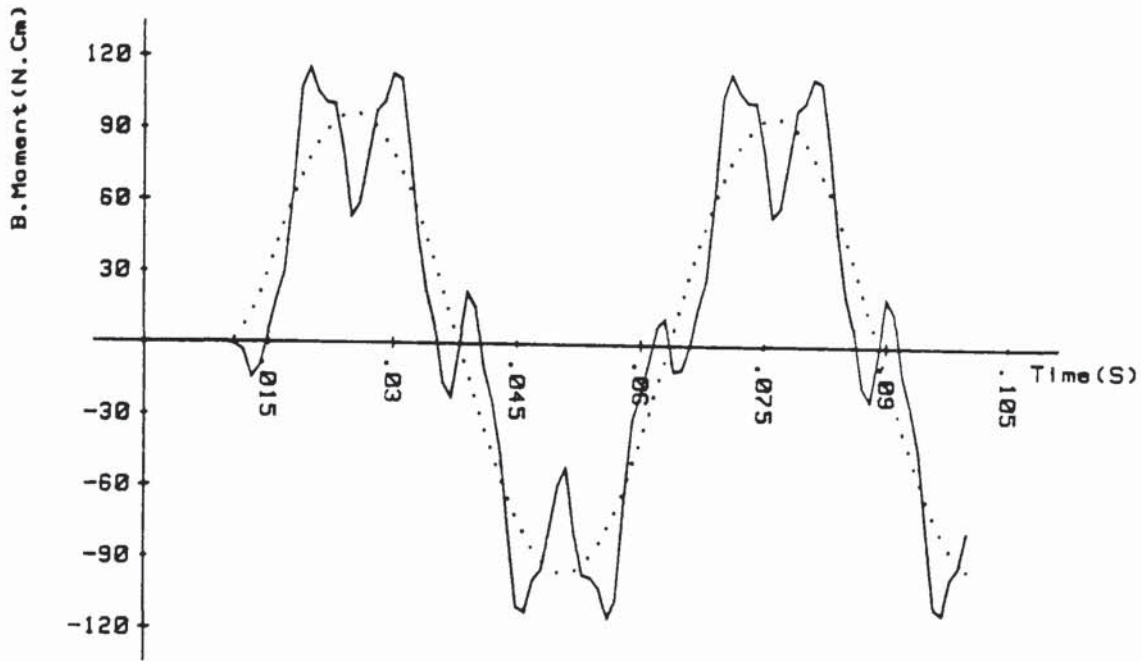
(a)



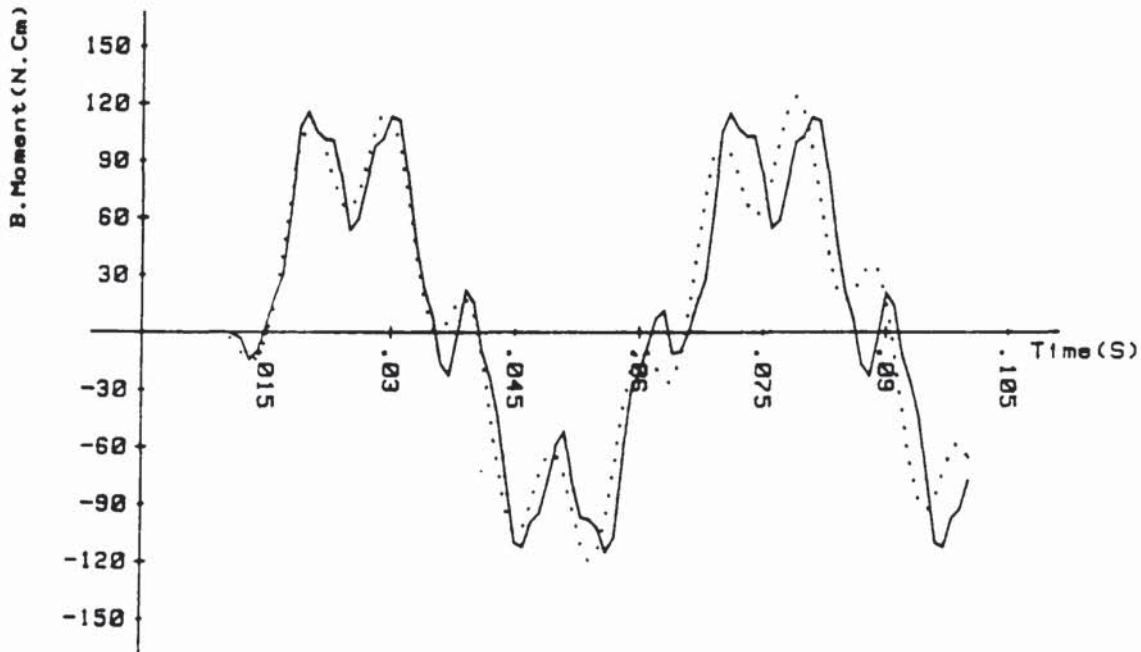
(b)

Fig 8.69 Displacement response by mode superposition method.
 (a-1mode,b-3modes used)

———— Exact
 F.E Model



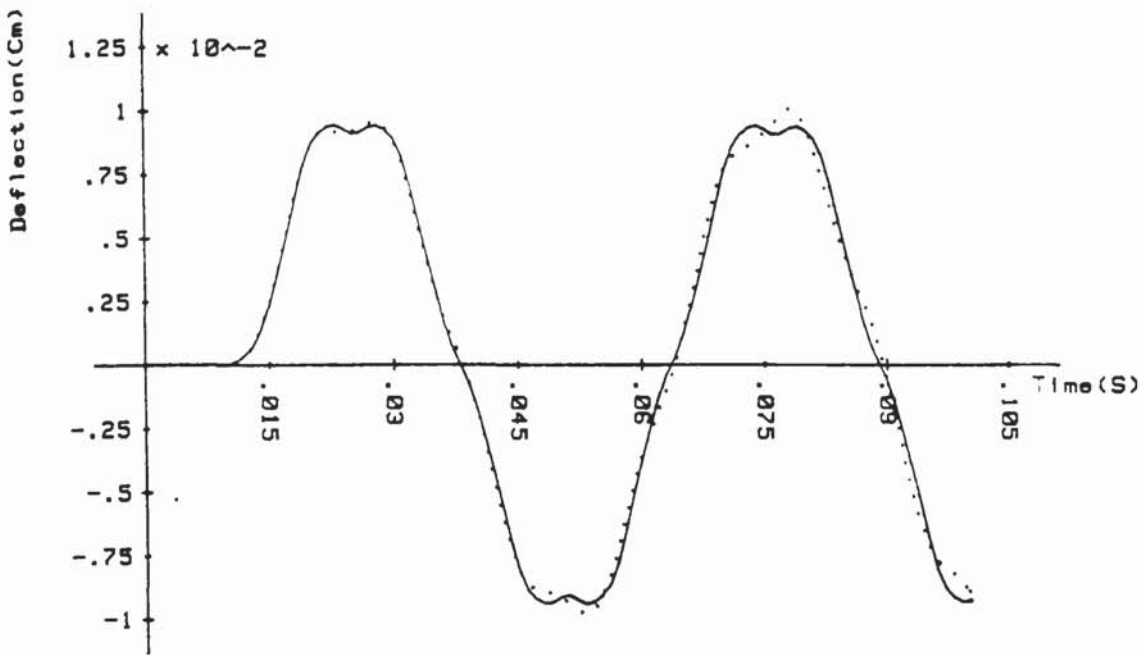
(a)



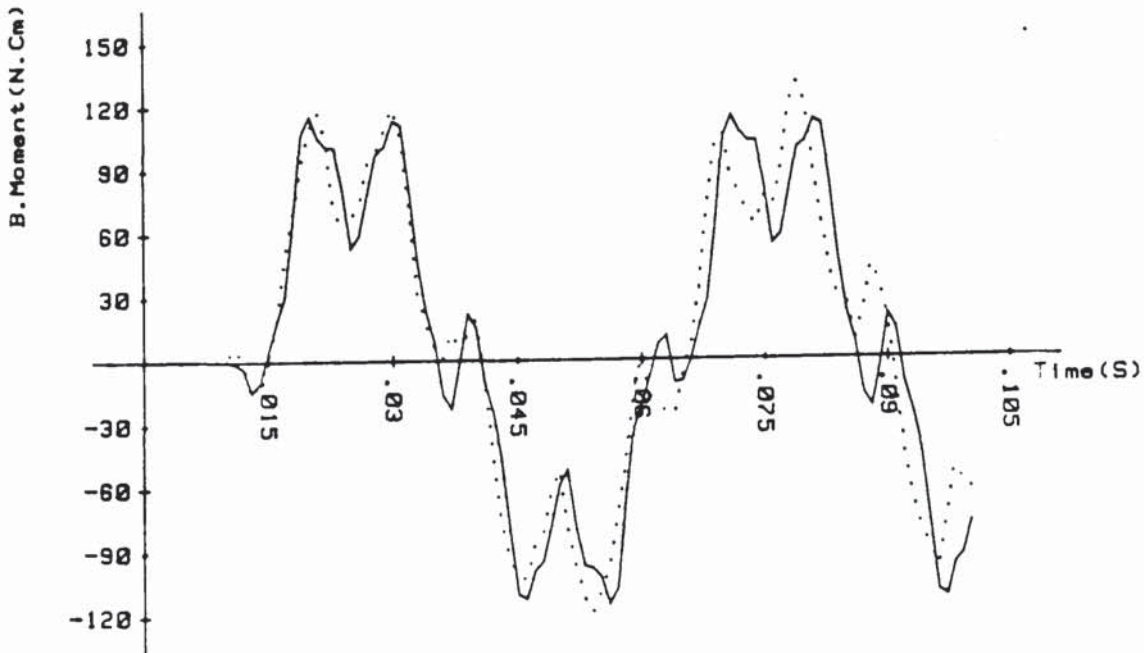
(b)

Fig 8.70 Bending moment response by mode superposition method.
 (a-1mode,b-3modes used)

———— Exact
 F.E Model



(a)



(b)

Fig 8.71 Forced response analysis of a SSSS plate by mode superposition method using 12 modes.

————— Exact
 F.E Model

(a) Mid point displacement response
 (b) Mid point bending moment response

CHAPTER 9

DISCUSSION
AND
CONCLUSIONS

9. DISCUSSION AND CONCLUSION

The application of Reissner's variational principle in the finite element analysis of structures has seen rapid progress during the past decade. This principle can be derived by the generalization of the minimum potential energy principle and is characterized by the use of both displacements and stresses as field variables. The so-called "mixed finite element" models by Reissner's principle have the following advantages:

- (i) The possibility of relaxing the continuity conditions along the interelement boundaries. Thus allowing the use of simple and low order shape functions for displacements and stresses. This property has been shown to be of particular advantage in the analysis of plate and shell type structures.
- (ii) Stresses, which are often of primary importance and interest, are calculated directly. Thus, the accuracy of the solution is comparable with that for displacements.

The earliest mixed finite element models were introduced by Herrmann (3, 61) in the static analysis of plate structures. He used a modified version of Reissner's principle which only imposes C_0 continuity on the field of displacement and stresses. As a result of the successful application of Herrmann's mixed models, a number of mixed finite element models for plate problems have appeared to date. Only a few of these investigations have dealt with dynamic (free vibration) problems, however.

The main objective of this project was to study the performance

in discretizing the bending moment M and displacement w . The elements are, in general, capable of predicting the natural frequencies with good accuracy and the results are in good agreement with the displacement type of solution. However, the solutions from two elements of $C0$ continuous class, namely MB7 with constant-parabolic shape functions and MB8 with parabolic-constant shape functions were wrong. The misbehaviour of those elements was attributed to the existence of untrue rigid body modes. These elements were excluded from the forced vibration analysis. The accuracy and convergency properties of mixed elements were also studied in the solution of beam response problems. It was observed that with a very few number of degrees of freedom, the elements are capable of predicting the transient response (deflection and moments) with very good accuracy. And in most cases, it was seen that the accuracy of the moments predicted by mixed elements is superior to that of displacement models, for the same number of degrees of freedom.

Determination of suitable shape functions of $C1$ continuity, in the formulation of plate elements is much more complex. If complete slope continuity is required on the interfaces between various elements, the mathematical and computational difficulties rise disproportionately fast. For this reason, the modified Reissner's principle introduced by Herrmann was employed in the development of mixed plate elements. The first element is a linear quadrilateral element with 16 degrees of freedom. This element has been tested in the solution of static, free vibration and buckling plate problems by Mota Soares (7), and good results were reported. The second element, developed in this work, is a parabolic quadrilateral element with 8 nodes, and 32 degrees of freedom. This element is suitable for representing plates of arbitrary shape. In addition to these, the two non-conforming displacement type elements of Ref. (9) were

of the mixed finite element models based on Reissner's variational principle in the solution of dynamic structural problems. These problems include both free and forced vibration analysis. In design work, a knowledge of the system natural frequencies and mode shapes, obtained from the free vibration analysis, is helpful in avoiding the peak response which occur in the vicinity of the natural frequencies. In the forced vibration analysis, the effects of dynamic loads on the behaviour of the structure are investigated. In large and complex structures, these effects can become dominant.

The work presented in this thesis deals with the free and forced vibration of beam and plate type structures. As a prerequisite for this work, it was necessary to derive a dynamic version of Reissner's principle. In Chapter 2, it was shown that this principle can be obtained from the minimum potential energy principle by introducing the strain-displacement equations as conditions of constraint and the corresponding Lagrange multipliers, which are the stresses, as additional variables, and then by eliminating the strains as variables using the stress-strain relations. The extension to dynamic problem, which also includes velocity dependent damping forces, was performed in a similar manner using Hamilton's generalized principle. A convenient version of Reissner's principle, for application to beam and plate problems can be derived by single integration by parts of the terms with second order derivatives of displacement. This version of Reissner's principle allows the use of C_0 continuous shape functions and was derived in section 3.3 for beam and in section 4.3.2 for plate analysis. The inclusion of C_1 continuous shape functions in the beam element formulation does not raise any difficulty. Thus both versions of Reissner's principle were employed in the derivation of beam elements characteristics. Eight elements were developed, with various sets of shape functions used

extended to the forced vibration case. The input data preparation was performed by means of an automatic mesh generation program.

In applications to free vibration plate problems, it was seen that the mixed models are capable of predicting the lower natural frequencies with good accuracy. The results from the linear mixed element are reasonable and the parabolic element results are significantly better than the linear ones. An advantage of the mixed models in the solution of eigenvalue problems is that the size of the eigen problem can be considerably reduced without affecting the solution accuracy. In this work, the eigenvalue problem was reduced to one having only nodal deflections as the unknowns.

In the forced vibration problems, the mixed equations were formulated in terms of the nodal deflections. Having determined the transient displacements, the bending or twisting moments could then be calculated by a simple matrix transformation procedure. Some numerical tests were performed and the results were compared with the available analytical and the non-conforming displacement type solutions. In all these applications relatively coarse meshes of mixed elements were capable of predicting the transient displacements and moments with comparable (in some cases with better) accuracy than the displacement models. In particular, it was observed that the computational time spent in the process of calculating the dynamic moments is considerably less than that in the displacement type formulation.

9.1 Further improvements

In this work, mixed isoparametric quadrilateral elements were used in the solution of dynamic plate problems. The discretization of plate structures was performed by an auto-mesh generation program. This program is also capable of generating meshes of 6-node triangular elements. The suite of programs can, with little modification, be made to accommodate this type of element. An advantage of the triangular element is that it is more versatile in representing the general shape of the boundary and contains fewer number of degrees of freedom than the 8-node quadrilateral element. (Moments and displacement may be assumed to vary parabolically within the element).

The modifications of the existing programs for the solution of static plate bending problems can be an objective of a further extension of the work of this thesis. For the solution of static problems, the mixed equations can be rearranged to yield a single matrix equation with nodal deflections and nodal bending moments as unknowns to be determined in a single operation. The corresponding mixed matrix is sparsely populated and the non-zero elements are located near the leading diagonal in a band form. In this way, it is only necessary to store the complete band form of the mixed matrix. This has the advantage of reducing the computer storage requirements. However, the overall mixed matrix is non-positive definite and the Gauss elimination method with row interchanges must be used in the solution of static equations.

REFERENCES

1. TURNER M.J., CLOUGH R.W., MARTIN H.C., and TOPP L.C. "Stiffness and deflection analysis of complex structures", *J. Aeronaut. Sci.* Vol. 23, No. 9, (1956)
2. REISSNER E. "On a variational theorem in elasticity", *J. Math. Phys.* 29, p.90, (1950)
3. HERRMANN L.R., "Finite element bending analysis of plates", *J. Eng. Mechanics. Div.*, ASCE, 94, No. EM5, pp 13-25 (1968)
4. VISSER W., "A refined mixed type plate bending element", *AIAA Journal* 7, pp 1801-1803, (1969)
5. COOK R.D., "Eigenvalue problems with mixed plate elements", *AIAA Journal*, Vol. 7, No. 4, pp 982-983, (1969)
6. KIKUCHI F., ANDO Y., "Rectangular finite element for plate bending analysis based on Hellinger-Reissner's variational principle", *J. Nucl. Sci. Techn.* 9, pp 28-35, (1972)
7. MOTA SOARES, C.M., "A study of mixed formulation for the finite element analysis of plates", PhD thesis, University of Aston in Birmingham, (1976)
8. TSAY C.S., and REDDY J.N., "Free vibration of thin rectangular plates by a mixed finite element; ASME, paper N77, (1977)
9. HENSHELL R.D., WALTERS D, and WARBURTON, G.B. "A new family of curvilinear plate bending elements for vibration and stability", *Journal of Sound and Vibration*, 20(3), pp 381-397, (1972)
10. LEISSA A.W., "The free vibration of rectangular plates", *Journal of Sound & Vibration*, 31(3), pp 257-293, (1973)
11. LEIPHOLZ H.H.E., "Six lectures on variational principles in structural engineering", Solid Mechanics Division, University of Waterloo, Waterloo, Canada, (1978)
12. LOVE A.E.H., "A treatise on the mathematical theory of elasticity," Cambridge University Press, 4th edition,(1927)
13. TIMOSHENKO S, AND GODIER J.N., "Theory of elasticity", McGraw-Hill, (1951)
14. WASHIZU K, "Variational methods in elasticity and plasticity", Pergamon Press, Oxford, (1968)
15. LANGHAAR H.L., "Energy methods in applied mechanics" John Wiley & Sons, Inc. New York, N.Y., (1962)
16. DYM C.L., and SHAMES I.H., "Solid mechanics: variational approach", McGraw-Hill, (1973)
17. KANTOROVICH L.V., "Approximate methods of high analysis", Inter Science Pub. (1964)

18. WILKINSON J.H., "*The algebraic eigenvalue problem*", Clarendon Press, Oxford, (1965)
19. CLOUGH R.W., "The finite element in plane stress analysis", Proc. 2nd ASCE Conf. on electronic computation, Pittsburgh, Pa. September 1960
20. ZIENKIEWICZ, O.C. "*The finite element method*" 3rd Edition, McGraw-Hill Book Co. (UK) Ltd. (1977)
21. DESAI C.S., and ABEL J.F., "*Introduction to the finite element method*", Van Nostrand Reinhold Co. New York (1972)
22. BEREBBIA C., TOTTENHAM H., "*Finite element techniques in structural mechanics*", Southampton University Press, (1971)
23. COOK R.D. "*Concepts and applications of finite element analysis*" John Wiley & Son (1974)
24. PIAN T.H.H., TONG P., "Basis of finite element methods for solid continua", *International Journal for Numerical Methods in Engineering*, Vol. 1, (1969), pp 3-28
25. LEISSA A., "Recent research in plate vibration 1973-1976: classical theory," *Shock and Vibration Digest*, 1977
26. LEISSA A., "Recent research in plate vibration 1973-1976: complicating effects", *Shock and Vibration Digest*, 1977
27. BISHOP R.E.D. and JOHNSON D.C., "*Vibration analysis tables*", Cambridge University Press, Cambridge (1956)
28. WARBURTON G.B., "*The dynamical behaviour of structures*", 2nd edition, (1976), Pergamon Press, Oxford
29. TIMOSHENKO S.P. and KRIEGER S.W., "*Theory of plates and shells*", 2nd edition, McGraw-Hill, Tokyo, (1959)
30. TIMOSHENKO S.P., GERE J.M. "*Theory of elastic stability*", McGraw-Hill, 2nd edition, (1961)
31. LEISSA W.A., "Vibration of plates", Nasa Sp-160, National Aeronautics and Space Administration, Washington, (1969)
32. MEIROVITCH L., "*Analytical methods in vibration*", McMillan Co. New York (1967)
33. TONG P., "New displacement hybrid finite element models for solid continua", *Int. J. Num. Meth. Engng.* 2, pp 73-83, (1970)
34. de VEUBEKE B.F. "Displacement and equilibrium models in finite element method", in *Stress analysis* (eds. Zienkiewicz and Hollister), Wiley, (1965)
35. SPILKER R.L. and MUNIR R.L., "The hybrid stress model for thin plates", *Int. J. Num. Meth. Engng.* 15, pp 1239-1260, (1980)
36. MIRZA F.A., OLSON M.D. "The mixed finite element method in plane elasticity", *Int. J. Num. Meth. Engng.* 15, p 273-289, (1980)

37. PRAGER W., "Variational principles of linear elastostatics for discontinuous displacements, strains and stresses", *Recent progress in applied mechanics, The Folke Odqvist Volume B.* Brberg, J. Hult, and F. Niodson (eds) Odqvist & Wiksell, Stockholm, pp 463-474, (1967)
38. NEMAT-NASSER, S., "Application of general variational methods with discontinuous fields to bending, buckling and vibration of beams", *Computer Meth. in Appl. Mech. and Engng*, 2, pp 33-41, (1973)
39. PIAN, T.H.H., and TONG P., "Reissner's principle in finite element formulation", *Mechanics Today*, Vol. 5, pp 377-395, (1980)
40. LAZAN B.J. *Damping of materials and members in structural mechanics*, Pergamon Press, 1968, Oxford
41. BERT, C.W. "Material damping: an introductory review of mathematical models, measures and experimental techniques", *Journal of Sound and Vibration*, 29(2), pp 129-153, (1973)
42. CLOUGH R.W., and PENZIEN J., *Dynamics of structures* McGraw-Hill Book Co., New York, (1975)
43. WILSON E.L. and PENZIEN J., "Evaluation of orthogonal damping matrices," *International Journal for Numerical Methods in Engineering*, Vol. 4, No. 1, pp 5-10, January (1972)
44. BATHE K.J. and WILSON E.L. *Numerical methods in finite element analysis*, Prentice-Hall, Inc. New Jersey (1976)
45. HITCHINGS D and DANCE S.H., "Response of nuclear structural systems to transient and random excitations, using both deterministic and probabilistic methods", *Nuclear Engineering and Design*, 29 (1974), pp 311-337
46. GALLAGHER R.H., "Analysis of plate and shell structures", Proc. of Conf. on Application of Finite Element Method in Civil Eng., Vanderbilt University, Nashville, pp 155-206, (1969)
47. BOGNER F.K., FOX R.L., and SCHMIT L.A., "The generation of interelement, compatible stiffness and mass matrices by the use of interpolation formulas", Proc. (1st) Conf. on Matrix Methods in Struct. Mech., AFFDL TR 66-80, Nov., (1965)
48. BUTLIN G.A. and LECKIE F.A. "A study of finite elements applied to plate flexure", Symposium papers, Numerical Methods for Vibration Problems, Vol. 3, July (1966), University of Southampton
49. MASON V., "Rectangular finite elements for analysis of plate vibration", *Journal of Sound and Vibration*, Vol. 7, (1968), pp 437-448
50. COWPER G.R., KOSKO E., LINDBERG G.M. and OLSON M.D. "Static and dynamic applications of a high-precision triangular plate bending element", *AIAA Journal*, Vol. 7, No. 10, October (1969)
51. BAZELEY G.P. et al., "Triangular elements in plate bending - conforming and non-conforming solutions" Matrix methods in structural mechanics, AFFDL - TR - 66-80, (1966), Wright-Patterson Air Force Base, Ohio, pp 547-576

52. CLOUGH R.W. and TOCHER J.L., "Finite element stiffness matrices for analysis of plate bending", Matrix methods in structural mechanics, AFFDL - TR - 66-80, (1966), Wright Patterson Air Force Base, Ohio, pp 515-545
53. MINDLIN, R.D., "Influence of rotatory inertia and shear on flexural motion of isotropic elastic plates", *J. Appl. Mech.* 18, pp31-38, (1951)
54. WEMPNER G.A., ODEN J.T., and KROSS D.A., "Finite element analysis of thin shells", Proceedings of the American Society of Civil Engineering, Vol. 94, EM6, December (1968), pp1273-1294
55. FRIED I., "Shear in C^0 and C^1 plate bending elements", *Int. J. Solids and Structures*, 9, 449-460 (1973)
56. ZIENKIEWICZ O.C., TAYLOR R.L. and TOO J.M., "Reduced integration techniques in general analysis of plates and shells", *Int. J. Num. Meth. Engng.* 3, 275-290 (1971)
57. PAWSEY S.E., and CLOUGH R.W., "Improved numerical integration of thick shell finite elements", *Int. J. Num. Meth. Engng.*, 3, 545-586 (1971)
58. LEE S.W. and PIAN T.H.H., "Improvement of plate and shell finite elements by mixed formulation", *AIAA Journal*, Vol. 16, No. 1, January (1978)
59. MORLEY L.S.D., "A triangular equilibrium element with linearly varying bending moments for plate bending problems", *J. Royal Aero. Soc.* 71, pp 715-721, (1967)
60. FRAEIJIS de VEUBEKE B. and SANDER G "An equilibrium model for plate bending", *Int. Jnl. Solids and Structs. (G.B.)*, 4, 447-468 (1968)
61. HERRMANN L.R. "A bending analysis for plates", Proc. (1st) Conf. on Matrix Methods in Struct. Mech., AFFDL - TR 66-80, pp 577-604, October (1965)
62. TAHIANI C., "*Analyse des Voiles Minces dans les Domaines Lineaire et Geometriquement Non-Lineaire par la Method des Elements Finis Mixtes*", Theses de Doctorat, Department de Genie Civil, Universite Laval, Aout (1971)
63. BRON J., DHATT G., "Mixed quadrilateral elements for bending", *AIAA Journal*, Vol. 10, October(1972)
64. RICHARDS T.H., *Energy methods in stress analysis*, Ellis Horwood Ltd. (1977)
65. FROBERG C.E., *Introduction to numerical analysis*, 2nd edition, Addison-Wesely Publishers, Comp. (1970)
66. GUNNAR E.N., "*Computer solution of the eigenvalue problem in vibration analysis*", MSc dissertation, University of Aston in Birmingham, November (1979)
67. WOOD P.C. "*Application of finite element method to problems in fracture mechanics*", PhD thesis, University of Aston in Birmingham, (1979)

68. WILKINSON J.H., MARTIN R.S., PETERS G., "Symmetric decomposition of a positive definite matrix", *Numerische Mathematik*, 7, pp 362-383, (1965)
69. RIPPERPER E.A., DALLY J.W., "Experimental values of natural frequencies for skew and rectangular cantilever plates", Report No. DRL 231, CF - 1354, Defence Research Lab. University of Texas, Austin (1949)
70. BARTON M.V., "Vibration of rectangular and skew plates", *Journal of Appl. Mech.*, 18, 2, (1951)

The undamped free vibration mode shapes and frequencies for an N degree of freedom system are determined by solving the eigenvalue equation (A.1),

$$[K][\hat{U}] = [M][\hat{U}][\omega^2] \quad (A.1)$$

in which $[\hat{U}]$ is the full (N x N) mode shape matrix and $[\omega^2]$ is an N x N diagonal frequency matrix containing the N squared natural frequencies. The undamped normal modes are then used to uncouple the equation of motion (A.2),

$$[M]\{\ddot{U}\} + [C]\{\dot{U}\} + [K]\{U\} = \{R\} \quad (A.2)$$

Thus, introducing normal-coordinate transformation,

$$\{U\} = [\hat{U}] \{q\} \quad (A.3)$$

into equation (A.2), we obtain:

$$m_r \ddot{q}_r + c_r \dot{q}_r + k_r q_r = R_r \quad (A.4)$$

$$r = 1, 2, \dots, N$$

where

$$m_r = \{\hat{U}\}_r^t [M] \{\hat{U}\}_r \quad (a)$$

$$c_r = \{\hat{U}\}_r^t [C] \{\hat{U}\}_r = 2m_r \omega_{nr} \zeta_r \quad (b) \quad (A.5)$$

$$k_r = \{\hat{U}\}_r^t [K] \{\hat{U}\}_r = m_r \omega_{nr}^2 \quad (c)$$

$$R_r = \{\hat{U}\}_r^t \{R\} \quad (d)$$

and ζ_r is the damping ratio of the r th mode of vibration.

After simple matrix manipulation, the following relation is obtained:

$$[C] = [\hat{U}]^{-t} [c_r] [\hat{U}]^{-1} \quad (A.6)$$

Using the first part of equation (A.5), it can be shown that

$$[\hat{U}]^{-t} = [M][\hat{U}][m_r]^{-1} \quad (a)$$

and $[\hat{U}]^{-1} = [m_r]^{-1} [\hat{U}]^t [M] \quad (b)$

(A.7)

substituting from (A.7) into (A.6) yields:

$$[C] = [\phi][\beta][\phi]^t \quad (A.8)$$

where $[\phi]$ is the mass normalized mode shape matrix defined by:

$$[\phi] = [M][\hat{U}] \quad (A.9)$$

and $[\beta]$ is a diagonal matrix in which the terms are given by

$$\beta_r = \frac{2\omega_r \zeta_r}{m_r} \quad (A.10)$$

Equation (A.8) can be written in an alternate form as a summation of modal damping matrices c_r i.e.

$$[C] = \sum_{r=1}^N [c_r]$$

where $[c_r]$ produces damping in mode r only and may be calculated directly from the mass normalized shape vector $\{\phi\}_r$ thus:

$$c_r = \beta_r \{\phi\}_r \{\phi\}_r^t \quad (\text{A.11})$$

The damping matrix $[C]$ is particularly useful in the evaluation of the dynamic response of structures when the direct step-by-step integration method is preferred to the normal mode superposition method.

B.1 Introduction

The mesh generation scheme is based on using "isoparametric" curvilinear mapping of quadrilaterals, which allows a unique coordinate mapping of curvilinear and cartesian coordinates (20).

In this program, a structure is divided into a "chequer board" pattern of quadrilateral zones. Each of these may define a material with a single property - and if such property is specified as zero - a void is achieved, allowing multiply connected zones to be mapped.

In this section, the input data required by the mesh generation program are described. Two data files are created. Data input by the operator is output onto the first file, and the data obtained from the mesh generation program onto the second data file. The second data file is accessed by the programs described in Chapter 7 to provide the necessary input data. At the end of this section an example is given to provide a guide to data preparation. For details on mesh generation program consult Reference (67).

B.1.1 Input data

Data is input in the following order:

(a) Program Code

- Code - Program classification number
- Qort - Type of element used (1 - Quadrilateral,
0 - Triangular)

Njob	-	Number of jobs to run
Nelemt	-	Number of elements
Nnode	-	Number of nodes
Cw	-	Number of nodes with prescribed w
Cx	-	Number of nodes with prescribed M_x
Cy	-	Number of nodes with prescribed M_y
C _{xy}	-	Number of nodes with prescribed M_{xy}
Nmat	-	Number of materials
Nskew	-	Number of nodes with coordinate transformation

(b) Control variables

Tnspds	-	Number of specified super nodes, i.e. not including standard generated nodes. If straight sided zone, only corner nodes are considered. If curve, mid-side nodes should also be included. Also if 2 super-nodes coincide only one is considered.
Pzone	-	Number of zones being used, ie. not including voids or generated zones
Vzone	-	Number of vertical zones (row of zones)
Hzone	-	Number of horizontal zones (column of zones)
Gh	-	Graphical output required? (1/Yes, 0/No)

(c) Standard geometries

Ntip	-	Number of crack tips (it should be specified as 0 here)
Ngm	-	Number of generated sections. If > 0 then input the following parameters:
Nstart	-	Super-node number starting the core
Zns	-	Zone number starting the core
N1	-	Number of super-nodes on the core face

X1,Y1 - Coordinates of the tip
 R1,R2,R3 - Radii for the inner core, grading node and outer node respectively
 A - Starting angle
 A1 - Incremental angle
 Dx,Dy - Zone's sub-divisions

(d) X and Y coordinates of specified super-nodes

Data sequence entered for each node

Q - Number of super-nodes occupying the position
 Xcod, Ycod - X and Y coordinates
 W - String of super-node numbers

(e) Defining zones

Zone - Number of like zones
 Mn - Material number
 Divx,Divy - Zone sub-divisions in x and y directions
 p - string of like zone numbers

(f) Identifying closing sides

Nd - Number of closing faces. If > 0 then input the following parameters for each face:
 Zn - Zone number
 Side - Side of face to be joined (1,2,3 or 4)
 Coin - Number of coinciding nodes. If > 0 then input the following parameters for each pair of nodes:
 Nd - Node number retained

Cnd - Corresponding node number

(g) Boundary conditions - material properties

Sequence of nodes with prescribed W

Sequence of nodes with prescribed M_x

Sequence of nodes with prescribed M_y

Sequence of nodes with prescribed M_{xy}

Data sequence for each material ..

Thick, Density, E, ν , G, E, ν ..

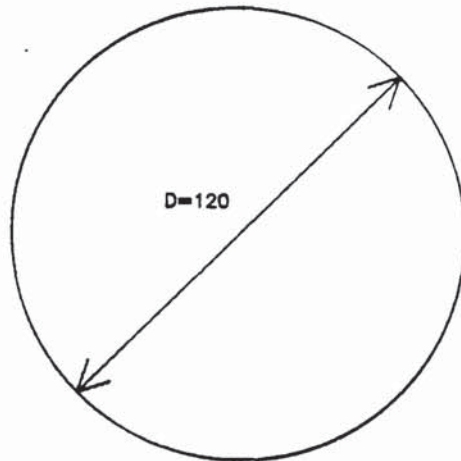
Data sequence for each skewed node ..

Nosk - Node number

Angsk - Angle of skew

B.1.2 Data input example.

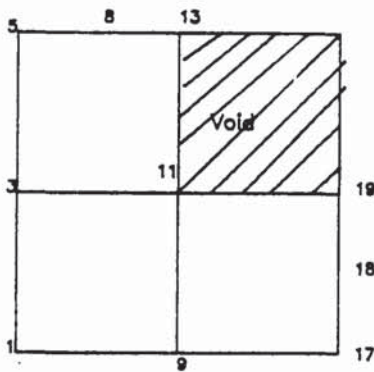
Simply supported circular plate.



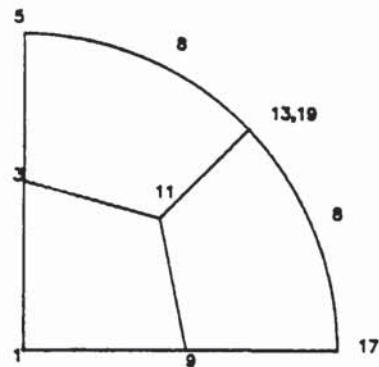
Material properties:
 $E=2.07 \times 10^7 \text{ N/Cm}^2$
 $\nu=.3$
 $\rho=7.8 \times 10^{-3} \text{ Kg/Cm}^3$
 $h=1\text{cm}$

The discretized plate

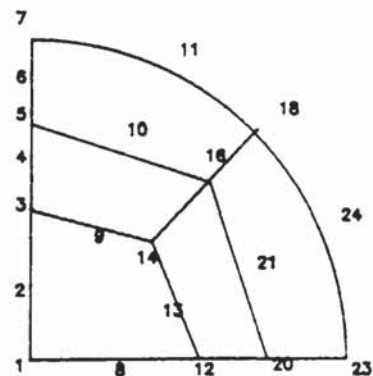
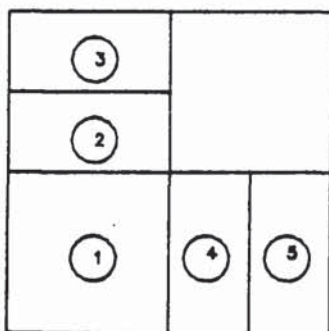
Due to symmetry only a quarter of the plate is required.



(a) "Chequer board" pattern



(b) Specified super nodes



(c) Element array with nodal numbering.

The input data

(a) 6, 1, 1, 5, 24, 5, 0, 3, 13, 1, 5

(b) 9, 3, 2, 2, 1

(c) 0, 0

(d) 1, 0, 0, 1 1, 0, 20, 3 1, 0, 60, 5 1, 20, 0, 9

1, $10\sqrt{2}$, $10\sqrt{2}$, 11 1, 60, 22.961, 55.4327, 8

2, 42.426, 42.426, 13, 19 1, 55.4327, 22.961, 18

1, 60, 0, 17

(e) 1, 1, 1, 1, 1

1, 1, 1, 2, 2

1, 1, 2, 1, 3

(f) 1, 2, 3, 0

(g) c_w : 7, 11, 18, 24, 23

$c_y(M_n)$: 11, 18, 24

c_{xy} : 1, 2, 3, 4, 5, 6, 7, 8, 12, 19, 20, 22, 23

Material properties: 1, $7.8E-3$

$2.07E7$, .3, $\frac{2.07E7}{2.6}$, $2.07E7$, .3

Nosk, Angsk: 11, 67.5°

18, 45°

24, 22.5°

APPENDIX C

Listing of computer programs:

MBRSP5	(Mixed beam response analysis)
RFPLT1	(Plate free vibration)
RFPLT2	(Plate forced vibration by mode superposition)
RFPLT3	(Plate forced vibration by Direct integration)

```

10  REM *****PROGRAM MBRSP5*****
20  REM *           Based on           *
30  REM *           Reissner principle  *
40  REM * Version#1:This program calculates the dynamic *
50  REM * displacements and stresses of a beam by means of *
60  REM * mixed finite element method.A direct integration *
70  REM * method known as Wilson thta is used.The method is *
80  REM * unconditionally stable.Damping is assumed to be *
90  REM * viscous and proportional.    *
100 REM * A complete damping matrix is thus derived ,based *
110 REM * on the orthogonality relations.A 3 node deflection*
120 REM * and a 3 node moment mixed element is used.      *
130 REM * Version#2:Mode superposition method is used to  *
140 REM * solve the equations.Modal dampings can be directly*
150 REM * employed in each uncoupled equation.            *
160 REM *****
170 OPTION BASE 1
180 PRINTER IS 16
190 PRINT "Dynamic analysis of beams by mixed formulation"
200 PRINT
210 DIM Xcod(120),Leg(50),E(50),Ro(50),A(50,2),Mi(50,2)
220 DIM Th(50,2),P(45),V(4),Kode(100,2),Ge(3,3),He(6,6)
230 DIM Me(3,3),U(6),H(20,20),M(20,20),G(43,43),K(43,43)
240 DIM Vec(43,43),Eval(43),Apfo(30,1),F0(20),D(43),OfFd(43)
250 DIM OfFd2(43,1),D1(43),Fo(43),C(20,20),A0(9),Dratio(50)
260 DIM I#[160],T#[80],A#[20],B#[20],Wcnt(3001),Mcnt(3001)
270 INTEGER N,Sol,Type,R,Pw,Pm,Neq,Nmod,Wpos,Mpos,Wplt,Mplt
280 MAT K=ZER
290 MAT M=ZER
300 MAT G=ZER
310 DISP "Before running the program for response analysis the"
320 DISP
330 DISP "following data files should be created on the current"
340 DISP
350 DISP "mass storage unit:"
360 DISP
370 DISP "1-Data file (Init1) to be used for recording the "
380 DISP
390 DISP "initial conditions. "
400 DISP
410 DISP "2-Data file (Eqn) to be used for excitation "
420 DISP
430 DISP "functions.The program is halted.Create the"
440 DISP
450 DISP "files and press CONT"
460 PAUSE
470 INPUT "Choose the printer,0 for paper 16 for CRT ",Printer
480 PRINTER IS Printer
490 INPUT "What is your mass storage unit for data files?",Data#
500 DISP "Structural data[Geometric and material]"
510 INPUT "Type of the problem[S-S,etc]",Type#
520 INPUT "Number of elements",Nelemt
530 DISP "Number of elements=",Nelemt
540 Nnode=2*Nelemt+1
550 REM ----Nodal coordinates
560 Z=-1
570 FOR M=1 TO Nelemt+1
580 Z=Z+2
590 DISP "X-coordinate of node";Z;"
600 INPUT Xcod(Z)
610 IF M>1 THEN Leg(M-1)=Xcod(Z)-Xcod(Z-2)
620 NEXT M
630 FOR M=1 TO Nelemt
640 Xcod(2*M)=(Xcod(2*M+1)-Xcod(2*M-1))/2+Xcod(2*M-1)
650 NEXT M

```

```

660 FOR M=1 TO Nnode
670 DISP "X-coordinate of node";M;"=";Xcod(M)
680 NEXT M
690 DISP "press CLEAR then CONT"
700 PAUSE
710 REDIM Xcod(Nnode),Leg(Nelemt),E(Nelemt),Ro(Nelemt)
720 REDIM A(Nelemt,2)
730 REDIM Mi(Nelemt,2),Th(Nelemt,2),Kode(Nnode,2),Fo(Nnode)
740 DISP "Element details"
750 INPUT "How many groups of like elements?(Mat)",Glik
760 FOR G=1 TO Glik
770 DISP "Number of like elements in group";G;"",
780 INPUT K
790 INPUT "Elasticity modulus?",E
800 INPUT "Mass density?",Ro
810 DISP "String of like elements in group";G;" "
820 FOR M=1 TO K
830 INPUT N
840 E(N)=E
850 Ro(N)=Ro
860 NEXT M
870 DISP "Material properties for group";G;" "
880 DISP "Elasticity modulus=";E
890 DISP "Mass density=";Ro
900 NEXT G
910 INPUT "Is the problem one of damped or undamped?1/0",Damp
920 IF NOT Damp THEN GOTO 990
930 INPUT "Number of modes with proportional damping?",Nmod
940 REDIM Dratio(Nmod)
950 FOR I=1 TO Nmod
960 DISP "Damping ratio in mode";I;"?"
970 INPUT Dratio(I)
980 NEXT I
990 DISP "Uniform cross section?if yes input the area,0 to "
1000 DISP " indicate nonuniform"
1010 INPUT T
1020 IF T=0 THEN GOTO 1100
1030 INPUT "Moment of inertia?",T1,"Extreme fiber location?",T2
1040 FOR I=1 TO Nelemt
1050 A(I,1)=A(I,2)=T
1060 Mi(I,1)=Mi(I,2)=T1
1070 Th(I,1)=Th(I,2)=T2
1080 NEXT I
1090 GOTO 1170
1100 FOR M=1 TO Nelemt
1110 DISP "Input the following for element";M;" ""
1120 DISP "Area?,Moment of inertia?,Extreme fiber location? At1"
1130 INPUT A(M,1),Mi(M,1),Th(M,1)
1140 DISP "Area?,Moment of inertia?,Extreme fiber location At2"
1150 INPUT A(M,2),Mi(M,2),Th(M,2)
1160 NEXT M
1170 DISP "press CLEAR then CONT"
1180 PAUSE
1190 MAT kode=ZER
1200 DISP "Introduction of prescribed freedoms[m,w] ""
1210 INPUT "Number of nodes with prescribed moments?",Pm
1220 FOR I=1 TO Pm
1230 INPUT "Node number ",M
1240 Kode(M,1)=1
1250 NEXT I
1260 INPUT "Number of nodes with prescribed deflection?",Pw
1270 FOR I=1 TO Pw
1280 INPUT "Node number?",M
1290 Kode(M,2)=1
1300 NEXT I
1310 Pm=R=Nnode-Pm

```

**PAGE
NUMBERS
CUT OFF
IN
ORIGINAL**

```

1320 Pw=B=Nnode-Pw
1330 REDIM G(A,A),H(A,B),M(B,B),Apfo(B,1),F0(B),C(B,B)
1340 A=B
1350 REDIM K(A,A),Vec(A,A),Eval(A),D(A),D1(A),Offd2(A,1)
1360 REDIM P(Pm),Offd(A)
1370 A=B=0
1380 DISP "press CLEAR then CONT"
1390 PAUSE
1400 PRINT SPA(14),"Results of finite element by Reissner pri
nciple"
1410 PRINT USING "K";"Response analysis by Wilson Theta Method"
1420 PRINT USING "K,16X,K";"Type of problem",Type#
1430 PRINT
1440 PRINT USING "K,12X,2D";"Number of elements",Nelemt
1450 PRINT
1460 PRINT USING "K,15X,2D";"Number of nodes",Nnode
1470 PRINT
1480 PRINT "Element properties:"
1490 PRINT LIN(2),"Elemt";SPA(2);"Modulus";SPA(3);"Area 1";SP
A(5);"Area 2";SPA(3);"Moment";SPA(5);"Moment";SPA(5);"Le
ngth";SPA(4);"Density"
1500 PRINT "number";SPA(1);"elastic";SPA(22);"Inertia1";SPA(3
);"Inertia2"
1510 PRINT
1520 FOR M=1 TO Nelemt
1530 PRINT USING "2D,2X,7(MD.3DE,X)";M,E(M),A(M,1),A(M,2),Mi(
M,1),Mi(M,2),Leg(M),Ro(M)
1540 NEXT M
1550 PRINT
1560 PRINT "Boundary conditions",LIN(2),"Node";SPA(4);"Xcoord
";SPA(6);"Moment";SPA(5);"Deflection"
1570 FOR M=1 TO Nnode
1580 PRINT USING "3D,3X,MD.4DE,5X,2(D,9X)";M,Xcod(M),Kode(M,1
),Kode(M,2)
1590 NEXT M
1600 INPUT "What is the loading type?1-for concentrated,2-for
distributed,3-for both",Lcon
1610 IF (Lcon=1) OR (Lcon=3) THEN GOSUB Conf
1620 IF (Lcon=2) OR (Lcon=3) THEN GOSUB Disf
1630 G=0
1640 FOR I=1 TO Nnode
1650 IF Kode(I,2)=1 THEN 1680
1660 G=G+1
1670 F0(G)=Fo(I)+F0(G)
1680 NEXT I
1690 PRINT "Total nodal forces"
1700 PRINT "Node-coords";SPA(10);"Force"
1710 FOR I=1 TO Nnode
1720 IF Kode(I,2) THEN PRINT USING "MD.4DE,10X,K";Xcod(I),"Fixed"
1730 IF NOT Kode(I,2) THEN PRINT USING "2(MD.4DE,10X)";Xcod(I
),Fo(I)
1740 NEXT I
1750 PRINT "Response analysis data"
1760 REM Input excitation as a function of time.
1770 LINK "EXCITE",5500
1780 CALL Excitn(Neq)
1790 CALL Wtipt(Wcnt(*),Mcnt(*),Kode(*),Time,Delta,A0(*),Thet
a,#1,Nnode,Pw)
1800 REM Assembly of [G],[H],[mass],[C] matrices.
1810 MAT Me=ZER
1820 MAT M=ZER
1830 FOR Z=1 TO Nelemt!Mass matrix assembly
1840 GOSUB Matme
1850 GOSUB Masemb
1860 NEXT Z
1870 MAT U=ZER

```



```

1880 FOR Z=1 TO Nelemt!Assembly of [G] matrix
1890 GOSUB Matge
1900 GOSUB Gasemb
1910 NEXT Z
1920 FOR Z=1 TO Nelemt!Assembly of [H] matrix
1930 C=1/Leg(Z)
1940 He(1,2)=He(2,1)=He(5,6)=He(6,5)=7/3
1950 He(1,4)=He(4,1)=He(2,3)=He(3,2)=He(3,6)=He(6,3)=-8/3
1960 He(4,5)=He(5,4)=-8/3
1970 He(1,6)=He(6,1)=He(2,5)=He(5,2)=1/3
1980 He(3,4)=He(4,3)=16/3
1990 MAT He=(C)*He
2000 GOSUB Hasemb
2010 NEXT Z
2020 REM Response analysis starts here.
2030 LINK "FDAMP",5500
2040 CALL Eqsolv(H(*),G(*),K(*),P(*),Pw,Pm)
2050 REM Damping matrix evaluation
2060 IF NOT Damp THEN GOTO 2080
2070 CALL Dampmat(C(*),Vec(*),Eval(*),M(*),K(*),Dratio(*),D(*),
Offd(*),Offd2(*),Dl(*),Nmod,Pw,Type,Sol)
2080 MAT Vec=M
2090 LINK "FINITL",5500
2100 CALL Eqsolv1(M(*),Dl(*),1,Pw)
2110 REM Initial acceleration is calculated and printed on file#1.
2120 CALL Initial(D(*),Apfo(*),F0(*),K(*),C(*),Offd2(*),Offd(*),
M(*),Dl(*),Delta,1,Pw,Neq,#1)
2130 FOR K1=1 TO Neq!Loop round the number of forces.
2140 PRINT "Force set";K1;" "
2150 ASSIGN #1 TO "Init1"
2160 MAT READ #1;D
2170 MAT READ #1;Offd
2180 FOR I=1 TO K1
2190 MAT READ #1;Offd2
2200 NEXT I
2210 MAT P=H*D
2220 INPUT "Node number to plot the displacements for?",Wplt
2230 FOR I=1 TO Nnode
2240 IF Kode(I,2)=1 THEN 2290
2250 G=G+1
2260 IF Wplt<>I THEN 2290
2270 Wpos=G
2280 GOTO 2300
2290 NEXT I
2300 Wcnt(1)=D(Wpos)
2310 INPUT "Node number to plot the moments for ?",Mplt
2320 IF Kode(Mplt,1)=0 THEN 2360
2330 BEEP
2340 DISP "Node";Mplt;" is free .Try again"
2350 GOTO 2310
2360 ! Determines position of Mplt
2370 G=0
2380 FOR I=1 TO Nnode
2390 IF Kode(I,1)=1 THEN 2440
2400 G=G+1
2410 IF Mplt<>I THEN 2440
2420 Mpos=G
2430 GOTO 2450
2440 NEXT I
2450 Mcnt(1)=P(Mpos)
2460 REM Calculation of response by Wilson theta method.
2470 LINK "WILSH1",5500
2480 LINK "Eqn",7250
2490 CALL Wilsh1(K(*),Vec(*),C(*),Apfo(*),F0(*),Dl(*),Offd(*),
Offd2(*),Dl(*),R0(*),Time,Delta,Theta,K1,P(*),H(*),Wcnt(*),
Mcnt(*),Mpos,Wpos,Pw,Pm)

```

```

2500 A$="DEFLECTION RESPONSE "
2510 B$="MOMENT RESPONSE"
2520 REM Response plots.
2530 LINK "FPLOT",5190
2540 CALL Plot(Wcnt(*),A$,Time,Delta,Wplt)
2550 CALL Plot(Mcnt(*),B$,Time,Delta,Mplt)
2560 LINPUT "File name for displacements?",Y$
2570 LINPUT "File name for moments?",M$
2580 ASSIGN #2 TO Y$
2590 ASSIGN #3 TO M$
2600 MAT PRINT #2;Wcnt
2610 MAT PRINT #3;Mcnt
2620 ASSIGN #2 TO *
2630 ASSIGN #3 TO *
2640 NEXT K1
2650 ASSIGN * TO #1
2660 BEEP
2670 PRINT "Execution terminated"
2680 END!OF PROGRAM
2690 Matge: ! SUBROUTINE TO EVALUATE [Ge]MATRIX
2700 Zeta(1)=.774596669241
2710 Zeta(2)=-Zeta(1)
2720 Zeta(3)=0
2730 MAT Ge=ZER(3,3)
2740 Y(1)=Y(2)=.555555555555
2750 Y(3)=.888888888888
2760 A=(Mi(Z,1)+Mi(Z,2))/2
2770 B=(Mi(Z,2)-Mi(Z,1))/2
2780 C=Leg(Z)/(2*E(Z))
2790 FOR I=1 TO 3
2800 Ge(1,1)=Ge(1,1)+Y(I)*(1/4*Zeta(I)^2*(-1+Zeta(I))^2)
2810 Ge(1,1)=Ge(1,1)/(A+B*Zeta(I))
2820 Ge(1,3)=Ge(1,3)-Y(I)*(-1/4*Zeta(I)^2*(Zeta(I)^2-1))
2830 Ge(1,3)=Ge(3,1)=Ge(1,3)/(A+B*Zeta(I))
2840 Ge(1,2)=Ge(1,2)-Y(I)*(-1/2*Zeta(I)*(Zeta(I)-1)*(1-Zeta(I)
)^2))
2850 Ge(1,2)=Ge(2,1)=Ge(1,2)/(A+B*Zeta(I))
2860 Ge(3,3)=Ge(3,3)+Y(I)*(1/4*Zeta(I)^2*(1+Zeta(I))^2)
2870 Ge(3,3)=Ge(3,3)/(A+B*Zeta(I))
2880 Ge(2,3)=Ge(2,3)+Y(I)*(1/2*Zeta(I)*(Zeta(I)+1)*(1-Zeta(I)^2))
2890 Ge(2,3)=Ge(3,2)=Ge(2,3)/(A+B*Zeta(I))
2900 Ge(2,2)=Ge(2,2)+Y(I)*(1-Zeta(I)^2)^2/(A+B*Zeta(I))
2910 NEXT I
2920 MAT Ge=(C)*Ge
2930 RETURN
2940 Matme: ! Subroutine to evaluate [Me] matrix
2950 Zeta(1)=.774596669241
2960 Zeta(2)=-Zeta(1)
2970 Zeta(3)=0
2980 MAT Me=ZER(3,3)
2990 Y(1)=Y(2)=.555555555555
3000 Y(3)=.888888888888
3010 A=(A(Z,1)+A(Z,2))/2
3020 B=(A(Z,2)-A(Z,1))/2
3030 C=Leg(Z)/2*Ro(Z)
3040 FOR I=1 TO 3
3050 Me(1,1)=Me(1,1)+Y(I)*(1/4*Zeta(I)^2*(-1+Zeta(I))^2)
3060 Me(1,1)=Me(1,1)*(A+B*Zeta(I))
3070 Me(1,3)=Me(1,3)-Y(I)*(-1/4*Zeta(I)^2*(Zeta(I)^2-1))
3080 Me(1,3)=Me(3,1)=Me(1,3)*(A+B*Zeta(I))
3090 Me(1,2)=Me(1,2)-Y(I)*(-1/2*Zeta(I)*(Zeta(I)-1)*(1-Zeta(I)
)^2))
3100 Me(1,2)=Me(2,1)=Me(1,2)*(A+B*Zeta(I))
3110 Me(3,3)=Me(3,3)+Y(I)*(1/4*Zeta(I)^2*(1+Zeta(I))^2)
3120 Me(3,3)=Me(3,3)*(A+B*Zeta(I))
3130 Me(2,3)=Me(2,3)+Y(I)*(1/2*Zeta(I)*(1+Zeta(I))*(1-Zeta(I)^2))

```

```

3140 Me(2,3)=Me(3,2)=Me(2,3)*(A+B*Zeta(I))
3150 Me(2,2)=Me(2,2)+Y(I)*(1-Zeta(I))^2/2*(A+B*Zeta(I))
3160 NEXT I
3170 MAT Me=(C)+Me
3180 RETURN
3190 Gasemb: ! Construction of [G]
3200 IF Z:=2 THEN GOTO 3320
3210 MAT U=ZER
3220 Gp=0
3230 IF Kode(Z,1)<>0 THEN 3260
3240 U(1)=1
3250 Gp=Gp+1
3260 U(2)=Gp+1
3270 Gp=U(2)
3280 IF Kode(2+Z+1,1)<>0 THEN 3390
3290 U(3)=Gp+1
3300 Gp=U(3)
3310 GOTO 3390
3320 U(1)=U(3)
3330 U(2)=Gp+1
3340 Gp=U(2)
3350 U(3)=0
3360 IF Kode(2*Z+1,1)<>0 THEN GOTO 3390
3370 U(3)=Gp+1
3380 Gp=U(3)
3390 GOSUB Gs
3400 RETURN
3410 Masemb: ! Construction of [G] matrix in reduced square
3420 ! form.
3430 IF Z:=2 THEN GOTO 3550
3440 MAT U=ZER
3450 Gp=0
3460 IF Kode(Z,2)<>0 THEN 3490
3470 U(1)=1
3480 Gp=Gp+1
3490 U(2)=Gp+1
3500 Gp=U(2)
3510 IF Kode(2+Z+1,2)<>0 THEN 3620
3520 U(3)=Gp+1
3530 Gp=U(3)
3540 GOTO 3620
3550 U(1)=U(3)
3560 U(2)=Gp+1
3570 Gp=U(2)
3580 U(3)=0
3590 IF Kode(2*Z+1,2)<>0 THEN GOTO 3620
3600 U(3)=Gp+1
3610 Gp=U(3)
3620 GOSUB Ms
3630 RETURN
3640 Hasemb: ! Construction of [H] matrix in reduced rectangular
3650 ! form.
3660 IF Z:=2 THEN GOTO 3910
3670 U(1)=U(2)=1
3680 U(3)=U(4)=2
3690 U(5)=U(6)=3
3700 IF Kode(Z,1)=0 THEN 3760
3710 U(1)=0
3720 U(3)=U(3)-1
3730 U(5)=U(5)-1
3740 V(1)=V(1)+1
3750 V(3)=V(3)+1
3760 IF Kode(Z,2)=0 THEN GOTO 3820
3770 U(2)=0
3780 U(4)=U(4)-1
3790 U(6)=U(6)-1

```

```

3800 V(2)=V(2)+1
3810 V(4)=V(4)+1
3820 IF Kode(2*Z+1,1)=0 THEN GOTO 3860
3830 U(5)=0
3840 V(1)=V(1)+1
3850 V(3)=V(3)+1
3860 IF Kode(2*Z+1,2)=0 THEN 3900
3870 U(6)=0
3880 V(2)=V(2)+1
3890 V(4)=V(4)+1
3900 GOTO 4070
3910 U(1)=U(5)
3920 U(2)=U(6)
3930 U(3)=2*Z-V(1)
3940 U(4)=2*Z-V(2)
3950 IF Kode(2*Z+1,1)=0 THEN 4000
3960 U(5)=0
3970 V(1)=V(1)+1
3980 V(3)=V(3)+1
3990 GOTO 4010
4000 U(5)=2*Z+1-V(3)
4010 IF Kode(2*Z+1,2)=0 THEN 4060
4020 U(6)=0
4030 V(2)=V(2)+1
4040 V(4)=V(4)+1
4050 GOTO 4070
4060 U(6)=2*Z+1-V(4)
4070 GOSUB Hs
4080 RETURN
4090 Gs: FOR I=1 TO 3
4100 FOR J=1 TO 3
4110 G=U(I)
4120 L=U(J)
4130 IF (G=0) OR (L=0) THEN 4150
4140 G(G,L)=G(G,L)+Gs(I,J)
4150 NEXT J
4160 NEXT I
4170 RETURN !Ms
4180 Ms: FOR I=1 TO 3
4190 FOR J=1 TO 3
4200 G=U(I)
4210 L=U(J)
4220 IF (G=0) OR (L=0) THEN 4240
4230 M(G,L)=M(G,L)+Ms(I,J)
4240 NEXT J
4250 NEXT I
4260 RETURN !Rs1
4270 Hs: FOR I=1 TO 5 STEP 2
4280 FOR J=2 TO 6 STEP 2
4290 G=U(I)
4300 L=U(J)
4310 IF (G=0) OR (L=0) THEN 4330
4320 H(G,L)=H(G,L)+Hs(I,J)
4330 NEXT J
4340 NEXT I
4350 RETURN !Hs
4360 Conf: ! Subroutine for concentrated loads
4370 DISP "Details of loading"
4380 INPUT "Number of nodes with concentrated loads?",W
4390 FOR I=1 TO W
4400 INPUT "Node number?",M,"Load value?",Fo
4410 Fo(M)=Fo
4420 NEXT I
4430 INPUT "Number of nodes with concentrated moments?",W
4440 FOR I=1 TO W
4450 INPUT "Node number?",M,"Concentrated moment?",Mo

```

```

4460 IF (M=1) OR (M=Nnode) THEN 4510
4470 Fo(M-1)=Fo(M-1)-1/Leg(M-1)*Mo
4480 Fo(M+1)=Fo(M+1)+1/Leg(M)*Mo
4490 Fo(M)=Fo(M)+Mo/Leg(M-1)-Mo/Leg(M)
4500 GOTO 4570
4510 IF M=1 THEN 4550
4520 Fo(M-1)=Fo(M-1)-1/Leg(M-1)*Mo
4530 Fo(M)=Fo(M)+Mo/Leg(M-1)
4540 GOTO 4570
4550 Fo(M+1)=Fo(M+1)+Mo/Leg(1)
4560 Fo(M)=Fo(M)-Mo/Leg(1)
4570 NEXT I
4580 RETURN
4590 Disf: ! Subroutine to evaluate for distributed loadings
4600 ! Load is assumed to vary linearly
4610 DISP "Details of distributed loading"
4620 PRINT
4630 DISP "Element number subjected to loading?"
4640 INPUT M
4650 INPUT "Load intensity at position 1",P1,"Load at 2?",P2
4660 Fo(2*M-1)=Fo(2*M-1)+(2*P1+P2)*(Leg(M)/6)
4670 Fo(2*M+1)=Fo(2*M+1)+(2*P2+P1)*(Leg(M)/6)
4680 INPUT "More loaded elements?if yes input the number ,else
0",M
4690 IF M THEN GOTO 4650
4700 DISP "Press CLEAR then CONT"
4710 PAUSE
4720 PRINT "Distributed loading information"
4730 PRINT
4740 PRINT "Node-coords";SPR(10);"Equivalent force"
4750 FOR N=1 TO Nnode
4760 PRINT USING "2(MD.4DE,10X)";Xcod(N),Fo(N)
4770 NEXT N
4780 RETURN
4790 SUB Wtipt(Wcnt(*),Mcnt(*),Kode(*),Time,Delta,A0(*),T,#1,
Nnode,INTEGER Pw)
4800 OPTION BASE 1
4810 REM Integration constants!Wilson method input subprogram
4820 DIM D(43),Offd(43)
4830 REDIM D(Pw),Offd(Pw)
4840 DISP "Integration constants"
4850 INPUT "What is the time duration?",Time
4860 INPUT "What is the time interval?",Delta
4870 PRINT
4880 PRINT USING "K,6X,MD.4DE";"Response duration",Time
4890 PRINT
4900 PRINT USING "K,7X,MD.4DE";"Time incremental",Delta
4910 REDIM Wcnt(INT(Time/Delta)+1),Mcnt(INT(Time/Delta)+1)
4920 INPUT "Select Theta[usually 1.4]?",T
4930 A0(1)=6/(T*Delta)^2
4940 A0(2)=3/(T*Delta)
4950 A0(3)=2*A0(2)
4960 A0(4)=T*Delta/2
4970 A0(5)=A0(1)/T
4980 A0(6)=-A0(3)/T
4990 A0(7)=1-3/T
5000 A0(8)=Delta/2
5010 A0(9)=Delta^2/6
5020 REM Initial displacement-velocity input
5030 DISP "Initial conditions"
5040 INPUT "If zero initial conditions press 0 otherwise 1
",In
5050 IF In<>0 THEN 5090
5060 MAT D=ZER
5070 MAT Offd=ZER
5080 GOTO 5230

```

```
5090 A=0
5100 FOR I=1 TO Nnode
5110 IF Kode(I,2) THEN GOTO 5150
5120 A=A+1
5130 DISP "Initial displacement of node";I;"
5140 INPUT D(I,A)
5150 NEXT I
5160 A=0
5170 FOR I=1 TO Nnode
5180 IF Kode(I,2) THEN 5220
5190 A=A+1
5200 DISP "Initial velocity of node";I;"
5210 INPUT Offd(I,A)
5220 NEXT I
5230 ASSIGN #1 TO "Initil:F"
5240 MAT PRINT #1;D
5250 MAT PRINT #1;Offd
5260 SUBEND
```

```

10  REM *****
20  REM * Free vibration analysis of thin plates by *
30  REM * Reissner's method. *
40  REM * *
50  REM * Program name:"RFPLT1:F8" *
60  REM * [Reissner's Plate Vibration] *
70  REM * *
80  REM * Version#1 Free vibration analysis. *
90  REM *****
100 OPTION BASE 1
110 PRINTER IS 16
120 PRINT PAGE,SPA(10),"PROGRAM INTRODUCTION#1",LIN(2)
130 PRINT "Thin plate vibration by mixed formulation:"
140 PRINT "The program is based on a mixed variational"
150 PRINT "principle known as Hellinger-Reissner's "
160 PRINT "principle.An 8 node quadrilateral finite "
170 PRINT "element is used for discretisation of the "
180 PRINT "plate.Lateral deflection is assumed to vary"
190 PRINT "parabolically inside the element.Bending and"
200 PRINT "twisting moments are also assumed to vary "
210 PRINT "parabolically.Latch PRT ALL press CONT"
220 PAUSE
230 DIM J(2,2),Ge(24,24),He(24,8),A#[30],Vec(27,27)
240 DIM Eval(27),D(27),Xx(65),Yy(65),Offd(27)
250 DIM Offd2(27,1),Me(8,8),C(10,6),Th(8),H(95,27),G(95,95)
260 DIM Dens(8),M(43,43),Dl(43),Cr(27,27),Ar(27,27),Bm(2,8)
270 DIM Sf(8),Sfm(8,8),W(9,4),Angsk(20),K(27,79)
280 INTEGER Nodc(65,4),Node(16,9),Nosk(20)
290 INTEGER Nmat,Matno,I,K,Jo,Z,Sol,N,Op,Cw,Cx,R,Type,Cy
300 INTEGER Cxy,Nskew,Fw,Fm,Nnode,Nelemt
310 REM Gause points and weights for numerical.integration.
320 A=.774596669241
330 B=0
340 C=.555555555555
350 D=.888888888888
360 W(1,1)=W(1,2)=W(2,2)=W(3,2)=W(4,1)=W(7,1)=-A
370 W(2,1)=W(4,2)=W(5,1)=W(5,2)=W(6,2)=W(8,1)=0
380 W(3,1)=W(6,1)=W(7,2)=W(8,2)=W(9,1)=W(9,2)=A
390 W(1,3)=W(1,4)=W(6,4)=W(2,3)=W(7,3)=W(7,4)=C
400 W(9,3)=W(9,4)=W(3,3)=W(3,4)=W(8,3)=W(4,3)=C
410 W(6,3)=W(2,4)=W(8,4)=W(4,4)=W(5,3)=W(5,4)=D
420 A=B=C=D=0
430 PRINT
440 DISP "Type in name of the input data file?,press CONT"
450 INPUT Data$
460 ASSIGN #1 TO Data$,C
470 IF NOT C THEN GOTO 520
480 BEEP
490 DISP "File not found.Try again"
500 WAIT 2000
510 GOTO 440
520 INPUT "What is the printer 16/0?",Printer
530 PRINTER IS Printer
540 INPUT "Type of the solution?1 for deflection,2 for m
oment eigenvectors",Type
550 PRINT ,SPA(1);"Vibration analysis of thin plates"
560 PRINT ,SPA(1);"-----"
570 PRINT
580 LINPUT "Type in name of the job.Not more than 30 charact
ers",A$
590 PRINT "Job name.....";A$;" "
600 READ #1;Njob,Nelemt,Nnode
610 PRINT LIN(2)
620 PRINT "Element selected:"
630 PRINT "8-node quadrilateral"

```

```

640 PRINT LIN(3)
650 PPRINT "Number of elements.....";Nelemt,LIN(2)
660 PRINT "Number of nodes .....";Nnode
670 READ #1;Cw,Cx,Cy,Cxy,Nmat,Nskew
680 Fm=3*Nnode-(Cx+Cy+Cxy)
690 Fw=Nnode-Cw
700 REDIM Xx(Nnode),Yy(Nnode),C(Nmat,6),Th(Nmat)
710 REDIM Dens(Nmat),G(Fm,Fm),H(Fm,Fw),M(Fw,Fw),Angsk(Nskew+1)
720 REDIM Node(Helemt,9),Nodc(Nnode,4),Nosk(Nskew+1)
730 IF Tipe=2 THEN GOTO 770
740 REDIM Vec(Fw,Fw),Eval(Fw),D(Fw),Offd(Fw)
750 REDIM Offd2(Fw,1),D1(Fw),K(Fw,Fw)
760 GOTO 790
770 REDIM Vec(Fm,Fm),Eval(Fm),D(Fm),Offd(Fm)
780 REDIM Offd2(Fm,1),D1(Fm),K(Fm,Fm)
790 LINK "INPPLT",1740
800 CALL Feinpt(Xx(*),Yy(*),#1,Nnode,Helemt,Cw,Cx,Cy,Cxy,Nod
e(*),Nodc(*))
810 FOR Matno=1 TO Nmat
820 CALL Cmatnx(C(*),Th(*),Dens(*),#1,Matno)
830 NEXT Matno
840 IF Nskew=0 THEN GOTO 880
850 FOR I=1 TO Nskew
860 READ #1;Nosk(I),Angsk(I)
870 NEXT I
880 REM Generation of mixed matrices [Ge] AND [He]
890 LINK "HEPLT",1740
900 IF Nskew=0 THEN GOTO 1000
910 PRINT
920 LINK "TRNPLT",3800
930 PPRINT "Nodal transformation."
940 PRINT
950 PPRINT "Node number",SPR(6),"N-X angle( DEG)"
960 PRINT
970 FOR I=1 TO Nskew
980 PRINT USING "(3D,22X,MD.4DE)";Nosk(I),Angsk(I)
990 NEXT I
1000 FOR Z=1 TO Nelemt
1010 MAT He=ZER
1020 MAT Sfm=ZER
1030 FOR U=1 TO 9
1040 CALL Qauv(W(U,1),W(U,2),Xx(*),Yy(*),Detj,Bm(*),Sf(*),Be,
Ds,Z,Node(*),6)
1050 FOR I=1 TO 8
1060 FOR J=I TO 8
1070 Sfm(I,J)=Sfm(I,J)+Sf(I)*Sf(J)+Detj+W(U,3)+W(U,4)
1080 NEXT J
1090 NEXT I
1100 CALL Heform(He(*),Bm(*),Detj,W(U,3),W(U,4))
1110 NEXT U
1120 CALL Geform(Ge(*),Sfm(*),C(*),Node(Z,9))
1130 CALL Mnsus(He(*),Xx(*),Yy(*),Bm(*),Sf(*),Be,Ds,Node(*),Z,K)
1140 IF Nskew=0 THEN GOTO 1210
1150 FOR I=1 TO Nskew
1160 FOR J=1 TO 8
1170 IF Nosk(I) .Node(Z,J) THEN GOTO 1190
1180 CALL Transf(Ge(*),He(*),Angsk(I),J)
1190 NEXT J
1200 NEXT I
1210 CALL Ghasemb(G(*),Ge(*),H(*),He(*),Fm,Z,Node(*),Nodc(*))
1220 NEXT Z
1230 FOR I=1 TO Fm
1240 FOR J=I TO Fm
1250 G(I,J)=G(J,I)
1260 NEXT J
1270 NEXT I

```



```

1280 REM Generation of mass matrix[M].
1290 LINK "ME1PLT",1740
1300 FOR Z=1 TO NElement
1310 MAT Me=ZER
1320 CALL Meform(Dens(*),Th(*),Me(*),Kx(*),Yy(*),W(*),Detj,Sf
(*),Bm(*),Node(*),Node(Z,9),Z)
1330 CALL Masemb(M(*),Me(*),Fw,Z,Node(*),Nodc(*))
1340 NEXT Z
1350 FOR I=1 TO Fw
1360 FOR J=I TO Fw
1370 M(I,J)=M(J,I)
1380 NEXT J
1390 NEXT I
1400 ! LINK "Eqsolv",1740 Choleski decomposition
1410 ! LINK "Gauss",1740 Simple Gaussian elimination
1420 LINK "PGauss",1740! Triangular decomposition with partial
pivoting.
1430 IF Type=1 THEN GOSUB Weigen
1440 IF Type=2 THEN GOSUB Meigen
1450 ASSIGN #1 TO *
1460 END!Of the program main routine.
1470 Weigen: ! Sub program for eigenvectors of <W>.
1480 CALL Eqsolv(G(*),H(*),K(*),Fw,Fm,Type)
1490 LINK "EGNIPT",1740
1500 CALL Eignipt(M1,M2,Lb,Ub,Fw,Sol)
1510 LINK "TRANS",1740
1520 CALL Trans(M(*),F(*),Vec(*),Eval(*),M1,M2,Lb,Ub,D(*),Offd
d(*),Offd2(*),D1(*),An(*),Cr(*),Type,Fw,Sol)
1530 IF Sol>3 THEN 1560
1540 LINK "EIGEN",1740
1550 CALL Eigen(M(*),K(*),Vec(*),Eval(*),M1,M2,Lb,Ub,D(*),Offd
d(*),Offd2(*),D1(*),An(*),Cr(*),Type,Fw,Sol)
1560 LINK "EVLV",1740
1570 CALL Evlv(M(*),K(*),Vec(*),Eval(*),M1,M2,Lb,Ub,D(*),Offd
(*),Offd2(*),D1(*),An(*),Cr(*),Type,Fw,Sol)
1580 RETURN !End of sub W
1590 Meigen: ! Sub program for eigenvectors of <M>.
1600 CALL Eqsolv(H(*),M(*),K(*),Fm,Fw,Type)
1610 LINK "EGNIPT",1640
1620 CALL Eignipt(M1,M2,Lb,Ub,Fm,Sol)
1630 LINK "TRANS",1640
1640 CALL Trans(G(*),K(*),Vec(*),Eval(*),M1,M2,Lb,Ub,D(*),Offd
d(*),Offd2(*),D1(*),An(*),Cr(*),Type,Fm,Sol)
1650 IF Sol>3 THEN GOTO 1680
1660 LINK "EIGEN",1740
1670 CALL Eigen(G(*),K(*),Vec(*),Eval(*),M1,M2,Lb,Ub,D(*),Offd
d(*),Offd2(*),D1(*),An(*),Cr(*),Type,Fm,Sol)
1680 LINK "EVLV",1740
1690 CALL Evlv(G(*),K(*),Vec(*),Eval(*),M1,M2,Lb,Ub,D(*),Offd
(*),Offd2(*),D1(*),An(*),Cr(*),Type,Fm,Sol)
1700 RETURN !End of sub M.

```

```

10  REM *****
20  REM +Forced vibration analysis of thin plates by *
30  REM +Reissner's method. *
40  REM +Program name is:"RFPLT2:F" *
50  REM + *
60  REM +Version#1:Free vibration analysis. *
70  REM +Version#2:Forced vibration response analysis*
80  REM +by mode superposition method. *
90  REM +Version#3:Forced vibration response analysis*
100 REM +by direct integration method. *
110 REM *****
120 OPTION BASE 1
130 PRINTER IS 16
140 PRINT PAGE,SPA(24),"PROGRAM INTRODUCTION #2",LIN(1)
150 PRINT "Thin plate vibration by mixed formulation:"
160 PRINT "The program is based on a mixed variational"
170 PRINT "principle known as Hellinger-Reissner's principle."
180 PRINT "An 8 node quadrilateral finite element is "
190 PRINT "used for discretisation of the plate."
200 PRINT "Lateral deflection is assumed to vary parabolically"
210 PRINT "inside the element:"
220 PRINT SPA(18);"W=a1+a2X+a3Y+a4XY+a5XY^2+a6YX^2+a7Y^2+a8X
^2",LIN(1)
230 PRINT "Bending and twisting moments also vary parabolically"
240 PRINT "inside the element:",LIN(1)
250 PRINT SPA(10);"Mx,My,Mxy=b1+b2X+b3Y+b4XY+b5XY^2+b6YX^2+b
7Y^2+b8X^2",LIN(1)
260 PRINT "Changes in input include:
"
270 PRINT "1-Nodal connections,2-Material number,"
280 PRINT "3-Element properties and 4-Element thickness."
290 PRINT "Orthotropic & isotropic materials may be used."
300 PRINT "In version#2 of this program,mode superposition "
310 PRINT "method is used in order to calculate time "
320 PRINT "response history of the plate displacements and"
330 PRINT "moments under the action of external loads.Press
CONT "
340 PAUSE
350 PRINT PAGE,SPA(15),"Data files required are",LIN(1)
360 PRINT
370 PRINT "Before running the program the following data "
380 PRINT
390 PRINT "files should be created:"
400 PRINT
410 PRINT "1-Data file[Initil:F]to be used for recording "
420 PRINT
430 PRINT "the initial conditions."
440 PRINT
450 PRINT "2-Data file[Eqn:F] to be used in order to "
460 PRINT
470 PRINT "print the excitation forces on."
480 PRINT "Create the data files,Latch PRT ALL and press
CONT."
490 PAUSE
500 DIM J(2,2),Ge(24,24),He(24,8),A#[20],Vec(26,26)
510 DIM Eval(26),D(26),Xx(65),Yy(65),Offd(26),Th(8)
520 DIM Offd2(26,1),Me(8,8),Const(10,6),H(95,26),G(95,95)
530 DIM Dens(8),M(26,26),Dl(26),Bm(2,8),K(27,96),Wt#[1][20]
540 DIM Vect(16,16),P1(45),Angsk(20),Mcont(1001),Initil(5)
550 DIM P(96),M1#[5][20],Wcont(1000),I#[160],T#[80]
560 DIM Sfr(8),Sfm(8,8),W(9,4),Apfo(30),F0(20),Dratio(20)
570 INTEGER Nodc(65,4),Node(16,9),Nosk(20),Type,R,Cv
580 INTEGER I,k,Jo,Z,Sol,N,Op,Cw,Cx
590 INTEGER Fw,Fm,Nnode,Helemt,Nmat,Matno
600 INTEGER Cxy,Nskew,J2,Nmode,Wplt,Mplt,Neq,Njob,Ndmode

```

```

610 REM Gauss points and weights for numerical integration.
620 A=.774596669241
630 B=0
640 C=.555555555555
650 D=.888888888888
660 W(1,1)=W(1,2)=W(2,2)=W(3,2)=W(4,1)=W(7,1)=-A
670 W(2,1)=W(4,2)=W(5,1)=W(5,2)=W(6,2)=W(8,1)=0
680 W(3,1)=W(5,1)=W(7,2)=W(8,2)=W(9,1)=W(9,2)=A
690 W(1,3)=W(1,4)=W(6,4)=W(2,3)=W(7,3)=W(7,4)=C
700 W(9,3)=W(9,4)=W(3,3)=W(3,4)=W(8,3)=W(4,3)=C
710 W(6,3)=W(2,4)=W(8,4)=W(4,4)=W(5,3)=W(5,4)=D
720 A=B=C=D=0
730 PRINT
740 DISP "Type in name of the input data file?,press CONT"
750 INPUT Data$
760 ASSIGN #1 TO Data$,C
770 IF NOT C THEN GOTO 820
780 BEEP
790 DISP "File not found.Try again"
800 WAIT 4000
810 GOTO 740
820 DISP "What is the printing device?16/0"
830 INPUT P
840 PRINTER IS P
850 P=0
860 PRINT ,SPR(1);"Vibration analysis of thin plates"
870 PRINT ,SPR(1);"-----"
880 PRINT
890 LINPUT "Type in name of the job.Not more than 20 characters",A$
900 PPINT "Job name.....";A$;" "
910 LINK "INPPLT",2860
920 CALL Feinpt(Xx(+),Yy(+),#1,Nnode,Nelemt,Njob,Cw,Cx,Cy,Cxy,
Nmat,Nskew,Nodc(+),Nodc(+))
930 Fm=3*Nnode-(Cx+Cy+Cxy)
940 Fw=Nnode-Cw
950 REDIM Xx(Nnode),Yy(Nnode),Cons(Nmat,6),Th(Nmat),Node(Nelemt,9)
960 REDIM Dens(Nmat),G(Fm,Fm),H(Fm,Fw),M(Fw,Fw),Apfo(Fw),F0(Fw)
970 REDIM Vec(Fw,Fw),Eval(Fw),D(Fw),Offd(Fw),Offd2(Fw,1),D1(Fw),k(Fw,Fw)
980 PEDIM P(Fw),Nodc(Nnode,4),P1(Fw),Vect(Fw,Fw),Angsk(Nskew+1),Hosk(Nskew+1)
990 FOR Matno=1 TO Nmat
1000 CALL Cmatrix(Cons(+),Th(+),Dens(+),#1,Matno)
1010 NEXT Matno
1020 IF Nskew=0 THEN GOTO 1060
1030 FOR I=1 TO Nskew
1040 READ #1;Hosk(I),Angsk(I)
1050 NEXT I
1060 REM Loading conditions.
1070 LINK "FLOAD",2860
1080 CALL Loadap(F0(+),W(+),Xx(+),Yy(+),Detj,Bm(+),Sf(+),Node(+),Nodc(+),Nnode,Nelemt)
1090 PRINT
1100 PPINT "Response analysis data:"
1110 REM Input excitation as a function of time.
1120 LINK "EXCITE",2860
1130 CALL Excitn(Neq)
1140 REM Input information concerning the forced vibration of plate.
1150 LINK "RFINPT",2860
1160 CALL Rsppt(Wcnt(+),Mcnt(+),Offd(+),D(+),Time,Delta,Init1(+),M#+(+),Wt#+(+),Dratio(+),Neq,Nnode,Fw,J2,Nmode,Wplt,Mplt,Nodc(+),Hdmode)
1170 REM Generation of mixed matrices [Ge] AND [He]

```

```

1180 LINK "HEPLT",2860
1190 IF Nskew=0 THEN GOTO 1290
1200 PRINT
1210 LINK "TRNPLT",5090
1220 PRINT "Nodal transformation."
1230 PRINT
1240 PRINT "Node number";SPA(7);"N-X angle(DEG)"
1250 PRINT
1260 FOR I=1 TO Nskew
1270 PRINT USING "(3D,22%,MD.4DE)";Nosk(I),Angsk(I)
1280 NEXT I
1290 FOR Z=1 TO Nelemt
1300 MAT He=ZER
1310 MAT Sfm=ZER
1320 FOR U=1 TO 9
1330 CALL Qaux(W(U,1),W(U,2),Xx(*),Yy(*),Detj,Bm(*),Sf(*),Be,
Ds,Z,Node(*),6)
1340 FOR I=1 TO 8
1350 FOR J=I TO 8
1360 Sfm(I,J)=Sfm(I,J)+Sf(I)*Sf(J)*Detj*W(U,3)+W(U,4)
1370 NEXT J
1380 NEXT I
1390 CALL Heform(He(*),Bm(*),Detj,W(U,3),W(U,4))
1400 NEXT U
1410 CALL Geform(Ge(*),Sfm(*),Const(*),Node(Z,9))
1420 CALL Mnsas(He(*),Xx(*),Yy(*),Bm(*),Sf(*),Be,Ds,Node(*),Z,K)
1430 IF Nskew=0 THEN GOTO 1500
1440 FOR I=1 TO Nskew
1450 FOR J=1 TO 8
1460 IF Nosk(I)<>Node(Z,J) THEN GOTO 1480
1470 CALL Transf(Ge(*),He(*),Angsk(I),J)
1480 NEXT J
1490 NEXT I
1500 CALL Ghasemb(G(*),Ge(*),H(*),He(*),Fm,Z,Node(*),Nodc(*))
1510 NEXT Z
1520 FOR I=1 TO Fm
1530 FOR J=I TO Fm
1540 G(I,J)=G(J,I)
1550 NEXT J
1560 NEXT I
1570 REM Generation of mass matrix[M].
1580 LINK "ME1PLT",2860
1590 FOR Z=1 TO Nelemt
1600 MAT Me=ZER
1610 CALL Meform(Dens(*),Th(*),Me(*),Xx(*),Yy(*),W(*),Detj,Sf
(*),Bm(*),Node(*),Node(Z,9),Z)
1620 CALL Masemb(M(*),Me(*),Fw,Z,Node(*),Nodc(*))
1630 NEXT Z
1640 FOR I=1 TO Fw
1650 FOR J=I TO Fw
1660 M(I,J)=M(J,I)
1670 NEXT J
1680 NEXT I
1690 ASSIGN #1 TO *!To close the finite element input data file.
1700 REM Response analysis starts here
1710 LINK "MODAL",2860
1720 CALL Eqso1o(H(*),G(*),f(*),P(*),Fw,Fm)
1730 CALL Modal(Vect(*),Eval(*),M(*),K(*),Dnat1o(*),D(*),Offd1(
*),Offd2(*),D1(*),Nnode,Fw,1,Sol,Ndmode)
1740 MAT Vect=TRN(Vect)
1750 REM Load vector transformation.
1760 MAT P1=Vect*F0
1770 MAT F0=P1
1780 REM Loop round the number of excitation forces.
1790 ASSIGN #1 TO "Initil:F"!To read non zero initial conditions.
1800 LINK "DUHAML",2860

```

```

1810 LINK "Eqn",5250
1820 FOR K1=1 TO Neq!Loop round the number of forces
1830 PRINT "Force set";K1;"
1840 IF Initial(K1) >0 THEN GOTO 1900
1850 MAT I=ZER!The 1st two columns of [K] are used as initial
      conditions
1860 !           in transformed coordinates.
1870 Wcnt(1)=0
1880 Mcnt(1)=0
1890 GOTO 2100
1900 MAT READ #1;D
1910 MAT READ #1;Offd
1920 REM Initial bending moments are calculated.
1930 P1=0
1940 FOR J=1 TO Fw
1950 P(Nodec(Mplt,J2))=P1+H(Nodec(Mplt,J2),J)+D(J)
1960 P1=P(Nodec(Mplt,J2))
1970 NEXT J
1980 Wcnt(1)=D(Nodec(Wplt,4))
1990 Mcnt(1)=P(Nodec(Mplt,J2))
2000 MAT P1=M*D
2010 MAT D=Vect+P1
2020 MAT P1=M*Offd
2030 MAT Offd=Vect*P1
2040 FOR I=1 TO Fw
2050 K(I,1)=D(I)
2060 K(I,2)=Offd(I)
2070 NEXT I
2080 MAT D=ZER
2090 MAT Offd=ZER
2100 REM Loop round the integration points
2110 Cnt=1
2120 T=0
2130 Npts=INT(Time/Delta)+1
2140 FOR Count=1 TO Npts-1
2150 T=T+Delta
2160 Cnt=Cnt+1
2170 CALL Eqn(T,F,K1)
2180 FOR Deg=1 TO Nmode
2190 F0=F*F0(Deg)
2200 Nf=SQR(Eval(Deg))
2210 IF Deg>Ndmode THEN GOTO 2240
2220 Ze=Dratio(Deg)
2230 GOTO 2250
2240 Ze=0
2250 Dnf=Nf*SQR(1-Ze^2)
2260 CALL Duhamel(T,Nf,Dnf,Ze,Delta,F0,D1(Deg),Offd(Deg),D(D
      eg),Offd2(Deg,1),Y,K(Deg,1),K(Deg,2),Initial(+),K1)
2270 Apfo(Deg)=1/Dnf+Y
2280 NEXT Deg
2290 REM Back transformation to system coordinates.
2300 FOR I=1 TO Fw
2310 A=0
2320 FOR J=1 TO Nmode
2330 P1(I)=A+Vec(I,J)*Apfo(J)
2340 A=P1(I)
2350 NEXT J
2360 NEXT I
2370 P1=0
2380 FOR J=1 TO Fw
2390 P(Nodec(Mplt,J2))=P1+H(Nodec(Mplt,J2),J)+P1(J)
2400 P1=P(Nodec(Mplt,J2))
2410 NEXT J
2420 Wcnt(Cnt)=P1(Nodec(Wplt,4))
2430 Mcnt(Cnt)=P(Nodec(Mplt,J2))
2440 MAT P1=ZER

```

```
2450 NEXT Count
2460 REM Response plots.
2470 CALL Plot(Wcnt(*),Wt$(1),Time,Delta,Wplt)
2480 CALL Plot(Mcnt(*),Mt$(J2),Time,Delta,Mplt)
2490 LINPUT "File name to print displacements on?",Fdisp$
2500 LINPUT "File name to print moments on?",Fstrs$
2510 ASSIGN #2 TO Fdisp$
2520 ASSIGN #3 TO Fstrs$
2530 MAT PRINT #2;Wcnt
2540 MAT PRINT #3;Mcnt
2550 ASSIGN #2 TO *
2560 ASSIGN #3 TO *
2570 NEXT K1
2580 ASSIGN * TO #1!To close file Initial
2590 BEEP
2600 PRINT "Execution terminated"
2610 END!Of program
```

```

10  REM *****
20  REM *Forced vibration analysis of thin plates by *
30  REM *
40  REM *Reissner's method Program name is:"RFPLT3:F" *
50  REM *
60  REM *Version#1:Free vibration analysis. *
70  REM *Version#2:Forced vibration response analysis. *
80  REM *by mode superposition method. *
90  REM *Version#3:Forced vibration response analysis. *
100 REM *by direct integration method. *
110 REM *****
120 OPTION BASE 1
130 PRINTER IS 16
140 PRINT PAGE,SPA(24),"PROGRAM INTRODUCTION #3",LIN(1)
150 PRINT "Thin plate vibration by mixed formulation:The"
160 PRINT "program is based on a mixed variational principle"
170 PRINT "known as Hellinger-Reissner's principle."
180 PRINT "An 8 node quadrilateral finite element is used"
190 PRINT "for discretisation of the plate.Lateral deflection"
200 PRINT "is assumed to vary parabolically inside the element"
210 PRINT SPA(18);"W=a1+a2X+a3Y+a4XY+a5XY^2+a6YX^2+a7Y^2+a8X
    ^2",LIN(1)
220 PRINT "Bending and twisting moments also vary parabolically"
230 PRINT "inside the element:",LIN(1)
240 PRINT SPA(18);"Mx,My,Mxy=b1+b2X+b3Y+b4XY+b5XY^2+b6YX^2+b
    7Y^2+b8X^2",LIN(1)
250 PRINT "Changes in input include: "
260 PRINT "1-Nodal connections,2-Material number,"
270 PRINT "3-Element properties and 4-Element thickness."
280 PRINT "Orthotropic & isotropic materials may be used."
290 PRINT "In version#3 of this program,an unconditionally"
300 PRINT "stable direct integration method known as "
310 PRINT "Wilson theta is used in order to calculate time "
320 PRINT "response history of the plate displacement and
    "
330 PRINT "moments under external loads.Press CONT.
    "
340 PAUSE
350 PRINT PAGE,SPA(15),"Data files required by the programs
    ",LIN(1)
360 PRINT
370 PRINT "Before running the program the following data "
380 PRINT
390 PRINT "files should be created: "
400 PRINT
410 PRINT "1-Data file[Initil:F]to be used for recording "
420 PRINT
430 PRINT "the initial conditions. "
440 PRINT
450 PRINT "2-Data file[Eqn:F] to be used in order to print "
460 PRINT
470 PRINT "the excitation forces on."
480 PRINT "Create the data files,Latch PRT ALL and press
    CONT."
490 PAUSE
500 DIM J(2,2),Ge(24,24),He(24,8),A$[20],Vec(27,27)
510 DIM Eval(27),D(27),Xx(65),Yy(65),OfFd(27),OfFd2(27,1)
520 DIM Me(8,8),Cons(10,6),Th(8),H(96,27),G(96,96),Dens(8)
530 DIM M(27,27),DI(27),Bm(2,8),K(27,96),C(27,27)
540 DIM P(96),Mt$(5)[20],Wcnt(1000),Angsk(20),Wt$(1)[20]
550 DIM Sf(8),Sfm(8,8),W(9,4),Apfo(30,1),F0(27)
560 DIM Dratio(20),Mcnt(1000),A0(9)
570 INTEGER Nodc(65,4),Node(16,9),Nosk(20),Fw,Fm,Nnode,Cy
580 INTEGER Nelemt,Nmat,Matno,I,K,Jo,Z,Sol,N,Op,Cw,Cx,R,Type
590 INTEGER Cxy,Nskew,J2,Nmode,Wplt,Mplt,Neq,Njob
    
```

```

600 REM Gauss points and weights for numerical integration.
610 A=.774596669241
620 B=0
630 C=.555555555555
640 D=.888888888888
650 W(1,1)=W(1,2)=W(2,2)=W(3,2)=W(4,1)=W(7,1)=-A
660 W(2,1)=W(4,2)=W(5,1)=W(5,2)=W(6,2)=W(8,1)=0
670 W(3,1)=W(6,1)=W(7,2)=W(8,2)=W(9,1)=W(9,2)=A
680 W(1,3)=W(1,4)=W(6,4)=W(2,3)=W(7,3)=W(7,4)=C
690 W(9,3)=W(9,4)=W(3,3)=W(3,4)=W(8,3)=W(4,3)=C
700 W(6,3)=W(2,4)=W(8,4)=W(4,4)=W(5,3)=W(5,4)=D
710 A=B=C=D=0
720 PRINT
730 DISP "Type in name of the input data file?,press CONT"
740 INPUT Data#
750 ASSIGN #1 TO Data#,C
760 IF NOT C THEN GOTO 810
770 BEEP
780 DISP "File not found.Try again"
790 WAIT 4000
800 GOTO 730
810 DISP "What is the printing device?16/0"
820 INPUT P
830 PRINTER IS P
840 P=0
850 PRINT ,SPA(1);"Vibration analysis of thin plates"
860 PRINT ,SPA(1);"-----"
870 PRINT
880 LINPUT "Type in name of the job.Not more than 20 characters",A#
890 PRINT "Job name.....";A#;" "
900 LINK "INPPLT",2300
910 CALL Feinpt(Xx(*),Yy(*),#1,Nnode,Nelemt,Njob,Cw,Cx,Cy,Cx
y,Nmat,Nskew,Node(*),Nodc(*))
920 PRINT LIN(2)
930 PRINT "Element selected:"
940 PRINT "8-node quadrilateral"
950 PRINT LIN(3)
960 PRINT "Number of elements.....";Nelemt,LIN(2)
970 PRINT "Number of nodes .....";Nnode
980 Fm=3+Nnode-(Cx+Cy+Cx)
990 Fw=Nnode-Cw
1000 REDIM Dens(Nmat),G(Fm,Fm),H(Fm,Fw),M(Fw,Fw),C(Fw,Fw)
1010 REDIM Vec(Fw,Fw),Eval(Fw),D(Fw),Offd1(Fw),Offd2(Fw,1)
1020 REDIM P(Fm),Angsk(Nskew+1),Nosk(Nskew+1),Cons(Nmat,6)
1030 REDIM Apfo(Fw,1),F0(Fw),Dl(Fw),K(Fw,Fw),Th(Nmat)
1040 FOR Matno=1 TO Nmat
1050 CALL Cmatrx(Cons(*),Th(*),Dens(*),#1,Matno)
1060 NEXT Matno
1070 IF Nskew=0 THEN GOTO 1110
1080 FOR I=1 TO Nskew
1090 READ #1;Nosk(I),Angsk(I)
1100 NEXT I
1110 REM Loading conditions.
1120 LINK "FLOAD",2300
1130 CALL Loadap(F0(*),W(*),Xx(*),Yy(*),Detj,Bm(*),Sf(*),Node
(*),Nodc(*),Nnode,Nelemt)
1140 PRINT
1150 PRINT "Response analysis data:"
1160 REM Input excitation as a function of time.
1170 LINK "EXCITE",2300
1180 CALL Excite(Neq)
1190 REM Input information concerning the forced vibration of
plate.
1200 LINK "FINPUT",2300
1210 CALL Rspipt(Wcnt(*),Mcnt(*),D(*),Offd(*),Mt$(*),Wt$(*),T
ime,Delta,Dratio(*),R0(*),Theta,#2,Neq,Nnode,Fw,J2,Nmode
,Wplt,Mplt,Nodc(*))

```



```

1220 REM Generation of mixed matrices [Ge] AND [He]
1230 LINK "HEPLT",2300
1240 IF Nskew=0 THEN GOTO 1340
1250 PRINT
1260 LINK "TRNPLT",6290
1270 PRINT "Nodal transformation."
1280 PRINT
1290 PRINT "Node number";SPA(7);"N-X angle(DEG)"
1300 PRINT
1310 FOR I=1 TO Nskew
1320 PRINT USING "<3D,22X,MD.4DE)";Nosk(I),Angsk(I)
1330 NEXT I
1340 FOR Z=1 TO Nelemt
1350 MAT He=ZER
1360 MAT Sfm=ZER
1370 FOR U=1 TO 9
1380 CALL Qaux(W(U,1),W(U,2),Xx(*),Yy(*),Detj,Bm(*),Sf(*),Be,
Ds,Z,Node(*),6)
1390 FOR I=1 TO 8
1400 FOR J=I TO 8
1410 Sfm(I,J)=Sfm(I,J)+Sf(I)*Sf(J)*Detj*W(U,3)*W(U,4)
1420 NEXT J
1430 NEXT I
1440 CALL Heform(He(*),Bm(*),Detj,W(U,3),W(U,4))
1450 NEXT U
1460 CALL Geform(Ge(*),Sfm(*),Cons(*),Node(Z,9))
1470 CALL Mnsws(He(*),Xx(*),Yy(*),Bm(*),Sf(*),Be,Ds,Node(*),Z,K)
1480 IF Nskew=0 THEN GOTO 1550
1490 FOR I=1 TO Nskew
1500 FOR J=1 TO 8
1510 IF Nosk(I)<>Node(Z,J) THEN GOTO 1530
1520 CALL Transf(Ge(*),He(*),Angsk(I),J)
1530 NEXT J
1540 NEXT I
1550 CALL Ghasemb(G(*),Ge(*),H(*),He(*),Fm,Z,Node(*),Nodc(*))
1560 NEXT Z
1570 FOR I=1 TO Fm
1580 FOR J=I TO Fm
1590 G(I,J)=G(J,I)
1600 NEXT J
1610 NEXT I
1620 REM Generation of mass matrix[M].
1630 LINK "ME1PLT",2300
1640 FOR Z=1 TO Nelemt
1650 MAT Me=ZER
1660 CALL Meform(Dens(*),Th(*),Me(*),Xx(*),Yy(*),W(*),Detj,Sf
(*),Bm(*),Node(*),Node(Z,9),Z)
1670 CALL Masemb(M(*),Me(*),Fw,Z,Node(*),Nodc(*))
1680 NEXT Z
1690 FOR I=1 TO Fw
1700 FOR J=I TO Fw
1710 M(I,J)=M(J,I)
1720 NEXT J
1730 NEXT I
1740 ASSIGN #1 TO *!To close the finite element input data file.
1750 REM Response analysis starts here
1760 LINK "FDAMP",2300
1770 CALL Eqsolu(H(*),G(*),K(*),P(*),Fw,Fm)
1780 REM Damping matrix evaluation
1790 IF Nmode=0 THEN GOTO 1810
1800 CALL Dampmat(C(*),Vec(*),Eval(*),M(*),K(*),Dratio(*),D(*
),Offd(*),Offd2(*),Dl(*),Nmode,Fw,Type,Sol)
1810 LINK "FINITL",2300
1820 MAT Vec=M
1830 CALL Eqsolu1(M(*),Dl(*),1,Fw)
1840 REM Initial acceleration is calculated and printed on file
#2.

```

```

1850 CALL Initial(D(*),Apfo(*),F0(*),K(*),C(*),Offd2(*),Offd(
*)M(*),Dl(*),Delta,1,Fw,Neq,#2)
1860 FOR K1=1 TO Neq!Loop round the number of forces
1870 PRINT "Force set";K1;"
1880 ASSIGN #1 TO "Initil"
1890 MAT READ #1;D
1900 MAT READ #1;Offd
1910 FOR I=1 TO K1
1920 MAT READ #1;Offd2
1930 NEXT I
1940 REM Calculation of displacement & bending moment at time
0
1950 Pi=0
1960 FOR J=1 TO Fw
1970 P(Nodc(Mplt,J2))=Pi+H(Nodc(Mplt,J2),J)*D(J)
1980 Pi=P(Nodc(Mplt,J2))
1990 NEXT J
2000 Wcnt(1)=D(Nodc(Wplt,4))
2010 Mcnt(1)=P(Nodc(Mplt,J2))
2020 REM Calculation of response by Wilson theta method.
2030 LINK "WILSNT",2300
2040 LINK "Eqn",4450
2050 CALL Wilnsol(K(*),Vec(*),C(*),Apfo(*),F0(*),D(*),Offd(
*),Offd2(*),Dl(*),A0(*),Time,Delta,Theta,K1,P(*),H(*),Wcn
t(*),Mcnt(*),Nodc(*),Mplt,Wplt,Fw,Fm,J2)
2060 REM Response plots.
2070 LINK "FPLOT",2300
2080 CALL Plot(Wcnt(*),Wt$(1),Time,Delta,Wplt)
2090 CALL Plot(Mcnt(*),Mt$(J2),Time,Delta,Mplt)
2100 LINPUT "File name to print displacements on?",Fdisp$
2110 LINPUT "File name to print stresses on?",Fstrs$
2120 ASSIGN #2 TO Fdisp$
2130 ASSIGN #3 TO Fstrs$
2140 MAT PRINT #2;Wcnt
2150 MAT PRINT #3;Mcnt
2160 ASSIGN #2 TO *
2170 ASSIGN #3 TO *
2180 NEXT K1
2190 ASSIGN * TO #1!To close file Initil
2200 BEEP
2210 PRINT "Execution terminated"
2220 END!Of program

```

```

10  SUB F=inpnt(X(*),Y(*),#1,INTEGER H,N1,Njb,Cw,Cx,Cy,Cxy,Nm
    at,Nskw,N(+),Ndc(*))
20  OPTION BASE 1
30  ! Nodal connection matrix is evaluated.
40  DIM K(32,4)
50  READ #1;Njb,N1,N,Cw,Cx,Cy,Cxy,Nmat,Nskw
60  REDIM X(N),Y(N),N(N1,9),Ndc(N,4)
70  Big=Cx
80  IF Cy>=Big THEN Big=Cy
90  IF Cxy>=Big THEN Big=Cxy
100 IF Cw>=Big THEN Big=Cw
110 IF Big<>0 THEN REDIM K(Big,4)
120 FOR I=1 TO N
130 READ #1;X(I),Y(I)
140 NEXT I
150 READ #1;N(*)
160 PRINT LIN(4)
170 PRINT "Nodal point data:",LIN(2)
180 PRINT "Node";SPA(4);"X-coord";SPA(5);"Y-coord"
190 FOR I=1 TO N
200 PRINT USING "3D,3X,2(MD.4DE,2X)";I,X(I),Y(I)
210 NEXT I
220 PRINT LIN(4)
230 PRINT "Element Data:";LIN(2)
240 PRINT "Element";SPA(18);"Nodal connections";SPA(19);"Mat
    erial"
250 FOR W=1 TO N1
260 PRINT USING "3D,7X,8(3D,2X),13X,2D";W,N(W,1),N(W,2),N(W,
    3),N(W,4),N(W,5),N(W,6),N(W,7),N(W,8),N(W,9)
270 NEXT W
280 MAT Ndc=ZER
290 FOR J=1 TO Cw
300 READ #1;K(J,1)
310 NEXT J
320 FOR J=1 TO Cx
330 READ #1;K(J,2)
340 NEXT J
350 FOR J=1 TO Cy
360 READ #1;K(J,3)
370 NEXT J
380 FOR J=1 TO Cxy
390 READ #1;K(J,4)
400 NEXT J
410 A=0
420 FOR I=1 TO N
430 FOR J=1 TO Cx
440 IF K(J,2)=I THEN My
450 NEXT J
460 Ndc(I,1)=A+1
470 A=Ndc(I,1)
480 My: FOR J=1 TO Cy
490 IF K(J,3)=I THEN Mxy
500 NEXT J
510 Ndc(I,2)=A+1
520 A=Ndc(I,2)
530 Mxy: FOR J=1 TO Cxy
540 IF K(J,4)=I THEN GOTO 580
550 NEXT J
560 Ndc(I,3)=A+1
570 A=Ndc(I,3)
580 NEXT I
590 FOR I=1 TO N
600 Ndc(I,4)=0
610 NEXT I
620 A=0

```

```

630   FOR I=1 TO N
640   FOR J=1 TO Cw
650   IF K(J,1)=I THEN GOTO 690
660   NEXT J
670   Ndc(I,4)=A+1
680   A=Ndc(I,4)
690   NEXT I
700   DISP "Nodal connection matrix is[for reducing [K] and [M]"
710   DISP Ndc(*);
720   SUBEND!End of feinput
730   SUB Cmatn(Z(*),Th(*),D(*),#1,INTEGER Mat)
740   REM Calculation of elastic constants for plate element
750   ! when several materials are present.
760   OPTION BASE 1
770   DIM A(5)
780   READ #1;Th(Mat),D(Mat)
790   READ #1;A(*)
800   IF Mat=1 THEN GOTO 840
810   PRINT LIN(3)
820   PRINT "Material and elastic properties",LIN(1)
830   PRINT "Mat.no";SPR(2);"Mat.Dens";SPR(3);"Elemt.thick";SP
A(3);"Exx      Eyy      Vxy      Gxy",LIN(1)
840   PRINT USING "2D,4X,6(MD.4DE, X)";Mat,D(Mat),Th(Mat),A(1)
,A(4),A(2),A(3)
850   C0=12/Th(Mat)^3
860   C11=C0*A(1)
870   C12=-C0*A(2)/A(4)
880   C13=0
890   C22=C0*A(4)
900   C23=0
910   C33=C0/A(3)
920   Z(Mat,1)=C11
930   Z(Mat,2)=C12
940   Z(Mat,3)=C13
950   Z(Mat,4)=C22
960   Z(Mat,5)=C23
970   Z(Mat,6)=C33
980   SUBEND !End of Cmatn.

```

```

10  SUB Daur(L1,L2,N(+),Y(+),U,Pm(+),Sf(*),Be,De,INTEGER Z,N
    (+),Jo)
20  OPTION BASE 1
30  DEFAULT ON
40  DIM J(2,2)
50  REM This sub program evaluates the jacobian J,
60  ! its determinant U ,and shape function
70  ! derivatives of W and M.
80  Dn1=1/4*(1-L2)*(2*L1+L2)
90  Dn2=1/4*(1-L1)*(2*L2+L1)
100 Dn3=1/4*(1-L2)*(2*L1-L2)
110 Dn4=-1/4*(1+L1)*(L1-2*L2)
120 Dn5=1/4*(1+L2)*(2*L1+L2)
130 Dn6=1/4*(1+L1)*(2*L2+L1)
140 Dn7=-1/4*(1+L2)*(-2*L1+L2)
150 Dn8=1/4*(1-L1)*(2*L2-L1)
160 Dn9=-L1*(1-L2)
170 Dn10=-1/2*(1-L1^2)
180 Dn11=1/2*(1-L2^2)
190 Dn12=-L2*(1+L1)
200 Dn13=-L1*(1+L2)
210 Dn14=-Dn10
220 Dn15=-Dn11
230 Dn16=-L2*(1-L1)
240 REM Shape functions
250 Sf(1)=1/4*(1-L1)*(1-L2)*(-L1-L2-1)
260 Sf(2)=1/4*(1+L1)*(1-L2)*(L1-L2-1)
270 Sf(3)=1/4*(1+L1)*(1+L2)*(L1+L2-1)
280 Sf(4)=1/4*(1-L1)*(1+L2)*(-L1+L2-1)
290 Sf(5)=1/2*(1-L1^2)*(1-L2)
300 Sf(6)=1/2*(1+L1)*(1-L2^2)
310 Sf(7)=1/2*(1-L1^2)*(1+L2)
320 Sf(8)=1/2*(1-L1)*(1-L2^2)
330 J(1,1)=Dn1*X(N(Z,1))+Dn3*X(N(Z,2))+Dn5*X(N(Z,3))+Dn7*X(N
    (Z,4))
340 J(1,1)=J(1,1)+Dn9*X(N(Z,5))+Dn11*X(N(Z,6))+Dn13*X(N(Z,7)
    )+Dn15*X(N(Z,8))
350 U1=J(1,1)
360 J(1,2)=Dn1*Y(N(Z,1))+Dn3*Y(N(Z,2))+Dn5*Y(N(Z,3))+Dn7*Y(N
    (Z,4))
370 J(1,2)=J(1,2)+Dn9*Y(N(Z,5))+Dn11*Y(N(Z,6))+Dn13*Y(N(Z,7)
    )+Dn15*Y(N(Z,8))
380 U2=J(1,2)
390 J(2,1)=Dn2*X(N(Z,1))+Dn4*X(N(Z,2))+Dn6*X(N(Z,3))+Dn8*X(N
    (Z,4))
400 J(2,1)=J(2,1)+Dn10*X(N(Z,5))+Dn12*X(N(Z,6))+Dn14*X(N(Z,7)
    )+Dn16*X(N(Z,8))
410 U3=J(2,1)
420 J(2,2)=Dn2*Y(N(Z,1))+Dn4*Y(N(Z,2))+Dn6*Y(N(Z,3))+Dn8*Y(N
    (Z,4))
430 J(2,2)=J(2,2)+Dn10*Y(N(Z,5))+Dn12*Y(N(Z,6))+Dn14*Y(N(Z,7)
    )+Dn16*Y(N(Z,8))
440 U4=J(2,2)
450 REM U replaces DETJ
460 U=U1+U4-U2+U3
470 IF Jo=5 THEN SUBEXIT
480 J(1,1)=J(2,2)/U
490 J(1,2)=-J(1,2)/U
500 J(2,1)=-J(2,1)/U
510 J(2,2)=U1/U
520 ! Determination of p[2,8],derivatives of W shape functions.
530 FOR I=1 TO 2
540 Pm(I,1)=Dn1*J(I,1)+Dn2*J(I,2)
550 Pm(I,2)=Dn3*J(I,1)+Dn4*J(I,2)
560 Pm(I,3)=Dn5*J(I,1)+Dn6*J(I,2)

```

```
570 Pm(I,4)=Dn7*J(I,1)+Dn8*J(I,2)
580 Pm(I,5)=Dn9*J(I,1)+Dn10*J(I,2)
590 Pm(I,6)=Dn11*J(I,1)+Dn12*J(I,2)
600 Pm(I,7)=Dn13*J(I,1)+Dn14*J(I,2)
610 Pm(I,8)=Dn15*J(I,1)+Dn16*J(I,2)
620 NEXT I
630 IF Jo=5 THEN SUBEXIT
640 ON Jo GOSUB Side1,Side2,Side3,Side4
650 DEFAULT OFF
660 SUBEXIT
670 Side1: Be=ATN(ABS(U1/U2))
680 Ds=SQR(U1^2+U2^2)
690 IF U2<0 THEN Be=PI+Be
700 IF U2>=0 THEN Be=-Be
710 RETURN
720 Side3: Be=ATN(ABS(U1-U2))
730 Ds=SQR(U1^2+U2^2)
740 U1=-1*U1
750 U2=-1*U2
760 IF U2<0 THEN Be=PI-Be
770 RETURN
780 Side2: Be=ATN(ABS(U3/U4))
790 Ds=SQR(U3^2+U4^2)
800 IF (U4>0) AND (U3>0) THEN Be=-Be
810 RETURN
820 Side4: Be=ATN(ABS(U3/U4))
830 Ds=SQR(U3^2+U4^2)
840 U3=-U3
850 U4=-U4
860 IF (U4<0) AND (U3>0) THEN Be=PI+Be
870 IF (U4>=0) OR (U3<=0) THEN Be=PI-Be
880 RETURN
890 SUBEND!End of Qaux.
```

```

10  SUB Excitn(INTEGER Neq)
20  OPTION BASE 1
30  DIM I$(160),T$(80)
40  DISP "Excitation as a function of time"
50  REM File "Eqn:F" is opened to input the forces.
60  INPUT "Is this a re-run 1=yes,0=no?",Re
70  IF NOT Re THEN GOTO 110
80  BEEP
90  INPUT "How many equations?",Neq
100 GOTO 450
110 ASSIGN #2 TO "Eqn:F"
120 T$="SUB EXIT"
130 J=0
140 FOR N=2010 TO 2100 STEP 10
150 J=J+1
160 I$(1,5)=VAL$(N)
170 I$(6,10)="L"&VAL$(J)&": "
180 LINPUT "Equation is?(e.g type F=SIN(10*T))",I$(11)
190 PRINT "E citation function(";J;") is: ";I$(11)
200 PRINT #2;I$
210 BEEP
220 DISP "Any more statements concerning",I$(11)
230 INPUT "1 or 0",A
240 IF NOT A THEN 310
250 N=N+1
260 I$(1,5)=VAL$(N)
270 LINPUT "Type in the statement",I$(6)
280 PRINT #2;I$
290 PRINT SPA(23),I$(6)
300 GOTO 210
310 I$(1,5)=VAL$(N+1)
320 I$(6)=T$
330 PRINT #2;I$
340 INPUT "Any more equations?1/0",More
350 IF More THEN GOTO Nextn
360 Neq=J
370 I$(1,5)=VAL$(2110)
380 I$(6)="SUB END"
390 PRINT #2;I$
400 GOTO Ed
410 Nextn: PRINT
420 NEXT N
430 Ed: PRINT #2;END
440 ASSIGN #2 TO *
450 SUBEND

```

```

10  SUB Pspipt(Wc(*),Mc(*),D(*),Of(*),Mt$(*),Wt$(*),Time,Delta,Dr(*),A0(*),T,#1,INTEGER Ndc,Nnode,Fw,J2,Nmod,Wp,Mp,Ndc(*))
20  OPTION BASE 1
30  REM Input information regarding Wilson theta
40  ! direct integration method for forced
50  ! vibration analysis of plates.
60  DISP "Integration constants"
70  INPUT "What is the time duration?",Time
80  INPUT "What is the time interval?",Delta
90  PRINT
100 PRINT USING "K,1K,MD.4DE";"Response duration",Time
110 PRINT
120 PRINT USING "K,2X,MD.4DE";"Time incremental",Delta
130 REDIM Wc(INT(Time/Delta)+1),Mc(INT(Time/Delta)+1)
140 INPUT "Select theta[usually 1.4]",T
150 A0(1)=6/(T*Delta)^2
160 A0(2)=3/(T*Delta)
170 A0(3)=2*A0(2)
180 A0(4)=T*Delta/2
190 A0(5)=A0(1)/T
200 A0(6)=-A0(3)/T
210 A0(7)=1-3/T
220 A0(8)=Delta/2
230 A0(9)=Delta^2/6
240 REM Initial displacement-velocity input
250 DISP "Initial conditions"
260 INPUT "If initial conds are zero press 0 otherwise 1",In
270 IF In<>0 THEN GOTO 310
280 MAT D=ZER
290 MAT Of=ZER
300 GOTO 410
310 FOR I=1 TO Nnode
320 IF Ndc(I,4)=0 THEN GOTO 350
330 DISP "Initial displ.of node";I;"?"
340 INPUT D(Ndc(I,4))
350 NEXT I
360 FOR I=1 TO Nnode
370 IF Ndc(I,4)=0 THEN GOTO 400
380 DISP "Initial veloc.of node";I;"?"
390 INPUT Of(Ndc(I,4))
400 NEXT I
410 ASSIGN #1 TO "Initil:F"
420 MAT PRINT #1;D
430 MAT PRINT #1;Of
440 DISP "Information regarding damping"
450 INPUT "Is the damping significant?1=0",Damp
460 IF NOT Damp THEN GOTO 530
470 INPUT "Number of modes with damping?",Nmod
480 REDIM Dr(Nmod)
490 FOR I=1 TO Nmod
500 DISP "Damping ratio in mode";I;"?"
510 INPUT Dr(I)
520 NEXT I
530 BEEP
540 DISP "Displacement/moment time history plot"
550 INPUT "Node number to plot the displacements for?",Wp
560 INPUT "Node number to plot moment for?",Mp
570 INPUT "Code?[1 for Mx-2 for My-3 for Mxy]",J2
580 Mt$(1)="BENDING MOMENT-X"
590 Mt$(2)="BENDING MOMENT-Y"
600 Mt$(3)="TWISTING MOMENT-XY"
610 Wt$(1)="DEFLECTION-Z"
620 SUBEND

```



```

10    SUB Loadap(R(*),W(*),Z(*),Y(*),Det,j,Bm(*),Sf(*),INTEGER
      N(*),Ndc(*),Nnode,Nelemt)
20    OPTION BASE 1
30    DIM P(8),Re(8),E1(20)
40    INTEGER E1
50    REM Equivalent nodal forces due to concentrated or
60    ' distributed loading conditions are determined
70    DISP "Load information"
80    DISP "The following load cases can be accomodated:"
90    DISP "1) Concentrated nodal forces consisting of "
100   DISP "   loads acting in Z directn."
110   DISP "2) Constantly distributed load acting normal to pl
      ate."
120   DISP "3) Varying distributed load acting normal to plate."
130   DISP "Such loading is converted into equivalent nodal fo
      rces."
140   INPUT "Load type?1 for conc.2 for constant distrd.3
      for varying distrd",Type
150   IF Type=1 THEN GOSUB Conc
160   IF Type=2 THEN GOSUB Cdis
170   IF Type=3 THEN GOSUB Vdis
180   BEEP
190   DISP "Press 1 if more loading and 0 to stop loading"
200   INPUT M
210   IF NOT M THEN Printout
220   GOTO 140
230   Conc: INPUT "Number of nodes with concentrated loads",N
240   FOR I=1 TO N
250    INPUT "Node number?",S1,"Value of load?",Val
260    IF Ndc(S1,4) <> 0 THEN GOTO 300
270    BEEP
280    DISP "Made a mistake.Try again"
290    GOTO 250
300    R(Ndc(S1,4))=R(Ndc(S1,4))+Val
310    NEXT I
320    RETURN
330   Cdis: INPUT "Number of elements with loading",Nel
340   IF Nel <= Nelemt THEN GOTO 370
350    BEEP
360    GOTO 330
370    PEDIM E1(Nel)
380    INPUT "Load per unit area?",P
390    FOR I=1 TO 8
400    P(I)=P
410    NEXT I
420    IF Nel=Nelemt THEN 480
430    DISP "Input elements under pressure one by one.Each time
      press CONT"
440    FOR Z=1 TO Nel
450    INPUT "Element number?",E1(Z)
460    NEXT Z
470    GOTO 510
480    FOR Z=1 TO Nelemt
490    E1(Z)=Z
500    NEXT Z
510    FOR Z=1 TO Nel
520    E1=E1(Z)
530    GOSUB Calc
540    MAT Pe=ZER
550    NEXT Z
560    RETURN
570    Vdis: INPUT "Number of elements with loading",Nel
580    FOR Z=1 TO Nel
590    INPUT "Element number?",E1
600    FOR I=1 TO 8

```

```

610  DISP "Load intensity at station";I;"?"
620  INPUT PrI
630  NEXT I
640  GOSUB Calc
650  MAT Re=ZER
660  NEXT Z
670  RETURN
680 Calc:  FOR U=1 TO 9
690  CALL Qaux(W(U,1),W(U,2),X(*),Y(*),Det,j,Bm(*),Sf(*),Be,Da
      ,E1,N(*),5)
700  FOR I=1 TO 8
710  FOR J=1 TO 8
720  Pe(I)=Pe(I)+Sf(I)+Sf(J)+P(J)+Det.j+W(U,3)*W(U,4)
730  NEXT J
740  NEXT I
750  NEXT U
760  FOR I=1 TO 8
770  S1=Ndc(N(E1,I),4)
780  IF S1=0 THEN GOTO 800
790  R(S1)=R(S1)+Re(I)
800  NEXT I
810  RETURN
820 Printout:  PPINT
830  PPINT "Equivalent nodal forces"
840  PRINT
850  PRINT "Node number";SPA(7);"Applied loads"
860  FOR I=1 TO Nnode
870  IF Ndc(I,4)=0 THEN GOTO 900
880  PRINT USING "3D,15X,MD.4DE";I,R(Ndc(I,4))
890  GOTO 910
900  PRINT USING "3D,15X,MD.4DE";I,0
910  NEXT I
920  SUBEXIT
930  RETURN
940  SUBEND

```

```

10  SUB Heform(He(*),Bm(*),Det j,T1,T2)
20  ! [He] matrix construction.
30  OPTION BASE 1
40  FOR I=1 TO 9
50  FOR J=1 TO 4
60  He(3*I-2,2*J-1)=He(3*I-2,2*J-1)+Bm(1,I)+Bm(1,2*J-1)+Det j
    *T1+T2
70  He(3*I-2,2*J)=He(3*I-2,2*J)+Bm(1,I)+Bm(1,2*J)+Det j*T1*T2
80  He(3*I-1,2*J-1)=He(3*I-1,2*J-1)+Bm(2,I)+Bm(2,2*J-1)+Det j
    +T1+T2
90  He(3*I-1,2*J)=He(3*I-1,2*J)+Bm(2,I)+Bm(2,2*J)+Det j*T1*T2
100 He(3*I,2*J-1)=He(3*I,2*J-1)+(Bm(2,I)+Bm(1,2*J-1)+Bm(1,I)
    +Bm(2,2*J-1))+Det j*T1*T2
110 He(3*I,2*J)=He(3*I,2*J)+(Bm(2,I)+Bm(1,2*J)+Bm(1,I)+Bm(2,
    2*J))+Det j+T1*T2
120 NEXT J
130 NEXT I
140 SUBEND!End of Heform.
150 SUB Geform(Ge(*),A(*),C(*),INTEGER Matno)
160 MAT Ge=ZER
170 FOR I=1 TO 8
180 FOR S=I TO 8
190 A=A(I,S)
200 IF I=S THEN GOTO 290
210 Ge(3*I-2,3*S-2)=A+C(Matno,1)
220 Ge(3*I-2,3*S-1)=A+C(Matno,2)
230 Ge(3*I-1,3*S-2)=A+C(Matno,2)
240 Ge(3*I-1,3*S-1)=A+C(Matno,4)
250 Ge(3*I,3*S-2)=A+C(Matno,3)
260 Ge(3*I,3*S-1)=A+C(Matno,5)
270 Ge(3*I,3*S)=A+C(Matno,6)
280 GOTO 330
290 Ge(3*I-2,3*S-2)=A*C(Matno,1)
300 Ge(3*I-2,3*S-1)=A*C(Matno,2)
310 Ge(3*I-1,3*S-1)=A*C(Matno,4)
320 Ge(3*I,3*S)=A+C(Matno,6)
330 NEXT S
340 NEXT I
350 FOR I=1 TO 24
360 FOR J=I TO 24
370 Ge(J,I)=Ge(I,J)
380 NEXT J
390 NEXT I
400 SUBEND!End of Geform.
410 SUB Mnsus(He(*),X(*),Y(*),Bm(*),Sf(*),Be,Ds,INTEGER N(*),
    Z,K)
420 OPTION BASE 1
430 DIM C(24,1),D(1,8),Zn(2,8)
440 A=.577350269
450 FOR I=1 TO 2
460 FOR J=2 TO 7 STEP 5
470 Zn(I,J)=-1
480 NEXT J
490 FOR J=3 TO 6 STEP 3
500 Zn(I,J)=1
510 NEXT J
520 NEXT I
530 Zn(1,1)=Zn(1,4)=Zn(1,5)=Zn(1,8)=-A
540 Zn(2,1)=Zn(2,4)=Zn(2,5)=Zn(2,8)=A
550 FOR I=1 TO 4
560 FOR I=1 TO 2
570 CALL Dau(Zn(I,2+K-1),Zn(I,2+K),X(*),Y(*),Det j,Bm(*),Sf(
    *),Be,Ds,Z,N(*),K)
580 Be=Be*360/(2*PI)
590 DEG
    
```

```

600 L1=-COS(Be)*SIN(Be)
610 L2=COS(Be)*SIN(Be)
620 L3=COS(Be)^2-SIN(Be)^2
630 L4=-SIN(Be)
640 L5=COS(Be)
650 FOR S=1 TO 8
660 C(3+S-2,1)=L1*Sf(S)
670 C(3+S-1,1)=L2*Sf(S)
680 C(3+S,1)=L3*Sf(S)
690 NEXT S
700 FOR S=1 TO 8
710 D(1,S)=L4*Bm(1,S)+L5*Bm(2,S)
720 NEXT S
730 IF (K=1) OR (K=3) THEN Ds=-Ds
740 MAT D=(Ds)*D
750 FOR S=1 TO 24
760 FOR J=1 TO 8
770 He(S,J)=He(S,J)+C(S,1)+D(1,J)
780 NEXT J
790 NEXT S
800 NEXT I
810 NEXT K
820 SUBEND!End of Mnsus
830 SUB Ghasemb(K(*),Ke(*),H(*),He(*),INTEGER Fm,Z,N(*),Ndc(*))
840 ! Assembly of coefficient matrices [G] and[H].
850 FOR I=1 TO 8
860 FOR J=1 TO 8
870 FOR V=2 TO 0 STEP -1
880 S1=Ndc(N(Z,I),1)
890 S3=Ndc(N(Z,I),2)
900 S5=Ndc(N(Z,I),3)
910 IF V=2 THEN S2=Ndc(N(Z,J),1)
920 IF V=1 THEN S2=Ndc(N(Z,J),2)
930 IF V=0 THEN S2=Ndc(N(Z,J),3)
940 IF S2=0 THEN L1
950 IF (S1=0) OR (S1<S2) THEN L2
960 K(S1,S2)=K(S1,S2)+Ke(3*I-2,3*J-V)
970 L2: IF S3=0 THEN GOTO L3
980 IF S3<S2 THEN L3
990 K(S3,S2)=K(S3,S2)+Ke(3*I-1,3*J-V)
1000 L3: IF S5=0 THEN L1
1010 IF S5>S2 THEN L1
1020 K(S5,S2)=K(S5,S2)+ke(3*I,3*J-V)
1030 L1: NEXT V
1040 NEXT J
1050 NEXT I
1060 FOR J=1 TO 8! [H] Assembly
1070 S4=Ndc(N(Z,J),4)
1080 IF S4=0 THEN Nexj
1090 FOR I=1 TO 8
1100 FOR V=0 TO 2
1110 S1=Ndc(N(Z,I),V+1)
1120 IF S1=0 THEN Nexv
1130 H(S1,S4)=H(S1,S4)+He(3*I-2+V,J)
1140 Nexv:NEXT V
1150 NEXT I
1160 Nexj:NEXT J
1170 SUBEND!End ofGhasemb

```

```

10  SUB Transf(Ge(+),He(+),Be,W)
20  OPTION BASE 1
30  DIM B(3,3)
40  GOSUB Cosd
50  FOR I=1 TO 24
60  FOR J=I TO 24
70  Ge(J,I)=Ge(I,J)
80  NEXT J
90  NEXT I
100 GOTO 300
110 Cosd: ! Transformation of coordinates.
120 DEG
130 B(1,1)=B(2,2)=SIN(Be)^2
140 B(1,2)=B(2,1)=COS(Be)^2
150 B(1,3)=-2*SIN(Be)*COS(Be)
160 B(2,3)=-B(1,3)
170 B(3,1)=B(1,3)/2
180 B(3,2)=-B(3,1)
190 B(3,3)=COS(Be)^2-SIN(Be)^2
200 MAT B=INV(B)
210 FOR T=1 TO W-1 STEP 1
220 CALL Matmult2(T,W,Ge(*),B(*))
230 NEXT T
240 FOR V=W+1 TO 8 STEP 1
250 CALL Matmult1(W,V,Ge(*),B(*))
260 NEXT V
270 CALL Matmult(W,W,Ge(*),B(*))
280 CALL Matmult3(W,1,He(*),B(*))
290 RETURN
300 SUBEND
310 SUB Matmult1(T,V,Ge(*),B(*))
320 OPTION BASE 1
330 DIM C(3,3)
340 REM [B]t+[C]
350 C(1,1)=Ge(3*T-2,3*V-2)
360 C(1,2)=Ge(3*T-2,3*V-1)
370 C(1,3)=Ge(3*T-2,3*V)
380 C(2,1)=Ge(3*T-1,3*V-2)
390 C(2,2)=Ge(3*T-1,3*V-1)
400 C(2,3)=Ge(3*T-1,3*V)
410 C(3,1)=Ge(3*T,3*V-2)
420 C(3,2)=Ge(3*T,3*V-1)
430 C(3,3)=Ge(3*T,3*V)
440 FOR I=1 TO 3
450 FOR J=1 TO 3
460 A=0
470 FOR R=1 TO 3
480 Ge(3*T-3+I,3*V-3+J)=A+B(R,I)*C(R,J)
490 A=Ge(3*T-3+I,3*V-3+J)
500 NEXT R
510 NEXT J
520 NEXT I
530 SUBEND!END OF Matmult1
540 SUB Matmult2(T,V,Ge(*),B(*))
550 OPTION BASE 1
560 DIM C(3,3)
570 REM [C]+[B]
580 C(1,1)=Ge(3*T-2,3*V-2)
590 C(1,2)=Ge(3*T-2,3*V-1)
600 C(1,3)=Ge(3*T-2,3*V)
610 C(2,1)=Ge(3*T-1,3*V-2)
620 C(2,2)=Ge(3*T-1,3*V-1)
630 C(2,3)=Ge(3*T-1,3*V)
640 C(3,1)=Ge(3*T,3*V-2)
650 C(3,2)=Ge(3*T,3*V-1)

```

```

660 C(3,3)=Ge(3*T,3*V)
670 FOR I=1 TO 3
680 FOR J=1 TO 3
690 A=0
700 FOR R=1 TO 3
710 Ge(3*T-3+I,3*V-3+J)=A+C(I,R)+B(R,J)
720 A=Ge(3*T-3+I,3*V-3+J)
730 NEXT R
740 NEXT J
750 NEXT I
760 SUBEND!End of Matmult2
770 SUB Matmult(T,V,Ge(*),B(*))
780 OPTION BASE 1
790 DIM C(3,3)
800 REM [B]t*[C]*[B]
810 C(1,1)=Ge(3*T-2,3*V-2)
820 C(1,2)=Ge(3*T-2,3*V-1)
830 C(1,3)=Ge(3*T-2,3*V)
840 C(2,2)=Ge(3*T-1,3*V-1)
850 C(2,3)=Ge(3*T-1,3*V)
860 C(3,3)=Ge(3*T,3*V)
870 FOR I=1 TO 3
880 FOR J=I TO 3
890 C(J,I)=C(I,J)
900 NEXT J
910 NEXT I
920 FOR P=1 TO 3
930 FOR S=1 TO 3
940 A=0
950 FOR I=1 TO 3
960 FOR J=1 TO 3
970 Ge(3*T-3+R,3*V-3+S)=A+B(I,R)+C(I,J)*B(J,S)
980 A=Ge(3*T-3+R,3*V-3+S)
990 NEXT J
1000 NEXT I
1010 NEXT S
1020 NEXT P
1030 SUBEND!End of Matmult
1040 SUB Matmult3(T,V,He(*),B(*))
1050 OPTION BASE 1
1060 DIM C(3,8),V(3)
1070 REM [B]t*[He]
1080 V(1)=2
1090 V(2)=1
1100 V(3)=0
1110 FOR I=1 TO 3
1120 FOR J=1 TO 8
1130 C(I,J)=He(3*T-V(I),J)
1140 NEXT J
1150 NEXT I
1160 FOR I=1 TO 3
1170 FOR J=1 TO 8
1180 A=0
1190 FOR R=1 TO 3
1200 He(3*T-3+I,J)=A+B(R,I)*C(R,J)
1210 A=He(3*T-3+I,J)
1220 NEXT R
1230 NEXT J
1240 NEXT I
1250 SUBEND !End of Matmult3

```

```

10  SUB Meform(D(*),Th(*),Me(*),X(*),Y(*),W(*),Detj,Sf(*),Bm
    (*),INTEGER N(*),Matno,Z)
20  REM Determination of consistant mass matrix for
30  ! plate element.
40  FOR U=1 TO 9
50  CALL Gau(W/U,1),W(U,2),X(*),Y(*),Detj,Bm(*),Sf(*),Be,Da
    (Z,H(*),5)
60  FOR I=1 TO 8
70  FOR J=I TO 8
80  Me(I,J)=Me(I,J)+Sf(I)+Sf(J)+Detj*W(U,3)*W(U,4)
90  NEXT J
100 NEXT I
110 NEXT U
120 MAT Me=(D(Matno)*Th(Matno))*Me
130 FOR I=1 TO 8
140 FOR J=I TO 8
150 Me(J,I)=Me(I,J)
160 NEXT J
170 NEXT I
180 SUBEND !End of Meform.
190 SUB Masemb(M(*),Me(*),INTEGER Fw,Z,N(*),Ndc(*))
200 ! Mass matrix assembly
210 FOR I=1 TO 8
220 S1=Ndc(N(Z,I),4)
230 IF S1=0 THEN GOTO 290
240 FOR J=1 TO 8
250 S2=Ndc(N(Z,J),4)
260 IF (S2=0) OR (S1=S2) THEN GOTO 280
270 M(S1,S2)=M(S1,S2)+Me(I,J)
280 NEXT J
290 NEXT I
300 SUBEND !End of Masemb.

```

```

10 SUB Dampmat(C(*),Vec(*),Eval(*),M(*),K(*),Zeta(*),D(*),O
ffd(*),Offd2(*),D1(*),INTEGER P,N,Type,Sol)
20 REM Evaluation of a full damping matrix with
30 ! known damping ratios.
40 OPTION BASE 1
50 DIM Theta(20)
60 REDIM Theta(N)
70 PRINT "Evaluation of normal modes of vibration "
80 PRINT "-----"
90 M1=1
100 M2=P
110 Sol=2
120 LINK "TRANS:F",9200
130 CALL Trans(M(*),K(*),Vec(*),Eval(*),Zeta(*),M1,M2,Lb,Ub,
D(*),Offd(*),Offd2(*),D1(*),Type,N,Sol,P)
140 LINK "EIGEN:F",9200
150 CALL Eigen(M(*),K(*),Vec(*),Eval(*),Zeta(*),M1,M2,Lb,Ub,
D(*),Offd(*),Offd2(*),D1(*),Type,N,Sol,P)
160 FOR R=1 TO P
170 Mr=0
180 ! Finds Mass of mode r
190 Br=2*Zeta(R)*SQR(Eval(R))
200 Vec=0
210 MAT Theta=ZER
220 FOR I=1 TO N
230 FOR J=1 TO N
240 Theta(I)=M(I,J)*Vec(J,R)+Theta(I)
250 NEXT J
260 NEXT I
270 FOR I=1 TO N
280 FOR J=I TO N
290 C(I,J)=Br*Theta(I)*Theta(J)+C(I,J)
300 C(J,I)=C(I,J)
310 NEXT J
320 NEXT I
330 NEXT R
340 MAT Offd=ZER
350 MAT Offd2=ZER
360 MAT D=ZER
370 MAT Vec=ZER
380 MAT D1=ZER
390 SUBEND
400 SUB Eqsolv(H(*),A(*),K(*),P(*),INTEGER R,N)
410 OPTION BASE 1
420 DIM B(89,10)
430 REDIM B(N,R)
440 MAT B=H
450 D1=1
460 D2=0
470 FOR I=1 TO N
480 FOR J=1 TO N
490 X=A(I,J)
500 FOR K=I-1 TO 1 STEP -1
510 X=X-A(J,K)*A(I,K)
520 NEXT K
530 IF J<>I THEN 630
540 D1=D1*X
550 IF X<>0 THEN L1
560 D2=0
570 GOTO Fail
580 L1: IF ABS(D1)<1 THEN L2
590 D1=D1*.0625
600 D2=D2+4
610 GOTO L1
620 L2: IF ABS(D1)>=.0625 THEN 660

```



```
630   D1=D1+16
640   D2=D2-4
650   GOTO L2
660   IF X.L0 THEN GOTO Fail
670   P(I)=1/SQP(X)
680   IF J.>I THEN A(J,I)=X+P(I)
690   NEXT J
700   NEXT I
710   FOR J=1 TO R
720   REM SOLUTION OF LY=B
730   FOR I=1 TO N
740   Z=B(I,J)
750   FOR K=I-1 TO 1 STEP -1
760   Z=Z-A(I,K)*B(K,J)
770   NEXT K
780   B(I,J)=Z+P(I)
790   NEXT I
800   REM SOLUTION OF UX=Y
810   FOR I=N TO 1 STEP -1
820   Z=B(I,J)
830   FOR K=I+1 TO N
840   Z=Z-A(K,I)*B(K,J)
850   NEXT K
860   B(I,J)=Z+P(I)
870   NEXT I
880   NEXT J
890   FOR I=1 TO R
900   FOR J=1 TO R
910   A=0
920   FOR S=1 TO N
930   K(I,J)=A+H(S,I)*B(S,J)
940   A=K(I,J)
950   NEXT S
960   NEXT J
970   NEXT I
980   MAT H=B
990   GOTO 1020
1000 Fail: DISP "PROGRAM FAILED IN EOSOLV SUBPROGRAM. COMPUTATION
STOPED"
1010 STOP
1020 SUBEND
```

```

10  SUB Eqsolv1(A(*),P(*),INTEGER R,N)
20  OPTION BASE 1
30  MAT P=ZER
40  REM [A]=[L]+[U] Triangularization of [A]
50  D1=1
60  D2=0
70  FOR I=1 TO N
80  FOR J=1 TO N
90  X=A(I,J)
100 FOR K=I-1 TO 1 STEP -1
110 X=X-A(K,I)*A(I,K)
120 NEXT K
130 IF J<>I THEN 280
140 D1=D1*X
150 IF X<>0 THEN L1
160 D2=0
170 GOTO Fail
180 L1: IF ABS(D1)<.1 THEN L2
190 D1=D1*.0625
200 D2=D2+4
210 GOTO L1
220 L2: IF ABS(D1)>=.0625 THEN 260
230 D1=D1*16
240 D2=D2-4
250 GOTO L2
260 IF X<0 THEN GOTO Fail
270 P(I)=1/SQR(X)
280 IF J<I THEN A(J,I)=X*P(I)
290 NEXT J
300 NEXT I
310 GOTO 340
320 Fail: DISP "PROGRAM FAILED IN EQSOLV SUBPROGRAM. COMPUTATION
        STOPED"
330 STOP
340 SUBEND
350 SUB Eqsolv2(B(*),A(*),P(*),INTEGER R,N)
360 OPTION BASE 1
370 FOR J=1 TO R
380 REM SOLUTION OF LY=B
390 FOR I=1 TO N
400 Z=B(I,J)
410 FOR K=I-1 TO 1 STEP -1
420 Z=Z-A(K,I)*B(K,J)
430 NEXT K
440 B(I,J)=Z*P(I)
450 NEXT I
460 REM Solution of UX=Y
470 FOR I=N TO 1 STEP -1
480 Z=B(I,J)
490 FOR K=I+1 TO N
500 Z=Z-A(K,I)*B(K,J)
510 NEXT K
520 B(I,J)=Z*P(I)
530 NEXT I
540 NEXT J
550 SUBEND
560 SUB Initial(D(*),Apfo(*),F0(+),K(+),C(*),Offd2(*),Offd(*),
        M(*),P(*),Delta,INTEGER R,N,Neq,#1)
570 OPTION BASE 1
580 ! This subprogram evaluates the acceleration vector
590 ! for different forcing functions.
600 READ #1,I
610 MAT READ #1;D
620 MAT READ #1;Offd
630 LINK "Eqn",9200,640
    
```

```
640   FOR K1=1 TO Neq
650   T=0
660   CALL Eqn(T,F,K1)
670   FOR I=1 TO N
680   Apfo(I,1)=F*F0(I)
690   NEXT I
700   FOR I=1 TO N
710   FOR J=1 TO N
720   Offd2(I,1)=-K(I,J)*D(J)-C(I,J)*Offd(J)+Apfo(I,1)
730   NEXT J
740   Apfo(I,1)=Offd2(I,1)
750   NEXT I
760   CALL Eqsolv2(Offd2(*),M(*),P(*),1,N)
770   MAT PRINT #1;Offd2
780   NEXT K1
790   ASSIGN * TO #1
800   SUBEND
810   SUB Eqn(T,F,K1)
820   OPTION BASE 1
830   ON K1 GOTO L1,L2,L3,L4,L5
```

```
10 SUB Wilsnsol(K(*),M(*),C(*),Apfo(*),F0(*),D(*),D1(*),D2(
*) ,D1(*),A0(*),Tm,De,Th,K1,P(*),H(*),Wcnt(*),Mcnt(*),INT
EGER Ndc(*),Mp,Wp,N,R,J2)
20 ! Direct numerical integration by Wilson theta.
30 OPTION BASE 1
40 REM Effective K,M,C matrices
50 ! [K]=[K]+A0*[M]+A1*[C]
60 FOR I=1 TO N
70 FOR J=I TO N
80 K(I,J)=K(I,J)+A0(1)*M(I,J)+A0(2)*C(I,J)
90 K(J,I)=K(I,J)
100 NEXT J
110 NEXT I
120 REM Matrix K the effective stiffness matrix is
130 ! triangularized.
140 CALL Eqsolv1(K(*),D1(*),R,N)
150 REM Loop round the integration points
160 Cnt=1
170 T=0
180 Npts=INT(Tm/De)+1
190 FOR Count=1 TO Npts-1
200 CALL Eqn(T,F,K1)
210 Cnt=Cnt+1
220 FOR I=1 TO N
230 Apfo(I,1)=F*F0(I)
240 NEXT I
250 T=T+De
260 CALL Eqn(T,F,K1)
270 FOR I=1 TO N
280 Apfo(I,1)=(1-Th)*Apfo(I,1)+Th*F*F0(I)
290 NEXT I
300 FOR I=1 TO N
310 FOR J=1 TO N
320 Apfo(I,1)=(A0(1)*M(I,J)+A0(2)*C(I,J))*D(J)+(A0(3)*M(I,J)
+2*C(I,J))*D1(J)+(2*M(I,J)+A0(4)*C(I,J))*D2(J,1)+Apfo(I,
1)
330 NEXT J
340 NEXT I
350 CALL Eqsolv2(Apfo(*),K(*),D1(*),1,N)
360 FOR I=1 TO N
370 Apfo(I,1)=A0(5)*(Apfo(I,1)-D(I))+A0(6)*D1(I)+A0(7)*D2(I,1)
380 NEXT I
390 FOR I=1 TO N
400 D(I)=D(I)+De*D1(I)+A0(9)*(Apfo(I,1)+2*D2(I,1))
410 NEXT I
420 FOR I=1 TO N
430 D1(I)=D1(I)+A0(8)*(Apfo(I,1)+D2(I,1))
440 NEXT I
450 MAT D2=Apfo
460 Pi=0
470 ! Calculation of bending moment for time T.
480 FOR J=1 TO N
490 P(Ndc(Mp,J2))=Pi+H(Ndc(Mp,J2),J)*D(J)
500 Pi=P(Ndc(Mp,J2))
510 NEXT J
520 Wcnt(Cnt)=D(Ndc(Wp,4))
530 Mcnt(Cnt)=P(Ndc(Mp,J2))
540 NEXT Count
550 SUBEND
```

```
10 SUB Duhammel(T,Nf,Dnf,Ze,Delta,F0,Abar,Bbar,Abar1,Bbar1,
Y,Ynlt,Dynlt,In(*),K1)
20 OPTION BASE 1
30 REM Evaluates Duhammel integral by trapezoidal rule.
40 IF (T<>0) AND (T<>Delta) THEN GOTO 120
50 IF T<>0 THEN GOTO 90
60 Abar=0
70 Abar1=F0
80 GOTO 140
90 Abar=(Abar+Abar1)*EXP(-Ze*Nf*Delta)+F0*COS(Dnf*Delta)
100 Abar1=F0*COS(Dnf*Delta)
110 GOTO 140
120 Abar=(Abar+Abar1)*EXP(-Ze*Nf*Delta)+F0*COS(Dnf*T)
130 Abar1=F0*COS(Dnf*T)
140 IF (T<>0) AND (T<>Delta) THEN GOTO 210
150 IF T<>0 THEN GOTO 180
160 Bbar=0
170 GOTO 230
180 Bbar=(Bbar+Bbar1)*EXP(-Ze*Nf*Delta)+F0*SIN(Dnf*Delta)
190 Bbar1=F0*SIN(Dnf*Delta)
200 GOTO 230
210 Bbar=(Bbar+Bbar1)*EXP(-Ze*Nf*Delta)+F0*SIN(Dnf*T)
220 Bbar1=F0*SIN(Dnf*T)
230 Y=Delta/2*(Abar*SIN(Dnf*T)-Bbar*COS(Dnf*T))
240 IF In(K1)=0 THEN SUBEXIT
250 Y0=(Dynlt+Ynlt*Ze*Nf)/Dnf*SIN(Dnf*T)+Ynlt*COS(Dnf*T)
260 Y0=Y0*EXP(-Ze*Nf*T)
270 Y=Y0+Y
280 SUBEND
290 SUB Modal(Vec(*),Eval(*),M(*),K(*),Zeta(*),D(*),Offd(*),
Offd2(*),D1(*),INTEGER P,N,Type,Sol,Ndm)
300 REM Evaluation of system modal characteristics.
310 OPTION BASE 1
320 DIM Ar(16,16),Cr(16,16)
330 REDIM Ar(N,N),Cr(N,N)
340 PRINT "-----"
350 Sol=1
360 M1=1
370 M2=P
380 LINK "TRANS:F",15570
390 CALL Trans(M(*),K(*),Vec(*),Eval(*),Zeta(*),M1,M2,Lb,Ub,
D(*),Offd(*),Offd2(*),D1(*),Ar(*),Cr(*),Type,N,Sol,Ndm)
400 LINK "EIGEN:F",15570
410 CALL Eigen(M(*),K(*),Vec(*),Eval(*),Zeta(*),M1,M2,Lb,Ub,
D(*),Offd(*),Offd2(*),D1(*),Ar(*),Cr(*),Type,N,Sol,Ndm)
420 MAT Offd=ZER
430 MAT Offd2=ZER
440 MAT D=ZER
450 MAT D1=ZER
460 SUBEND
```

```

10 SUB Plot(Drw(*),C#,Time,Delta,INTEGER Nd1)
20 OPTION BASE 1
30 REM This sub program plots the graphs for
40 | displacements and stresses against time.
50 BEEP
60 DISP "Choose the plotter,5 for incremental,13 for CR
70 T,7 for 9827A"
70 INPUT Pltr
80 ! Finds Max & Min of Drw(*)
90 Max=Min=Drw(1)
100 FOR I=2 TO Time/Delta
110 IF Drw(I)>Max THEN Max=Drw(I)
120 IF Drw(I)<Min THEN Min=Drw(I)
130 NEXT I
140 IF ABS(Max)>ABS(Min) THEN PRINT USING "K,4X,MD.4DE";"Max
150 |imum response is:",Max
150 IF ABS(Min)>ABS(Max) THEN PRINT USING "K,4X,MD.4DE";"Max
160 |imum response is:",Min
160 IF Pltr=13 THEN GOSUB Plt2
170 IF Pltr=5 THEN GOSUB Plt1
180 IF Pltr=7 THEN GOSUB Plt3
190 GOTO 340
200 Plt1: DISP "Set the plotter then press CONT"
210 PAUSE
220 PLOTTER IS 5,"INCREMENTAL"
230 LIMIT 20,920,10,500
240 RETURN
250 Plt2: PLOTTER IS 13,"GRAPHICS"
260 DISP "Do you need a hard copy?"
270 INPUT Dump
280 GRAPHICS
290 RETURN
300 Plt3: DISP "Set the plotter then press CONT"
310 PAUSE
320 PLOTTER IS 7,5,"9872A"
330 RETURN
340 FRAME
350 LOCATE 11,105,6,95
360 MOVE 4,29
370 CSIZE 2,1
380 LDIR PI/2
390 LABEL "";C#;" AT NODE";Nd1;""
400 LDIR 0
410 Xmax=Time
420 CALL Axes(0,Xmax,Min,Max,1)
430 MOVE 0,Drw(1)
440 FOR I=2 TO INT(Time/Delta)
450 DRAW Delta+(I-1),Drw(I)
460 NEXT I
470 IF Dump THEN DUMP GRAPHICS
480 GCLEAR
490 EXIT GRAPHICS
500 SUBEND
510 SUB Axes(Xmin,Xmax,Ymin,Ymax,Scay)
520 OPTION BASE 1
530 X3=(Xmax-Xmin)/8
540 Y3=(Ymax-Ymin)/8
550 Jx=5+10^(INT(LGT(X3))-1)
560 Jy=5+10^(INT(LGT(Y3))-1)
570 X3=Jx+INT(X3/Jx+.5)
580 Y3=Jy+INT(Y3/Jy+.5)
590 Sxmin=X3+INT(Xmin/X3)
600 Sxmin=Y3+INT(Ymin/Y3)
610 Sxmax=-X3*INT(-Xmax/X3)
620 Symax=-Y3*INT(-Ymax/Y3)

```

```

630 X4=(Sxmax-Sxmin)/17
640 Y4=(Symax-Symin)/17
650 SCALE Sxmin-X4, Sxmax+X4, Symin-Y4, Symax+Y4
660 Xint=Yint=0
670 IF SGN(Sxmax)*SGN(Sxmin)>0 THEN Xint=Sxmin
680 IF SGN(Symax)*SGN(Symin)>0 THEN Yint=Symin
690 AXES X3,Y3,Xint,Yint,2,2,Scay
700 CSIZE 3.5*Scay
710 LDIR ATH(0)
720 LORG 6
730 IF Sxmax<=0 THEN 760
740 P=INT(LGT(Sxmax))
750 GOTO 770
760 P=INT(LGT(-Sxmin))
770 J=0
780 IF (P<-1) OR (P>2) THEN J=1
790 FOR Lx=Sxmin TO Sxmax STEP X3
800 IF Lx=Xint THEN Next
810 MOVE Lx,Yint-Y3*.1
820 LABEL USING "K";" "%VAL$(Lx/10^(J*P))&" "
830 Next: NEXT Lx
840 IF J=0 THEN Skipx
850 MOVE Sxmax+X3/2,Yint-Y3*.1
860 LORG 3
870 LABEL USING "K";" x 10^",P
880 Skipx: LDIR 0
890 LORG 8
900 IF Symax<=0 THEN 930
910 P=INT(LGT(Symax))
920 GOTO 940
930 P=INT(LGT(-Symin))
940 J=0
950 IF (P<-1) OR (P>2) THEN J=1
960 LORG 2
970 MOVE Sxmax,Yint-.8*Y3
980 LABEL "TIME(Sec)"
990 LORG 8
1000 FOR Ly=Symin TO Symax STEP Y3
1010 IF Ly=Yint THEN 1040
1020 MOVE Xint,Ly
1030 LABEL USING "K";VAL$(Ly/10^(J*P))&" "
1040 NEXT Ly
1050 IF J=0 THEN Skip
1060 LORG 2
1070 MOVE Xint,Symax
1080 LABEL USING "K";" x 10^",P
1090 Skip: PENUP
1100 CSIZE 3.3*Scay
1110 Xmin=Symin
1120 Ymin=Symin
1130 Xmax=Sxmax
1140 Ymax=Symax
1150 SUBEND

```